

Cyclen Transition Metal Complexes as Biomimetic Catalysts, Phosphate Anion Sensors and Building-blocks in Supramolecular Assemblies

Dissertation

zur Erlangung des Doktorgrades der Naturwissenschaften

(Dr. rer. nat.)

der naturwissenschaftlichen Fakultät IV

– Chemie und Pharmazie –

der Universität Regensburg



vorgelegt von

Kristina Michaela Woinaroschy

aus Bukarest (Rumänien)

2007

The experimental part of this work was carried out between October 2003 and September 2007 at the Institute of Organic Chemistry at the University of Regensburg, under the supervision of Prof. Dr. B. König.

The PhD thesis was submitted on: 06. November 2007

The colloquium took place on: 27. November 2007

Board of examiners:	Prof. Dr. J. Heilmann	(Chairman)
	Prof. Dr. B. König	(1st Referee)
	Prof. Dr. R. Gschwind	(2nd Referee)
	Prof. Dr. S. Elz	(Examiner)

To Alex
and my family

Acknowledgements

I would like to express my sincere gratitude to Prof. Dr. B. König for his continued guidance, encouragement and advice throughout this work.

I would also like to thank the German Environmental Foundation (Deutsche Bundesstiftung Umwelt, DBU) for awarding me a PhD scholarship and offering me the occasion to make interesting contacts and learn about new valuable scientific projects during the yearly seminars and conferences. My special thanks to Dr. J. Lay and Nicole Redeker-Freyer for their support and valuable friendship.

Thanks are extended to the scientific staff members of the analytical department of the Faculty of Chemistry and Pharmacy at the University of Regensburg for the quick and precise measurements, and especially for their constant help when puzzling questions and problems troubled me. Special thanks to Dr. T. Burgemeister, Mr. F. Kastner, Ms. N. Pustet, Ms. A. Schramm and Ms. G. Stühler (NMR), Dr. K. K. Mayer, Mr. J. Kiermaier and Mr. W. Söllner (MS), Mr. H. Schüller (elemental analysis), Dr. M. Zabel and Ms. S. Stempfhuber (X-ray crystallography) and Mrs. H. Leffler-Schuster, Mrs. Britta Badziura and Mrs. Regina Hoheisel (potentiometric titrations). I thank also the scientific teams of Prof. Dr. O. Reiser and Prof. Dr. A. Buschauer for the use of the IR spectrometers and high temperature melting point apparatus. A special thanks to Prof. Dr. R. Winter from the Institute of Inorganic Chemistry at the University of Regensburg and Dr. Biprajit Sarkar from the University of Stuttgart for measurements of EPR spectra and the helpful discussions.

I would like to thank Michael Subat for the good collaboration on two of the projects, for giving me advice and for the long and interesting discussions, whether scientific or personal. Thanks go also to the two undergraduate students, Stefan Anthofer and Andrei Ursu, for the good cooperation and their industrious work in the lab. A special thanks to Dr. W. Braig, Dr. C. Braig, Mrs. E. Liebl, Ms. S. Graetz, Dr. R. Vasold and Mrs. S. Strauss for their support.

I would like to thank all my colleagues, past and present, for making the working environment positive, constructive, as well as relaxed. My special thanks go to:

Dr. C. Bonauer, Dr. C. Mandl and Dr. T. Graf for making me feel welcome and putting me at ease at my arrival in the working group. My lab colleagues Dr. Stefan Ritter, Andreas Grauer

and Alexander Riechers for making sure the days in the lab are lively and never boring or ordinary, for the discussions and great laughs. Andrea Späth for having always a cheer-up line and an open ear for discussion. Jiri Svoboda for the nice evenings playing board games and the great Czech meals. Robert Knappe for being always himself and for his sincerity. Giovanni Imperato for all the crazy stuff, for showing me to take things easier and the delicious food. Britta Badziura, Regina Hoheisel, Simone Strauss and Elisabeth Liebl for all the nice lunchtimes spent in the kitchen together.

My personal thanks goes to my school friends Alexandra Beca and Catalina Anitei and to Valentin Lupu for their friendship, all the nice moments spent on the holidays back home, the many laughs and the constant encouragements.

I would also like to thank the members of the theatre group “Babylon” in the years 2003-2006 for their friendship, for helping me adapt quicker to my new environment, for offering me unforgettable moments and interesting views on other cultures. Special thanks to Caren, Christine and Andi for keeping the group together, to Leo, Nazish, Moni, Lissy, Magda, Gokce, Bille, Pasquale for laughing with tears and to Witalij and Dragisa for sharing with me the Slavonic spirit.

My most special and biggest thanks go to my husband Alex and to my family (my parents, grandparents and aunt). A very big “Thank you” from all my heart for giving me all your love and trust, for never letting me down and giving me always 100% backup. I could not be where I am today and be the person that I am today without you.

*One never notices what has been done;
one can only see what remains to be done.*

Marie Curie

Table of Contents

A	Introduction	1
B	Main Part	5
1.	1,4,7,10 – Tetraazacyclododecane Metal Complexes as Potent Promoters of Carboxyester Hydrolysis under Physiological Conditions	5
1.1.	Introduction	6
1.2.	Results and discussion	8
1.2.1.	Syntheses of the ligands L1-L8 and their metal complexes	8
1.2.2.	Deprotonation constants (pK_a) of the metal-bound H_2O	12
1.2.3.	X-ray Crystal Structure of $[Zn_2L_2]\mu-OH(ClO_4)_3 \cdot CH_3CN \cdot H_2O$	17
1.2.4.	Hydrolysis of 4-nitrophenyl acetate (NA) promoted by the mononuclear metal complexes	19
1.2.5.	Hydrolysis of 4-nitrophenyl acetate (NA) promoted by the dinuclear metal complexes Zn_2L_2 , Zn_2L_4 and Zn_2L_5	24
1.2.6.	Hydrolysis of 4-nitrophenyl acetate (NA) promoted by the dinuclear metal complexes Cu_2L_2 , Ni_2L_2 , Zn_2L_6 and Zn_2L_7	27
1.3.	Conclusion	33
1.4.	Experimental section	35
1.5.	References	77
2.	1,4,7,10 – Tetraazacyclododecane Metal Complexes as Potent Promoters of Phosphodiester Hydrolysis under Physiological Conditions	81
2.1.	Introduction	81
2.2.	Experimental section	83
2.3.	Results and discussion	84
2.4.	Conclusion	99
2.5.	Supporting Information	100
2.6.	References	102
3.	Phosphate Anion Binding of Dinuclear Zinc-1,4,7,10 – tetraazacyclododecane Complexes at Physiological Conditions	107
3.1.	Introduction	107
3.2.	Results and discussion	111

3.3. Conclusion.....	126
3.4. Experimental section.....	127
3.5. Supporting Information.....	132
3.6. References.....	142
 4. Synthesis and characterization of 1-(2H-Tetrazol-5-yl)-1,4,7,10-tetraaza- cyclododecane and its Zn(II), Ni(II) and Cu(II) complexes.....	 145
4.1. Introduction.....	145
4.2. Results and discussion.....	146
4.2.1. Syntheses of the macrocyclic tetraazole ligand and its metal complexes ZnL, CuL and NiL.....	146
4.2.2. X-ray Crystal Structure of the dimer $[\text{Ni}_2(\text{LH}_{-1})_2(\text{H}_2\text{O})_2](\text{ClO}_4)_2$	148
4.2.3. Deprotonation Constants ($\text{p}K_{\text{a}}$) of the metal complexes.....	150
4.3. Experimental section.....	153
4.4. References.....	161
 C Summary.....	 165
 D Appendix.....	 166
Publication list.....	166
Curriculum Vitae.....	167

Abbreviations

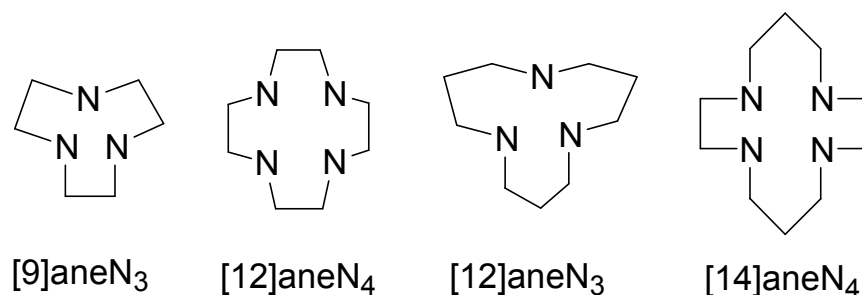
Bis/Tris	Bis[2-hydroxyethyl]-imino-Tris-[hydroxymethyl]-methane
BNPP	bis(4-nitrophenyl)phosphate
Boc	<i>tert</i> -butoxycarbonyl
BrCN	cyanogen bromide
C	Celsius
c	concentration
calcd.	Calculated
CDCl ₃	deuterated chloroform
CH ₃ CN	acetonitrile
CHES	N-cyclohexyl-2-aminoethanesulfonic acid
CI	chemical ionisation
ClO ₄	perchlorate (anion)
DCM	dichloromethane
DMSO	dimethylsulfoxide
EI	electron impact (MS)
EPR	electron paramagnetic resonance (spectra)
eq.	equivalent
ES	electron spray (MS)
Et ₂ NH	diethylamine
Et ₂ O	diethyl ether
EtOAc	ethyl acetate
EtOH	ethanol
FAB	fast atom bombardment
h	hours
HCl	hydrochloric acid
HClO ₄	perchloric acid
HEPES	N-2-Hydroxyethylpiperazin-N'-2-ethansulfonic acid
HPLC	high pressure liquid chromatography
HRMS	high resolution mass spectrum
<i>I</i>	ionic strength
IR	infra red (spectrum)
ITC	isothermal titration calorimetry

<i>J</i>	coupling constant
K	Kelvin
KBr	potassium bromide
K ₂ CO ₃	potassium carbonate
LiOH	lithium hydroxide
M	metal ion
MeOH	methanol
min	minutes
m.p.	melting point
MS	mass spectrum
<i>n</i> -BuNH ₂	N-buthylamine
NA	4-nitrophenyl acetate
NaCl	sodium chloride
NaN ₃	sodium azide
NH ₄ Cl	ammonium chloride
NMR	nuclear magnetic resonance
Ph	phenyl
R _f	retention factor
rt	room temperature
tert	tertiary
TEAP	triethylammonium perchlorate
TFA	trifluoroacetic acid
THF	tetrahydrofuran
TLC	thin layer chromatography
TMS	tetramethyl silane
TRIS	2-amino-2-hydroxymethyl-propane-1,3-diol
UV/Vis	ultraviolet/visible (spectroscopy)

A. Introduction

The field of coordination chemistry of polyazamacrocycles has known an immense interest since the publication of the first reports in the early 1960s by Curtis¹ and Thompson and Curtis².

Especially cyclic tri- and tetraamines (**Scheme 1**) have been extensively used in various applications, as these compounds are able to adapt to many metal ion coordination geometries,³ offer multiple donors sites and are able to hold two or more metal ions at short distances, mimicking thus the active sites of metalloenzymes.



Scheme 1. Structure of the most popular azamacrocycles.

The Zn(II) complexes of 1,5,9-triazacyclododecane ([12]aneN₃), 1,4,7,10-tetraazacyclododecane ([12]aneN₄, cyclen) and their derivatives have been suggested as chemical models of the active centre of alkaline phosphatase (AP)⁴, carbonic anhydrase (CA)⁵, carboxypeptidase⁶, liver alcohol dehydrogenase⁷ or β -lactamase.⁸ Likewise, Cu(II) complexes of 1,4,7-triazacyclononane [9]aneN₃ have been discussed as chemical models of phosphatases,⁹ nucleases¹⁰ and peptidases.¹¹ The detoxification of some pesticides and chemical weapons was envisaged as a possible application of the compounds.¹²

The metal ions are usually bound thermodynamically strongly by the macrocyclic ligand, but additionally, unoccupied coordination sites of Lewis-acidic metal ion allow reversible coordination of Lewis-basic binding partners.¹³ The strength of such an interaction is determined by the Lewis-acidic character of the metal, the basicity of the anions and the influence of the substituents on the azamacrocycle. Thus metal complexes of azamacrocycles are most suitable to be used not only as models of metalloenzymes, but also as sensors of various anions. Kimura et al used mono-, di- and trinuclear azamacrocyclic zinc complexes for the selective binding of several phosphates¹⁴, Parker et al. reported a lanthanide (Eu³⁺ or Tb³⁺) cyclen derivative with chiral amide side chains for carbonate, phosphate, lactate, citrate, acetate and malonate ions¹⁵, Zn(II)-1,5,9-triazacyclononane was shown to interact with

acetate, hydrogencarbonate, thiocyanate, halides and deprotonated sulfonamides¹⁶ and a Cu(II) complex of 1,4,8,11-tetraazacyclotetradecane ([14]aneN₄, cyclam) coordinated chloride, bromide, sulphate, phosphate, ADP and ATP¹⁷. Macrocyclic metal complexes also reversibly coordinate imide moieties, which led to their use as artificial receptors for barbiturates¹⁸, thymine¹⁹, uracil²⁰, and flavins²¹. For a more detailed coverage of the molecular interactions of Zn(II) cyclen and its derivatives²² and the molecular recognition by azamacrocycles²³ we refer to recent reviews.

Due to these exceptional properties, transitional metal complexes of azamacrocyclic compounds are better suited than synthetic receptors based on hydrogen bonding for the selective recognition of target molecules and offer the advantage of high association constants in biological media. Therefore they are ideal as binding sites for analytes, and offer many applications in bioanalytics, molecular biology, diagnostics or medicinal chemistry. Their coordination abilities could also enable their use as building blocks for self-assembled supramolecular coordination compounds and lead to interesting applications in material science.

References

- ¹ Curtis, N.F. *J. Chem. Soc.* **1960**, 4409.
- ² Tompson, M.C.; Busch, D. H. *J. Am. Chem. Soc.* **1964**, 86, 3561.
- ³ Review on thermodynamic and kinetic data for macrocycle interaction with cations, anions and neutral molecules: Izatt, R. M.; Pawlak, K.; Bradshaw, J. S.; Bruening, R. L. *Chem. Rev.* **1995**, 95, 2529-2586.
- ⁴ a) Koike, T.; Kajitani, S.; Nakamura, I.; Kimura, E.; Shiro, M. *J. Am. Chem. Soc.* **1995**, 117, 1210-1219; b) Kimura, E.; Kodama, Y.; Koike, T.; Shiro, M. *J. Am. Chem. Soc.* **1995**, 117, 8304-8311.
- ⁵ Zhang, Z.; van Eldic, R.; Koike, T.; Kimura, E. *Inorg. Chem.* **1993**, 32, 5749-5755.
- ⁶ Kim, D.H.; Lee, S.S. *Bioorg & Med. Chem.* **2000**, 8, 647-652.
- ⁷ Kimura, E.; Shionoya, M.; Hoshino, A.; Ikeda, T. ; Yamada, Y. *J. Am. Chem. Soc.* **1992**, 114, 10134-10137.
- ⁸ Koike, T.; Masahiro, M.; Kimura, E. *J. Am. Chem. Soc.* **1994**, 116, 8443-8449.
- ⁹ a) Belousoff, M. J.; Duriska, M. B.; Graham, B.; Batten, S. R.; Moubaraki, B.; Murray, K. S.; Spiccia, L. *Inorg. Chem.* **2006**, 45, 3746-3755; b) Burstyn, J. N.; Deal, K. A. *Inorg. Chem.* **1993**, 32, 3585-3586; c) Deal, K. A.; Burstyn, J. N. *Inorg. Chem.* **1996**, 35, 2792-2798;
- ¹⁰ a) McCue, K. P.; Voss, D. A. Jr. ; Marks, C. ; Morrow, J. R. *J. Chem. Soc. Dalton Trans.* **1998**, 2961-2963; b) Hegg, E. L.; Deal, K.; Kiessling, L.; Burstyn, J. N. *Inorg. Chem.* **1997**, 36, 1715-1718;
- ¹¹ Hegg, E. L.; Burstyn, J. N. *J. Am. Chem. Soc.* **1995**, 117, 7015-7016;
- ¹² Kimura, E.; Hashimoto, H.; Koike, T. *J. Am. Chem. Soc.* **1996**, 118, 10963-10970.
- ¹³ Reichenbach-Klinke, R.; König, Burkhard, *J. Chem. Soc. Dalton Trans.* **2002**, 121-130.
- ¹⁴ a) S. Aoki, M. Zulkefeli, M. Shiro, M. Kohsako, K. Takeda, E. Kimura, *J. Am. Chem. Soc.* **2005**, 127, 9129-9139; b) E. Kimura, S. Aoki, T. Koike, M. Shiro, *J. Am. Chem. Soc.* **1997**, 119, 3068-3076.
- ¹⁵ a) R. Dickins, T. Gunlaugsson, D. Parker, R. Peacock, *Chem. Comm.* 1998, 1643; b) J. Bruce, R. Dickins, L. Govenlock, T. Gunlaugsson, S. Lopinski, M. Lowe, D. Parker, R. Peacock, J. Perry, S. Aime, M. Botta, *J. Am. Chem. Soc.* **2000**, 122, 9674-9684.
- ¹⁶ E. Kimura, T. Shiota, T. Koike, M. Shiro, M. Kodama, *J. Am. Chem. Soc.* **1990**, 112, 5805-5811.
- ¹⁷ M. Padilla-Tosta, J. Lloris, R. Martinez-Manez, T. Pardo, F. Sancenon, J. Soto, M. Marcos, *Eur. J. Inorg. Chem.*, **2001**, 1221-1226.
- ¹⁸ T. Koike, M. Takashige, E. Kimura, H. Fujioka, M. Shiro, *Chem. Eur. J.* **1996**, 2, 617.
- ¹⁹ E. Kimura, M. Murata, N. Katsube, T. Koike, E. Kikuta, *J. Am. Chem. Soc.* **1999**, 121, 5426-5436 and references therein.
- ²⁰ E. Kimura, T. Koike, *J. Chem. Soc. Chem. Commun.* **1998**, 1495-1500.

-
- ²¹ a) B. König, M. Pelka, H. Zieg, T. Ritter, H. Bouas-Laurent, R. Bonneau, J.-P. Desvergne, *J. Am. Chem. Soc.*, **1999**, *121*, 1681-1687; b) B. König, H.-C. Gallmeier, R. Reichenbach-Klinke, *Chem. Commun.*, **2001**, 2390-2391.
- ²² S. Aoki, E. Kimura, *Chem. Rev.* **2004**, *104*, 769-788.
- ²³ M. Kruppa, T. Walenzyk, B. König, *Chem Rev.* **2006**, *106*, 3520 – 3560.

B. Main Part

1. 1,4,7,10 – Tetraazacyclododecane Metal Complexes as Potent Promoters of Carboxyester Hydrolysis under Physiological Conditions¹

Note

The research results reported in this chapter are the work of the PhD students Kristina Woinaroschy (synthesis and characterisation of the Cu(II) and Ni(II) complexes and study of their hydrolytic activity towards carboxyesters) and Michael Subat (synthesis and characterisation of the Zn(II) complexes, study of their behaviour in the hydrolysis of carboxyesters). The undergraduate students Barbara Malterer and Stefan Anthofer performed kinetic measurements (spectroscopic titrations) with the metal complexes during a six-month research project. The publication manuscript was written by Kristina Woinaroschy.

Abstract

New 1,4,7,10-tetraazacyclododecane ([12]aneN₄ or cyclen) ligands with different heterocyclic spacers (triazine, pyridine) of various lengths (bi- and tripyridine) or an azacrown-pendant and their mono- and dinuclear Zn(II), Cu(II) and Ni(II) complexes have been synthesised and characterised. The pK_a values of water molecules coordinated to the complexed metal ions were determined by potentiometric pH titrations and vary from 7.7 to 11.2, depending on the metal ion and the ligand properties. The X-ray structure of [Zn₂L2]μ-OH(ClO₄)₃ · CH₃CN · H₂O shows each Zn(II) ion in a tetrahedral geometry, binding to three N-atoms of cyclen (the average distance of Zn-N: 2.1 Å) and having a μ-OH bridge at the apical site linking the two metal ions (the average distance of Zn-O: 1.9 Å). The distance between the Zn(II) ion and the fourth N-atom is 2.6 Å. All Zn(II) complexes promote the hydrolysis of 4-nitrophenyl acetate (NA) under physiological conditions, while those of Cu(II) and Ni(II) do not have a significant effect on the hydrolysis reaction. The kinetic studies in buffered solutions (0.05 M TRIS, HEPES or CHES, I = 0.1 M, NaCl) at 25 °C in the pH range 6 to 11 under pseudo-first order reaction conditions (excess of metal complex) were analysed by applying the method of initial rates. Comparison of the second-order pH-independent rate constants (*k*_{NA}, M⁻¹s⁻¹) for the mononuclear complexes **ZnL1**, **ZnL3** and **ZnL8**, which are 0.39, 0.27 and 0.38, respectively, indicates that the heterocyclic moiety improves the rate of hydrolysis up to 4 times over the parent Zn([12]aneN₄) complex (*k*_{NA} =

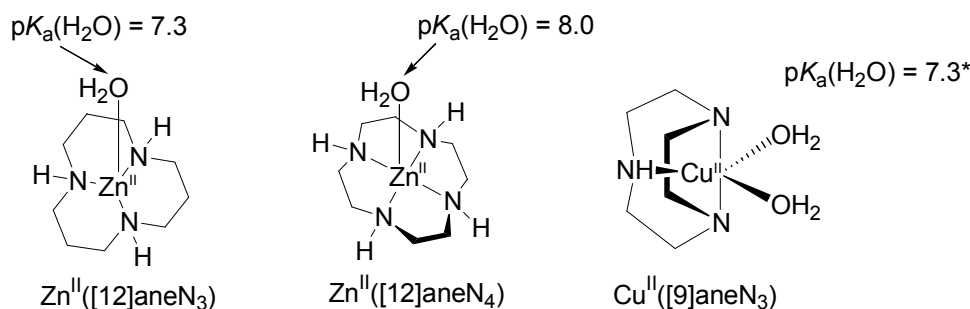
¹ The results of this chapter have been published:

Subat, M.; Woinaroschy, K.; Anthofer, S.; Malterer, B.; Koenig B. *Inorg. Chem.* **2007**, 46(10) pp 4336 - 4356.

0.09 M⁻¹s⁻¹). The reactive species is the Zn(II)-OH⁻ complex, in which the Zn(II)-bound OH⁻ acts as a nucleophile, which attacks intermolecularly the carbonyl group of the acetate ester. For dinuclear complexes **Zn₂L2**, **Zn₂L4**, **Zn₂L5**, **Zn₂L6** and **Zn₂L7**, the mechanism of reaction is defined by the degree of cooperation between the metal centres, determined by the spacer length. For **Zn₂L7**, having the longest tri-aryl spacer, the two metal centres act independently in the hydrolysis, therefore the reaction rate is twice as high as the rate of the mononuclear analogue ($k_{\text{NA}} = 0.78 \text{ M}^{-1}\text{s}^{-1}$). The complexes with mono-aryl spacer show saturation kinetics with formation of a Michaelis-Menten adduct. Their hydrolysis rates are 40 times higher than the Zn[12]aneN₄ system ($k_{\text{NA}} \sim 4 \text{ M}^{-1}\text{s}^{-1}$). **Zn₂L6** is a hybrid between these two mechanisms, a clear saturation curve is not visible, but neither are the metal cores completely independent from another. Some of the Zn(II) complexes show a higher hydrolytic activity under physiological conditions compared to other previously reported complexes of this type.

1.1 Introduction

Hydrolytic enzymes often use water molecules or protein hydroxy residues (e.g. of serine or threonine) as nucleophiles to react with electrophilic substrates (carboxyesters, phosphate esters and amides), wherein the prior activation of the nucleophiles (and/or electrophiles) is essential.¹ These enzymes often require metal cations for their activity² and many metal ion based model systems have been reported, generally featuring tridentate or tetradentate ligands with free coordination sites on the metal cation.³ Polyamine macrocyclic ligands have received special attention in this respect. They are able to adapt to many metal ion coordination geometries,⁴ offer multiple donors sites and are able to hold two metal ions at short distances, mimicking the active sites of metalloenzymes. The Zn(II) complexes of 1,5,9-triazacyclododecane ([12]aneN₃), 1,4,7,10-tetraazacyclododecane ([12]aneN₄) (**Scheme 1**) and their derivatives have been suggested as chemical models of the active centre of alkaline phosphatase (AP)⁵, carbonic anhydrase (CA)⁶, carboxypeptidase⁷, liver alcohol dehydrogenase⁸ or β -lactamase.⁹ Likewise, Cu(II) complexes of 1,4,7-triazacyclononane [9]aneN₃ (**Scheme 1**) have been discussed as chemical models of phosphatases,¹⁰ nucleases¹¹ and peptidases.¹² The detoxification of some pesticides and chemical weapons was envisaged as a possible application of the compounds.¹³



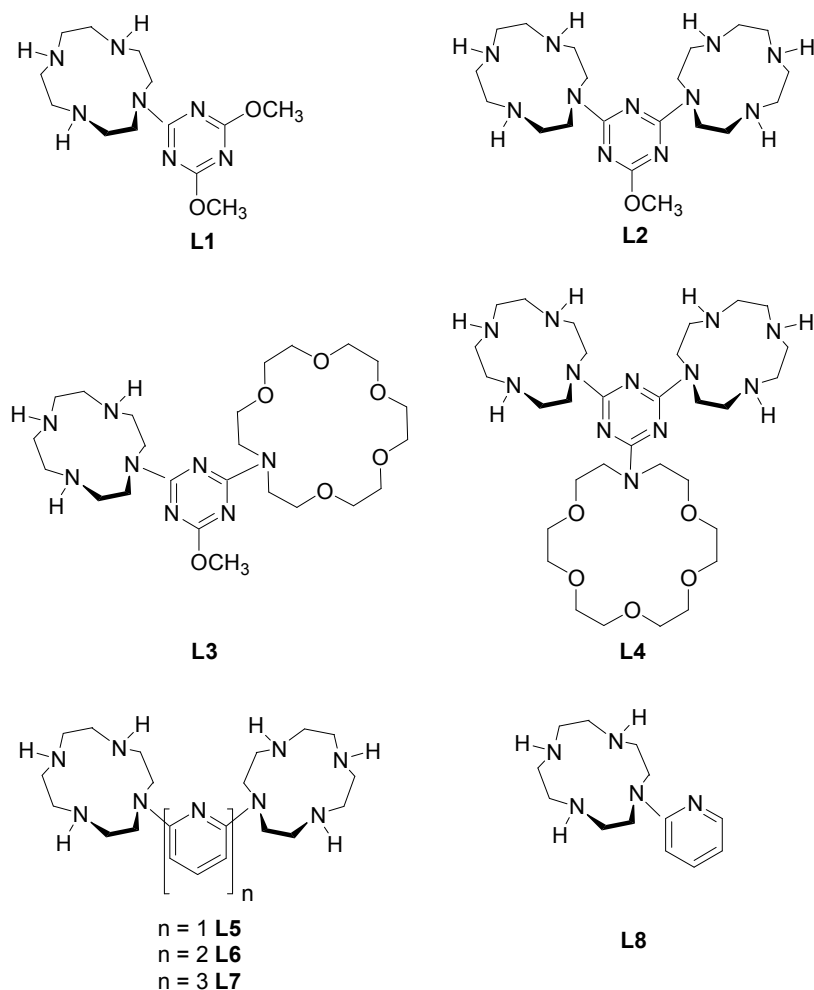
* Because of a monomer-dimer equilibrium, this $\text{p}K_{\text{a}}$ is not simply the $\text{p}K_{\text{a}}$ of the coordinated water; it is, however, the kinetically relevant $\text{p}K_{\text{a}}$.

Scheme 1

The proposed general mechanism of the hydrolysis reaction promoted by these complexes is based on the Lewis acidic metal ion reducing the $\text{p}K_{\text{a}}$ of the coordinated water, thus providing a metal-bound hydroxide nucleophile at neutral pH and at the same time activating the substrate towards nucleophilic attack by charge neutralization.^{3a,14} For dinuclear species, the two metal ions act cooperatively in the catalytic process, either one metal ion provides the nucleophile and the other one coordinates the substrate or both metal ions participate in substrate binding, activation and cleavage.¹⁵ This cooperative action renders dinuclear complexes far more reactive than their mononuclear analogues.

However, the hydrolytic activity of these synthetic systems with carboxyesters is moderate under physiological conditions. The second-order rate constants reach significant values only at pH values >9 . Therefore applications in biotechnology, medicine or environmental sciences of the complexes would suffer from low efficiencies.

It has been demonstrated that additional interactions in the active site influence the properties of the metal complexes and that the hydrolytic activity may increase by attachment of functional groups to a chelate ligand,¹⁶ such as a basic or nucleophilic auxiliary group^{5b,17} or an NH-acidic group.¹⁸ With the aim to develop more efficient metal complexes possessing hydrolytic activity under physiological conditions, we have synthesised the macrocyclic ligands **L1-L8** (Scheme 2) with different heterocyclic spacers of various lengths and determined the hydrolytic properties of their Zn(II), Cu(II) and Ni(II) complexes in aqueous solution with 4-nitrophenyl acetate (NA). The influence of the following parameters on the hydrolytic efficiency and the mechanism of the hydrolysis reaction were analysed: (i) metal complex spacer type and length, (ii) metal ion and its properties (synthesis of Cu(II) and Ni(II) complexes of **L1** and **L2**), (iii) number of metal ions present in the complex (comparison between mono- and dinuclear complexes).



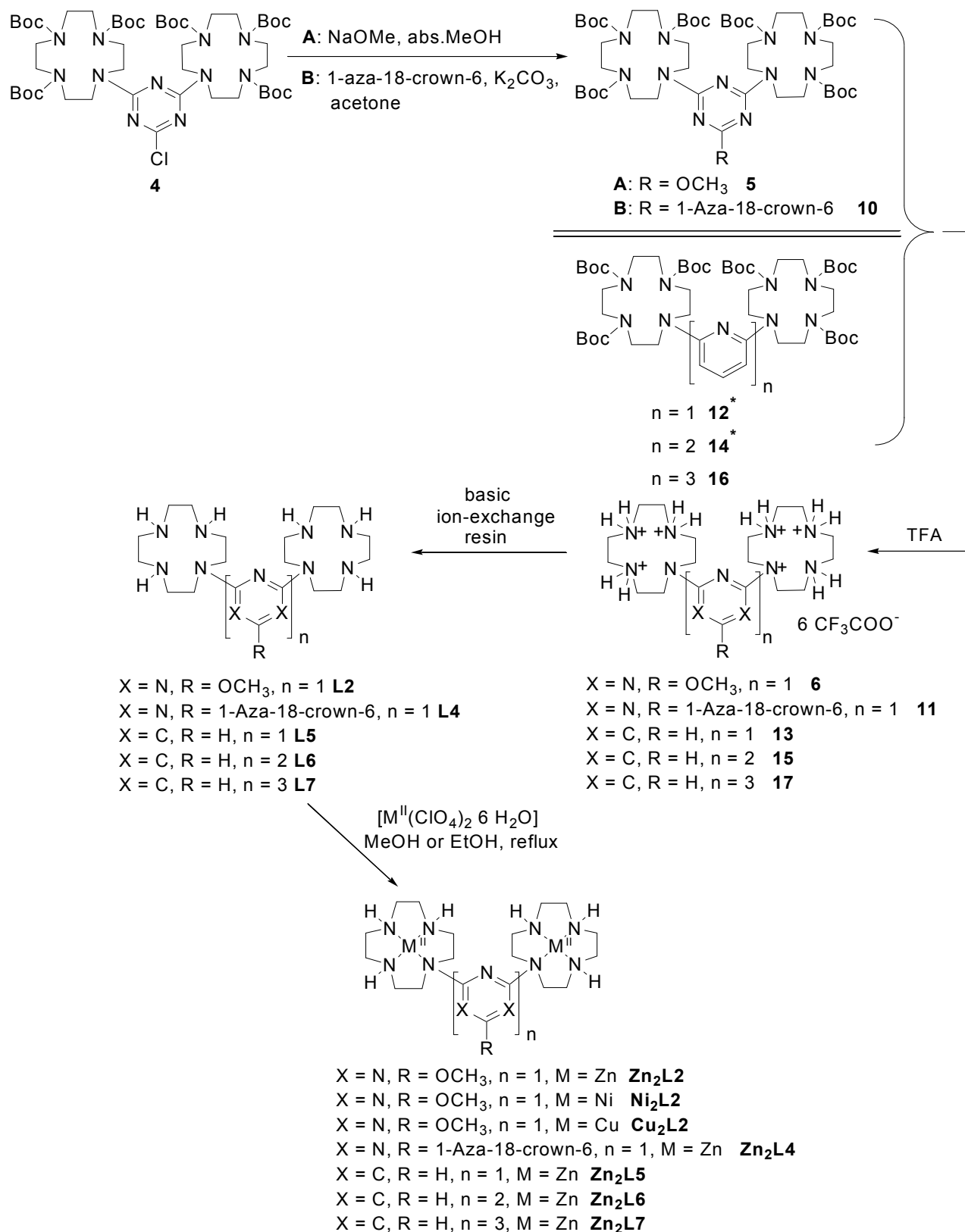
Scheme 2. Structure of the new [12]aneN₄ ligands **L1-L8**

1.2 Results and Discussion

1.2.1 Syntheses of the ligands **L1-L8** and their metal complexes (schemes 3-5).

Ligands **L1-L8** were obtained by a synthetic route previously developed. The first step of the synthesis has already been disclosed for the monosubstituted compound **1**.¹⁹ Ligand **L1** was obtained from compound **1** by nucleophilic substitution with sodium methylate, deprotection of the Boc-groups with TFA and elution from basic ion-exchange resin with an overall yield of 98% (**Scheme 3**). The same procedure gave **L8** starting from the previously reported compound tri-tert-butyl-10-(2-pyridinyl)-1,4,7,10-tetraaza-cyclododecane-1,4,7-tricarboxylate (**18**).²¹

The ligands **L2** and **L4** were prepared starting from the previously reported compound **4**²⁰ using the same synthetic pathways as for **L1**, respectively **L3** (**Scheme 5**). The ligands **L5** and **L6** were obtained starting from the previously reported compounds²¹ **12** and **14**. By following the same procedure²¹ as for **12** and **14**, the new compound **16** was synthesised, from which ligand **L7** was prepared (**Scheme 5**). Metal complexes were isolated in analytical purity with good yields (53% to 98%) from the reaction of the ligands with metal perchlorate salts in MeOH (for Zn(II)) or EtOH (for Ni(II) and Cu(II)) and characterized by different methods (¹H NMR, ¹³C NMR, UV/Vis, IR, ESI, elemental analysis, HRMS) to show a stoichiometry of 1:1 metal cation/ligand for mononuclear complexes, respectively 2:1 metal cation/ligand for dinuclear complexes. In all cases the heteroaromatic spacer is directly connected to the macrocycle, without any pendant arm,^{19,20,21} which leads to more rigid structures.



* Synthesis and characterisation of these compounds previously published see experimental part

Scheme 5. Synthesis of **L2**, **L4-L7** and their metal complexes.

1.2.2 Deprotonation constants (pK_a) of the metal-bound H_2O .

The pK_a values were determined by pH-metric titrations in aqueous or MeOH/ H_2O (1:9) solutions under nitrogen at 25 °C and $I = 0.1$ (tetraethylammonium perchlorate TEAP). The pH profiles of all the complexes and species distribution diagrams of the dinuclear metal complexes can be found in the experimental part. The pK_a values of the mononuclear metal complexes are summarized in **Table 1**.

Metal complex	pK_a
ZnL1	8.35 ± 0.03
NiL1	11.13 ± 0.02
CuL1 ^a	-
ZnL3	8.28 ± 0.05
ZnL8	7.89 ± 0.05
Zn-[12]aneN ₄ ^b	8.06 ± 0.01

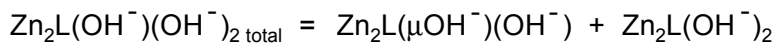
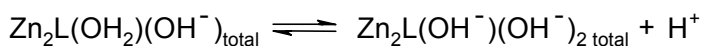
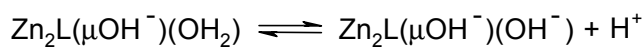
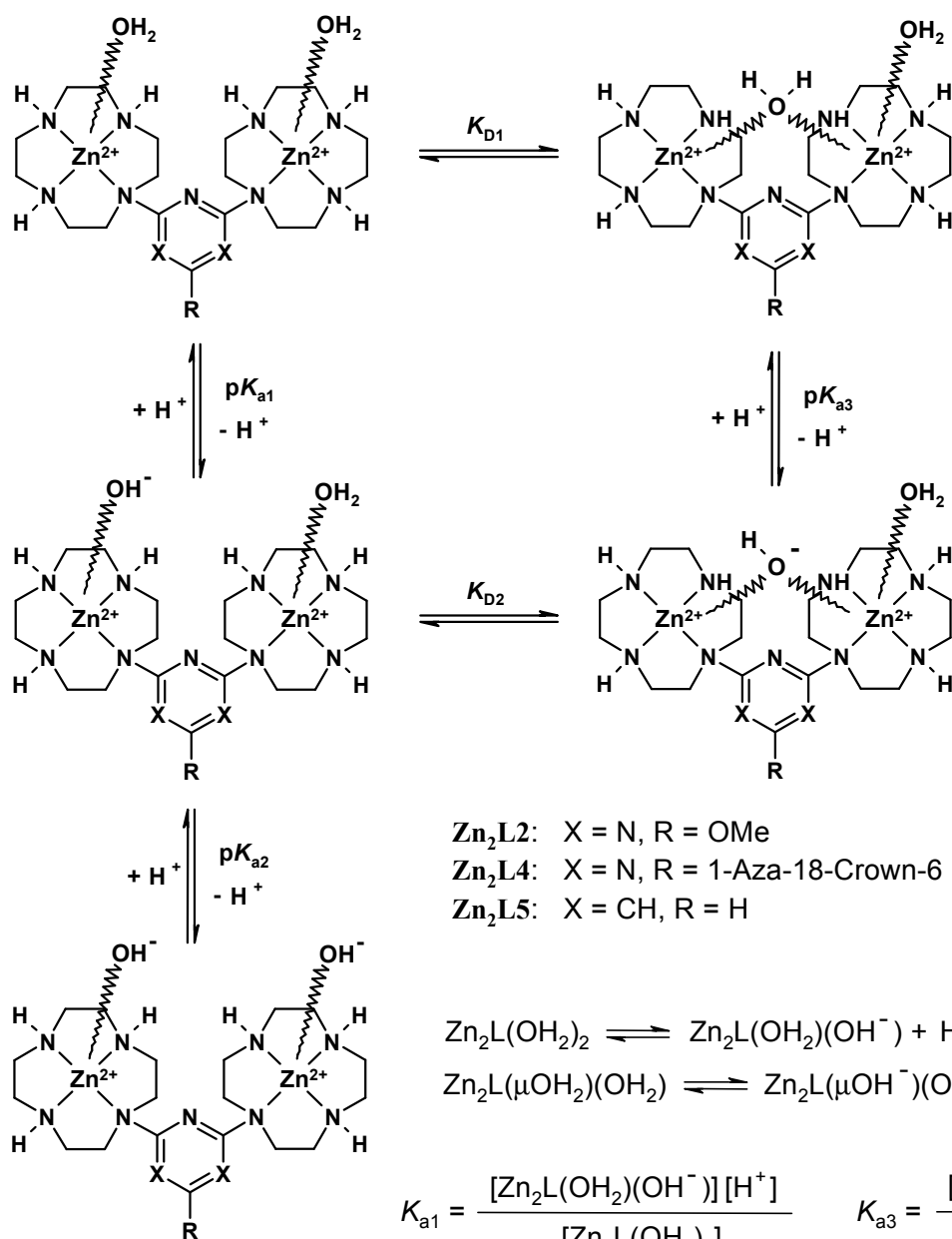
^a titration was not possible due to insufficient solubility. ^b this work.

Table 1. Deprotonation constants (pK_a) of metal-bound H_2O at 25 °C and $I = 0.10$ (TEAP).

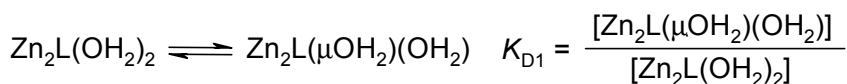
CuL1 was not sufficiently soluble under the given experimental conditions to allow a potentiometric pH titration. However, its UV and IR spectra indicate a square pyramidal complex with one molecule of water as fifth ligand, as reported in literature.²² The UV and IR spectra of **NiL1** coincide also to the usual structure of Ni[12]aneN₄ complexes, reported to have a high spin *cis*-octahedral geometry with two coordinated water molecules,²³ the pK_a value of the second water molecule being higher than pH 13. Among the mononuclear Zn complexes **ZnL8** shows the smallest pK_a value.

For the dinuclear complexes **Zn₂L4** (in aqueous solution) and **Zn₂L5** (in MeOH/ H_2O 9:1 solution) two distinct buffer regions were determined, one around pH 6, the other in the pH range 8 to 10, corresponding to three distinct pK_a values. The model curve fitted to the pH titration profiles corresponds to three pK_a values with complete deprotonation after the addition of two equivalents of base. The titration curves of **Zn₂L2** (in aqueous solution and in MeOH/ H_2O 9:1 solution) show only one deprotonation constant in the pH range of 9, but have a high similarity to the upper part of the titration curves of **Zn₂L4** and **Zn₂L5**. This observation is rationalized by the low solubility of **Zn₂L2**, which did not allow an exact determination of the buffer curve at lower pH range. Titration with a more diluted base (0.025 M instead of 0.1 M) did not improve the measurement. **Zn₂L2** is supposed to have three pK_a

values, but for the chosen experimental conditions only one of them could be determined. The proposed chemical model for the deprotonation steps of **Zn₂L4**, **Zn₂L5** and **Zn₂L2** is shown in **Scheme 6**. The model is based on an equilibrium in solution between the μ -hydroxo-bridged species $\text{Zn}_2\text{-L-(}\mu\text{OH}_2\text{)(OH}_2\text{)}$, analogous to the obtained crystal structure, and an open form corresponding to the species where each Zn(II) ion is coordinating a water molecule, $\text{Zn}_2\text{-L-(OH}_2\text{)}_2$. This model is supported by a good match of the calculated and the measured pH profiles, and reports from literature where a similar equilibrium between open and closed species was postulated.²⁴ The proton independent equilibrium K_{DI} can be determined indirectly. The $\text{p}K_a$ values of **Zn₂L2**, **Zn₂L4** and **Zn₂L5** are summarized in **Table 2**. Alternative models with two deprotonation steps, either consecutive or independent from one another, or a model with the dinuclear metal complex coordinating three water molecules, one at each metal ion and one as a μ -hydroxo-bridge, as observed for the crystal structure of **Zn₂L2** and reported for other macrocyclic Zn complexes,²⁵ do not fit the experimental data.



$$K_{a2} = \frac{[\text{Zn}_2\text{L}(\mu\text{OH}^-)(\text{OH}^-)] [\text{H}^+]}{[\text{Zn}_2\text{L}(\mu\text{OH}^-)(\text{OH}_2)]} = \frac{[\text{Zn}_2\text{L}(\text{OH}^-)(\text{OH}^-)_{2 \text{ total}}] [\text{H}^+]}{[\text{Zn}_2\text{L}(\text{OH}_2)(\text{OH}^-)_{\text{total}}]}$$



Scheme 6. Proposed model for the deprotonation steps of **Zn₂L4**, **Zn₂L5** and **Zn₂L2**

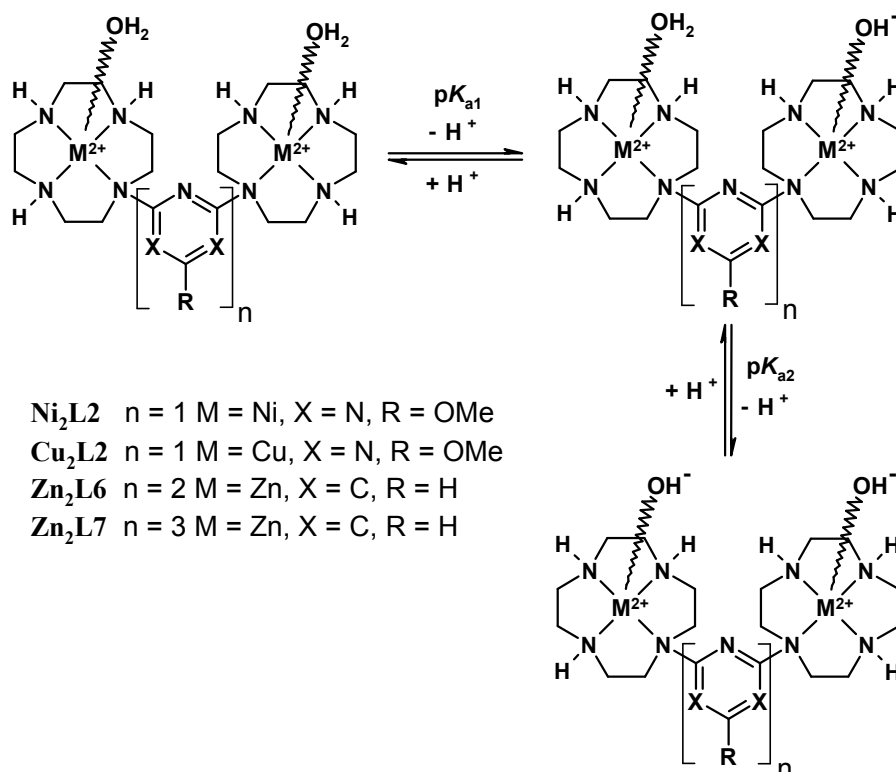
Metal complex	pK_a			$\log K_{D1}$
	pK_{a1}	pK_{a2}	pK_{a3}	
Zn_2L2	-	9.72 ± 0.03^a	-	-
Zn_2L4	8.27 ± 0.02	9.42 ± 0.06	5.96 ± 0.02	0.47 ± 0.04
Zn_2L5	8.14 ± 0.03	9.27 ± 0.05	5.85 ± 0.02	0.64 ± 0.04

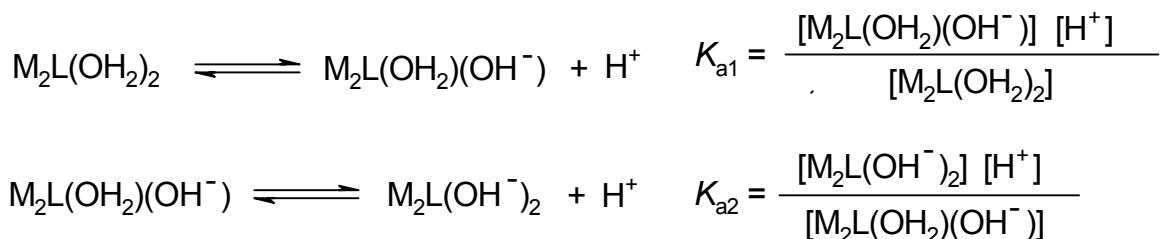
^a The titration curve does not permit a determination of pK_{a1} and pK_{a3} values due to the insufficient solubility of the complex in water and/or MeOH/water 9:1.

Table 2. Deprotonation constants (pK_a) of metal-bound H_2O at 25 °C and $I = 0.10$ (TEAP).

The pK_a value of the μ -hydroxo-coordinated water molecule, pK_{a3} , is smaller than those reported for similar compounds,^{27c} indicating an enhanced acidity and stability of the μ -hydroxo-bridge due to the close proximity of the two Zn(II) cyclen moieties.

For the remaining dinuclear complexes, Cu_2L2 , Ni_2L2 , Zn_2L6 and Zn_2L7 , the pH profiles correspond to the general model²⁶ with each metal ion coordinating a water molecule and two successive deprotonation steps leading to the species $M_2-L-(OH)_2$ (Scheme 7).





Scheme 7. Deprotonation steps and equilibrium equations for **Ni₂L2**, **Cu₂L2**, **Zn₂L6** and **Zn₂L7**

The $\text{p}K_a$ values of these complexes are summarized in **Table 3**.

Metal complex	$\text{p}K_{a1}$	$\text{p}K_{a2}$
Ni ₂ L2	9.75 ± 0.02	10.10 ± 0.02
Cu ₂ L2	8.34 ± 0.03	8.68 ± 0.03
Zn ₂ L6	7.45 ± 0.03	8.85 ± 0.03
Zn ₂ L7	7.65 ± 0.01	8.11 ± 0.03

Table 3. Deprotonation constants ($\text{p}K_a$) of metal-bound H₂O at 25 °C and $I = 0.10$ (TEAP).

The pH profile of **Cu₂L2**, together with its UV and IR spectra, indicate the structure of the complex, with each Cu(cyclen) unit possessing the already reported square pyramidal geometry,²⁵ each Cu(II) ion coordinating to the 4 N-atoms of the macrocycle and 1 H₂O molecule. Therefore there is neither a μ -hydroxo bridge present between the two metal centres as in the case of **Zn₂L2** or as reported in literature for Cu[9]aneN₃ complexes,^{10a,10c,27} nor any coordination of the Cu(II) ions to the N-atom of the bridging hetarene, as observed in a pyridyl-bridged Cu(II) bis(cyclen) complex.²⁸

The successive deprotonation of the water molecules indicates an interaction between the two metal centres. The strength of this interaction is influenced by the spacer length,^{24b,29} as observed from the differences between the two $\text{p}K_a$ values: a shorter spacer length leads to stronger interactions between the metal ions, making the second deprotonation step more difficult and thus increasing the difference between the two $\text{p}K_a$ values. For **Zn₂L6** with the shorter diaryl spacer, this difference is $\Delta\text{p}K_a = 1.4$, while for **Zn₂L7** with the longest spacer, only $\Delta\text{p}K_a = 0.5$. Compound **Zn₂L5** possessing a short aryl spacer was shown to form a μ -hydroxo-bridge between the two metal centers. For the Ni(II) and Cu(II) complexes, the small difference between the $\text{p}K_a$ values indicates a very weak interaction between the two metal ions.

1.2.3 X-ray Crystal Structure of the complex $[\text{Zn}_2\text{L2}]\mu\text{-OH}(\text{ClO}_4)_3 \cdot \text{CH}_3\text{CN} \cdot \text{H}_2\text{O}$.

A solution of $[\text{Zn}_2\text{L2}](\text{ClO}_4)_4 \cdot \text{CH}_3\text{CN}$ in acetonitrile was left to stand at room temperature. After 2 weeks colorless crystals were collected. **Figure 1** shows an ORTEP drawing of the complex with 50% probability thermal ellipsoids.³⁰

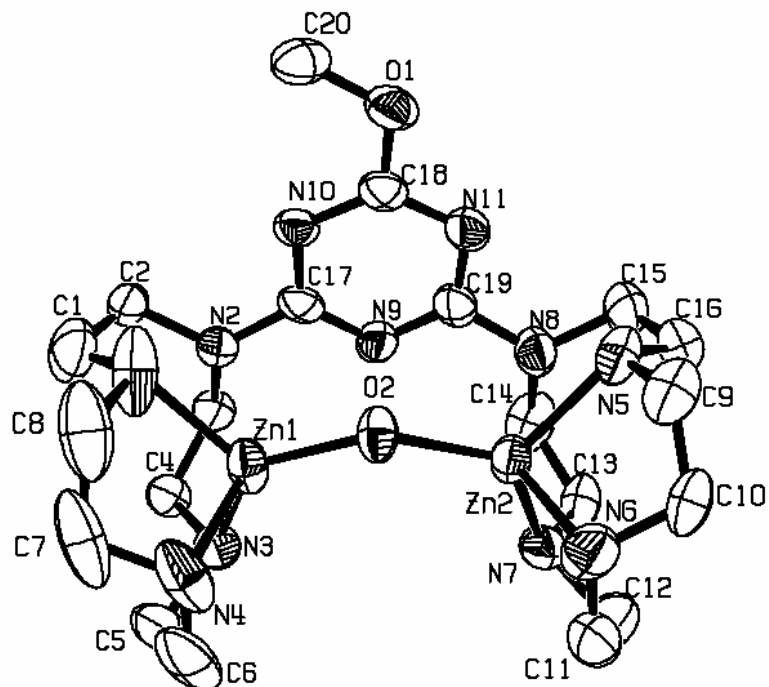


Figure 1. ORTEP drawing (50% probability ellipsoids) of $[\text{Zn}_2\text{L2}]\mu\text{-OH}(\text{ClO}_4)_3 \cdot \text{CH}_3\text{CN} \cdot \text{H}_2\text{O}$. All hydrogen atoms, three perchlorate anions, an acetonitrile atom and a water molecule are omitted for clarity.

Selected bond lengths and bond angles around the Zn(II) ions are presented in **Table 4**. Data collection parameters are given in the experimental part.

Bond distances, Å			
Zn(1)-O(2)	1.902(5)	Zn(2)-O(2)	1.909(5)
Zn(1)-N(1)	2.125(7)	Zn(2)-N(5)	2.101(6)
Zn(1)-N(3)	2.058(6)	Zn(2)-N(6)	2.074(8)
Zn(1)-N(4)	2.082(8)	Zn(2)-N(7)	2.036(6)
Bond angles, deg			
O(2)-Zn(1)-N(1)	113.9(3)	O(2)-Zn(2)-N(5)	117.2(2)
O(2)-Zn(1)-N(3)	125.4(2)	O(2)-Zn(2)-N(6)	113.9(3)
O(2)-Zn(1)-N(4)	110.9(3)	O(2)-Zn(2)-N(7)	122.2(2)

N(1)-Zn(1)-N(3)	117.9(3)	N(5)-Zn(2)-N(6)	85.7(3)
N(1)-Zn(1)-N(4)	88.2(3)	N(5)-Zn(2)-N(7)	117.2(2)
N(3)-Zn(1)-N(4)	87.0(3)	N(6)-Zn(2)-N(7)	88.1(3)
Distances Zn(1)-N(2), Zn(2)-N(8), Zn(1)-Zn(2), O(2)-N(9)			
Zn(1)-N(2)	2.592	Zn(2)-N(8)	2.663
O(2)-N(9)	3.002	Zn(1)-Zn(2)	3.602

^aESD in parentheses.

Table 4. Bond distances, bond angles and atomic distances for $[\text{Zn}_2\text{L2}]\mu\text{-OH}(\text{ClO}_4)_3 \cdot \text{CH}_3\text{CN} \cdot \text{H}_2\text{O}^{\text{a}}$.

Figure 1 shows the symmetrical structure and geometry of the Zn(II) complex. There is a OH^- bridge between the two Zn(II) ions, with equal distances Zn-O of 1.9 Å and parallel to the plane of the triazine spacer with a distance of 3 Å between the O-atom of the bridge and N(9) of triazine. Although the structure in solid state may not coincide with the situation in solution, it demonstrates the ability of the dinuclear complex of forming an OH^- -bridge, which may act as the active species in the hydrolysis of carboxyesters.

The distances between the Zn atom and three of the N atoms of cyclen are around 2.1 Å, as it is generally reported for the Zn-cyclen complex,^{5,8,31} but the distances to the aryl bound nitrogens N(2) and N(8) are 2.6 Å, which is too long to allow a bond. This longer distance is explained by the influence of the triazine, which withdraws as an electron-poor aromatic system electron density of cyclen nitrogen atom thus making coordination to the metal ion by this forth nitrogen atom less probable. Kimura et al. have shown a similar coordination pattern for two Zn cyclen complexes having dinitrobenzene³² and pyridine³³ as cyclen pendants. Each Zn(II) ion has a distorted tetrahedral geometry, coordinating to three N-atoms of cyclen and the apical O-atom of the OH^- bridge. In fact the coordination type, bond lengths and angles (especially those for Zn(1) and N(3), N(4), respectively Zn(2) and N(6), N(7)) of our complex resemble more to that of a $\text{Zn}[9]\text{aneN}_3$ ^{16c,34} complex, where the metal ion is coordinated by only three N atoms. The two metal ions are separated by 3.6 Å and the electrostatic interaction between them is shielded by the ionized hydroxo bridge. This distance is in the range (3.0-4.0 Å) observed for other related alkoxo-bridged dinuclear Zn(II) complexes^{17h,35} and for dinuclear Zn(II) cores of many metallohydrolases.^{2c}

1.2.4 Hydrolysis of 4-nitrophenyl acetate (NA) promoted by the mononuclear metal complexes.

The reaction rates of ester bond cleavage of 4-nitrophenyl acetate (NA) (0.003-2 mM) were measured by an initial slope method following the increase in 400 nm-absorption of 4-nitrophenolate in 10% (v/v) CH₃CN aqueous solution in the pH range 6.5-9.5 (50 mM HEPES, TRIS or CHES buffer, *I* = 0.1 M, NaCl) at 25 °C. The reactions were corrected for the degree of ionization of the 4-nitrophenol at the respective pH and temperature. The absorption increase was recorded immediately after mixing and then monitored generally until maximum 5% formation of 4-nitrophenolate. Correction for the spontaneous hydrolysis of the substrate by the solvent was accomplished either by directly measuring a difference between the production of 4-nitrophenolate in the reaction cell and a reference cell containing the same concentration of carboxyester as in the reaction cell in absence of metal complex, or by calculating the general rate of spontaneous hydrolysis in the pH range 7 to 8.5 for NA and subtracting it from the measured rate of hydrolysis. The calculation of the general rate of spontaneous hydrolysis for NA is presented in the experimental part. The second-order dependence of the rate constant k_{cat} on the concentration of NA and metal complex fits to the kinetic equation (1).

$$v_{cat} = k_{cat} [M-L] [NA] \quad (1)$$

In equation (1) k_{cat} is the observed NA hydrolysis rate caused by the metal complex, which was derived by subtraction of the solvent-promoted NA spontaneous hydrolysis rate from the total observed NA hydrolysis rate.

$$v = v_{cat} + v_{spontaneous\ hydrolysis} = k_{obs} [NA] = (k_{cat} [M-L] + k_{OH} [OH^-] + k_0) [NA]$$

The k_{OH} value is a second-order rate constant describing the nucleophilic attack of the OH⁻ ions. The k_0 value is a first-order constant describing the solvolysis of the ester due to solvent molecules (e.g. water or organic additives).

The reactions were carried out under pseudo-first-order conditions with an excess of metal complex over NA,^{24b,36} where the rate constants k_{obs} (s⁻¹) were obtained by an initial slope method ([produced 4-nitrophenolate]/time) using the log e values (experimentally determined, see supplementary information). A plot of k_{obs} versus the metal complex concentration at a given pH gave a straight line, the slope of this line being the second-order rate constant k_{cat} (M⁻¹s⁻¹).

CuL1 showed poor solubility under the given experimental conditions and could therefore not be used for the hydrolysis experiments. A change in solvent or an increase in temperature would have made the measurements possible, but prevents a meaningful comparison of

reactivity. **NiL1** did not show a significant effect on the hydrolysis (k_{obs} values in the range of 10^{-7} to 10^{-6} s^{-1}), a fact easily explained by the percentage of active species in solution, which is in the order of 0.0069 for pH 7, 0.069 for pH 8 and 0.69 for pH 9. It is obvious that at these pH values the rate of hydrolysis is very small, but at higher pH values the spontaneous hydrolysis of the substrates would be the predominant reaction taking place.

Kimura et al. have shown for the hydrolysis of NA with various $\text{Zn}[12]\text{aneN}_3$ and $\text{Zn}[12]\text{aneN}_4$ complexes that the active nucleophilic species attacking the ester is in fact the Zn-L-OH^- species.^{5a,9,36} The total concentration of the mononuclear metal complexes is composed of the following species, depending on the pH and the respective $\text{p}K_a$ value:

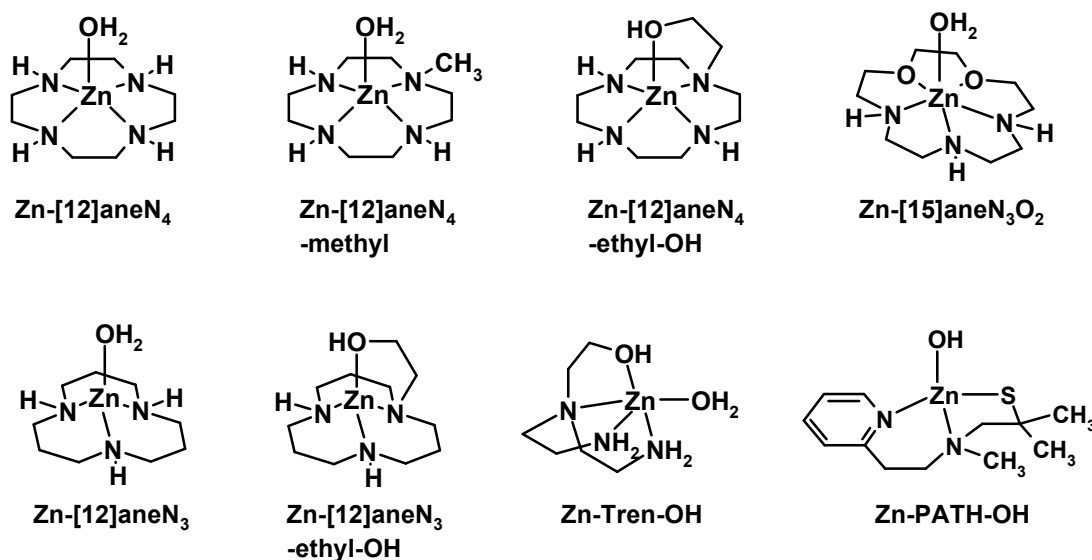
$$[\text{M-L}] = [\text{M-L-OH}_2] + [\text{M-L-OH}^-]$$

Thus equation (1) can be written as follows:

$$v_{\text{cat}} = k_{\text{NA}} [\text{M-L-OH}^-] \quad (2) \quad \text{with } k_{\text{NA}} = \frac{[\text{M-L}] k_{\text{cat}}}{[\text{M-L-OH}^-]}$$

By using the pH independent second-order reaction rate constant $k_{\text{NA}} (\text{M}^{-1} \text{s}^{-1})$ instead of the pH dependent second-order reaction rate constant $k_{\text{cat}} (\text{M}^{-1} \text{s}^{-1})$, we are able to compare the results of this work with previous works from literature. Reciprocally, starting from reported values of k_{NA} for other macrocyclic metal complexes their k_{cat} values for pH 7 and 8 can be calculated. In this way an indirect comparison between our results and previous work is possible and the effect of the reaction conditions becomes observable.

The structures of the most efficient previously studied mononuclear metal complexes are depicted in **Scheme 8** and their reported second-order reaction rates k_{cat} and k_{NA} are presented in **Table 5**, together with the hydrolysis rate constants of two carbonic anhydrases.



Scheme 8. Structures of previously studied mononuclear Zn(II) complexes

Metal complex	$10^2 k_{\text{NA}}$ ($\text{M}^{-1}\text{s}^{-1}$)	$10^2 k_{\text{cat}}$ ($\text{M}^{-1}\text{s}^{-1}$) (pH 7)	$10^2 k_{\text{cat}}$ ($\text{M}^{-1}\text{s}^{-1}$) (pH 8)	reaction conditions ^a	pK _a	Lit.
Zn-[12]aneN ₃	4.1	---	---	50 mM HEPES buffer, pH 8.2	7.2	38c
Zn-[12]aneN ₃	3.6 ± 0.3	1.4	3.1	20 mM CHES buffer pH 9.3	7.2	38d
Zn-[12]aneN ₃ - ethyl-OH	14 ± 1	4.0	11.2		7.4	38d
Zn-[12]aneN ₄	11 ± 2	1.1	5.6	20 to 50 mM CHES buffer, pH 9.2	7.9	38b 9
Zn-[12]aneN ₄ ^b	9.6 ± 0.1	1.063	5.38	50 mM Tris/HCl buffer	8.06	-
Zn-[12]aneN ₄ - ethyl-OH	46 ± 1	7.7	30.6	20 mM CHES buffer pH 9.3	7.7	5a
Zn-[12]aneN ₄ - methyl	4.9 ± 0.1	---	---		7.68	5a
Zn-[15]aneN ₃ - O ₂	60 ± 6	---	---	50 mM buffer, pH 7-9.5	8.8	37
Zn-Tren-OH	13 ± 1	---	---	20 mM Tris/HCl buffer, pH 8-9	7.74 ^c (9.78) ^d	38
Zn-PATH-OH	89 ± 0.3	---	---	20 mM buffer, pH 7-9.5	8.05	39
Carbonic anhydrase (CA II)	250.000 ± 20.000	---	---	50 mM buffer, pH = 6.8-9.6	6.8	40
His94Cys (CAII)	11.700 ± 2000	---	---		≥ 9.5	42

^a at T = 25 °C and 10 % CH₃CN. ^b this work. ^c pK_a value of Zn-ROH. ^d pK_a value of Zn-OH₂.

Table 5. A comparison of hydrolysis rate constants k_{NA} ($\text{M}^{-1}\text{s}^{-1}$) and k_{cat} ($\text{M}^{-1}\text{s}^{-1}$) for previously reported mononuclear metal complexes.

The k_{NA} value determined by us for **Zn[12]aneN₄** in the TRIS/HCl buffer system is about 10% lower than the one determined by Kimura for the CHES buffer system, which is a good agreement under the given error margins. The measured rate constant of **Zn[12]aneN₄** will be used for further analysis.

A comparison of hydrolysis rate constants for the new mononuclear metal complexes is presented in table **Table 6**.

Complex ^a	10 ² k_{cat} (M ⁻¹ s ⁻¹) pH 7	10 ² k_{cat} (M ⁻¹ s ⁻¹) pH 8	10 ² k_{NA} (M ⁻¹ s ⁻¹)
Zn[12]aneN ₄	1.06 ± 0.03	5.38 ± 0.05	9.57 ± 0.06
ZnL1	1.68 ± 0.02	12.01 ± 0.03	39.08 ± 0.1
ZnL3	1.39 ± 0.03	9.61 ± 0.02	27.91 ± 0.02
ZnL8	6.03 ± 0.05	25.29 ± 0.03	38.63 ± 0.02

^a determined with [complex] = 0.01-1.3 mM and [NA] = 0.03-2 mM.

Table 6: A comparison of hydrolysis rate constants, k_{cat} (M⁻¹s⁻¹) and k_{NA} (M⁻¹s⁻¹), for the mononuclear metal complexes at 25 °C in 10% (v/v) CH₃CN.

An example of a plot of k_{obs} vs Zn(II) complex concentration is presented in the experimental part.

In order to get a better insight, the hydrolysis of NA promoted by **ZnL3** and **ZnL8** in the pH range 6.5 to 9.5 was measured. For these experiments the spontaneous hydrolysis of the substrate was corrected by directly measuring a difference between the production of 4-nitrophenolate in the reaction cell and a reference cell containing only carboxyester in the same concentration as in the reaction cell. Therefore no information about the value of k_{OH} is available. The derived sigmoidal pH-rate profiles (**Figure 2**) are characteristic of a kinetic process controlled by an acid-base equilibrium and exhibit inflection points corresponding to the $\text{p}K_{\text{a}}$ values of the coordinated water molecules of **ZnL3** ($\text{p}K_{\text{a}} = 8.28$) and **ZnL8** ($\text{p}K_{\text{a}} = 7.89$). Therefore, the reactive species is concluded to be the Zn(II)-OH⁻ complex, in which the Zn(II)-bound OH⁻ acts as a nucleophile to attack intermolecularly the carbonyl group of the acetate ester and hydrolyse thus 4-nitrophenyl acetate to 4-nitrophenolate and acetate. This mechanism of NA hydrolysis has also been reported for other Zn(II) cyclen complexes.^{9,38b}

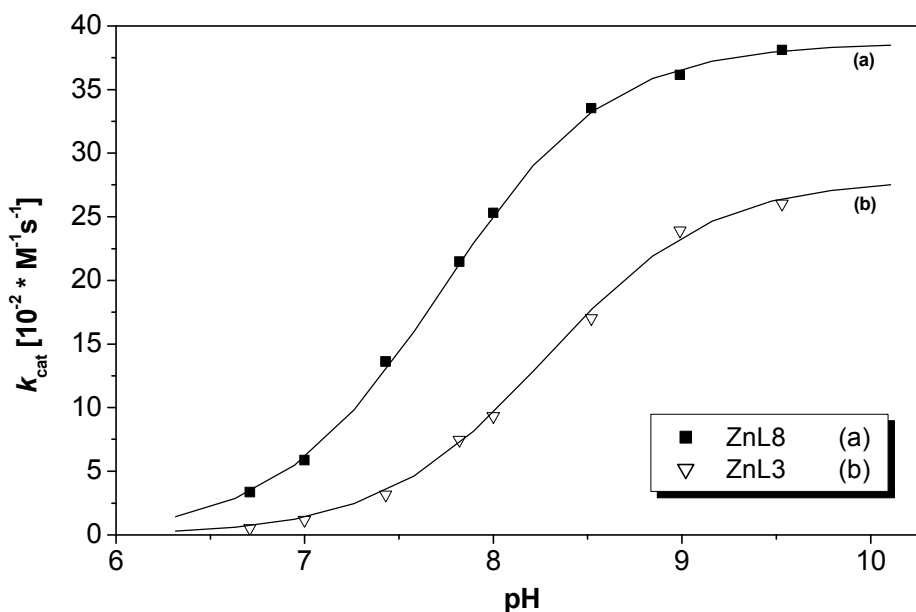


Figure 2. pH-Rate profile for the second-order rate constants of NA hydrolysis of **ZnL3** and **ZnL8** at 25 °C and $I = 0.10$ (NaCl) in 10% (v/v) CH₃CN.

The k_{NA} values of our Zn(II) cyclen complexes show a 3 to 4-fold higher hydrolysis rate than the simple Zn[12]aneN₄ system due to the aromatic substituent. π - π interactions of the heterocycle with the aromatic ring of the 4-nitrophenyl acetate may lead to a tighter binding and provides a more hydrophobic environment³⁴ with less solvation, and therefore a higher reactivity of the hydroxy species. Tang et al. previously reported on the influence of an aromatic substituent, emphasizing on its positive influence on the substrate orientation and stabilisation of the leaving group in the transition state.⁴¹

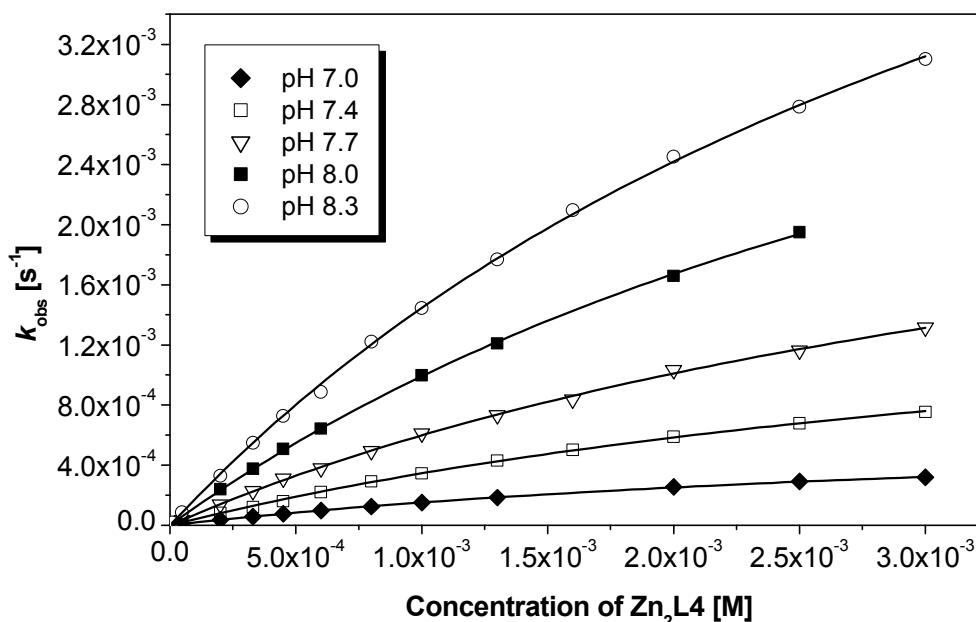
Among the mononuclear Zn complexes **ZnL8** has the highest hydrolytic activity. Due to its smaller $\text{p}K_a$ value it has a higher percentage of catalytically active species at lower pH values. The lower reaction rate of **ZnL3** may be explained due to the bulky azacrown ether in the *ortho* position.

Several conclusions can be drawn from the comparison of our complexes with previously reported catalysts. First, Zn[12]aneN₄ complexes show higher reaction rates than Zn[12]aneN₃ derivatives. For the latter complexes the metal ion is coordinated by only 3 nitrogen atoms, therefore the electron deficiency of the Zn(II) ion is less saturated leading to a higher Lewis acidic character of the metal ion, but also to a lower nucleophilic character of the Zn-L-OH⁻ species. The complexes with an ethylhydroxyl pendant arm show a higher hydrolytic activity, but operate by a different reaction mechanism with the alcoholate as reactive species and a transacylation reaction step. Among the previously reported complexes, Zn-[15]aneN₃-O₂ reported by Bencini et al. has the highest reaction rate (0.6 M⁻¹s⁻¹),

comparable to the k_{NA} value of **ZnL8** and **ZnL1** ($0.4 \text{ M}^{-1}\text{s}^{-1}$). However, these reaction rates are still far from those of natural enzymes, as given in **Table 5**.

Due to the chosen reaction conditions the metal complexes cannot act catalytically. Therefore an experiment with a catalytic amount of metal complex (ratio NA to **ZnL8** is of 30:1, $[\text{NA}] = 0.2 \text{ mM}$, $[\text{ZnL8}] = 0.007 \text{ mM}$) at pH 8 (50 mM TRIS/HCl buffer, 25°C , $I = 0.1$, NaCl) was performed and the reaction was followed for nine hours. After this reaction time a concentration of 0.0107 mM of 4-nitrophenolate was recorded, corresponding to a turnover of 151%, thus indicating the catalytic properties of the metal complexes for the hydrolysis of carboxyesters.

1.2.5 Hydrolysis of 4-nitrophenyl acetate (NA) promoted by the dinuclear metal complexes $\text{Zn}_2\text{L2}$, $\text{Zn}_2\text{L4}$ and $\text{Zn}_2\text{L5}$. The ester bond cleavage rates were measured in 10% (v/v) CH_3CN aqueous solution in the pH range 7-8.3 (50 mM TRIS/HCl buffer, $I = 0.1 \text{ M}$, NaCl) at 25°C . The concentrations of complex varied in the range $0.005\text{--}3 \text{ mM}$, those of NA in the range $0.003\text{--}2 \text{ mM}$. In contrast to the mononuclear complexes, here the plots of k_{obs} versus the metal complex concentration at a given pH did not give a straight line, but a curve, due to saturation kinetics at higher complex concentrations (**Figure 3**). The plots for the other two complexes are presented in the experimental part.



^a 50 mM TRIS/HCl buffer, 10 % CH_3CN , $I = 0.1 \text{ M}$ (NaCl), 25°C , $[\text{NA}] = 1.0 - 4.0 \cdot 10^{-5} \text{ M}$, $\Delta \text{pH} = \pm 0.01$, $\Delta k_{\text{obs}} \pm 0.5 - 2.9 \%$

Figure 3: Saturation kinetics for **$\text{Zn}_2\text{L4}$** ^a

This is typical for a *Michaelis-Menten* reaction mechanism, where an intermediate substrate-catalyst adduct is formed which then breaks down to release catalyst and reaction product.⁴² But unlike the classical *Michaelis-Menten* reaction, here the metal complex is the reaction partner present in excess, due to the necessary experimental conditions, also emphasized for other complexes of this type.^{16c,24b,36,43} Therefore the reaction order for the complex concentration is lower than one. The model for the calculation of the maximum reaction rate k'_{cat} (s^{-1}), of the apparent association constant for the ester-metal complex-adduct and of the second-order rate constant $k'_{\text{cat}}/K_{\text{M}}$ ($\text{M}^{-1}\text{s}^{-1}$) was established on the basis of previously reported models.⁴⁴

The total rate of reaction v at a constant pH is the sum of the spontaneous hydrolysis and of the metal catalysed hydrolysis.⁴⁵

$$v = \frac{d(\text{Abs})}{d(t) \epsilon_{\text{obs}}} = k'_{\text{obs}} ([\text{NA}] + [\text{Zn}_2\text{-L-NA}]) = k_{\text{spontaneous}} [\text{NA}] + k'_{\text{cat}} [\text{Zn}_2\text{-L-NA}] \quad (3)$$

For saturation kinetics the concentration of metal complex forming the substrate-catalyst adduct, $[\text{Zn}_2\text{-L-NA}]$, is the most important. The relationship between this value and the total amount of metal complex $[\text{Zn}_2\text{-L}]$ is expressed in equation (4):

$$\text{Zn}_2\text{-L} + \text{NA} \rightleftharpoons \text{Zn}_2\text{-L-NA} \quad K_{\text{A}} = \frac{[\text{Zn}_2\text{-L-NA}]}{[\text{Zn}_2\text{-L}] [\text{NA}]} \quad \text{with: } K_{\text{M}} = K_{\text{A}}^{-1} \quad (4)$$

The K_{M} , respectively the K_{A} values correspond to the apparent association constant for the ester-metal complex-adduct.

By extrapolation we obtain equation (5):

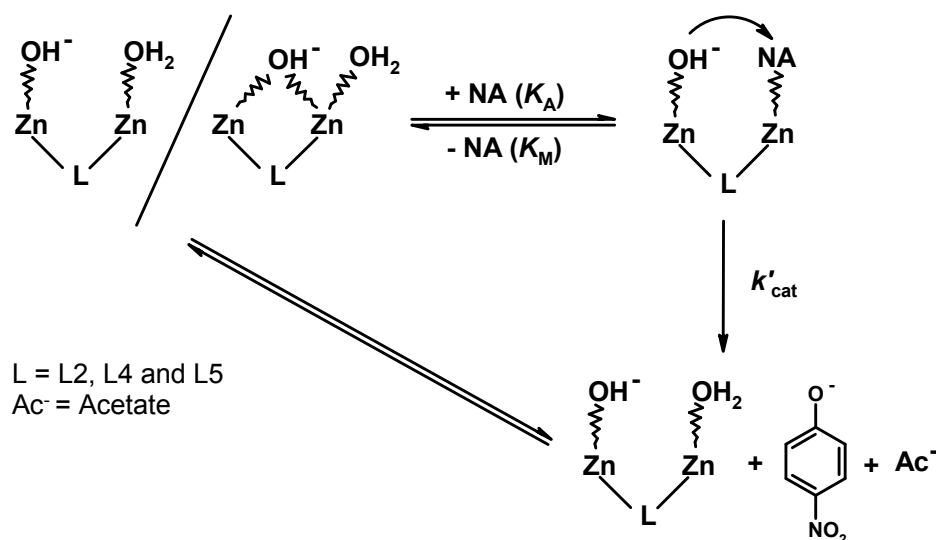
$$k'_{\text{obs}} = \frac{K_{\text{M}} k_{\text{spontaneous}} + k'_{\text{cat}} [\text{Zn-L}]}{K_{\text{M}} + [\text{Zn-L}]} = \frac{K_{\text{M}} k_{\text{spontaneous}}}{K_{\text{M}} + [\text{Zn-L}]} + \frac{k'_{\text{cat}} [\text{Zn-L}]}{K_{\text{M}} + [\text{Zn-L}]} \quad (5)$$

By subtracting from the k'_{obs} value the value of the spontaneous hydrolysis, equation (5) can be written as follows:

$$k_{\text{obs}} = \frac{k'_{\text{cat}} [\text{Zn-L}]}{K_{\text{M}} + [\text{Zn-L}]} \quad \text{with: } k_{\text{obs}} = k'_{\text{obs}} - k_{\text{spontaneous}} \quad (6)$$

The curves in **Figure 3** were obtained by a non-linear fit of equation (6). The values of the apparent pH independent *Michaelis-Menten* constants K_{M} (M) are of 3.86 M, 4.34 M and 4.2 M for **Zn₂L2**, **Zn₂L4**, respectively **Zn₂L5**. From these values the apparent binding constant K_{A} (M^{-1}) for the three complexes can be derived, $0.23 \pm 0.02 \text{ M}^{-1}$. The pH independent k_{NA} values are extrapolated from the second-order reaction rate constants k_{cat} defined as $k'_{\text{cat}}/K_{\text{M}}$. For these calculations we assume the monohydroxy species $\text{Zn}_2\text{-L-(OH}_2\text{)(OH}^-)$ to be the

catalytically active species, as the bishydroxy form $\text{Zn}_2\text{-L-(OH)}_2$ is present in very low concentration for this pH range (at pH 8.3 <3%). Consequently, the values of k_{NA} are of $4.1 \pm 0.27 \text{ M}^{-1}\text{s}^{-1}$, $3.1 \pm 0.19 \text{ M}^{-1}\text{s}^{-1}$ and $4.4 \pm 0.31 \text{ M}^{-1}\text{s}^{-1}$ for **Zn₂L2**, **Zn₂L4**, respectively **Zn₂L5**. The $\text{p}K_{\text{a}}$ value can be also determined kinetically (see also equation (4) in the experimental part).^{16c} The obtained $\text{p}K_{\text{a}}$ values of 8.09 ± 0.17 , 8.17 ± 0.16 and 8.37 ± 0.19 for **Zn₂L2**, **Zn₂L4**, respectively **Zn₂L5**⁴⁶ correspond within the error margin to the $\text{p}K_{\text{a1}}$ values determined by potentiometric titrations. Therefore the reactive species is in this case the monohydroxy species $\text{Zn}_2\text{-L-(OH)}_2(\text{OH}^-)$ in its opened form. The intramolecular reaction mechanism is pictured in **Scheme 9**.



Scheme 9. Proposed associative reaction mechanism for the hydrolysis of **NA** by **Zn₂L2**, **Zn₂L4** and **Zn₂L5**

The monohydroxy species (opened and/or closed structure) forms a substrate-catalyst adduct, whereby the ester is displacing a water molecule. Most likely the ester is coordinating to the metal center through its carbonyl group. The opened form is more suitable for the coordination of the substrate. Once the hydrolytically relevant species is formed, the intramolecular nucleophilic attack takes place. This attack is facilitated by the additional activation of the ester through its coordination to the metal. A product inhibition study of **Zn₂L2** and **Zn₂L4** with 4-nitrophenolate showed no binding affinity. The same mechanism was reported for the hydrolysis of **NA** with other **Zn(II)** complexes of this type.^{10c,46,47}

Zn₂L2 and **Zn₂L5** have almost the same catalytic activity, while **Zn₂L4** is about 25% less efficient, due to the aforementioned steric factors. The dinuclear complexes are cleaving the ester about 10 times faster than their mononuclear analogues and about 30 to 44 times faster

than the Zn[12]aneN₄ complex. This high acceleration rates indicate a cooperation of the two metal centers and supports the proposed mechanism presented in **Scheme 9**.

1.2.6 Hydrolysis of 4-nitrophenyl acetate (NA) promoted by the dinuclear metal complexes Cu₂L2, Ni₂L2, Zn₂L6 and Zn₂L7. The ester bond cleavage rates were measured in 10% (v/v) CH₃CN aqueous solution in the pH range 6-9.5 (50 mM TRIS/HCl buffer, HEPES, CHES *I* = 0.1 M, NaCl) at 25 °C under pseudo-first order rate reaction conditions (excess of metal complex).

The reaction rate is proportional to the concentrations of the metal complex and the substrate, such that equation (7) can be postulated, from which equation (8) is then easily derived.

$$v_{\text{cat}} = k_{\text{cat}} [\text{Zn-L}]^{\text{Total}} [\text{NA}] \quad (7)$$

$$v_{\text{cat}} = \frac{d(\text{Abs})}{d(t) \epsilon_{\text{obs}}} = k_{\text{obs } 1, 2} [\text{NA}] = k_{\text{cat } 1, 2} [\text{Zn-L}]^{\text{Total}} [\text{NA}] \quad (8)$$

The reaction rate v_{cat} reflects in this case the contribution of two reactive species, the monohydroxy and the dihydroxy species. Therefore equation (8) can be interpolated to equation (9).

$$k_{\text{cat } 1, 2} [\text{Zn-L}]^{\text{Total}} = k_{\text{cat } 1} [\text{Zn}_2\text{-L-(OH}_2\text{)(OH}^-)] + k_{\text{cat } 2} [\text{Zn}_2\text{-L-(OH}^-)_2] \quad (9)$$

For **Ni₂L2**, low hydrolysis rates (k_{obs} in the range of 10^{-6} s^{-1}) were obtained due to the weak Lewis acidic character of the metal ion reflected in the high pK_a values of the complex (9.74 and 10.13). Therefore at physiological pH there is no active species present in solution. For the measurement with this complex, as well as with **Cu₂L2**, difficulties were encountered when measuring the hydrolysis rates under the chosen reaction conditions. The concentration range needed for these complexes in order to have a stable baseline and acceptable experimental errors required low concentrations of metal complex, which led to low concentrations of substrate in order to have $C_0 \gg S_0$, reaching the detection limits of the apparatus. Together with long induction periods for **Cu₂L2**, for which we do not yet have a rational explanation, the kinetic measurements remain difficult to interpret. To the best of our knowledge no Cu(II) or Ni(II) cyclen complexes promoting the hydrolysis of a carboxyester are reported, while phosphate ester hydrolysis was reported for Cu[9]aneN3 complexes⁴⁸ and Ni(II) complexes.²³ However, a successful carboxyester hydrolysis promoted by **Ni₂L2** is clearly not possible in the pH range 7 to 9 due to the low Lewis acidity of the metal, and most improbable for the **Cu₂L2** complex, due to the fact that the two metal centers do not act cooperatively (as indicated by the small difference between the two pK_a values) and that each

Cu(II) cation has only one available coordination site, making it impossible to bind both substrate and hydroxide on the same metal ion. Morrow et al.⁴⁹ and Burstyn et al.^{14a} have demonstrated that artificial metallohydrolases (mono- as well as dinuclear metal complexes) must possess two cis-oriented labile coordination sites in order to bind both substrate and nucleophile, which is not the case for **Cu₂L2**.

For **Zn₂L7** the difference between its pK_a values is too small to allow a separate study of the influence of the monohydroxy and dihydroxy species, as for **Zn₂L6** or for previous reported compounds.^{24a,37,43,50} From the plots of $k_{\text{obs}1,2}$ versus the metal complex concentration at a given pH the $k_{\text{cat}1,2}$ values for **Zn₂L7** were obtained. The pH-rate profile is presented in **Figure 4**. For pH <6 no hydrolytic activity is measurable, therefore both species are active species. For pH >10, only the dihydroxy species Zn₂-L-(OH)₂ is present in solution, hence $k_{\text{cat}1,2}$ is in this case equal to $k_{\text{cat}2}$.

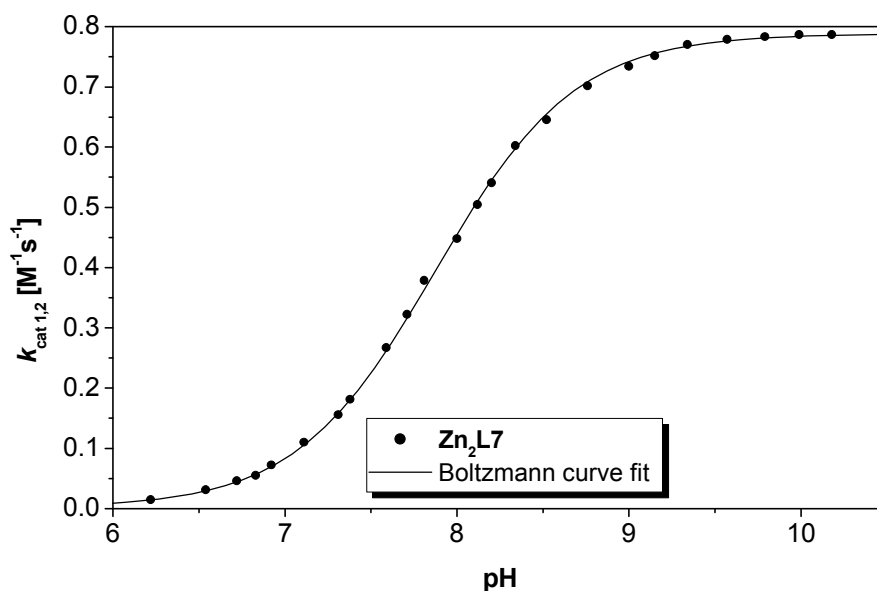


Figure 4. pH-rate profile for the second-order rate constants of NA hydrolysis of **Zn₂L7** at 25 °C and $I = 0.10$ (NaCl) in 10% (v/v) CH₃CN.

From the species distribution diagram and the experimentally determined $k_{\text{cat}1,2}$ values it is possible to derive the values of $k_{\text{cat}1}$ and $k_{\text{cat}2}$ from calculations⁵¹ (**Figure 5**; for more details see **Figures 22** and **23** of the experimental part).

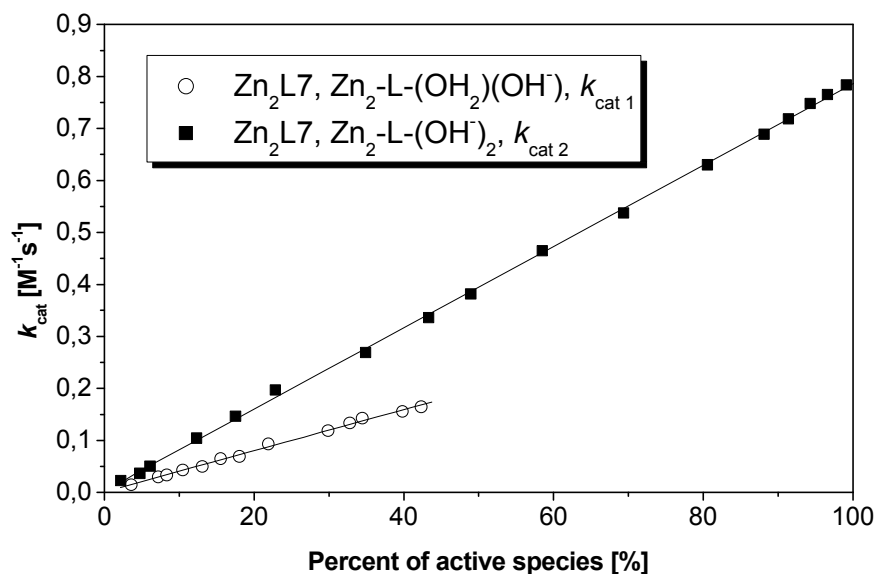


Figure 5. Deduction of $k_{cat 1}$ and $k_{cat 2}$ from the values of $k_{cat 1,2}$ for **Zn₂L7**.

Once the pH-dependent $k_{cat 1}$ and $k_{cat 2}$ values are known, the k_{NA} values can be easily derived. The values of $k_{NA 1}$ and $k_{NA 2}$ for **Zn₂L7**, corresponding to the monohydroxy species $Zn_2-L-(OH_2)(OH^-)$, respectively the dihydroxy species $Zn_2-L-(OH^-)_2$, are $0.40 \pm 0.007 M^{-1}s^{-1}$, respectively $0.78 \pm 0.006 M^{-1}s^{-1}$. A comparison of these values with those of the mononuclear complexes shows that the k_{NA} values of **ZnL1** and **ZnL8** are almost identical to the $k_{NA 1}$ value and that the value of $k_{NA 2}$ is 2 times higher than that of the mononuclear complexes. Hence, it seems that for **Zn₂L7** the two metal centres are acting independently in the hydrolysis of 4-nitrophenolate.

The same calculations based on equation (8) were performed for **Zn₂L6**. The pH-rate profile (**Figure 6**) has a sigmoidal shape with the velocity of reaction tending to zero for lower pH values and reaching a maximum for high pH values.

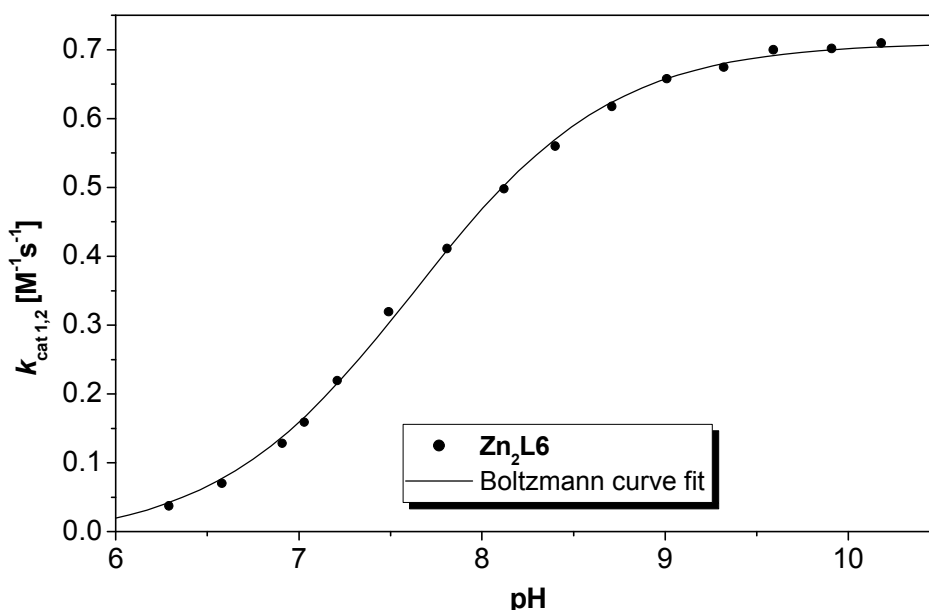


Figure 6. pH-rate profile for the second-order rate constants of NA hydrolysis of **Zn₂L6** at 25 °C and $I = 0.10$ (NaCl) in 10% (v/v) CH₃CN.

The pK_a values of **Zn₂L6** are more differentiated, permitting thus a better separation of the two reactive species and of their second-order reaction rate constants $k_{cat\ 1}$ and $k_{cat\ 2}$. For pH values below 7 the amount of dihydroxy species present in solution is less than 0.5 %, hence the $k_{cat\ 1,2}$ value corresponds in this range to the $k_{cat\ 1}$ value. For the remaining pH range we used the same calculation method as for **Zn₂L7** (Figure 7).

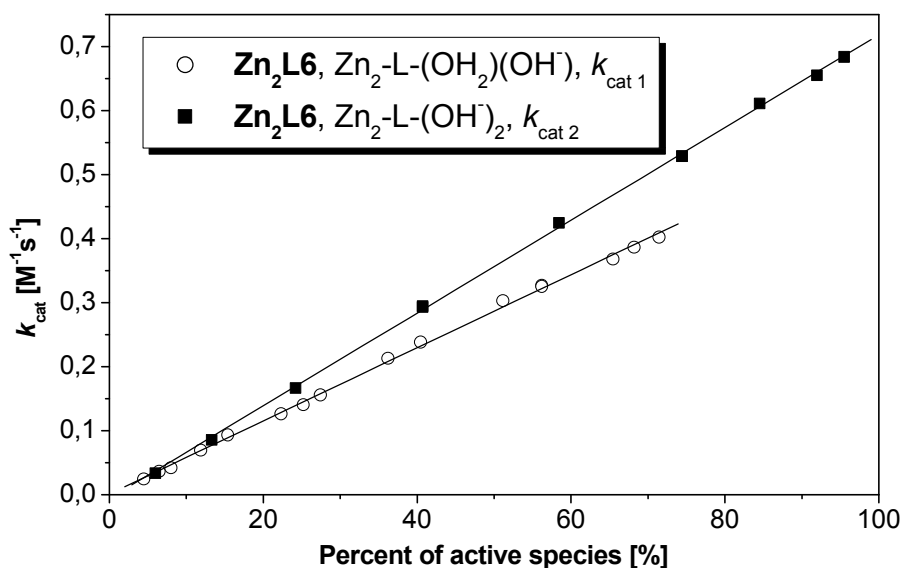
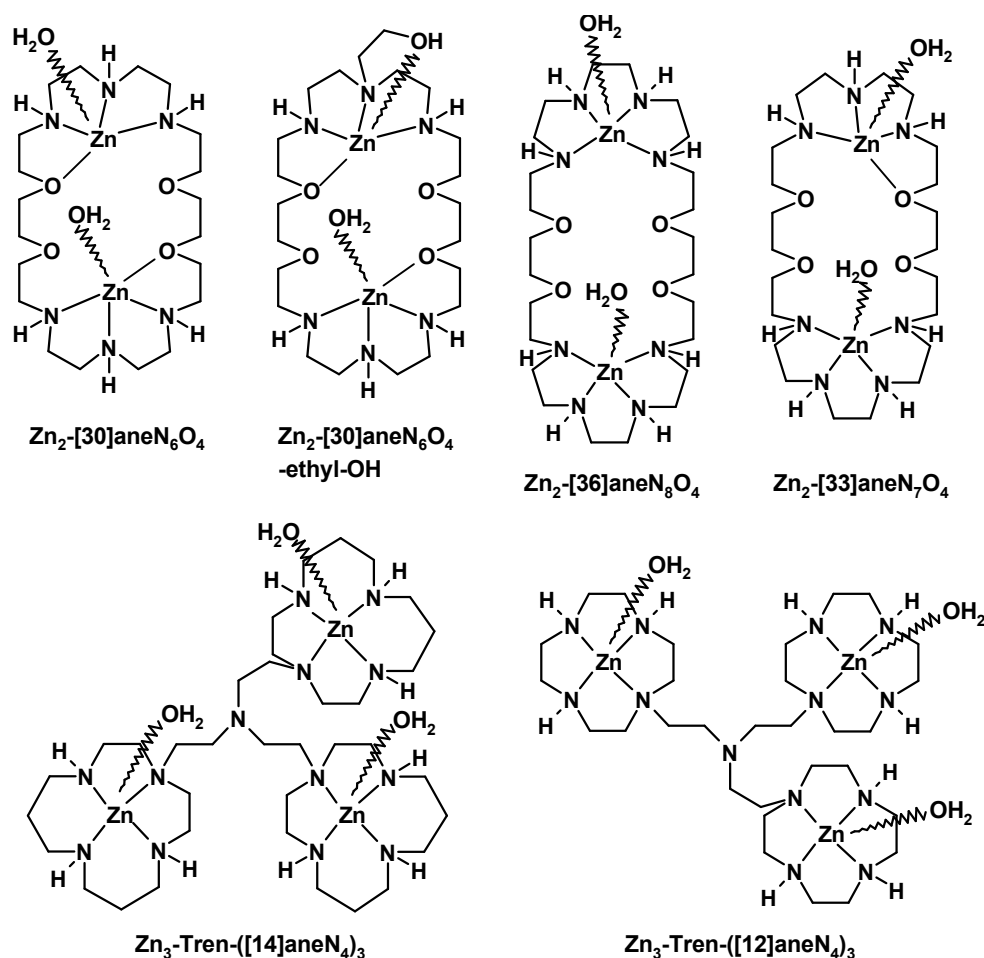


Figure 7. Deduction of $k_{cat\ 1}$ and $k_{cat\ 2}$ from the values of $k_{cat\ 1,2}$ for **Zn₂L6**.

The values of $k_{NA\ 1}$ and $k_{NA\ 2}$ for **Zn₂L6** are $0.57 \pm 0.003\ M^{-1}s^{-1}$, respectively $0.72 \pm 0.004\ M^{-1}s^{-1}$. A comparison of the reaction rates of **Zn₂L6**, **Zn₂L7** and **ZnL8** show the

monohydroxy species of **Zn₂L6** possessing a 45% higher rate than the others, whereas the monohydroxy species of **Zn₂L7** is in the same range to that of **ZnL8**. Moreover, the rate of the dihydroxy species of **Zn₂L6** is about 10% lower than the rate of **Zn₂L7**. These facts indicate a different behaviour of the metal centres. Actually, the mechanism of hydrolysis for **Zn₂L6** seems to be a hybrid between the one postulated for the aryl-bridged **Zn₂L5** (cooperation of the metal centres, intramolecular nucleophilic attack) and the one established for the triaryl-bridged **Zn₂L7** (independence of the metal centres, intermolecular nucleophilic attack). Indeed, the experimental data for the diaryl-bridged **Zn₂L6** could be also fitted to the saturation kinetics model with similar regression coefficients.⁵² We conclude that the mechanism of reaction is defined by the degree of cooperation between the metal centres, influenced by the spacer length.

The structures of the most efficient previously reported di- and trinuclear metal complexes are depicted in **Scheme 10** and their reported second-order reaction rates k_{NA} and $\text{p}K_{\text{a}}$ values are presented in **Table 7**.



^a Charges and counter-ions are omitted for clarity reasons.

Scheme 10. Structure of previously studied di- and trinuclear Zn(II) complexes for the hydrolysis of NA^a .

Complex / Nucleophile	$10^2 k_{\text{NA}} (\text{M}^{-1}\text{s}^{-1})^a$	$\text{p}K_{\text{a}}^b$	Lit.
$\text{Zn}_2\text{-[30]aneN}_6\text{O}_4 / \text{Zn}_2\text{-(OH}^-)$	9.4 ± 0.1	7.6	39
$\text{Zn}_2\text{-[30]aneN}_6\text{O}_4 / \text{Zn}_2\text{-(OH}^-)_2$	130 ± 10	9.2	39
$\text{Zn}_2\text{-[30]aneN}_6\text{O}_4\text{-ethyl-OH} / \text{Zn}_2\text{-(ethyl-OH}^-)$	21 ± 2	6.9	37
$\text{Zn}_2\text{-[30]aneN}_6\text{O}_4\text{-ethyl-OH} / \text{Zn}_2\text{-(ethyl-OH}^-)(\text{OH}^-)$	160 ± 10	8.5	37
$\text{Zn}_2\text{-[36]aneN}_8\text{O}_4 / \text{Zn}_2\text{-(OH}^-)$	35 ± 4	7.9	⁵³
$\text{Zn}_2\text{-[36]aneN}_8\text{O}_4 / \text{Zn}_2\text{-(OH}^-)_2$	350 ± 30	9.4	53
$\text{Zn}_2\text{-[33]aneN}_7\text{O}_4 / \text{Zn}_2\text{-(OH}^-)$	16 ± 2	7.5	53
$\text{Zn}_2\text{-[33]aneN}_7\text{O}_4 / \text{Zn}_2\text{-(OH}^-)_2$	200 ± 20	9.1	53
$\text{Zn}_3\text{-Tren-([14]aneN}_4)_3 / \text{Zn}_3\text{-(OH}^-)_2^c$	34 ± 4	8.1	51
$\text{Zn}_3\text{-Tren-([14]aneN}_4)_3 / \text{Zn}_3\text{-(OH}^-)_3$	370 ± 40	8.9	51
$\text{Zn}_3\text{-Tren-([12]aneN}_4)_3 / \text{Zn}_3\text{-(OH}^-)_2^c$	56 ± 6	8.6	51
$\text{Zn}_3\text{-Tren-([12]aneN}_4)_3 / \text{Zn}_3\text{-(OH}^-)_3$	420 ± 40	9.7	51

^a various buffer systems [50 mM], 10 % CH_3CN , $I = 0.1 - 0.15 \text{ M}$ (NaCl or NMe_4NO_3), 25°C . ^b 25°C , water, the first decimal was rounded up. ^c $\text{p}K_{\text{a}}$ and k_{NA} values of the monohydroxy species were not determined due to their negligible effect on the hydrolysis.

Table 7: A comparison of hydrolysis rate constants, $k_{\text{NA}} (\text{M}^{-1}\text{s}^{-1})$ and $\text{p}K_{\text{a}}$ values for previously reported di- and trinuclear Zn(II) metal complexes.

For all the reported complexes a bimolecular mechanism is postulated, with the coordinated hydroxide acting as the nucleophile. For the complexes with a pendant arm another mechanism is valid and has already been described for the mononuclear complexes. The metal centres in these complexes are not rigidly bound, as it is the case for the here reported compounds. This leads to much lower hydrolysis rates of the monohydroxy species compared to the bishydroxy species, due to intramolecular folding leading to steric hindrance. Hence, a rigid structure is advantageous for the hydrolytic efficiency of the complex.

The monohydroxy species of **Zn₂L6** and **Zn₂L7** hydrolyse NA 1.5 to 5.5 times faster than the complexes in **Table 7**, while **Zn₂L2**, **Zn₂L4** and **Zn₂L5** are about in the same range as the $\text{Zn}_3\text{-Tren-([12]aneN}_4)_3$ complex. Overall, our complexes are in the same range with previously reported similar compounds, but have a higher hydrolytic activity at physiological pH values (e.g. **Zn₂L2** has at pH 8.3 $k_{\text{cat}} > 2 \text{ M}^{-1}\text{s}^{-1}$, a value which for $\text{Zn}_3\text{-Tren-([12]aneN}_4)_3$ is reached only at pH >10).⁵¹ Therefore, the complexes reported in this paper are better suited for the hydrolysis of esters under physiological conditions.

The catalytic property of all dinuclear Zn(II) complexes was tested by performing experiments with an excess amount of 4-nitrophenyl acetate ($[NA] = 1-2 \text{ mM}$, $[metal \text{ complex}] = 0.005-0.01 \text{ mM}$) in the pH range 6.7 to 7.1 (50 mM HEPES buffer, 25 °C, $I = 0.1$, NaCl) and following the reaction for longer time periods. The turnovers of NA are 3.9 times higher than the complex concentrations, thus indicating the catalytic properties of the metal complexes for the hydrolysis of carboxyesters.⁵⁴

1.3 Conclusion

All determined k_{NA} and pK_a values of the active species of the mono- and dinuclear metal complexes are summarized in **Table 8**.

Complex / Nucleophile	$10^2 k_{NA} (M^{-1}s^{-1})$	pK_a
Zn-cyclen	9.6 ± 0.01	7.9
ZnL1 ; $Zn_1L(OH^-)$	39.1 ± 0.1	8.35
ZnL3 ; $Zn_1L(OH^-)$	27.9 ± 0.01	8.28
ZnL8 ; $Zn_1L(OH^-)$	38.6 ± 0.02	7.89
Zn₂L2 ; $Zn_2L(OH^-)(OH_2)$	410 ± 27	8.09^a
Zn₂L4 ; $Zn_2L(OH^-)(OH_2)$	310 ± 19	8.27
Zn₂L5 ; $Zn_2L(OH^-)(OH_2)$	440 ± 31	$8.37^a, 8.14^b$
Zn₂L6 ; $Zn_2L(OH^-)(OH_2)$	57.3 ± 0.3	7.45
Zn₂L6 ; $Zn_2L(OH^-)(OH^-)$	71.7 ± 0.4	8.85
Zn₂L7 ; $Zn_2L(OH^-)(OH_2)$	39.9 ± 0.74	7.65
Zn₂L7 ; $Zn_2L(OH^-)(OH^-)$	78.6 ± 0.6	8.11

^a determined kinetically. ^b MeOH/H₂O (9:1)

Table 8: Summary of the hydrolytic assays for NA.

The k_{NA} values of the mononuclear Zn(II) cyclen complexes show a 3 to 4-fold higher hydrolysis rate than the simple Zn[12]aneN₄ system due to the aromatic substituent, which provides a more hydrophobic environment³⁴ and interacts with the aromatic ring of the 4-nitrophenyl acetate by p-p interactions. The reactive species is the Zn(II)-OH⁻ complex, in which the Zn(II)-bound OH⁻ acts as a nucleophile to attack intermolecularly the carbonyl group of the acetate ester.

For the dinuclear complexes the mechanism of reaction is defined by the degree of cooperation between the metal centres, influenced by the spacer length. The spacer type does not have an important influence on the catalytic activity, as can be observed from the similar k_{NA} values of **Zn₂L2** and **Zn₂L5**. For **Zn₂L7**, possessing the longest spacer, the two metal centres act independently in the hydrolysis, therefore the reaction rate is twice as high as the rate of the mononuclear analogue. The complexes with one aryl spacer show saturation kinetics with formation of a *Michaelis-Menten* adduct. Their rates are 40 times higher than the simple Zn[12]aneN₄ system. **Zn₂L6** is a hybrid between a these two mechanism, a clear saturation curve is not visible, but neither are the metal cores completely independent from another.

The Cu(II) and Ni(II) complexes do not fulfil one of the two conditions needed for an artificial metallohydrolase: the Cu(II) complexes do not possess two *cis*-oriented coordination sites on the metal ion for binding the substrate and a water molecule, while Ni(II) is not a strong Lewis acid in **NiL1** and **Ni₂L2** and does not facilitate deprotonation of the coordinated water to generate the hydroxide nucleophile.

For all Zn(II) complexes the catalytic activity was proven. The Zn(II) complexes show a higher concentration of active species under physiological conditions than previously reported similar compounds and are therefore better suited for the hydrolysis of esters under physiological conditions.

1.4 Experimental Section

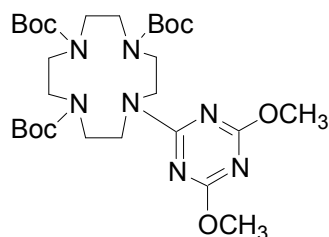
1.4.1 General information.

UV/VIS spectra were recorded on a Varian Cary BIO 50 UV/VIS/NIR spectrophotometer equipped with a jacketed cell holder using 1-cm cuvettes (quartz or glass) from Hellma and on a Zeiss SPECORD M500 equipped with 6 cuvette holders using disposable acrylic (PMMA) 1-cm cuvettes from Sarstedt. For all UV/VIS measurements the temperature was kept constant at 25 °C (± 0.1 °C). IR spectra were recorded on a Bio-Rad FT-IR FTS 155 spectrometer and a Bruker Tensor 27 spectrometer with an ATR unit. Elemental analysis was performed on a Vario EL III. Mass spectra were performed on a ThermoQuest Finnigan TSQ 7000 (ESI) and Finnigan MAT 95 (HRMS). Potentiometric titrations were performed with a Metrohm Dosimat 665. ^1H and ^{13}C NMR spectra were obtained on the following machines: Bruker AC-250 (^1H : 250.1 MHz, ^{13}C : 62.9 MHz, 24 °C), Bruker Avance 300 (^1H : 300.1 MHz, ^{13}C : 75.5 MHz, 27 °C), Bruker Avance 400 (^1H : 400.1 MHz, ^{13}C : 100.6 MHz, 27 °C), Bruker Avance 600 (^1H : 600.1 MHz, ^{13}C : 150.1 MHz, 27 °C). Melting points were determined with a Büchi SMP 20 and are uncorrected.

1.4.2 Synthesis of ligands and metal complexes.

The synthetic intermediates 10-(4,6-dichloro-[1,3,5]triazin-2-yl)-1,4,7,10-tetraazacyclododecane-1,4,7-tricarboxylic acid tri-*tert*-butyl ester **1**,⁵⁵ 4,6-bis-(1,4,7,10-tetraazacyclododecane-1,4,7-tricarboxylic acid tri-*tert*-butyl ester)-2-chloro-[1,3,5]-triazin **4**,⁵⁶ 2,6-bis-(1,4,7-tris[*tert*-butyloxycarbonyl]-1,4,7,10-tetraazacyclododecan)-pyridine **12**,⁵⁷ 6,6'-bis-(1,4,7-tris[*tert*-butyloxycarbonyl]-1,4,7,10-tetraazacyclododecane)-[2,2']bipyridine **14**²¹ and 10-(2-pyridinyl)-1,4,7,10-tetraazacyclododecan-1,4,7-tricarboxylic acid tri-*tert*-butyl ester **18**²¹ were prepared according to published methods. Compound **16** was synthesized according to the published general procedure.²¹

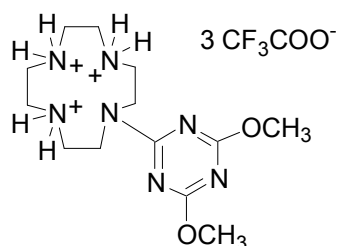
10-(4,6-Dimethoxy-[1,3,5]triazin-2-yl)-1,4,7,10-tetraaza-cyclododecane-1,4,7-tricarboxylic acid tri-*tert*-butyl ester (2)



A solution of **1**¹⁹ (3.50 g, 5.65 mmol) in absolute methanol (25 mL) was treated under nitrogen with sodium methylate (0.85g, 15.82 mmol) and the mixture was stirred for 18 h at room temperature. After completion of the reaction, the excess of NaOMe was quenched with a saturated aqueous solution of NH₄Cl (2 mL). The solvent was removed in vacuum and the residue was purified by chromatography on silica (ethyl acetate/petroleum ether, 1:2) to give a colorless solid (*R*_f = 0.47, ethyl acetate/petroleum ether, 1:1). Yield: 3.38 g (98%).

Melting point: 70 °C; IR (KBr): $\tilde{\nu}$ [cm⁻¹] = 2974, 2929, 1697, 1583, 1363, 1165, 679; UV/Vis (CH₃CN): λ_{max} [nm] (lg *e*) = 233 (4.489); ¹H NMR (400 MHz, CDCl₃): δ = 1.37 (s, 18 H, CH₃-Boc), 1.43 (s, 9 H, CH₃-Boc), 3.34-3.53 (m, 8 H, CH₂-cyclen), 3.60 (bs, 4 H, CH₂-cyclen), 3.68 (bs, 4 H, CH₂-cyclen), 3.91 (s, 6 H, OCH₃); ¹³C NMR (100 MHz, CDCl₃): δ = 28.4, 28.5 (+, CH₃-Boc), 50.0, 50.3, 51.5 (-, CH₂-cyclen), 54.6 (+, OCH₃) 80.0, 80.3 (C_{quat}, C-Boc), 156.3, 157.1 (C_{quat}, C=O Boc), 167.4 (C_{quat}, C_{Aryl}-N), 171.9 (C_{quat}, C_{Aryl}-OCH₃); MS (ESI, MeOH + 1 % AcOH): *m/z* (%) = 612 (100) [MH]⁺, 634 (10) [M + Na]⁺; Anal. Calcd for C₂₈H₄₉N₇O₈: C 54.98, H 8.07, N 16.03. Found: C 54.88, H 8.02, N 15.60.

10-(4,6-Dimethoxy-[1,3,5]triazin-2-yl)-10-aza-1,4,7-triazonia-cyclododecane-tris-trifluoro-acetate (3)

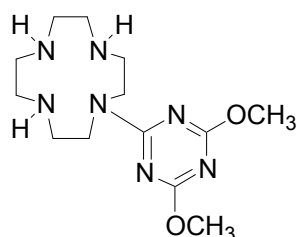


A solution of **2** (1.10 g, 1.80 mmol) in dichloromethane (60 mL) was treated under nitrogen with TFA (5.8 mL, 8.62 g, 75.60 mmol) and the mixture was stirred for 18 h at room temperature. The solvent and the excess of TFA were removed under vacuum. The product **3** was obtained quantitatively as colorless, hygroscopic solid. Yield: 1.18 g (quantitative).

Melting point: 137 °C; IR (KBr): $\tilde{\nu}$ [cm⁻¹] = 2969, 1685, 1201, 1132, 796, 723; UV/Vis (CH₃CN): λ_{max} [nm] (lg *e*) = 223 (3.452); ¹H NMR (300 MHz, CD₃CN): δ = 3.14 (bs, 8 H,

CH₂-cyclen), 3.19-3.24 (m, 4 H, CH₂-cyclen), 3.88-3.91 (m, 10 H, CH₂-cyclen and OCH₃), 7.55 (bs, 6 H, NH₂⁺); (400 MHz, MeOH-d₄): δ = 3.19-3.24 (m, 8 H, CH₂-cyclen), 3.30-3.37 (m, 4 H, CH₂-cyclen and solvent MeOH), 3.98 (s, 6 H, OCH₃), 4.10-4.27 (m, 4 H, CH₂-cyclen), 4.99 (bs, 6 H, NH₂⁺ and solvent MeOH); (300 MHz, D₂O): δ = 3.05-3.12 (m, 4 H, CH₂-cyclen), 3.17-3.21 (m, 8 H, CH₂-cyclen), 3.83-3.94 (m, 10 H, CH₂-cyclen and OCH₃); ¹³C NMR (75 MHz, CD₃CN): δ = 44.6, 45.5, 47.0, 48.7 (-, CH₂-cyclen), 56.1 (+, OCH₃), 116.9 (C_{quat}, q, ¹J_{C,F} = 287.2 Hz, CF₃COO⁻), 160.6 (C_{quat}, q, ²J_{C,F} = 37.9 Hz, CF₃COO⁻), 169.3 (C_{quat}, C_{Aryl}-N), 171.3 (C_{quat}, C_{Aryl}-OCH₃); (100 MHz, MeOH-d₄): δ = 44.6, 46.1, 47.1, 48.4 (-, CH₂-cyclen), 55.7 (+, OCH₃), 117.4 (C_{quat}, q, ¹J_{C,F} = 289.6 Hz, CF₃COO⁻), 161.6 (C_{quat}, q, ²J_{C,F} = 36.8 Hz, CF₃COO⁻), 170.4 (C_{quat}, C_{Aryl}-N), 172.4 (C_{quat}, C_{Aryl}-OCH₃); (75 MHz, D₂O): δ = 43.6, 44.3, 45.4, 47.9 (-, CH₂-cyclen), 56.7 (+, OCH₃), 116.1 (C_{quat}, q, ¹J_{C,F} = 288.3 Hz, CF₃COO⁻), 162.6 (C_{quat}, q, ²J_{C,F} = 37.4 Hz, CF₃COO⁻), 164.6 (C_{quat}, C_{Aryl}-N), 167.0 (C_{quat}, C_{Aryl}-OCH₃); MS (ESI, CH₃CN): *m/z* (%) = 312 (100) [M³⁺ - 2 H]⁺; 334 (10) [M³⁺ - 3 H + Na]⁺.

1-(4,6-Dimethoxy-[1,3,5]triazin-2-yl)-1,4,7,10-tetraaza-cyclododecane (L1)

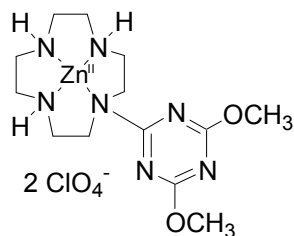


A basic ion exchange resin (OH⁻ capacity 0.9 mmol/mL) was swollen in water for 15 min and then washed several times. A chromatography column was charged with resin (15 mL). A solution of **3** (0.92 g, 1.37 mmol) in water (30 mL) was slowly passed through this column, followed by a solution of water and acetonitrile. The organic solvent was removed under reduced pressure and the aqueous solvent by lyophilisation to give a colorless solid. Yield: 0.42 g (98%).

Melting point: 103 °C; IR (KBr): $\tilde{\nu}$ [cm⁻¹] = 3441, 2924, 2856, 1556, 1486, 1359, 806; UV/Vis (CH₃CN): λ_{max} [nm] (lg *e*) = 234 (2.732); ¹H NMR (300 MHz, MeOH-d₄): δ = 2.64-2.74 (m, 8 H, CH₂-cyclen), 2.95-2.99 (m, 4 H, CH₂-cyclen), 3.82-3.89 (m, 4 H, CH₂-cyclen), 3.94 (s, 6 H, OCH₃); (400 MHz, CDCl₃): δ = 2.66-2.68 (m, 4 H, CH₂-cyclen), 2.77-2.80 (m, 4 H, CH₂-cyclen), 2.96-2.99 (m, 4 H, CH₂-cyclen), 3.80-3.83 (m, 4 H, CH₂-cyclen), 3.94 (s, 6 H, OCH₃); ¹³C NMR (75 MHz, MeOH-d₄): δ = 47.1, 48.7, 49.5, 50.5 (-, CH₂-cyclen), 55.2 (+, OCH₃), 169.8 (C_{quat}, C_{Aryl}-N), 173.1 (C_{quat}, C_{Aryl}-OCH₃); (100 MHz, CDCl₃): δ = 47.2,

47.8, 48.8, 49.8 (-, CH₂-cyclen), 54.5 (+, OCH₃), 167.2 (C_{quat}, C_{Aryl}-N), 171.9 (C_{quat}, C_{Aryl}-OCH₃); MS (ESI, MeOH + 1 % AcOH): m/z (%) = 312 (100) [MH]⁺; 334 (7) [M + Na]⁺; HRMS (C₁₃H₂₆N₇O₂): calcd 312.2148 [MH]⁺, obsd 312.2146 [MH]⁺ ± 0.88 ppm.

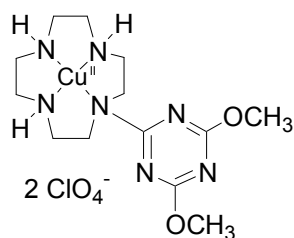
[ZnL1](ClO₄)₂ · H₂O



A solution of **L1** (0.315 g, 1.01 mmol) in methanol (15 mL) was treated under stirring with a solution of Zn(ClO₄)₂ · 6 H₂O (0.376 g, 1.01 mmol) in methanol (10 mL). A colorless precipitate immediately appeared. The mixture was refluxed for 3 h. Colorless crystals were obtained after recrystallization from a mixture of MeOH/water (4:1). Some petroleum ether was added to the filtrate solution to yield also colorless crystals. Both filter residues showed the same analytical purity. Yield: 0.554 g (95%).

Melting point: 284 °C (decomposition); IR (KBr): $\tilde{\nu}$ [cm⁻¹] = 3428, 3293, 2943, 1576, 1469, 1287, 1140, 812, 627; UV/Vis (CH₃CN): λ_{max} [nm] (lg ϵ) = 226 (3.935); ¹H NMR (300 MHz, DMSO-d₆): δ = 2.66-2.70 (m, 4 H, CH₂-cyclen), 2.82-2.89 (m, 4 H, CH₂-cyclen), 3.41-3.44 (m, 4 H, CH₂-cyclen and H₂O), 3.89 (s, 6 H, OCH₃), 3.98-4.08 (m, 4 H CH₂-cyclen); ¹³C NMR (75 MHz, DMSO-d₆): δ = 44.9, 45.5, 46.2, 47.2 (-, CH₂-cyclen), 54.2 (+, OCH₃), 169.0 (C_{quat}, C_{Aryl}-N), 171.1 (C_{quat}, C_{Aryl}-OCH₃); MS (ESI, CH₂Cl₂/MeOH + 10 mmol/l NH₄Ac): m/z (%) = 434 (100) [M²⁺ + CH₃COO]⁺; 187 (85) [M]²⁺, 474 (8) [M²⁺ + ClO₄]⁺; (ESI, negative, CH₂Cl₂/MeOH + 10 mmol/l NH₄Ac): m/z (%) = 674 (100) [M²⁺ + 3 ClO₄]⁻, 634 (8) [M²⁺ + 2 ClO₄ + CH₃COO]⁻; HRMS (C₁₃H₂₅N₇O₆Cl₁Zn₁): calcd 474.0846 [M²⁺ + ClO₄]⁺, obsd 474.0842 [M²⁺ + ClO₄]⁺ ± 0.95 ppm; Anal. Calcd. for C₁₃H₂₅N₇ O₁₀Cl₂Zn · 1 H₂O: C 26.30, H 4.58, N 16.52. Found: C 26.38, H 4.49, N 16.41.

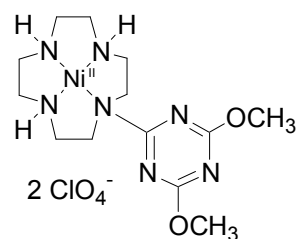
[CuL1](ClO₄)₂ · H₂O



A procedure analogous to that described for **ZnL1** was followed starting from a solution of **L1** (0.15 g, 0.5 mmol) in ethanol (2 mL) and a solution of $\text{Cu}(\text{ClO}_4)_2 \cdot 6 \text{H}_2\text{O}$ (0.18 g, 0.5 mmol) in ethanol (3 mL). The resulting blue mixture was refluxed for 18 h. After cooling, the solid compound was filtered off, washed with ethanol and dried under vacuum to obtain the product as a pale blue solid. Yield: 0.28 g (0.49 mmol, 98%).

Melting point: 194-196 °C; IR (ATR unit): $\tilde{\nu}$ [cm^{-1}] = 3313, 3270, 2941, 1604, 1561, 1486, 1381, 1099, 815, 621; UV/Vis (Millipore H_2O): λ_{max} [nm] (lg ϵ) = 229 (3.889), 272 (3.368), 641 (2.064), 650 (2.033); MS (ESI, $\text{H}_2\text{O}/\text{CH}_3\text{CN}$): m/z (%) = 186.8 (65) $[\text{M}]^{2+}$, 207.4 (100) $[\text{M}^{2+} + \text{CH}_3\text{CN}]^{2+}$, 473 (15) $[\text{M}^{2+} + \text{ClO}_4]^{+}$; (ESI, negative, $\text{H}_2\text{O}/\text{CH}_3\text{CN}$): m/z (%) = 672.8 (100) $[\text{M}^{2+} + 3 \text{ClO}_4]^{-}$; Anal. Calcd for $\text{C}_{13}\text{H}_{25}\text{N}_7\text{O}_{10}\text{Cl}_2\text{Cu} \cdot 1 \text{H}_2\text{O}$: C 26.44; H 4.61; N 16.61. Found: C 26.53; H 4.74; N 16.70.

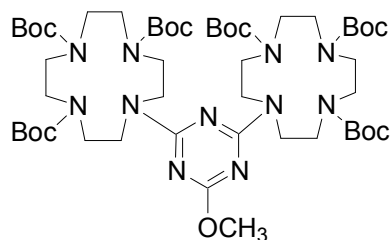
[NiL1](ClO₄)₂ · 2 H₂O



A procedure analogous to that described for **CuL1** was followed starting from a solution of **L1** (0.127 g, 0.4 mmol) in ethanol (2 mL) and a solution of $\text{Ni}(\text{ClO}_4)_2 \cdot 6 \text{H}_2\text{O}$ (0.15 g, 0.4 mmol) in ethanol (3 mL). The resulting turquoise mixture was refluxed for 24 h. After evaporation of the solvent the product was dried under vacuum to obtain a pale green, hygroscopic solid. Yield: 0.158 g (70%).

Melting point: 242 °C (decomposition); IR (KBr): $\tilde{\nu}$ [cm^{-1}] = 3398, 3270, 2940, 2360, 1585, 1479, 1366, 1091, 974, 809, 626; UV/Vis (Millipore H_2O): λ_{max} [nm] (lg ϵ) = 228 (4.175), 368 (1.514), 590 (1.212), 964 (1.447); MS (ESI, $\text{H}_2\text{O}/\text{CH}_3\text{CN}$): m/z (%) = 184.3 (60) $[\text{M}^{2+}]^{2+}$, 204.9 (100) $[\text{M}^{2+} + \text{CH}_3\text{CN}]^{2+}$, 225.3 (15) $[\text{M}^{2+} + 2 \text{CH}_3\text{CN}]^{2+}$, 468 (25) $[\text{M}^{2+} + \text{ClO}_4]^{+}$; (ESI, negative, $\text{H}_2\text{O}/\text{CH}_3\text{CN}$): m/z (%) = 667.9 (100) $[\text{M}^{2+} + 3 \text{ClO}_4]^{-}$; HRMS ($\text{C}_{13}\text{H}_{25}\text{N}_7\text{O}_6\text{ClNi}$): calcd 468.0908 $[\text{M}^{2+} + \text{ClO}_4]^{+}$, obsd 474.0906 $[\text{M}^{2+} + \text{ClO}_4]^{+} \pm 0.48$ ppm; Anal. Calcd. for $\text{C}_{13}\text{H}_{25}\text{N}_7\text{O}_{10}\text{Cl}_2\text{Ni} \cdot 2 \text{H}_2\text{O}$: C 25.81; H 4.83; N 16.21. Found: C 25.31; H 5.04; N 16.02.

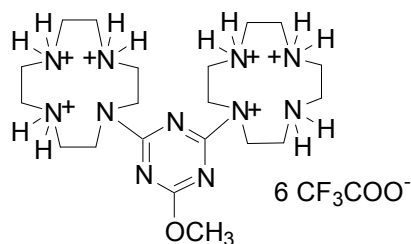
4,6-Bis-(1,4,7,10-tetraaza-cyclododecane-1,4,7-tricarboxylic acid tri-tert-butyl ester)-2-methoxy-[1,3,5]-triazine (5)



A procedure analogous to that described for **2** was followed starting from a solution of **4**²⁰ (5.28 g, 5.00 mmol) in absolute methanol (50 mL) and NaOMe (0.41 g, 7.59 mmol) under nitrogen. The solvent was removed under vacuum and the residue was purified by chromatography on silica (ethyl acetate/petroleum ether, 1:4 to 4:1) to give a colorless solid (R_f = 0.47, ethyl acetate/petroleum ether, 1:1). Yield: 5.17 g (98%).

Melting point: 109 °C; IR (KBr): $\tilde{\nu}$ [cm^{-1}] = 2976, 2933, 1695, 1571, 1365, 1163, 739; UV/Vis (CH_3CN): λ_{max} [nm] (lg ϵ) = 234 (4.617); ^1H NMR (400 MHz, CDCl_3): δ = 1.37 (s, 18 H, CH_3 -Boc), 1.41 (s, 36 H, CH_3 -Boc), 3.27-3.62 (m, 32 H, CH_2 -cyclen), 3.85 (s, 3 H, OCH_3); ^{13}C NMR (100 MHz, CDCl_3): δ = 28.4, 28.5 (+, CH_3 -Boc), 50.1 (-, very broad peak, CH_2 -cyclen), 53.9 (+, OCH_3), 79.9, 80.0 (C_{quat} , C-Boc), 156.3 (C_{quat} , C=O Boc), 166.3 (C_{quat} , $\text{C}_{\text{Aryl-N}}$), 170.6 (C_{quat} , $\text{C}_{\text{Aryl-OCH}_3}$); MS (ESI, MeOH + 1 % AcOH): m/z (%) = 1052 (100) $[\text{MH}]^+$, 952 (7) $[\text{MH} - \text{Boc}]^+$; Anal. Calcd for $\text{C}_{50}\text{H}_{89}\text{N}_{11}\text{O}_{13}$: C 57.05, H 8.52, N 14.64. Found: C 57.28, H 8.37, N 14.21.

[4,6-Bis-(10-aza-1,4,7-triazonia-cyclododec-10-yl)-[1,3,5]triazine-2-yl]-methylether-hexakis-trifluoroacetate (6)

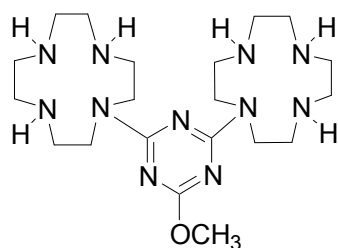


A procedure analogous to that described for **3** was followed. The product **6** was obtained quantitatively as a colorless, hygroscopic solid.

Melting point: 124 °C; IR (KBr): $\tilde{\nu}$ [cm^{-1}] = 2961, 1681, 1208, 1145, 781; UV/Vis (CH_3CN): λ_{max} [nm] (lg ϵ) = 224 (4.502); ^1H NMR (250 MHz, D_2O): δ = 3.02-3.09 (m, 16 H, CH_2 -cyclen), 3.15-3.18 (m, 8 H, CH_2 -cyclen), 3.81-3.94 (m, 11 H, CH_2 -cyclen and OCH_3); (300 MHz, CD_3CN): δ = 3.01-3.17 (m, 16 H, CH_2 -cyclen), 3.28-3.39 (m, 16 H, CH_2 -cyclen), 3.85 (s, 3 H, OCH_3), 7.17 (bs, 12 H, NH_2^+); ^{13}C NMR (62 MHz, D_2O): δ = 43.4, 44.4, 45.6, 47.3 (-

,CH₂-cyclen), 55.7 (+, OCH₃), 116.2 (C_{quat}, q, ¹J_{C,F} = 291.7 Hz, CF₃COO⁻), 162.5 (C_{quat}, q, ²J_{C,F} = 35.6 Hz, CF₃COO⁻), 164.5 (C_{quat}, C_{Aryl}-N), 166.4 (C_{quat}, C_{Aryl}-OCH₃); (75 MHz, CD₃CN): δ = 43.6, 43.9, 45.3, 45.9, 46.0, 47.1, 47.4, 47.6 (-, CH₂-cyclen), 55.0 (+, OCH₃), 117.4 (C_{quat}, q, ¹J_{C,F} = 291.2 Hz, CF₃COO⁻), 161.0 (C_{quat}, q, ²J_{C,F} = 35.8 Hz, CF₃COO⁻), 169.8 (C_{quat}, C_{Aryl}-N), 171.8 (C_{quat}, C_{Aryl}-OCH₃); MS (ESI, CH₃CN): *m/z* (%) = 452 (100) [M⁶⁺ - 5 H]⁺, 226 (95) [M⁶⁺ - 4 H]²⁺.

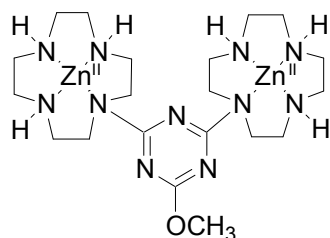
2-Methoxy-4,6-di-(1,4,7,10-tetraaza-cyclododecan-1-yl)-[1,3,5]triazine (L2)



A procedure analogous to that described for **L1** was followed. The free amine **L2** was obtained quantitatively as a colorless solid.

Melting point: 83 °C; IR (KBr): $\tilde{\nu}$ [cm⁻¹] = 3396, 2926, 2841, 1583, 1116, 812, 722; UV/Vis (CH₃CN): λ_{max} [nm] (lg ϵ) = 232 (4.531); ¹H NMR (300 MHz, MeOH-d₄): δ = 2.65-2.73 (m, 16 H, CH₂-cyclen), 2.87-2.96 (m, 8 H, CH₂-cyclen), 3.75-3.85 (m, 8 H, CH₂-cyclen), 3.89 (s, 3 H, OCH₃); (300 MHz, CDCl₃): δ = 2.62-2.65 (m, 8 H, CH₂-cyclen), 2.74-2.78 (m, 8 H, CH₂-cyclen), 2.90-2.94 (m, 8 H, CH₂-cyclen), 3.72-3.76 (m, 8 H, CH₂-cyclen), 3.84 (s, 3 H, OCH₃); ¹³C NMR (75 MHz, D₂O): δ = 45.5, 47.5, 48.3, 49.6 (-, CH₂-cyclen), 52.9 (+, OCH₃), 167.1 (C_{quat}, C_{Aryl}-N), 170.3 (C_{quat}, C_{Aryl}-OCH₃); MS (ESI, MeOH + 10 mmol/l NH₄Ac): *m/z* (%) = 452 (100) [MH]⁺, 226 (8) [M + 2 H]²⁺; HRMS (C₂₀H₄₂N₁₁O₁): calcd 452.3574 [MH]⁺, obsd 452.3578 [MH]⁺ ± 0.56 ppm.

[Zn₂L2](ClO₄)₄ · CH₃CN

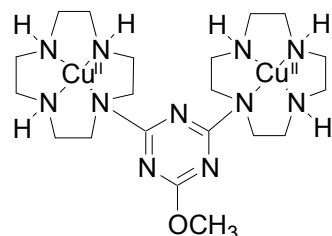


A procedure analogous to that described for **ZnL1** was followed. A solution of **L2** (0.61 g, 1.35 mmol) in methanol (15 mL) was treated under intense stirring with a solution of Zn(ClO₄)₂ · 6 H₂O (1.06 g, 2.70 mmol) in methanol (15 mL). Colorless crystals were obtained

after recrystallization from a mixture of MeOH/water/acetonitrile (8:1:1). The filtrate solution was reduced to half its volume and some petroleum ether was added to yield additional product as colorless crystals. Both filter residues showed the same analytical purity. Yield: 1.29 g (98%).

Melting point: 248 °C; IR (KBr): $\tilde{\nu}$ [cm⁻¹] = 3600, 3435, 3292, 2931, 1572, 1471, 1350, 1076, 814, 628; UV/Vis (CH₃CN): λ_{max} [nm] (lg ϵ) = 226 (4.735); ¹H NMR (600 MHz, CH₃CN): δ = 2.70-2.74 (m, 4 H, CH₂-cyclen), 2.85-2.89 (m, 8 H, CH₂-cyclen), 3.04-3.06 (m, 8 H, CH₂-cyclen), 3.18-3.22 (m, 4 H, CH₂-cyclen), 3.36-3.38 (m, 4 H, CH₂-cyclen), 3.51-3.53 (t, 2 H, ³J = 5.4 Hz, NH), 3.59 (bs, 4 H, NH), 3.98 (s, 3 H, OCH₃), 4.48-4.51 (m, 4 H, CH₂-cyclen); ¹³C NMR (150 MHz, CD₃CN): δ = 44.4 (-, CH₂-cyclen), 47.0 (-, CH₂-cyclen), 47.8 (-, CH₂-cyclen), 55.8 (+, OCH₃), 172.0 (C_{quat}, C_{Aryl}-N), 172.4 (C_{quat}, C_{Aryl}-OCH₃); MS (ESI, CH₃CN): m/z (%) = 349 (100) [M⁴⁺ + 2 CH₃COO]²⁺, 319 (60) [M⁴⁺ - H + CH₃COO]²⁺; (ESI, negative, CH₃CN): m/z (%) = 1038 (100) [M⁴⁺ + 4 ClO₄⁻ + CH₃COO]⁻, 1078 (15) [M⁴⁺ + 5 ClO₄⁻]⁻; Anal. Calcd for C₂₀H₄₁N₁₁O₁₇Cl₄Zn₂ · 1 CH₃CN: C 25.98, H 4.36, N 16.54. Found: C 26.25, H 4.66, N 16.74.

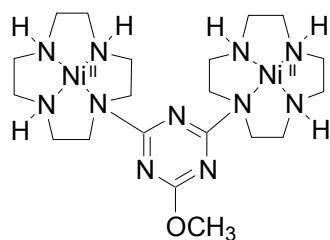
[Cu₂L2](ClO₄)₄ · 2 H₂O



A procedure analogous to that described for **CuL1** was followed. A solution of **L2** (0.115 g, 0.25 mmol) in ethanol (4 mL) was treated under intense stirring with a solution of Cu(ClO₄)₂ · 6 H₂O (0.19 g, 0.5 mmol) in ethanol (3 mL). The resulting dark blue solution was stirred at room temperature for 2 h, and then refluxed for 1 h. The solid compound was filtered off, washed with ethanol and dried under vacuum to obtain a blue solid. Yield: 0.185 g (77%).

Melting point: 235 °C; IR (ATR unit): $\tilde{\nu}$ [cm⁻¹] = 3267, 2959, 2884, 1556, 1469, 1332, 1070, 826, 621; UV/Vis (Millipore H₂O): λ_{max} [nm] (lg ϵ) = 230 (4.355), 650 (2.490); MS (ESI, H₂O/CH₃CN): m/z (%) = 216 (75) [M⁴⁺ + 7 CH₃CN]⁴⁺, 253 (55) [M⁴⁺ + ClO₄⁻ + 2 CH₃CN]³⁺, 266 (100) [M⁴⁺ + ClO₄⁻ + 3 CH₃CN]³⁺, 356 (50) [M⁴⁺ + ClO₄⁻ + Cl]²⁺, 388 (100) [M⁴⁺ + 2 ClO₄⁻]²⁺; (ESI, negative, H₂O/CH₃CN): m/z (%) = 1076 (100) [M⁴⁺ + 5 ClO₄⁻]⁻; Anal. Calcd for C₂₀H₄₁N₁₁O₁₇Cl₄Cu₂ · 2 H₂O: C 23.79, H 4.49, N 15.27. Found: C 24.01, H 4.69, N 15.22.

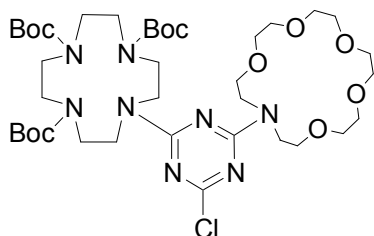
[Ni₂L2](ClO₄)₄



A procedure analogous to that described for **NiL1** was followed. A solution of **L2** (0.105 g, 0.23 mmol) in ethanol (6 mL) was treated under intense stirring with a solution of Ni(ClO₄)₂ · 6 H₂O (0.17 g, 0.46 mmol) in ethanol (6 mL). The resulting pale blue solution was refluxed for 24 h. After reflux the solution and the residue were green. The solid compound was filtered off, washed with ethanol and dried under vacuum to obtain the product as a green, hygroscopic solid. Yield: 0.155 g (72%).

Melting point: 222 °C; IR (KBr): $\tilde{\nu}$ [cm⁻¹] = 3421, 3279, 2949, 2889, 2023, 1568, 1458, 1408, 1349, 1105, 1091, 980, 927, 816, 626; UV/Vis (Millipore H₂O): λ_{max} [nm] (lg ϵ) = 228 (4.205), 361 (1.970), 589 (1.970), 1029 (1.636); MS (ESI, H₂O/CH₃CN): m/z (%) = 203.2 (85) [M⁴⁺ + 6 CH₃CN]⁴⁺, 241.7 (100) [M⁴⁺ + Cl⁻ + 3 CH₃CN]³⁺, 263.1 (80) [M⁴⁺ + ClO₄⁻ + 3 CH₃CN]³⁺, 351.4 (70) [M⁴⁺ + ClO₄⁻ + Cl⁻]²⁺, 383.5 (30) [M⁴⁺ + 2 ClO₄⁻]²⁺, 802.2 (15) [M⁴⁺ + 2 ClO₄⁻ + Cl⁻]⁺; (ESI, negative, H₂O/CH₃CN): m/z (%) = 937.9 (55) [M⁴⁺ + 3 ClO₄⁻ + 2 Cl⁻]⁻, 1002 (100) [M⁴⁺ + 4 ClO₄⁻ + Cl⁻]⁻, 1064 (60) [M⁴⁺ + 5 ClO₄⁻]⁻; HRMS (C₂₀H₃₉N₁₁ClO₅Ni₂): calcd 664.1531 [M⁴⁺ + ClO₄⁻ - 2 H⁺]⁺, obsd 664.1518 [M⁴⁺ + ClO₄⁻ - 2 H⁺]⁺ ± 1.96 ppm.

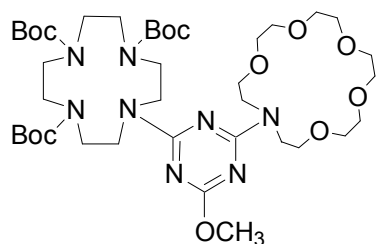
10-[4-Chloro-6-(1,4,7,10,13-pentaoxa-16-aza-cyclooctadec-16-yl)-[1,3,5]triazine-2-yl]-1,4,7,10-tetraaza-cyclododecane-1,4,7-tricarboxylic acid tri-*tert*-butyl ester (**7**)



A solution of **1** (2.0 g, 3.22 mmol) and 1-aza-18-crown-6 (0.85 g, 3.22 mmol) in acetone (15 mL) was treated under nitrogen with K₂CO₃ (0.67 g, 4.83 mmol) and the mixture was refluxed for 3 h. The solvent was removed under vacuum and the residue was purified by chromatography on silica (ethyl acetate/methanol, 98:2) to give a colorless solid (R_f = 0.16; ethyl acetate/methanol, 95:5). Yield: 2.45 g (91%).

Melting point: 153 °C; IR (KBr): $\tilde{\nu}$ [cm⁻¹] = 3446, 2974, 2870, 1695, 1570, 1249, 1133, 972, 803, 778; UV/Vis (CH₃CN): λ_{max} [nm] (lg e) = 234 (4.574); ¹H NMR (300 MHz, CDCl₃): δ = 1.43 (s, 18 H, CH₃-Boc), 1.47 (s, 9 H, CH₃-Boc), 3.39-3.51 (m, 12 H, CH₂-cyclen), 3.62-3.75 (m, 24 H, CH₂-azacrown), 3.83-3.87 (m, 4 H, CH₂-cyclen); ¹³C NMR (75 MHz, CDCl₃): δ = 28.4, 28.5 (+, CH₃-Boc), 48.0, 48.3, 50.0, 50.5, 50.9, 51.0 (-, CH₂-cyclen and CH₂-azacrown), 69.1, 69.4, 70.4, 70.5, 70.5, 70.6, 70.7, 70.8 (-, CH₂-azacrown), 80.0, 80.3 (C_{quat}, C-Boc), 156.3, 157.2 (C_{quat}, C=O Boc), 164.6, 165.0 (C_{quat}, C_{Aryl}-N), 168.9 (C_{quat}, C_{Aryl}-Cl); MS (FAB, CH₂Cl₂/MeOH, Glycerin): m/z (%) = 847 (100) [MH]⁺, 547 (35) [MH - 3 Boc]⁺, 747 (11) [MH - Boc]⁺, 869 (5) [M + Na]⁺; Anal. Calcd for C₃₈H₆₇N₈O₁₁Cl₁: C 53.87, H 7.97, N 13.22. Found: C 54.21, H 8.17, N 13.67.

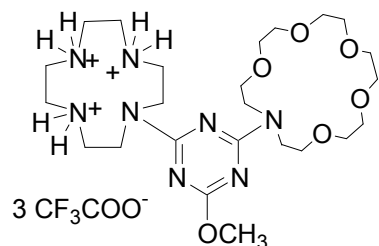
10-[4-Methoxy-6-(1,4,7,10,13-pentaoxa-16-aza-cyclooctadec-16-yl)-[1,3,5]triazine-2-yl]-1,4,7,10-tetraaza-cyclododecane-1,4,7-tricarboxylic acid tri-*tert*-butyl ester (8)



A procedure analogous to that described for **2** was followed starting from a solution of **7** (2.05 g, 2.42 mmol) in absolute methanol (20 mL) and NaOMe (0.21 g, 3.89 mmol) under nitrogen. The residue was suspended in a solution of ethyl acetate/methanol (98:2) and filtered through a very small amount of silica in order to avoid adsorption of the polar product on the silica. Product **8** was isolated as a colorless solid (R_f = 0.25, ethyl acetate/methanol, 95:5). Yield: 2.02 g (99%).

Melting point: 81 °C; IR (KBr): $\tilde{\nu}$ [cm⁻¹] = 3495, 2975, 2869, 1692, 1573, 1250, 1167, 974, 814, 778; UV/Vis (CH₃CN): λ_{max} [nm] (lg e) = 231 (4.538); ¹H NMR (300 MHz, CDCl₃): δ = 1.41 (s, 18 H, CH₃-Boc), 1.47 (s, 9 H, CH₃-Boc), 3.22-3.52 (m, 12 H, CH₂-cyclen), 3.61-3.69 (m, 24 H, CH₂-azacrown), 3.82-3.97 (m, 7 H, OCH₃ and CH₂-cyclen); ¹³C NMR (75 MHz, CDCl₃): δ = 28.5, 28.6 (+, CH₃-Boc), 48.1, 48.4, 50.4, 51.9 (-, CH₂-cyclen and CH₂-azacrown), 53.9 (+, OCH₃), 69.6, 69.7, 70.5, 70.6, 70.7, 70.9 (-, CH₂-azacrown), 79.8, 80.1 (C_{quat}, C-Boc), 156.3, 156.9 (C_{quat}, C=O Boc), 165.7, 166.6 (C_{quat}, C_{Aryl}-N), 170.4 (C_{quat}, C_{Aryl}-OCH₃); MS (ESI, MeOH/CH₂Cl₂ + 1% AcOH): m/z (%) = 844 (100) [MH]⁺, 866 (5) [M + Na]⁺; Anal. Calcd for C₃₉H₇₀N₈O₁₂: C 55.56, H 8.37, N 13.29. Found: C 55.22, H 8.22, N 13.76.

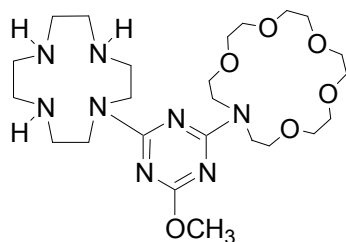
10-[4-Methoxy-6-(1,4,7,10,13-pentaoxa-16-aza-cyclooctadec-16-yl)-[1,3,5]triazine-2-yl]-10-aza-1,4,7-triazonia-cyclododecane-*tris*-trifluoroacetate (9)



A procedure analogous to that described for **3** was followed starting from a solution of **8** (1.52 g, 1.80 mmol) in dichloromethane (30 mL) and TFA (4.2 mL, 6.22 g, 54.53 mmol). The product **9** was obtained quantitatively as pale yellow, viscous oil. Yield: 1.62 g (quantitative). UV/Vis (CH₃CN): λ_{max} [nm] (lg ϵ) = 227 (4.472); ¹H NMR (600 MHz, CD₃CN): δ = 3.15-3.29 (m, 12 H, CH₂-cyclen and CH₂-azacrown), 3.47-3.99 (m, 28 H, CH₂-cyclen and CH₂-azacrown), 4.07 (s, 3 H, OCH₃), 8.13 (bs, 6 H, NH₂⁺); (300 MHz, MeOH-d₄): δ = 3.17-3.22 (m, 8 H, CH₂^{*}), 3.29-3.39 (m, 4 H, CH₂^{*} and solvent MeOH), 3.53-3.64 (m, 16 H, CH₂^{*}), 3.71-3.78 (m, 4 H, CH₂^{*}), 3.86-3.90 (m, 4 H, CH₂^{*}), 3.98-4.01 (m, 7 H, CH₂^{*} and OCH₃); (250 MHz, D₂O): δ = 3.09-3.27 (m, 14 H, CH₂-cyclen and CH₂-azacrown), 3.42-3.77 (m, 22 H, CH₂-cyclen and CH₂-azacrown), 3.81-3.89 (m, 7 H, CH₂-cyclen-CH₂ and OCH₃); ¹³C NMR (150 MHz, CD₃CN): δ = 45.5, 45.7, 47.3, 49.7, 50.4, 52.4 (-, CH₂-cyclen and CH₂-azacrown), 57.5 (+, OCH₃), 68.6, 69.7, 69.9, 70.2, 70.4, 71.0, 71.1, 71.4 (-, CH₂-azacrown), 117.0 (C_{quat}, q, ¹J_{C,F} = 289.4 Hz, CF₃COO⁻), 157.7 (C_{quat}, C_{Aryl}-N), 160.7 (C_{quat}, q, ²J_{C,F} = 37.6 Hz, CF₃COO⁻), 163.3 (C_{quat}, C_{Aryl}-N), 165.1 (C_{quat}, C_{Aryl}-OCH₃); (100 MHz, D₂O): δ = 44.0, 44.6, 46.0, 48.0, 49.2 (-, CH₂-cyclen and CH₂-azacrown), 56.7 (+, OCH₃), 67.5, 68.4, 69.4, 69.6, 69.8, 70.1 (-, CH₂-azacrown), 116.4 (C_{quat}, q, ¹J_{C,F} = 291.8 Hz, CF₃COO⁻), 156.9, 162.2 (C_{quat}, C_{Aryl}-N), 162.8 (C_{quat}, q, ²J_{C,F} = 35.4 Hz, CF₃COO⁻), 163.8 (C_{quat}, C_{Aryl}-OCH₃); **MS** (ESI, MeOH + 1 % AcOH): m/z (%) = 543 (100) [M³⁺ - 2 H]⁺, 272 (33) [M³⁺ - 1 H]²⁺, 565 (21), [M³⁺ - 3 H + Na]⁺.

[*] A more accurate distinction between the cyclen- and azacrown-CH₂ groups was not possible in this solvent due to a strong overlap of the signals. 2D-spectra did not provide further information.

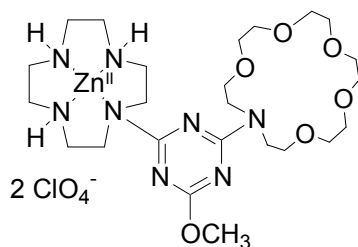
16-[4-Methoxy-6-(1,4,7,10-tetraaza-cyclododec-1-yl)-[1,3,5]triazine-2-yl]-1,4,7,10,13-pentaoxa-16-aza-cyclooctadecane (L3)



A procedure analogous to that described for **L1** was followed. A solution of **9** (1.40 g, 1.55 mmol) in water (15 mL) was slowly passed through a column of basic ion exchange resin. The column was then washed with water (120 mL) and acetonitrile (30 mL). The free amine **L3** was obtained quantitatively as a colorless solid. Yield: 0.84 g (quantitative).

Melting point: 76 °C; IR (KBr): $\tilde{\nu}$ [cm⁻¹] = 3440, 2868, 1574, 1358, 1115, 941, 812; UV/Vis (CH₃CN): λ_{max} [nm] (lg ϵ) = 231 (4.501); ¹H NMR (600 MHz, MeOH-d₄): δ = 2.67-2.68 (m, 4 H, CH₂-cyclen), 2.74-2.76 (m, 4 H, CH₂-cyclen), 2.95-2.97 (m, 4 H, CH₂-cyclen), 3.56-3.65 (m, 8 H, CH₂-azacrown), 3.66-3.69 (m, 8 H, CH₂-cyclen), 3.71-3.75 (m, 4 H, CH₂-azacrown), 3.76-3.79 (m, 4 H, CH₂-cyclen), 3.85-3.89 (m, 4 H, CH₂-azacrown), 3.90 (s, 3 H, OCH₃); ¹³C NMR (150 MHz, MeOH-d₄): δ = 45.8 (-, CH₂-cyclen), 47.6, 47.9 (-, CH₂-cyclen and CH₂-azacrown), 48.2, 48.9 (-, CH₂-cyclen), 52.9 (+, OCH₃), 69.1, 70.1, 70.2, 70.3, 70.4 (-, CH₂-azacrown), 165.8 (C_{quat}, C_{Aryl}-N_{azacrown}), 167.4 (C_{quat}, C_{Aryl}-N_{cyclen}), 170.6 (C_{quat}, C_{Aryl}-OCH₃); MS (ESI, MeOH + 10 mmol/l NH₄Ac): m/z (%) = 543(100) [MH]⁺, 565 (21) [M + Na]⁺, 272 (17), [M + 2 H]²⁺; HRMS (C₂₄H₄₇N₈O₆): calcd 543.3619 [MH]⁺, obsd 543.3624 [MH]⁺ ± 1.23 ppm.

[ZnL3](ClO₄)₂

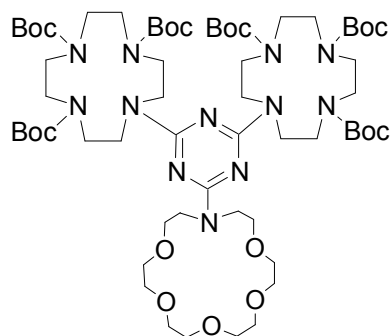


A procedure analogous to that described for **ZnL1** was followed. To a solution of **L3** (0.65 g, 1.20 mmol) in methanol (15 mL) were added under intense stirring portions of a solution of Zn(ClO₄)₂ · 6 H₂O (0.446 g, 1.20 mmol) in methanol (10 mL). The solution remained clear even after the addition of the zinc salt. The mixture was refluxed for 18 h. After removal of the solvent under vacuum the residue was washed three times with 2 mL of cold methanol

over a sintered-glass funnel. The product was isolated as colorless crystals. Yield: 0.887 g (92%).

Melting point: 181 °C; IR (KBr): $\tilde{\nu}$ [cm⁻¹] = 3435, 3269, 2926, 1580, 1471, 1352, 1108, 980, 815, 625; UV/Vis (CH₃CN): λ_{max} [nm] (lg e) = 228 (4.409); ¹H NMR (300 MHz, CD₃CN): δ = 2.68-3.12 (m, 12 H, CH₂), 3.34-3.86 (m, 26 H, CH₂), 3.92 (s, 3 H, OCH₃), 4.16-4.28 (m, 2 H, CH₂); ¹³C NMR (75 MHz, CD₃CN): δ = 44.8, 46.8, 47.5, 48.9, 49.4 (-, CH₂-cyclen and CH₂-azacrown), 55.4 (+, OCH₃), 70.0, 70.6, 70.7, 70.8, 71.1 (-, CH₂-azacrown), 166.9, 171.8 (C_{quat}, C_{Aryl}-N), 172.8 (C_{quat}, C_{Aryl}-OCH₃); MS (ESI, CH₃CN): m/z (%) = 665 (100) [M²⁺ + CH₃COO⁻]⁺, 344 (28) [M²⁺ + CH₃CN]²⁺, 705 (10) [M²⁺ + ClO₄⁻]⁺; (ESI, negative, CH₃CN): m/z (%) = 865 (100) [M²⁺ + 2 ClO₄⁻ + CH₃COO⁻]⁻, 905 (65) [M²⁺ + 3 ClO₄⁻]⁻; HRMS (C₂₄H₄₅N₈O₆Zn): calcd 605.2754 [M²⁺ - H]⁺, obsd 605.2756 [M²⁺ - H]⁺ ± 1.48 ppm.

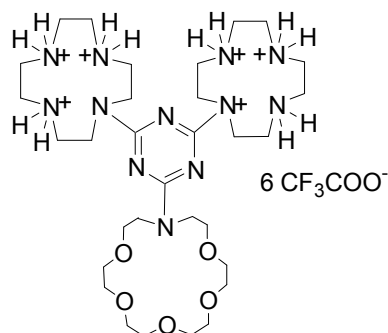
4,6-Bis-(1,4,7-tricarboxylic acid tri-*tert*-butyl ester-1,4,7,10-tetraaza-cyclododecane)-2-(1,4,7,10,13-pentaoxa-16-aza-cyclooctadecane-16-yl)-[1,3,5]triazine (10)



A procedure analogous to that described for **7** was followed starting from a solution of **4**²⁰ (1.2 g, 1.14 mmol), 1-aza-18-crown-6 (0.45 g, 1.71 mmol) and K₂CO₃ (0.47 g, 3.42 mmol) in acetone (25 mL) and the mixture was refluxed for 24 h. The solvent was removed under vacuum and the residue was purified by chromatography on silica (ethyl acetate/methanol, 97:3) to give a colorless solid (R_f = 0.31; ethyl acetate/methanol, 97:3). Yield: 1.27 g (87%).

Melting point: 97 °C; IR (KBr): $\tilde{\nu}$ [cm⁻¹] = 3449, 2975, 2932, 1697, 1541, 1249, 1166, 777; UV/Vis (CH₃CN): λ_{max} [nm] (lg e) = 232 (4.695); ¹H NMR (300 MHz, CDCl₃): δ = 1.38 (s, 18 H, CH₃-Boc), 1.40 (s, 36 H, CH₃-Boc), 3.24-3.88 (m, 56 H, CH₂-cyclen and CH₂-azacrown); ¹³C NMR (75 MHz, CDCl₃): δ = 28.5, 28.6 (+, CH₃-Boc), 48.1 (-, CH₂-azacrown), 50.5 (-, CH₂-cyclen), 70.0, 70.5, 70.6, 70.7, 70.9 (-, CH₂-azacrown), 79.7, 79.8 (C_{quat}, C-Boc), 156.2 (C_{quat}, C=O Boc), 164.6, 166.6 (C_{quat}, C_{Aryl}-N); MS (ESI, CH₂Cl₂/MeOH + 1 % AcOH): m/z (%) = 1284 (100) [MH]⁺, 1306 (10) [M + Na]⁺; Anal. Calcd for C₆₁H₁₁₀N₁₂O₁₇: C 57.08, H 8.64, N 13.09. Found: C 57.25, H 8.78, N 13.24.

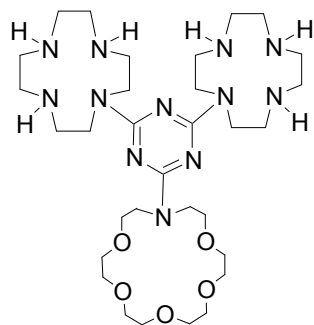
[4,6-Bis-(10-aza-1,4,7-azonia-cyclododec-10-yl)-[1,3,5]triazine-2-yl]-1,4,7,10,13-pentaoxa-16-azacyclooctadecane-hexakis-trifluoroacetate (11)



A procedure analogous to that described for **3** was followed starting from a solution of **10** (0.90 g, 0.70 mmol) in dichloromethane (30 mL) and TFA (3.3 mL, 4.88 g, 42.8 mmol). The product **11** was obtained as highly viscous oil. The oily residue was dissolved in a small amount of acetonitrile and the solvent was removed under vacuum. This procedure was repeated for three times in order to remove all traces of TFA. Product **11** was obtained quantitatively as pale yellow, very hygroscopic solid. Yield: 0.958 g (quantitative).

Melting point: 47-49 °C; IR (KBr): $\tilde{\nu}$ [cm⁻¹] = 3429, 2970, 2802, 1571, 1195, 781; UV/Vis (CH₃CN): λ_{max} [nm] (lg ϵ) = 225 (4.221); ¹H NMR (300 MHz, CD₃CN): δ = 2.98-3.29 (m, 28 H, CH₂-cyclen and CH₂-azacrown), 3.52-3.63 (m, 16 H, CH₂-cyclen and CH₂-azacrown), 3.46-3.79 (m, 8 H, CH₂-cyclen and CH₂-azacrown), 3.95-3.99 (m, 4 H, CH₂-cyclen), 7.74 (bs, 12 H, NH₂⁺); ¹³C NMR (75 MHz, CD₃CN): δ = 44.2, 45.0, 46.2, 47.5, 50.5 (-, CH₂-cyclen and CH₂-azacrown), 70.8, 71.1, 71.3, 71.4, 71.5 (-, CH₂-azacrown), 117.0 (C_{quat}, q, ¹J_{C,F} = 287.8 Hz, CF₃COO⁻), 160.6 (C_{quat}, q, ²J_{C,F} = 36.5 Hz, CF₃COO⁻), 162.1, 165.8 (C_{quat}, C_{Aryl}-N); MS (ESI, MeOH + 10 mmol/l NH₄Ac): m/z (%) = 342 (100) [M⁶⁺ - 4 H]²⁺, 683 (30) [M⁶⁺ - 5 H]⁺, 353 (28) [M⁶⁺ - 5 H + Na]²⁺, 705 (9) [M⁶⁺ - 6 H + Na]⁺.

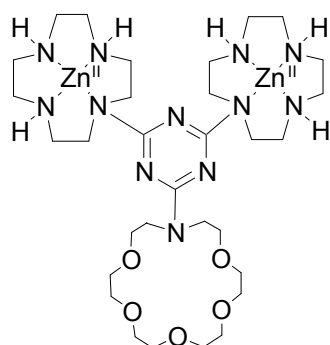
16-[4,6-Bis-(1,4,7,10-tetraaza-cyclododec-1-yl)-[1,3,5]triazine-2-yl]-1,4,7,10,13-pentaoxa-16-aza-cyclooctadecane (L4)



A procedure analogous to that described for **L1** was followed. The free amine **L4** was obtained quantitatively as a colorless solid.

Melting point: 58 °C; IR (KBr): $\tilde{\nu}$ [cm⁻¹] = 3441, 2952, 2867, 1572, 1348, 1125, 773; UV/Vis (CH₃CN): λ_{max} [nm] (lg ϵ) = 228 (4.482); ¹H NMR (300 MHz, MeOH-d₄): δ = 2.65-2.67 (m, 8 H, CH₂-cyclen), 2.72-2.74 (m, 8 H, CH₂-cyclen), 2.91-2.94 (m, 8 H, CH₂-cyclen), 3.54-3.87 (m, 32 H, CH₂-cyclen and CH₂-azacrown); ¹³C NMR (75 MHz, MeOH-d₄): δ = 47.3, 49.0, 49.5, 49.6, 50.1 (-, CH₂-cyclen and CH₂-azacrown), 70.9, 71.6, 71.7, 71.8, 71.9 (-, CH₂-azacrown), 166.0 (C_{quat}, C_{Aryl}-N_{azacrown}), 168.0 (C_{quat}, C_{Aryl}-N_{cyclen}); MS (ESI, MeOH + 10 mmol/l NH₄Ac): m/z (%) = 684 (100) [MH]⁺, 342 (25) [M + 2 H]²⁺; HRMS (C₃₁H₆₃N₁₂O₅): calcd 683.6044 [MH]⁺, obsd 683.6051 [MH]⁺ \pm 0.73 ppm.

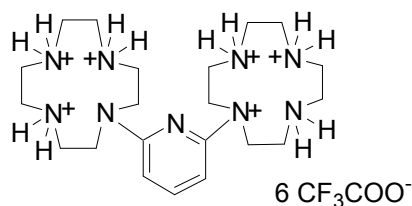
[Zn₂L4](ClO₄)₄



A procedure analogous to that described for **Zn₂L2** was followed. To a solution of **L4** (0.39 g, 0.57 mmol) in methanol (20 mL) under intense stirring portions of a solution of Zn(ClO₄)₂ · 6 H₂O (0.424 g, 1.14 mmol) in methanol (12 mL) were added. At the beginning a colorless precipitate appeared, which dissolved after addition of the total amount of zinc salt. The mixture was refluxed for 24 h. After removal of all solvents under vacuum the residue was dissolved in methanol, cooled in an ice bath and some petroleum ether was added to yield the product as colorless crystals. Yield: 0.571 g (82%).

Melting point: 168 °C; IR (KBr): $\tilde{\nu}$ [cm⁻¹] = 3537, 3261, 2963, 2883, 1567, 1347, 1085, 814, 627; UV/Vis (CH₃CN): λ_{max} [nm] (lg ϵ) = 225 (4.575); ¹H NMR (300 MHz, CD₃CN): δ = 2.65-3.16 (m, 24 H, cyclen-CH₂), 3.34-3.91 (m, 34 H, CH₂-cyclen, CH₂-azacrown and NH), 4.24-4.28 (m, 4 H, CH₂-cyclen); ¹³C NMR (75 MHz, CD₃CN): δ = 44.5, 45.9, 46.8, 48.0, 49.4 (-, CH₂-cyclen and CH₂-azacrown), 70.2, 70.6, 70.7, 71.0, 71.1 (-, CH₂-azacrown), 165.9 (C_{quat}, C_{Aryl}-N_{azacrown}), 170.9 (C_{quat}, C_{Aryl}-N_{cyclen}); MS (ESI, CH₃CN): m/z (%) = 465 (100) [M⁴⁺ + 2 CH₃COO⁻]²⁺, 486 (55) [M⁴⁺ + ClO₄⁻ + CH₃COO⁻]²⁺, 1071 (10) [M⁴⁺ + 2 ClO₄⁻ + CH₃COO⁻]⁺; (ESI, negative, CH₃CN): 1227 (100) [M⁴⁺ + 4 ClO₄⁻ + OH]⁻, 1269 (85) [M⁴⁺ + 4 ClO₄⁻ + CH₃COO⁻]⁻, 1309 (22) [M⁴⁺ + 5 ClO₄⁻]⁻.

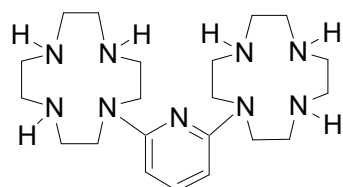
2,6-Bis-(10-aza-1,4,7-azonia-cyclododec-10-yl)-pyridine-hexakis-trifluoroacetate (**13**)



A procedure analogous to that described for **3** was followed starting from a solution of **12**²¹ (0.60 g, 0.59 mmol) in dichloromethane (20 mL) and TFA (2.7 mL, 4.03 g, 35.42 mmol). Compound **13** was isolated quantitatively as colorless solid.

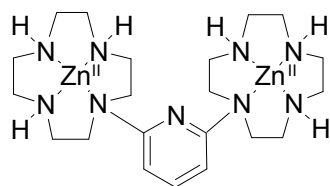
Melting point: 98-100 °C; IR (KBr): $\tilde{\nu}$ [cm⁻¹] = 3299, 2995, 2875, 1571, 1196, 778; UV/Vis (CH₃CN): λ_{max} [nm] (lg ϵ) = 221 (4.145), 255 (3.978), 317 (3.981); ¹H NMR (300 MHz, CD₃CN): δ = 3.07-3.25 (m, 24 H, CH₂-cyclen), 3.73-3.88 (m, 8 H, CH₂-cyclen), 6.07 (d, 2 H, ³J = 8.2 Hz, CH-pyridine), 7.34 (t, 1 H, ³J = 8.2 Hz, CH-pyridine), 8.53 (bs, 12 H, NH₂⁺); ¹³C NMR (75 MHz, CD₃CN): δ = 44.5, 45.9, 46.9, 47.8 (-, CH₂-cyclen), 98.7 (+, C_{Aryl}-H pyridine), 117.1 (C_{quat}, q, ¹J_{C,F} = 288.1 Hz, CF₃COO⁻), 140.7 (+, C_{Aryl}-H pyridine), 158.6 (C_{quat}, C_{Aryl}-N pyridine), 160.7 (C_{quat}, q, ²J_{C,F} = 36.8 Hz, CF₃COO⁻); MS (ESI, CH₃CN): m/z (%) = 420 (100) [M⁶⁺ - 5 H]⁺, 211 (45) [M⁶⁺ - 4 H]²⁺.

2,6-Di-(1,4,7,10-tetraaza-cyclododecane-1-yl)-pyridine (**L5**)



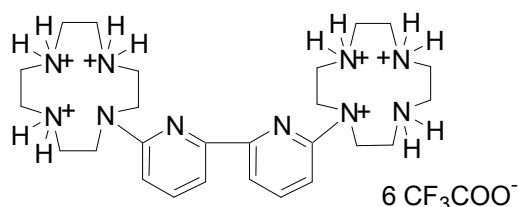
A procedure analogous to that described for **L1** was followed. A solution of **13** (0.55 g, 0.49 mmol) in water (10 mL) was slowly passed through a column of basic ion exchange resin (30 mL). The free amine **L5** was obtained as colorless solid. Yield: 0.203 g (99%).

Melting point: 85 °C; IR (KBr): $\tilde{\nu}$ [cm⁻¹] = 3352, 2981, 2874, 1582, 1342, 1212, 777; UV/Vis (CH₃CN): λ_{max} [nm] (lg ϵ) = 225 (4.221), 258 (4.060), 321 (4.167); ¹H NMR (300 MHz, CDCl₃): δ = 2.62-2.66 (m, 8 H, CH₂-cyclen), 2.76-2.87 (m, 8 H, CH₂-cyclen), 2.91-2.99 (m, 8 H, CH₂-cyclen), 3.62-3.68 (m, 8 H, CH₂-cyclen), 6.07 (d, 2 H, ³J = 8.1 Hz, CH-pyridine), 7.28 (t, 1 H, ³J = 8.1 Hz, CH-pyridine and CDCl₃); ¹³C NMR (75 MHz, CDCl₃): δ = 46.4, 48.1, 48.8, 50.8 (-, CH₂-cyclen), 96.3 (+, C_{Aryl}-H-pyridine), 138.4 (+, C_{Aryl}-H-pyridine), 158.7 (C_{quat}, C_{Aryl}-N-pyridine); MS (ESI, MeOH/CH₂Cl₂ + 1 % AcOH): m/z (%) = 420 (100) [MH]⁺, 442 (15) [M + Na]⁺; HRMS (C₂₁H₄₂N₉): calcd 420.3563 [MH]⁺, obsd 420.3561 [MH]⁺ ± 0.82 ppm.

[Zn₂L5](ClO₄)₄ · H₂O

A procedure analogous to that described for **Zn₂L2** was followed. To a solution of **L5** (0.18 g, 0.43 mmol) in methanol (20 mL) were added slowly under stirring portions of a solution of Zn(ClO₄)₂ · 6 H₂O (0.32 g, 0.86 mmol) in methanol (10 mL). A colorless precipitate immediately appeared. The mixture was stirred for 18 h at room temperature and then refluxed for 30 min. The precipitate was dissolved during reflux and the clear solution became slightly brown. Half of the amount of solvent was removed under vacuum. The mixture was cooled overnight. Colorless crystals were obtained after filtration and were washed with cold methanol. Yield: 0.216 g (53%).

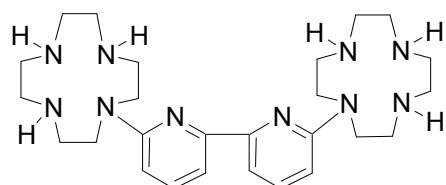
Melting point: 201 °C (decomposition); IR (KBr): $\tilde{\nu}$ [cm⁻¹] = 3580, 3372, 2997, 2878, 1575, 1346, 1211, 779; UV/Vis (CH₃CN): λ_{max} [nm] (lg ϵ) = 223 (4.170), 256 (4.001), 319 (4.121); ¹H NMR (300 MHz, CD₃CN): δ = 2.81-2.89 (m, 4 H, CH₂-cyclen), 2.95-3.18 (m, 8 H, CH₂-cyclen), 3.29-3.50 (m, 8 H, CH₂-cyclen), 3.75-3.99 (18 H, CH₂-cyclen and NH), 7.35 (d, 2 H, ³J = 8.0 Hz, CH-pyridine), 8.06 (t, 1 H, ³J = 8.1 Hz, CH-pyridine); ¹³C NMR (75 MHz, CD₃CN): δ = 43.9, 44.5, 45.1, 52.9 (-, CH₂-cyclen), 106.9 (+, C_{Aryl}-H-pyridine), 141.1 (+, C_{Aryl}-H-pyridine), 159.9 (C_{quat}, C_{Aryl}-N-pyridine); MS (ESI, CH₃CN): m/z (%) = 215 (100) [M⁴⁺ + ClO₄]³⁺, 229 (80) [M⁴⁺ + ClO₄ + CH₃CN]³⁺; Anal. Calcd for C₂₁H₄₁N₉O₁₆Cl₄Zn₂ · H₂O: C 26.11, H 4.49, N 13.05. Found: C 25.98, H 4.45, N 12.81.

6,6'-Bis-(10-aza-1,4,7-azonia-cyclododec-10-yl)-[2,2']bipyridine-hexakis-trifluoroacetate (15)


A procedure analogous to that described for **3** was followed starting from a solution of **14**²¹ (1.20 g, 1.09 mmol) in dichloromethane (40 mL) and TFA (5 mL, 7.48 g, 65.63 mmol). After addition of TFA the solution is colored intensively yellow. The solvent and the excess of TFA were removed under vacuum. The salt **15** was isolated quantitatively as yellow, viscous oil. Yield: 1.29 g (quantitative).

IR (KBr): $\tilde{\nu}$ [cm⁻¹] = 3432, 3261, 2915, 2878, 1677, 1615, 1435, 1201, 787, 718; UV/Vis (CH₃CN): λ_{max} [nm] (lg ϵ) = 227 (4.170), 259 (3.237), 339 (3.091); ¹H NMR (400 MHz, CD₃CN): δ = 3.16-3.18 (m, 8 H, CH₂-cyclen), 3.25-3.28 (m, 16 H, CH₂-cyclen), 3.89-3.94 (m, 8 H, CH₂-cyclen), 7.02 (d, 2 H, ³*J* = 8.7 Hz, CH-pyridine), 7.56 (d, 2 H, ³*J* = 7.3 Hz, CH-pyridine), 7.88 (dd, 2 H, ³*J* = 8.7 Hz, ³*J* = 7.3 Hz, CH-pyridine), 8.54 (bs, 12 H, NH₂⁺); ¹H NMR (250 MHz, D₂O): δ = 3.06-3.10 (m, 8 H, CH₂-cyclen), 3.15-3.19 (m, 16 H, CH₂-cyclen), 3.78-3.82 (m, 8 H, CH₂-cyclen), 7.04 (d, 2 H, ³*J* = 8.9 Hz, CH-pyridine), 7.53 (d, 2 H, ³*J* = 7.5 Hz, CH-pyridine), 7.87 (dd, 2 H, ³*J* = 8.9 Hz, ³*J* = 7.5 Hz, CH-pyridine); ¹³C NMR (100 MHz, CD₃CN): δ = 45.5, 45.6, 47.1, 50.4 (-, CH₂-cyclen), 112.0 (+, C_{Aryl}-H-pyridine), 112.7 0 (+, C_{Aryl}-H-pyridine), 118.4 (C_{quat}, q, ¹*J*_{C,F} = 289.9 Hz, CF₃COO⁻), 142.4 0 (+, C_{Aryl}-H-pyridine), 148.1 (C_{quat}, C_{Aryl}-N-pyridine), 156.9 (C_{quat}, C_{Aryl}-N-pyridine), 161.0 (C_{quat}, q, ²*J*_{C,F} = 36.9 Hz, CF₃COO⁻); (63 MHz, D₂O): δ = 43.9, 44.3, 45.4, 48.8 (-, CH₂-cyclen), 112.3, 113.0 (+, C_{Aryl}-H-pyridine), 116.2 (C_{quat}, q, ¹*J*_{C,F} = 291.2 Hz, CF₃COO⁻), 142.9 (+, C_{Aryl}-H-pyridine), 143.5 (C_{quat}, C_{Aryl}-N-pyridine), 154.9 (C_{quat}, C_{Aryl}-N-pyridine), 162.6 (C_{quat}, q, ²*J*_{C,F} = 35.9 Hz, CF₃COO⁻); MS (ESI, MeOH/H₂O + 10 mmol/l NH₄Ac): *m/z* (%) = 497 (100) [M⁶⁺ - 5 H]⁺, 249 (50) [M⁶⁺ - 4 H]²⁺.

6, 6'-Bis-(1,4,7,10-tetraaza-cyclododec-1-yl)-[2,2']bipyridinyl (L6)

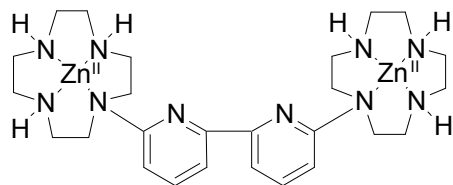


A procedure analogous to that described for **L1** was followed. A solution of **15** (1.10 g, 0.93 mmol) in water (25 mL) was slowly passed through a column of basic ion exchange resin (60 mL). The free amine **L6** was obtained as pale yellow solid. Yield: 0.451 g (98%).

Melting point: 95 °C; IR (KBr): $\tilde{\nu}$ [cm⁻¹] = 3415, 2926, 2833, 1651, 1574, 1471, 1363, 787, 737; UV/Vis (CH₃CN): λ_{max} [nm] (lg ϵ) = 230 (3.877), 269 (3.675), 351 (3.391); ¹H NMR (400 MHz, MeOH-d₄): δ = 2.61-2.64 (m, 8 H, CH₂-cyclen), 2.71-2.73 (m, 8 H, CH₂-cyclen), 2.95-3.19 (m, 8 H, CH₂-cyclen), 3.68-3.73 (m, 8 H, CH₂-cyclen), 6.83 (d, 2 H, ³*J* = 8.4 Hz, CH-pyridine), 7.62 (dd, 2 H, ³*J* = 8.4 Hz, ³*J* = 7.4 Hz, CH-pyridine), 7.73 (d, 2 H, ³*J* = 7.4 Hz, CH-pyridine); ¹³C NMR (100 MHz, MeOH-d₄): δ = 46.8, 48.4, 49.0, 51.6 (-, CH₂-cyclen), 109.8 (+, C_{Aryl}-H-pyridine), 111.6 (+, C_{Aryl}-H-pyridine), 139.2 (+, C_{Aryl}-H-pyridine), 155.6 (C_{quat}, C_{Aryl}-N-pyridine), 160.7 (C_{quat}, C_{Aryl}-N-pyridine); MS (ESI, MeOH + 10 mmol/l

NH₄Ac): m/z (%) = 497 (100) [MH]⁺, 249 (60) [M + 2 H]²⁺; HRMS (C₂₆H₄₅N₁₀): calcd 497.3829 [MH]⁺, obsd 497.3828 [MH]⁺ ± 0.49 ppm.

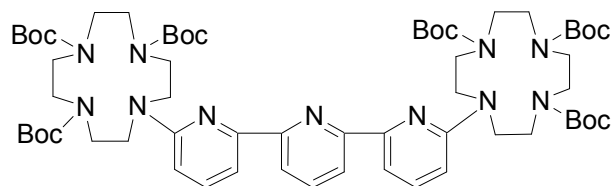
[Zn₂L6](ClO₄)₄ · H₂O



A procedure analogous to that described for **Zn₂L2** was followed. To a solution of **L6** (0.38 g, 0.77 mmol) in methanol (20 mL) were added slowly under intense stirring portions of a solution of Zn(ClO₄)₂ · 6 H₂O (0.57 g, 1.53 mmol) in methanol (15 mL). A colorless precipitate immediately appeared. The mixture was stirred for 22 h at room temperature and then refluxed for 4 h. The solvent was removed under vacuum. Pale yellow crystals were obtained after recrystallization from a mixture of MeOH/water (4:1). The concentrated filtrate solution showed the same analytical purity of the product and thus both fractions were united. Yield: 0.765 g (98%).

Melting point: 235-237 °C; IR (KBr): $\tilde{\nu}$ [cm⁻¹] = 3429, 2945, 2869, 1649, 1576, 1468, 1362, 786, 739; UV/Vis (CH₃CN): λ_{max} [nm] (lg ϵ) = 227 (3.801), 291 (3.569), 342 (2.956); ¹H NMR (600 MHz, CD₃CN): δ = 2.78-2.91 (m, 16 H, CH₂-cyclen), 2.94-2.97 (m, 4 H, CH₂-cyclen), 3.01-3.05 (m, 4 H, CH₂-cyclen), 3.08-3.11 (m, 2 H, NH), 3.17-3.21 (m, 4 H, CH₂-cyclen), 3.32-3.36 (m, CH₂-cyclen), 3.53-3.58 (m, 4 H, NH), 7.67 (d, 2 H, ³J = 8.04 Hz, CH-pyridine), 8.06 (d, 2 H, ³J = 7.65 Hz, CH-pyridine), 8.17 (dd, 2 H, ³J = 8.04 Hz, ³J = 7.65 Hz, CH-pyridine); ¹³C NMR (150 MHz, CD₃CN): δ = 44.3 (-, CH₂-cyclen), 44.9 (-, CH₂-cyclen), 45.8 (-, CH₂-cyclen), 53.5 (-, CH₂-cyclen), 119.7 (+, C_{Aryl}-H-pyridine), 122.9 (+, C_{Aryl}-H-pyridine), 142.9 (+, C_{Aryl}-H-pyridine), 154.8 (C_{quat}, C_{Aryl}-N-pyridine), 162.7 (C_{quat}, C_{Aryl}-N-pyridine); MS (ESI, CH₃CN/H₂O): m/z (%) = 241 (100) [M⁴⁺ + ClO₄]³⁺, 228 (70) [M⁴⁺ + CH₃COO]³⁺, 370 (50) [M⁴⁺ + ClO₄ + OH]²⁺; (ESI, negative, CH₃CN/H₂O): m/z (%) = 1041 (100) [M⁴⁺ + 4 ClO₄ + OH]⁻; Anal. Calcd for C₂₆H₄₄N₁₀O₁₆Cl₄Zn₂ · H₂O: C 29.93, H 4.44, N 13.43. Found: C 29.81, H 4.21, N 13.11.

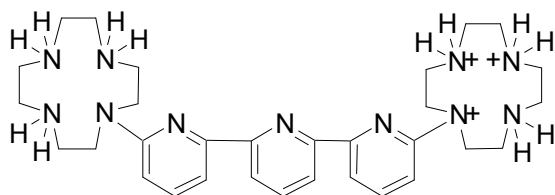
6,6''-Bis-(1,4,7-tris[*tert*-butyloxycarbonyl]-1,4,7,10-tetraazacyclododecane)-[2,2':6',2'']-terpyridine (16)



Compound **16** was prepared according to the procedure **B** described in literature.²¹ A mixture of 1,4,7,10-tetraazacyclododecane-1,4,7-tricarboxylic acid tri-*tert*-butyl ester (1.90 g, 4.03 mmol) and 6,6'-dibrom-[2,2':6',2'']terpyridine (0.75 g, 1.92 mmol) was treated with sodium *tert*-butylate. Pd(OAc)₂/PPh₃ was used as catalyst. The reaction mixture was heated for 34 h at 80 °C and then purified by column chromatography on silica. Compound **16** (*R_f* = 0.11, ethyl acetate/petroleum ether, 3:7) was isolated as the main product. Yield: 1.54 g (68%, 81% corrected yield according to starting material conversion). The dehydrohalogenation product (0.125 g, 9%, 11% corrected yield according to starting material conversion; *R_f* = 0.19, EE/PE, 3:7) was isolated as side product. The homoaryl coupling product was not formed in a significant amount and was only observed by mass spectroscopy in the raw reaction mixture (MS (ESI, CH₂Cl₂/MeOH + 1 % AcOH): *m/z* (%) = 1406 (9) [MH]⁺).

Melting point: 127 °C; IR (KBr): $\tilde{\nu}$ [cm⁻¹] = 2974, 2930, 1703, 1568, 1412, 1250, 1171, 860, 778, 633; UV/Vis (CH₃CN): λ_{max} [nm] (lg ϵ) = 226 (3.592), 271 (3.429), 350 (2.984); ¹H NMR (600 MHz, CDCl₃): δ = 1.45 (s, 54 H, CH₃-Boc), 3.25-3.78 (m, 32 H, CH₂-cyclen), 6.64 (d, 2 H, ³*J* = 8.3 Hz, CH-pyridine), 7.61 (dd, 2 H, ³*J* = 8.3 Hz, ³*J* = 7.4 Hz, CH-pyridine), 7.86 (t, 1 H, ³*J* = 7.8 Hz, CH g), 7.97 (d, 2 H, ³*J* = 7.4 Hz, CH-pyridine), 8.30 (d, 2 H, ³*J* = 7.8 Hz, CH-pyridine); ¹³C NMR (150 MHz, CDCl₃): δ = 28.4, 28.5 (+, CH₃-Boc), 50.3, 50.7, 52.2 (-, CH₂-cyclen), 79.9, 80.2 (C_{quat}, C-Boc), 108.0 (+, C_{Aryl}-H-pyridine), 110.1 (+, C_{Aryl}-H-pyridine), 120.1 (+, C_{Aryl}-H-pyridine), 137.4 (+, C_{Aryl}-H-pyridine), 138.1 (+, C_{Aryl}-H-pyridine), 154.0, 155.8 (C_{quat}, C_{Aryl}-N-pyridine), 156.4 (C_{quat}, C=O Boc), 159.1 (C_{quat}, C_{Aryl}-N-pyridine); MS (ESI, CH₂Cl₂/MeOH + 10 mmol/l NH₄Ac): *m/z* (%) = 1175 (100) [MH]⁺, 588 (20) [M + 2 H]²⁺, 1197 (10) [M + Na]⁺; Anal. Calcd for C₆₁H₉₅N₁₁O₁₂: C 62.37, H 8.16, N 13.12. Found: C 62.05, H 8.15, N 12.58.

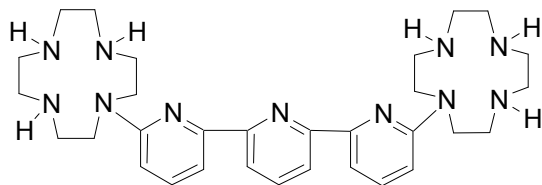
6,6''-Bis-(10-aza-1,4,7-azonia-cyclododec-10-yl)-[2,2':6',2'']terpyridine-hexakis-trifluoro-acetate (17)



A procedure analogous to that described for **3** was followed starting from a solution of **16** (0.90 g, 0.77 mmol) in dichloromethane (40 mL) and TFA (3.5 mL, 5.18 g, 45.44 mmol). After addition of TFA the color of the solution turns intensively yellow. The salt **17** was isolated quantitatively as yellow, very viscous oil, in quantitative yield.

IR (KBr): $\tilde{\nu}$ [cm⁻¹] = 3445, 2991, 2889, 1679, 1610, 1202, 1136, 866, 789, 718; UV/Vis (CH₃CN): λ_{max} [nm] (lg e) = 224 (3.738), 261 (3.504), 334 (3.210); ¹H NMR (300 MHz, CD₃CN): δ = 3.12-3.14 (m, 8 H, CH₂-cyclen), 3.20-3.26 (m, 16 H, CH₂-cyclen), 3.89-3.92 (m, 8 H, CH₂-cyclen), 7.06 (d, 2 H, ³J = 8.7 Hz, CH), 7.71 (d, 2 H, ³J = 7.4 Hz, CH), 7.86-7.99 (m, 3 H, CH), 8.28 (bs, 12 H, NH₂⁺), 8.45 (d, 2 H, ³J = 7.9 Hz, CH); ¹³C NMR (75 MHz, CD₃CN): δ = 45.4, 45.6, 47.3, 50.2 (-, CH₂-cyclen), 112.9, 113.6 (+, C_{Aryl}-H), 117.0 (C_{quat}, q, ¹J_{C,F} = 287.5 Hz, CF₃COO⁻), 124.5, 141.4, 145.5 (+, C_{Aryl}-H), 146.9, 150.9, 158.5 (C_{quat}, C_{Aryl}-N), 160.8 (C_{quat}, q, ²J_{C,F} = 36.9 Hz, CF₃COO⁻); MS (ESI, MeOH + 10 mmol/l NH₄Ac): *m/z* (%) = 574 (40) [M⁶⁺ - 5 H]⁺, 288 (100) [M⁶⁺ - 4 H]²⁺.

6,6''-Bis-(1,4,7,10-tetraaza-cyclododec-1-yl)-[2,2':6',2'']terpyridine (L7)

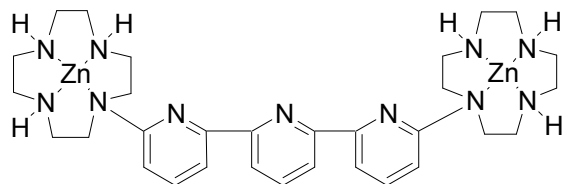


A procedure analogous to that described for **L1** was followed. A solution of **17** (0.706 g, 0.56 mmol) in water (20 mL) was slowly passed through a column of basic ion exchange resin (35 mL). The free amine **L7** was obtained as pale yellow solid. Yield: 0.311 g (97%).

Melting point: 98-100 °C; IR (KBr): $\tilde{\nu}$ [cm⁻¹] = 3448, 2925, 2854, 1621, 1568, 1428, 1365, 787; UV/Vis (CH₃CN): λ_{max} [nm] (lg e) = 226 (4.082), 270 (3.910), 349 (3.475); ¹H NMR (300 MHz, MeOH-d₄): δ = 2.68-2.71 (m, 8 H, CH₂-cyclen), 2.75-2.79 (m, 8 H, CH₂-cyclen), 3.03-3.11 (m, 8 H, CH₂-cyclen), 3.71-3.79 (m, 8 H, CH₂-cyclen), 6.89 (d, 2 H, ³J = 8.4 Hz, CH-pyridine), 7.72 (dd, 2H, ³J = 8.4 Hz, ³J = 7.4 Hz, CH-pyridine), 7.94-8.02 (m, 3 H, CH-pyridine), 8.39 (d, 2 H, ³J = 7.8 Hz, CH-pyridine); ¹³C NMR (75 MHz, MeOH-d₄): δ = 45.2,

47.0, 48.1, 49.9 (-, CH₂-cyclen), 108.2 (+, C_{Aryl}-H-pyridine), 110.1 (+, C_{Aryl}-H-pyridine), 120.0 (+, C_{Aryl}-H-pyridine), 137.2 (+, C_{Aryl}-H-pyridine), 137.9 (+, C_{Aryl}-H-pyridine), 153.5, 155.6 (C_{quat}, C_{Aryl}-N-pyridine), 158.9 (C_{quat}, C_{Aryl}-N-pyridine); MS (ESI, MeOH + 10 mmol/l NH₄Ac): m/z (%) = 574 (100) [MH]⁺, 288 (60) [M + 2 H]²⁺; HRMS (C₃₁H₄₈N₁₁): calcd 574.4094 [MH]⁺, obsd 574.4096 [MH]⁺ ± 1.27 ppm.

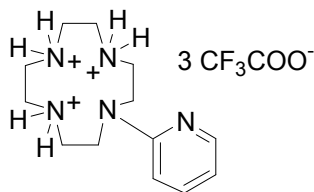
[Zn₂L7](ClO₄)₄ · CH₃CN



A procedure analogous to that described for **Zn₂L2** was followed. To a solution of **L7** (0.214 g, 0.37 mmol) in methanol (20 mL) were added slowly under intense stirring portions of a solution of Zn(ClO₄)₂ · 6 H₂O (0.28 g, 0.74 mmol) in methanol (15 mL). A colorless precipitate immediately appeared. The mixture was stirred for 21 h at room temperature and then refluxed for 2 h. The solvent was removed under vacuum. Pale yellow crystals were obtained after recrystallization from a mixture of MeOH/CH₃CN and 0.1 N HCl (2:4:1). Yield: 0.29 g (71%).

Melting point: 232 °C; IR (KBr): $\tilde{\nu}$ [cm⁻¹] = 3429, 2965, 2891, 1652, 1570, 1467, 1365, 791; UV/Vis (CH₃CN): λ_{max} [nm] (lg ϵ) = 224 (4.005), 265 (3.742), 343 (3.198); ¹H NMR (300 MHz, CD₃CN): δ = 2.70-2.78 (m, 4 H, CH₂-cyclen), 2.86-2.98 (m, 16 H, CH₂-cyclen), 3.19-3.25 (m, 8 H, CH₂-cyclen), 3.38-3.42 (m, 2 H, NH), 3.74-3.85 (m, 8 H, CH₂-cyclen and NH), 7.34 (d, 2 H, ³J = 8.1 Hz, CH), 7.89-8.09 (m, 3 H, CH), 8.37-8.43 (m, 4 H, CH); ¹³C NMR (75 MHz, CH₃CN): δ = 44.6, 44.8, 46.2, 52.5 (-, CH₂-cyclen), 117.8, 118.9, 123.0, 139.7, 141.1 (+, C_{Aryl}-H), 155.6, 156.8, 160.5 (C_{quat}, C_{Aryl}-N); MS (ESI, MeOH/CH₃CN): m/z (%) = 410 (100) [M⁴⁺ + 2 CH₃COO]²⁺, 450 (40) [M⁴⁺ + 2 ClO₄]²⁺; Anal. Calcd for C₃₁H₄₇N₁₁O₁₆Cl₄Zn₂ · CH₃CN: C 34.67, H 4.41, N 14.70. Found: C 34.71, H 4.49, N 14.92.

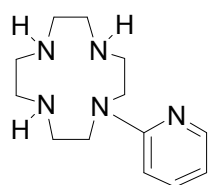
10-(2-Pyridinyl)-10-aza-1,4,7-triazonia-cyclododecane-*tris*-trifluoroacetate (**19**)



A procedure analogous to that described for **3** was followed starting from a solution of **18**²¹ (1 g, 1.82 mmol) in dichloromethane (35 mL) and TFA (4.2 mL, 6.22 g, 54.53 mmol). The product **19** was obtained quantitatively as pale yellow, viscous oil.

Melting point: 198-201 °C; IR (KBr): $\tilde{\nu}$ [cm⁻¹] = 3421, 2951, 1630, 1538, 1484, 1284, 1095, 774; UV/Vis (CH₃CN): λ_{max} [nm] (lg ϵ) = 249 (4.012), 304 (3.401); ¹H NMR (250 MHz, D₂O): δ = 3.09-3.15 (m, 8 H, CH₂-cyclen), 3.29-3.39 (m, 4 H, CH₂-cyclen), 3.82-3.86 (m, 4 H, CH₂-cyclen), 6.99 (dd, 1 H, ³*J* = 7.0 Hz, ³*J* = 7.2 Hz, CH-pyridine), 7.16 (d, 1 H, ³*J* = 9.3 Hz, CH-pyridine), 7.88 (m, 1 H, CH-pyridine), 8.01 (m, 1 H, CH-pyridine); (600 MHz, CD₃CN): δ = 3.19-3.21 (m, 8 H, CH₂-cyclen), 3.34-3.36 (m, 4 H, CH₂-cyclen), 3.89-3.90 (m, CH₂-cyclen), 7.09 (dd, 1 H, ³*J* = 7.13 Hz, ³*J* = 6.31 Hz CH-pyridine), 7.18 (d, 1 H, ³*J* = 9.26 Hz, CH-pyridine), 8.03 (dd, 1 H, ³*J* = 6.31 Hz, ⁴*J* = 1.78 Hz, CH-pyridine), 8.08 (ddd, 1 H, ³*J* = 9.26 Hz, ³*J* = 7.13 Hz, ⁴*J* = 1.78 Hz, CH-pyridine); ¹³C NMR (63 MHz, D₂O): δ = 44.3, 44.6, 45.7, 49.9 (-, CH₂-cyclen), 112.9, 114.3 (+, C_{Aryl}-H), 116.2 (C_{quart}, q, ¹*J*_{C,F} = 292.4 Hz, CF₃COO⁻), 136.6, 145.2 (+, C_{Aryl}-H), 152.1 (C_{quart}, C_{Aryl}-N), 162.8 (C_{quart}, q, ²*J*_{C,F} = 36.1 Hz, CF₃COO⁻); (150 MHz, CD₃CN): δ = 44.3, 44.9, 45.5, 50.1 (-, CH₂-cyclen), 112.8 (+, C_{Aryl}-H-pyridine), 113.9 (+, C_{Aryl}-H-pyridine), 116.5 (C_{quart}, q, ¹*J*_{C,F} = 291.9 Hz, CF₃COO⁻), 136.9 (+, C_{Aryl}-H-pyridine), 144.6 (+, C_{Aryl}-H 3), 152.5 (C_{quart}, C_{Aryl}-N-pyridine), 159.3 (C_{quart}, q, ²*J*_{C,F} = 36.4 Hz, CF₃COO⁻); MS (ESI, CH₃CN): *m/z* (%) = 250 (100) [M³⁺ - 2 H]⁺.

1-(2-Pyridinyl)-1,4,7,10-tetraazacyclododecane (**L8**)

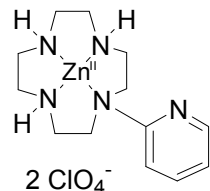


A procedure analogous to that described for **L1** was followed. A solution of **19** (0.8 g, 1.35 mmol) in water (20 mL) was slowly passed through a column of basic ion exchange resin (45 mL). The free amine **L8** was obtained as colorless solid. Yield: 0.32 g (95%).

Melting point: 89 °C; IR (KBr): $\tilde{\nu}$ [cm⁻¹] = 3410, 2927, 2831, 1628, 1558, 1360, 1283, 770, 599; UV/Vis (CH₃CN): λ_{max} [nm] (lg ϵ) = 251 (4.134), 309 (3.638); ¹H NMR (300 MHz, MeOH-d₄): δ = 2.56-2.65 (m, 4 H, CH₂-cyclen), 2.71-2.79 (m, 4 H, CH₂-cyclen), 2.87-2.94 (m, 4 H, CH₂-cyclen), 3.62-3.66 (m, 4 H, CH₂-cyclen), 6.62-6.67 (m, 1 H, CH-pyridine), 6.83 (d, 1 H, ³*J* = 8.7 Hz, CH-pyridine), 7.51-7.55 (m, 1 H, CH-pyridine), 8.06-8.10 (dd, 1 H, ³*J* = 6.7 Hz, ⁴*J* = 1.9 Hz, CH-pyridine); ¹³C NMR (75 MHz, MeOH-d₄): δ = 46.7, 48.4, 49.1, 51.2 (-, CH₂-cyclen), 109.8, 114.4, 138.7, 148.4 (+, C_{Aryl}-H), 161.0 (C_{quart}, C_{Aryl}-N); MS (ESI,

CH₂Cl₂/MeOH + 10 mmol/l NH₄Ac): m/z (%) = 250 (100) [MH]⁺; Anal. Calcd for C₁₃H₂₃N₅: C 62.62, H 9.30, N 28.09. Found C 62.43, H 9.11, N 27.72.

[ZnL8](ClO₄)₂



A procedure analogous to that described for **ZnL1** was followed. To a solution of **L8** (0.2 g, 0.80 mmol) in methanol (15 mL) were added under intense stirring portions of a solution of Zn(ClO₄)₂ · 6 H₂O (0.298 g, 0.80 mmol) in methanol (5 mL). The mixture was refluxed for 15 h. After removal of the solvent under vacuum the residue was recrystallized from a mixture of MeOH/H₂O 3:1. The product was isolated as colorless crystals. Yield: 0.409 g (95%).

Melting point: 234 °C; IR (KBr): $\tilde{\nu}$ [cm⁻¹] = 3214, 2920, 2872, 1588, 1383, 1285, 780, 592; UV/Vis (CH₃CN): λ_{max} [nm] (lg ϵ) = 250 (4.007), 305 (3.509); ¹H NMR (300 MHz, MeOH-d₄): δ = 2.50-2.62 (m, 2 H, CH₂-cyclen), 2.81-2.94 (m, 6 H, CH₂-cyclen), 2.99-3.09 (m, 4 H, CH₂-cyclen), 3.35-3.44 (m, 4 H, CH₂-cyclen), 7.61-7.66 (m, 1 H, CH-pyridine), 7.78 (d, 1 H, ³J = 8.2 Hz, CH-pyridine), 8.18-8.25 (m, 1 H, CH-pyridine), 8.49 (dd, 1 H, ³J = 7.8 Hz, ⁴J = 1.8 Hz, CH-pyridine); ¹³C NMR (75 MHz, MeOH-d₄): δ = 46.4, 46.5, 46.8, 53.1 (-, CH₂-cyclen), 121.6, 126.5, 144.7, 149.2 (+, C_{Aryl}-H), 160.1 (C_{quart}, C_{Aryl}-N); MS (ESI, MeOH/CH₂Cl₂ + 10 mmol/l NH₄Ac): m/z (%) = 372 (100) [M²⁺ + CH₃COO]⁺, 412 (35) [M²⁺ + ClO₄]⁺.

1.4.3 Crystallographic Study.

Colorless monoclinic crystals of [Zn₂L2]μ-OH(ClO₄)₃ · CH₃CN · H₂O (0.20 x 0.12 x 0.06 mm) were used for data collection at 173 (± 1) K with graphite-monochromated Mo-Kα radiation (λ = 0.71073 Å) on a STOE-IPDS diffractometer. The structure of the compound [Zn₂L2]μ-OH(ClO₄)₃ · CH₃CN · H₂O was solved by direct methods SIR97 and refined by full-matrix least-squares on F² using SHELXL-97. The molecular structure is illustrated in **Figure 1** by ORTEP drawing with 50% probability thermal ellipsoids. Selected interatomic distances and bond angles around the Zn(II) are presented in **Table 1**.

Crystal data for [Zn₂L2]μ-OH(ClO₄)₃ · CH₃CN · H₂O: C₂₂H₄₇Cl₃N₁₂Zn₂O₁₅, M_r = 956.81, monoclinic, space group P 2₁/n, a = 14.9051(8) Å, b = 10.5525(6) Å, c = 24.4935(13) Å, α = 90°, β = 105.687(6)°, γ = 90°, V = 3709.0 (4) Å³, Z = 4, D_x = 1.713 Mg/m³, μ = 1.592 mm⁻¹,

$F(000) = 1976$, θ -range for data collection from 2.11 to 25.85, index ranges $-18 < h < 18$, $-12 < k < 12$, $-29 < l < 29$, reflections collected = 32904, unique reflections = 7132, $R_{\text{int}} = 0.1253$, data/restraints/parameters 7132/0/490, goodness-of-fit on F^2 is 0.803, final R-index $R_1 = 0.0597$, ($wR_2 = 0.1181$), $\rho_{\text{min}} = -0.692 \text{ e } \text{\AA}^{-3}$, $\rho_{\text{max}} = 0.916 \text{ e } \text{\AA}^{-3}$.

1.4.4 Potentiometric pH Titrations.

The pH titrations were carried out under N_2 at 25°C with a computer controlled pH-meter (pH 3000, WTW) and dosimat (Dosimat 665 and 765, Metrohm). Aqueous or methanol (ratio water/methanol 9:1) solutions of the metal complexes (0.1 mM for the Zn(II) complexes, 0.25 mM for the Cu(II)- and Ni(II) complexes) were titrated with 0.1 M tetraethylammoniumhydroxide (TEAOH) aqueous solution. The ionic strength was adjusted to $I = 0.1$ with tetraethylammoniumperchlorate (TEAP). The TEAOH solutions were calibrated with mono sodium phthalate. A titration of 0.1 M perchloric acid with TEAOH solution was used for calibration and to determine $\log K_W$. For the dinuclear complexes **Zn₂L4** and **Zn₂L5** 0.5 eq. HClO_4 were added to the titration solution in order to determine values in the pH range of 5 to 8. The Irving-factor (A_I) was determined according to $\text{pH}_{\text{measurement}} = \text{pH}_{\text{real}} + A_I$ in the corresponding solvent. For each metal complex at least two independent titrations were made. The complex **CuL1** was not soluble enough to allow a potentiometric pH titration. Data analysis was performed with the program Hyperquad2000 (Version 2.1, P. Gans) and Origin 6.0. The deprotonation constants K_a are defined as $[\text{ML-OH}^-]a_{\text{H}^+}/[\text{ML}]$.

1.4.5 Kinetic Measurements.

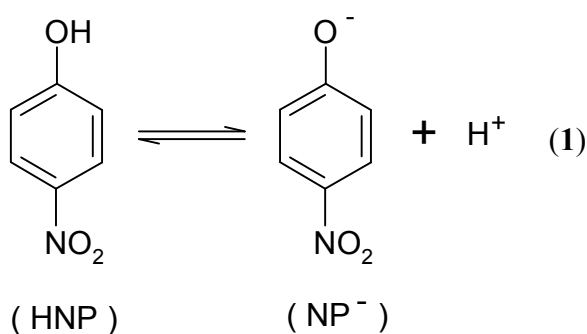
The hydrolysis rate of 4-nitrophenyl acetate (NA) promoted by ML-OH^- species was measured by an initial slope method following the increase in 400 nm-absorption of 4-nitrophenolate in 10% (v/v) CH_3CN aqueous solution in the pH range 6.5 to 9.5 for the Zn(II) complexes and 7 to 9 for the Cu(II) and Ni(II) complexes (50 mM HEPES, TRIS or CHES buffer, $I = 0.1 \text{ M}$, NaCl) at 25°C. The reactions were corrected for the degree of ionization of the 4-nitrophenol at the respective pH and temperature (see Figure 1, chapter 1.4.6). The kinetic data were collected under pseudo-first order conditions (excess of metal complex). Using the $\log e$ value of 4.26 for 4-nitrophenolate (experimentally determined, see chapter 1.4.6) the initial rate of 4-nitrophenolate release was calculated, whereby three independent measurements were made. From the obtained slope ($[\text{produced 4-nitrophenolate}]/\text{time}$) and the concentration of NA, the pseudo-first-order rate constant $k_{\text{obs}}(\text{NA})$ (s^{-1}) was determined.

A plot of these k_{obs} values vs metal complex concentrations at a given pH gave a straight line, its slope representing the second-order rate constant $k_{cat}(NA)$ ($M^{-1}s^{-1}$). All correlation coefficients are > 0.9989 . Correction for the spontaneous hydrolysis of the substrate by the solvent was accomplished either by directly measuring a difference between the production of 4-nitrophenolate in the reaction cell and a reference cell containing the same concentration of carboxyester as in the reaction cell in absence of metal complex, or by separate measurement of the general rate of spontaneous hydrolysis for NA (see Figure 2 chapter 1.4.7). The determined value of $8.16 M^{-1}s^{-1}$ for k_{OH} (the rate constant describing the attack of free OH^- anions) matches the values obtained from the intercepts of the plots of k_{obs} vs metal complex concentrations. The reaction solutions contained 0.1-0.5 mM Cu(II)-, 0.0002-0.075 mM Ni(II)-, 0.005-3.0 mM Zn(II)-complex, 0.003-2.0 mM NA and 50 mM buffer. The absorption increase was recorded immediately after mixing and then monitored until 5% formation of 4-nitrophenolate.

1.4.6 Calculation of the Molar Extinction Coefficients for *para*-nitrophenolate

The hydrolysis of 4-nitrophenyl acetate (NA) releases *p*-nitrophenolate as a product which can be detected spectrophotometrically. The molar extinction coefficient of the nitrophenol anion varies due to the protonation equilibrium, thus due to the pH value and the used buffer system. The molar extinction coefficient was determined experimentally for the pH range 7 to 9 in a buffer system TRIS/HCl (20-80 mM).

For the protonation equilibrium and its equilibrium constant K_a applies:



$$K_a = \frac{[\text{NP}^-][\text{H}^+]}{[\text{HNP}]} \quad (2)$$

According to the *Lambert-Beer* law the absorption in diluted solution is:

$$\text{Abs} = \epsilon_{\text{obs}} d [\text{HNP}]^{\text{total}} = \epsilon_{\text{NP}^-} d [\text{NP}^-] \quad (3)$$

where ϵ_{obs} is the measured extinction coefficient of HNP, ϵ_{NP^-} is the extinction coefficient of the *p*-nitrophenolate ion and d the thickness of the cell. Equations (2) and (3) give equation

(4) which describes the relationship between the molar extinction coefficient and the pH value.

$$\epsilon_{\text{obs}} = \frac{\epsilon_{\text{NP}} K_a}{K_a + [\text{H}^+]} \quad (4)$$

Plots of $1/\epsilon_{\text{obs}}$ versus $[\text{H}^+]$ allow the determination of the molar extinction coefficient of the *p*-nitrophenolate for various pH values and various buffer systems. In the pH range of 7 to 9 for the buffer system TRIS/HCl the respective ϵ_{obs} values were obtained with a regression coefficient of $R^2 > 0.9991$ using a dilution series ($c = 10^{-4}$ to $5 \cdot 10^{-7}$ mol L⁻¹ *p*-nitrophenol). The ϵ_{obs} values for 400 nm are summarised in **Table 1**.

pH ^a	ϵ_{obs} at 400 nm [mol ⁻¹ L cm ⁻¹]
7.01	7805
7.04	8201
7.21	9938
7.28	10628
7.50	12665
7.81	15119
8.11	16581
8.53	17602
8.75	17911
9.01	18097

^a Δ pH = \pm 0.005

Table 1: ϵ_{obs} -values for *p*-nitrophenolate at 400 nm (25 °C, 50 mM TRIS/HCl).

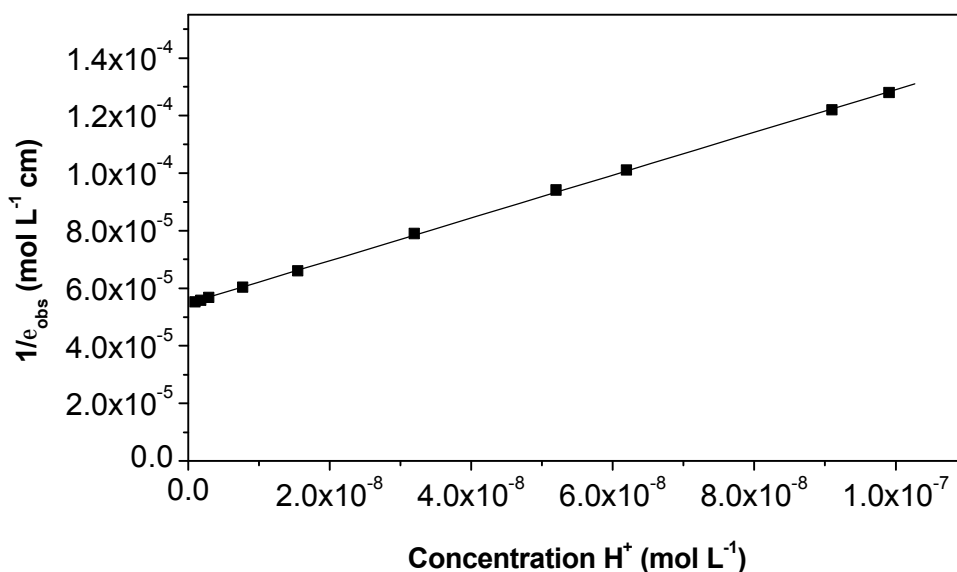


Figure 1: Calculation of the molar extinction coefficient for *p*-nitrophenolate at 400 nm (25 °C, 50 mM TRIS/HCl).

From the slope, respectively the axis segment we can calculate by using equation (4) the equilibrium constant ($pK_a = 7.14 \pm 0.01$) as well as the molar extinction coefficient at 400 nm ($\epsilon_{NP, 400nm} = 18279 \text{ mol}^{-1} \text{ L cm}^{-1}$). The value of the equilibrium constant calculated this way corresponds to the value from literature². Variations in the buffer concentration (TRIS/HCl 20 and 80 mM) or in the ionic strength show no significant changes in the molar extinction coefficient. Changes in the region of $\Delta\epsilon_{NP} \approx \pm 70 \text{ mol}^{-1} \text{ L cm}^{-1}$ were detected.

1.4.7 Calculation of the spontaneous hydrolysis of 4-nitrophenyl acetate (NA)

The nucleophilic attack of OH^- in the used solvent system competes with the metal catalyzed hydrolysis of NA. This spontaneous hydrolysis has to be taken into account when analyzing the reaction kinetics. The spontaneous hydrolysis is a bimolecular reaction, described by equation (5):

$$v = k_{x+y} [\text{OH}^-]^x [\text{Ester}]^y \quad (5)$$

Under the given reaction conditions the velocity of reaction ? is directly proportional to the concentration of the used ester and the concentration of the hydroxide ions. Therefore the spontaneous hydrolysis shows second-order kinetics, with each reactant having a first order dependence. For a constant pH value equation (5) becomes:

² a) J.A. Dean, *Lange's Handbook of Chemistry*, McGraw-Hill, New York, **1973**, Vol.11, Chapter 5; b) Robinson, R.A.; Briggs, A.T. *Trans. Faraday Soc.* **1955**, 51, 901 ($pK_a = 7.149$ at 25 °C).

$$v = \frac{d(\text{Abs})}{d(t) \cdot \epsilon_{\text{obs}}} = k'_{\text{obs}} [\text{Ester}] = (k_{\text{OH}} [\text{OH}^-] + k_0) [\text{Ester}] \quad (6)$$

$$k'_{\text{obs}} = k_0 + k_{\text{OH}} [\text{OH}^-] \quad (7)$$

Equation (7) shows the k'_{obs} -value as an additive value. The k_{OH} value is a second-order velocity constant describing the nucleophilic attack of the OH^- ions. The k_0 value is a first-order constant describing the solvolysis of the ester due to solvent molecules (e.g. water or organic additives).

The use of known values from literature for the spontaneous hydrolysis is not possible, as these constants depend on the reaction conditions (e.g. the type of buffer system used, the ionic strength, the presence of organic additives etc)³.

The k'_{obs} value was determined by the initial slope method at constant pH with various concentrations of NA ($[\text{NA}] = 2$ to 5 mM). The results are presented in **Table 2**.

pH ^a	7.00 ^c	7.20	7.34	7.52	7.82	7.93	8.00 ^c	8.23	8.51
$k'_{\text{obs}} [10^{-6} \text{ s}^{-1}]^b$	1.50	1.87	2.46	3.30	6.08	7.32	8.94	15.17	27.02

^a $\Delta \text{pH} = \pm 0.005$; ^b 25.0 ± 0.1 °C, 50 mM TRIS/HCl, 10 % CH_3CN , $\Delta k'_{\text{obs}} = \pm 2.0 \cdot 10^{-8} \text{ s}^{-1}$;

^c $I = 0$ to 50 mM NaCl

Table 2: k_{obs} values for the spontaneous hydrolysis of NA

From the plot of k'_{obs} versus $[\text{OH}^-]$ and equation (7) the following results were obtained:

$k_{\text{OH}} = 8.16 \pm 0.01 \text{ M}^{-1} \text{ s}^{-1}$ and $k_0 = 6.63 \pm 0.02 \cdot 10^{-7} \text{ s}^{-1}$ (**Fig. 2**)

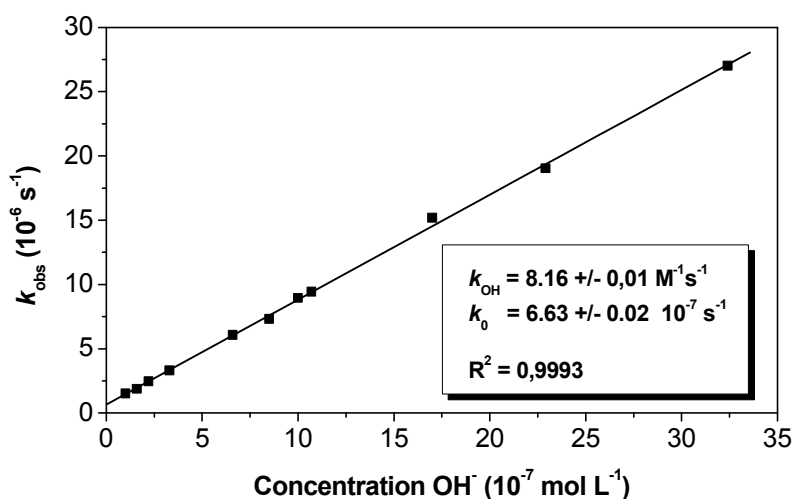


Fig. 2: k'_{obs} versus $[\text{OH}^-]$ in the pH range 7.0 - 8.5.

³ a) J. F. Kirsch, W. P. Jencks, *J. Am. Chem. Soc.* **1964**, *86*, 837-846; b) T. C. Bruice, C. L. Schmir, *J. Am. Chem. Soc.* **1957**, *79*, 1663-1667; c) W. P. Jencks, M. Gilchrist, *J. Am. Chem. Soc.* **1968**, *90*, 2622-2637

A variation of the ionic strength in the range 0 to 50 mM at two different pH values did not lead to any significant change in the value of k'_{obs} .

A comparison between the experimentally determined values and the values from literature (**Table 3**) shows the influence of the buffer system and of the added co-solvent on the rate constants.

k_{OH} ($\text{M}^{-1} \text{s}^{-1}$)	k_0 (s^{-1})	reaction conditions	literature
9.5	$< 1.66 \cdot 10^{-3}$	T = 25 °C, $I = 1.0$ M (KCl), 50 mM H ₂ O/triethylamine buffer	4a
23.5	---	T = 30 °C, $I = 1.0$ M (KCl), H ₂ O/Dioxan (1 %), pH control by 1 M KOH	3b
8.1	$7.28 \cdot 10^{-5}$	T = 25 °C, $I = 0$, H ₂ O/EtOH (28.5 %), phosphate buffer	3c
---	$4.3 \cdot 10^{-7}$	T = 25 °C, $I = 1.0$ M (KCl), H ₂ O, no buffer	3d
4.4; 8.1; 14.7	---	T = 15, 25, 35 °C, $I = 0.1$ M (NaNO ₃), 20 mM CHES buffer, H ₂ O/CH ₃ CN (10 %)	3e
7.84	$1.12 \cdot 10^{-5}$	T = 25 °C, $I = 0.1$ M (KNO ₃), 20 mM Tris buffer, H ₂ O/CH ₃ CN (10 %)	4a
19.41 ^a	$8.16 \cdot 10^{-7}$	T = 25 °C, $I = 0.1$ M (KNO ₃), 20 mM Tris buffer, H ₂ O/CH ₃ CN (10 %)	4b
12.41	$3.67 \cdot 10^{-6}$	T = 25 °C, $I = 0.1$ M (KNO ₃), 20 mM „Goods“-buffer, H ₂ O/CH ₃ CN (10 %)	4c
14.8	---	T = 25 °C, $I = 0.3$ M (NaCl or KCl), 10 mM H ₂ O/triethylamin buffer	4d

^a the k_{OH} -value is clearly very different from the other values. The authors have used for their calculations an unusual high value for ϵ_{NP} (20000 mol⁻¹ L cm⁻¹, 400 nm) which probably leads to this discrepancy.

Table 3: Literature values for k_{OH} and k_0 in the spontaneous hydrolysis of NA.

The spontaneous hydrolysis of NA is generally one order of magnitude faster than any metal catalysed hydrolysis known at present. Therefore the rate of spontaneous hydrolysis of NA has to be determined experimentally for the reaction conditions employed.

1.4.8 pH Profiles and species distribution diagrams of the metal complexes in aqueous solutions under nitrogen at 25 °C and $I = 0.10$ (TEAP).

In all graphs every second point is represented.

⁴ a) S. Zhu, W. Chen, H.-K. Lin, X. Yin, F. Kou, M. Lin, Y. Chen; *Polyhedron* **1997**, *16*, 3285 – 3291; b) X.-C. Su, H.-W. Sun, Z.-F. Zhou, H.-K. Lin, L. Chen, S. Zhu, Y.-T. Chen; *Polyhedron* **2001**, *20*, 91 – 95; c) Y.-H. Guo, Q.-C. Ge, H. Lin, H.-K. Lin, S.-R. Zhu; *Int. J. Chem. Kinet.* **2004**, *36*, 41 – 48; d) W. P. Jencks, J. Carrioulo *J. Am. Chem. Soc.* **1960**, *82*, 1778-1786.

1.4.8.1 Mononuclear complexes

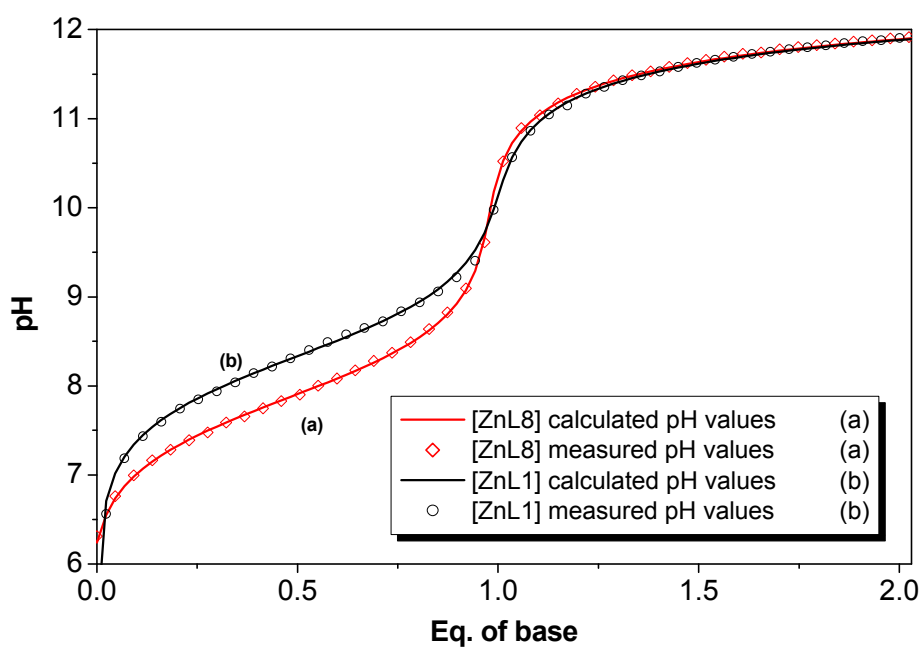
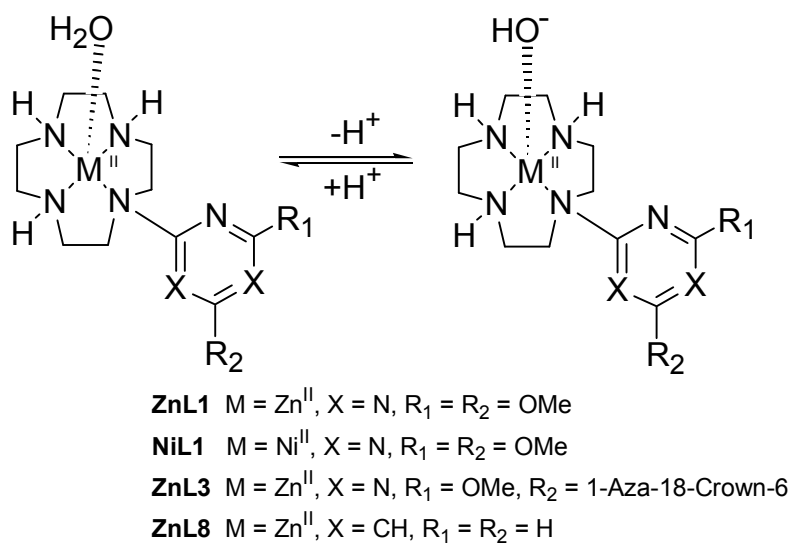


Figure 3. Titration curve for the complexes $[\text{ZnL1}](\text{ClO}_4)_2 \cdot \text{H}_2\text{O}$ and $[\text{ZnL8}](\text{ClO}_4)_2$ in aqueous solution. The pH profile of $[\text{ZnL3}](\text{ClO}_4)_2$ in aqueous solution is similar to that of $[\text{ZnL1}](\text{ClO}_4)_2 \cdot \text{H}_2\text{O}$ and was omitted for clarity reasons.

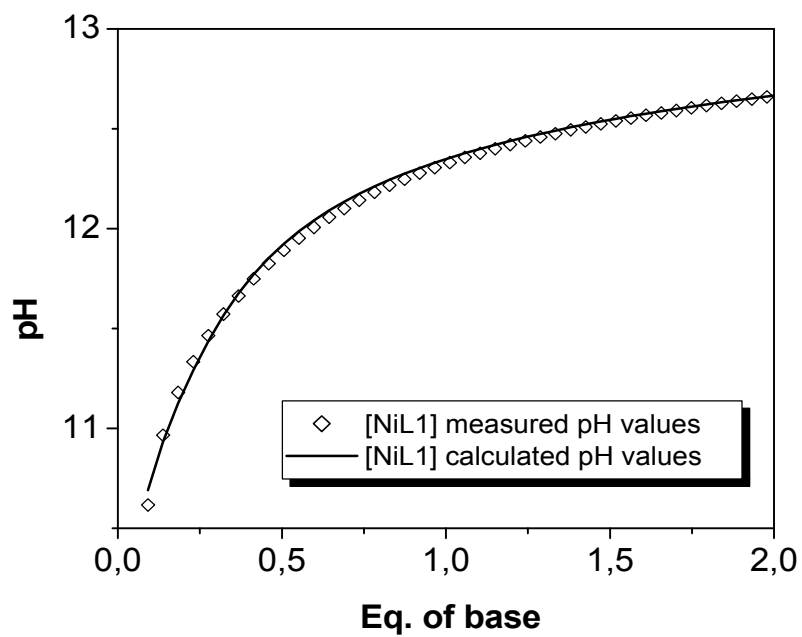


Figure 4. Titration curve for the complex $[\text{NiL1}](\text{ClO}_4)_2 \cdot 2 \text{H}_2\text{O}$ in aqueous solution

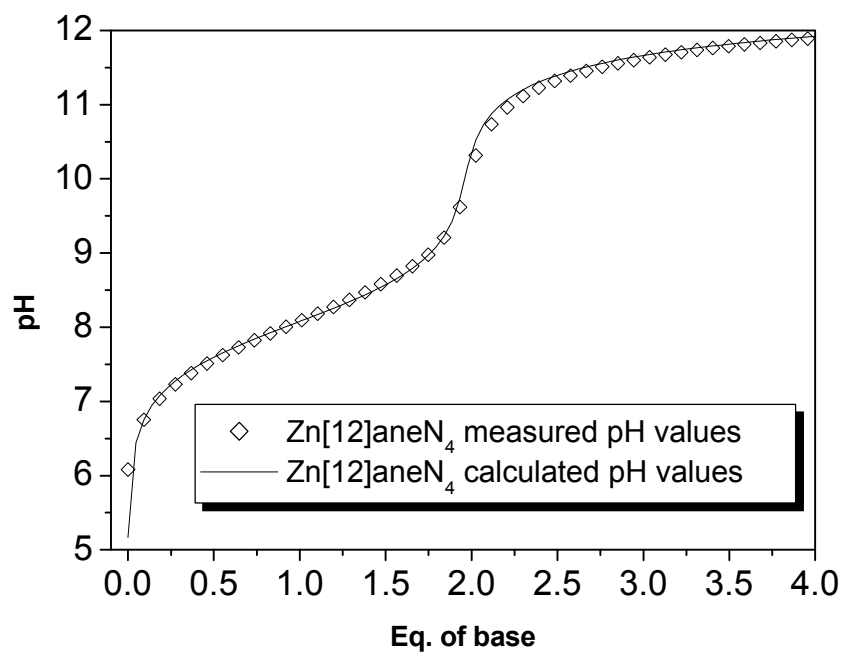


Figure 5. Titration curve for the complex $\text{Zn}[12]\text{aneN}_4 (\text{ClO}_4)_2$

1.4.8.2 Dinuclear complexes

A. pH Titration curves

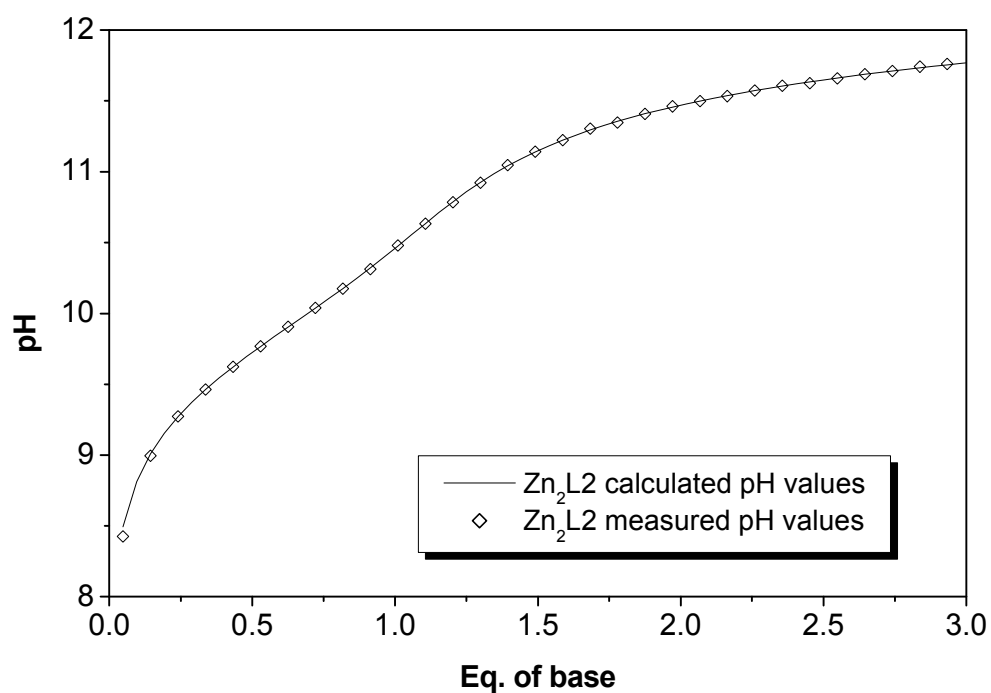


Figure 6. Titration curve for the complex $[\text{Zn}_2\text{L2}](\text{ClO}_4)_4 \cdot \text{CH}_3\text{CN}$ in aqueous solution

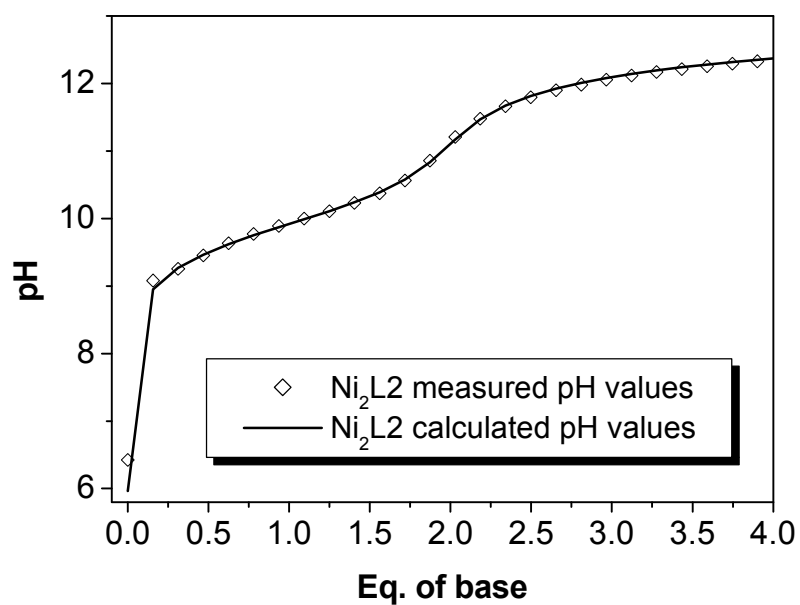


Figure 7. Titration curve for the complex $[\text{Ni}_2\text{L2}](\text{ClO}_4)_4$ in aqueous solution

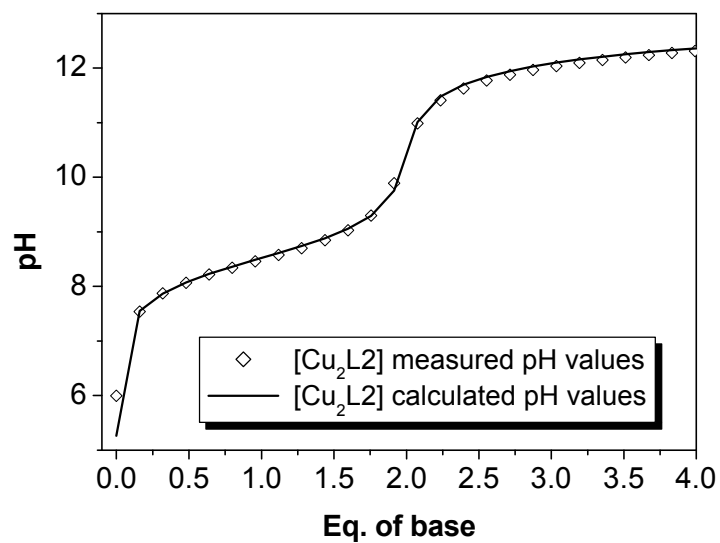


Figure 8. Titration curve for the complex $[\text{Cu}_2\text{L2}](\text{ClO}_4)_4 \cdot 2 \text{H}_2\text{O}$ in aqueous solution

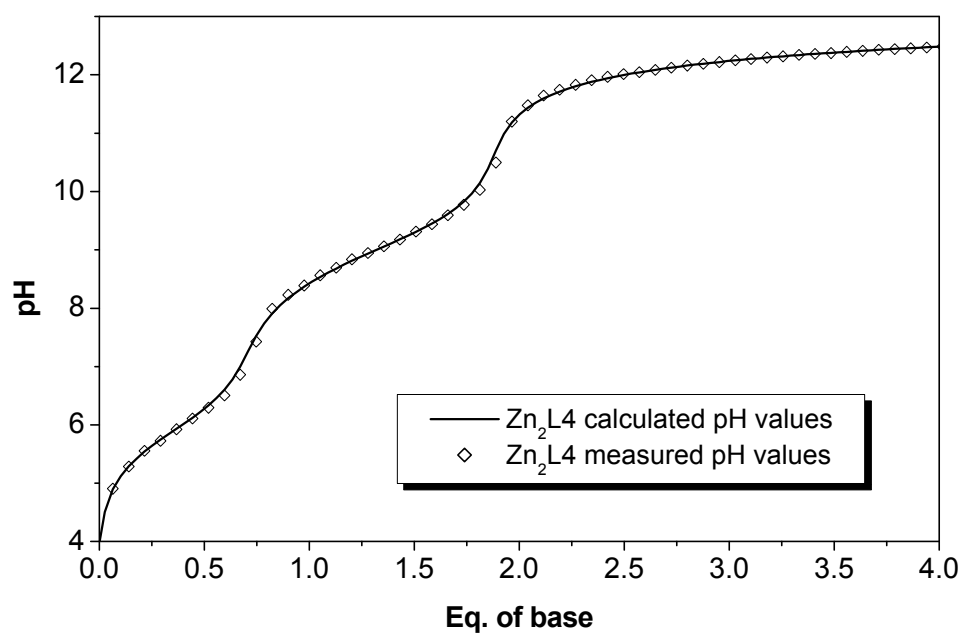


Figure 9. Titration curve for the complex $[\text{Zn}_2\text{L4}](\text{ClO}_4)_4$ in aqueous solution (0.5 eq. HClO_4)

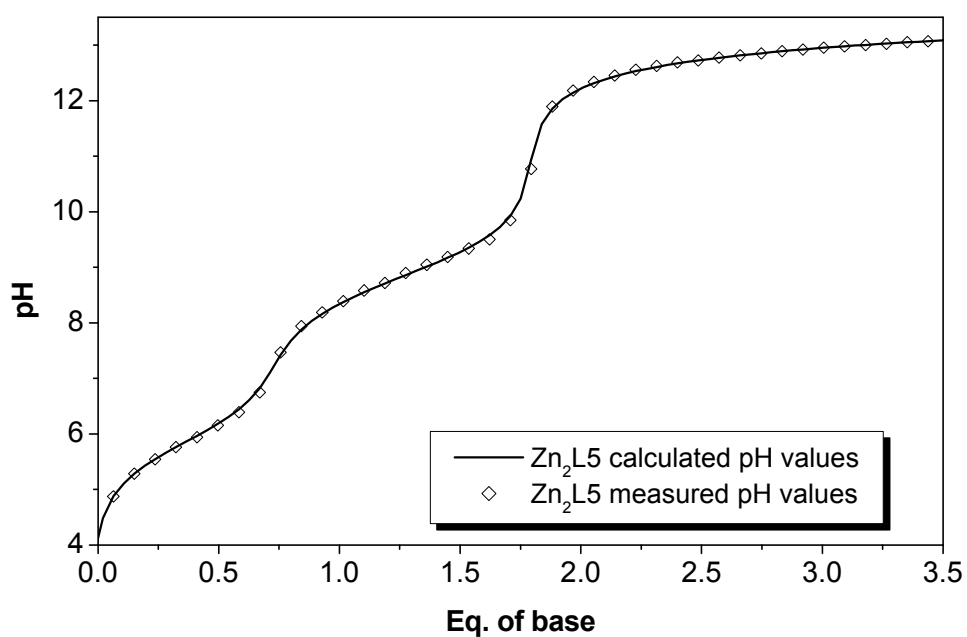


Figure 10. Titration curve for the complex $[\text{Zn}_2\text{L5}](\text{ClO}_4)_4 \cdot \text{H}_2\text{O}$ in $\text{MeOH}/\text{H}_2\text{O}$ (9:1) solution (0.5 eq. HClO_4)

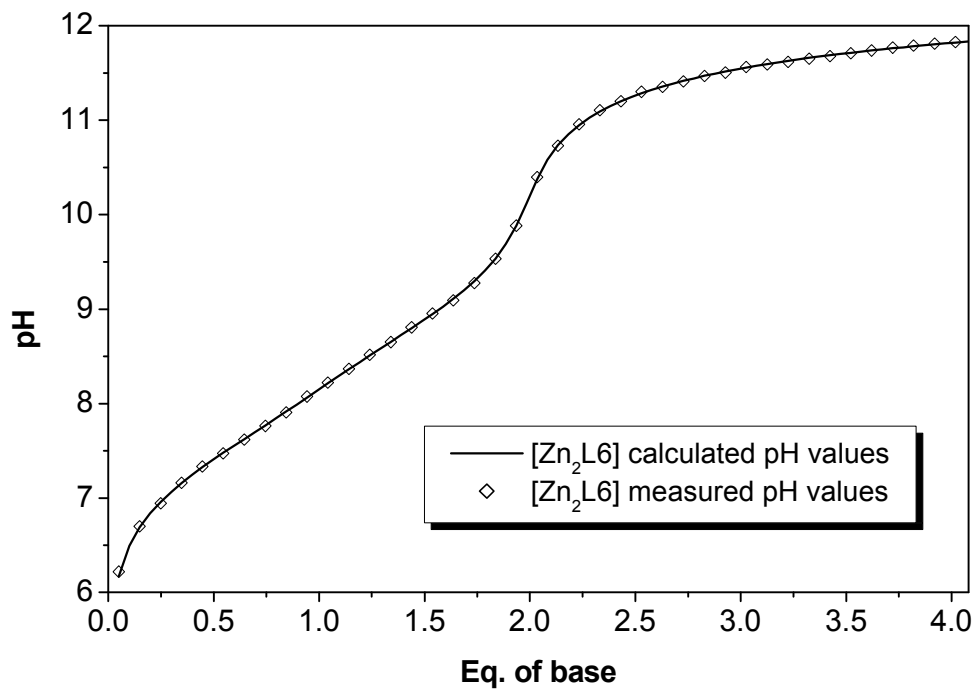


Figure 11. Titration curve for the complex $[\text{Zn}_2\text{L6}](\text{ClO}_4)_4 \cdot \text{H}_2\text{O}$ in aqueous solution.

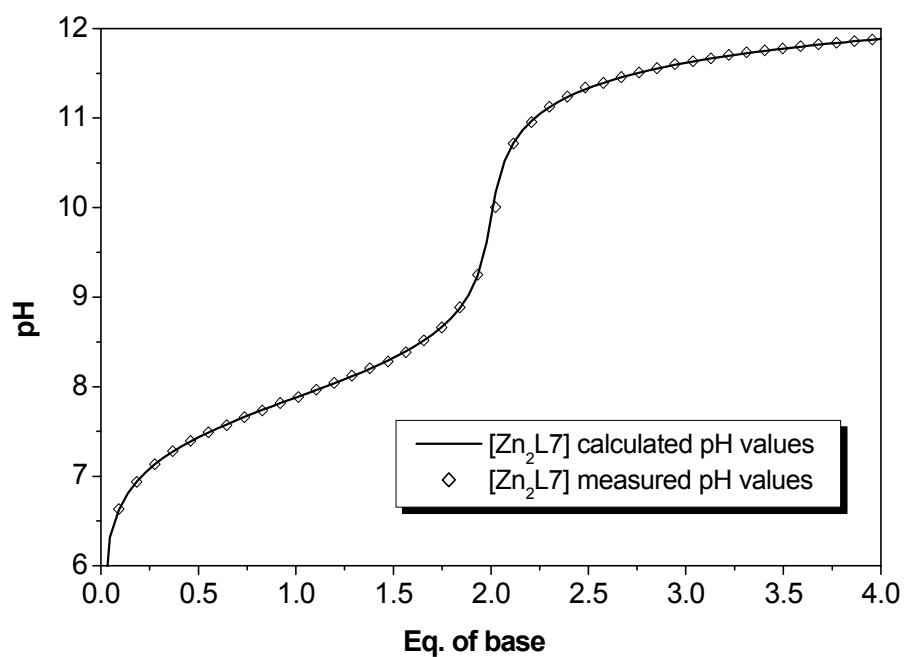


Figure 12. Titration curve for the complex $[\text{Zn}_2\text{L7}](\text{ClO}_4)_4 \cdot \text{CH}_3\text{CN}$ in aqueous solution.

B. Species distribution diagrams

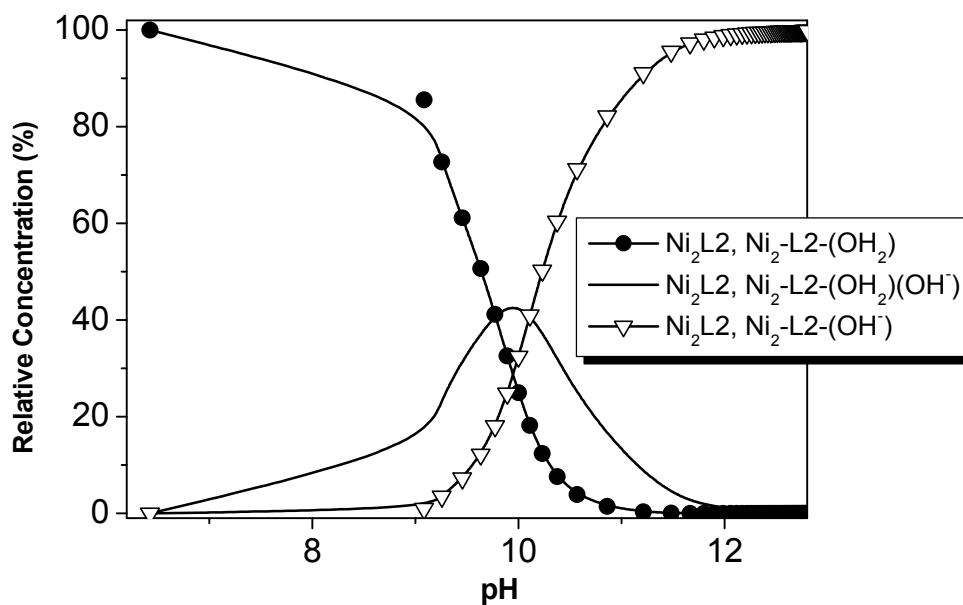


Figure 13. Species distribution diagram for $[\text{Ni}_2\text{L2}](\text{ClO}_4)_4$ in aqueous solution.

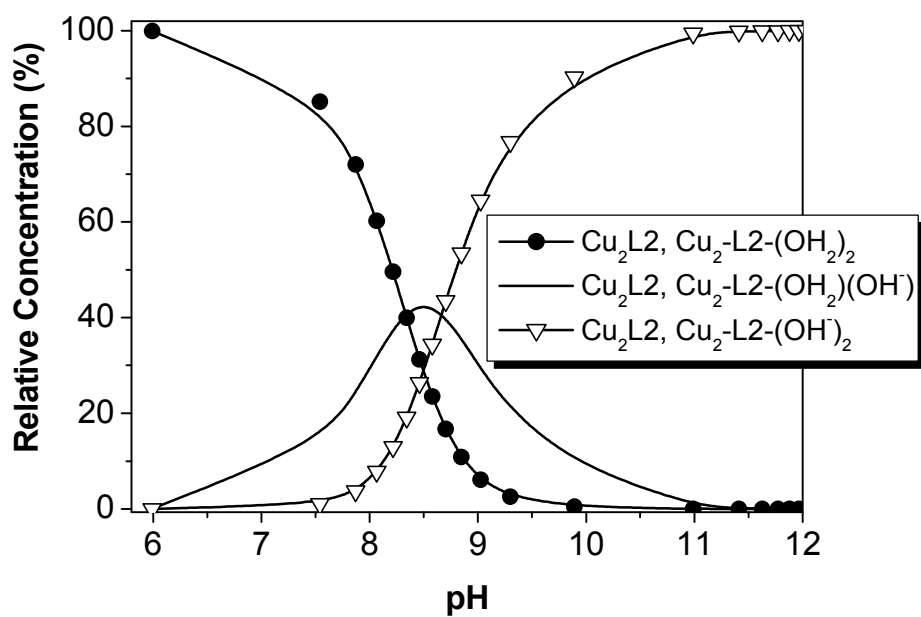


Figure 14. Species distribution diagram for $[\text{Cu}_2\text{L2}](\text{ClO}_4)_4 \cdot 2\text{H}_2\text{O}$ in aqueous solution.

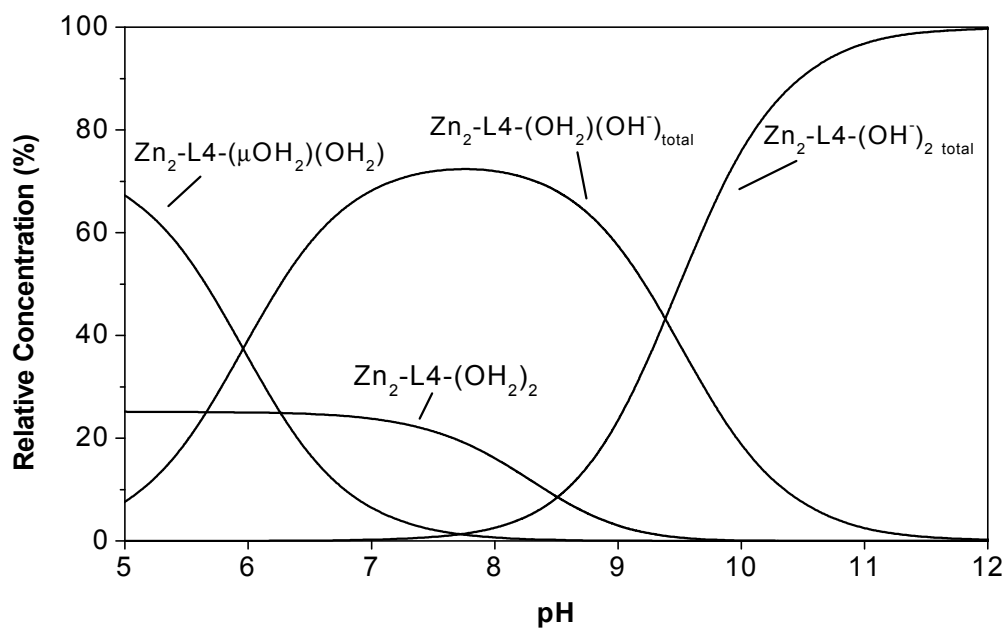


Figure 15. Species distribution diagram for $[\text{Zn}_2\text{L4}](\text{ClO}_4)_4$ in aqueous solution.

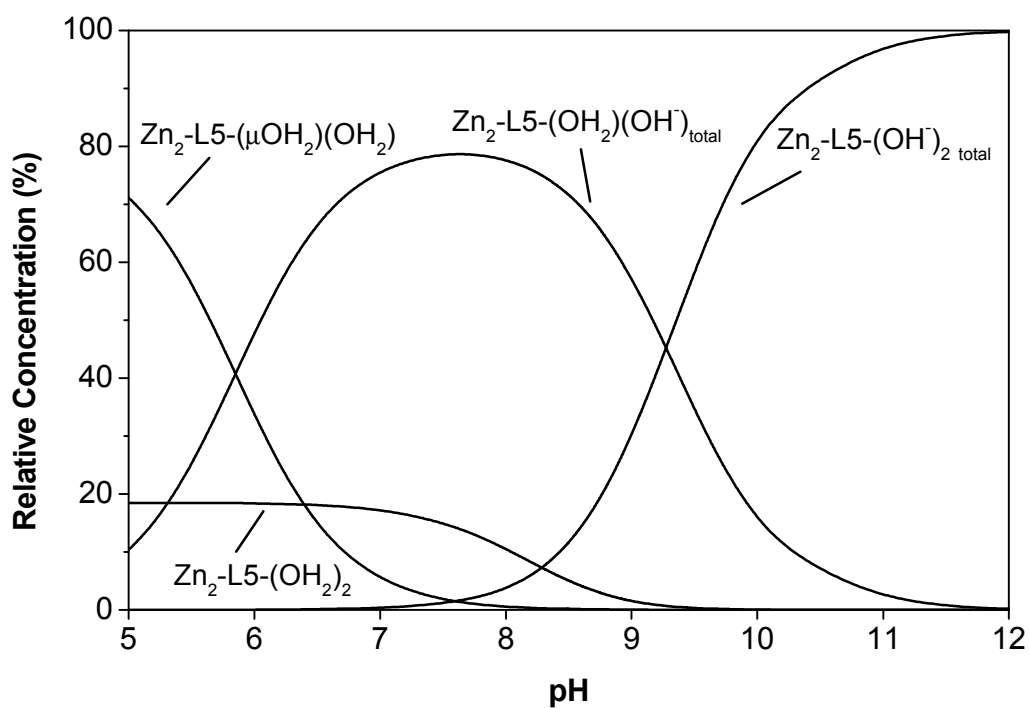


Figure 16. Species distribution diagram for $[\text{Zn}_2\text{L5}](\text{ClO}_4)_4 \cdot \text{H}_2\text{O}$ in MeOH/H₂O 9:1.

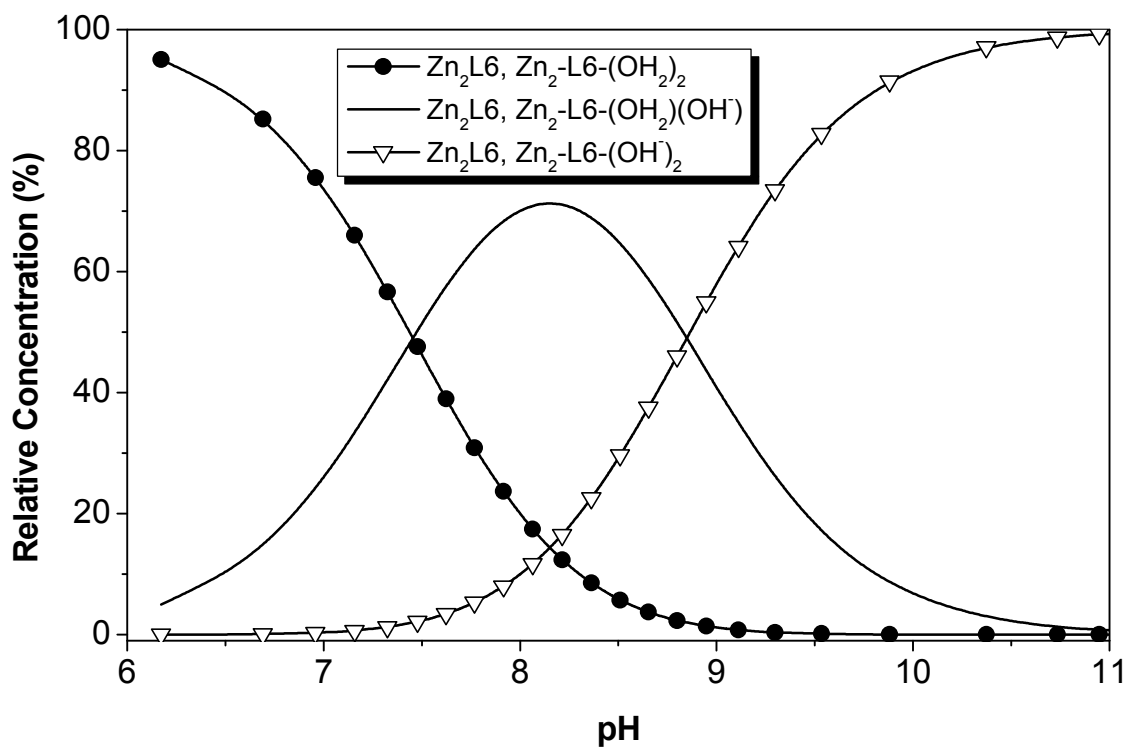


Figure 17. Species distribution diagram for $[\text{Zn}_2\text{L6}](\text{ClO}_4)_4 \cdot \text{H}_2\text{O}$ in aqueous solution.

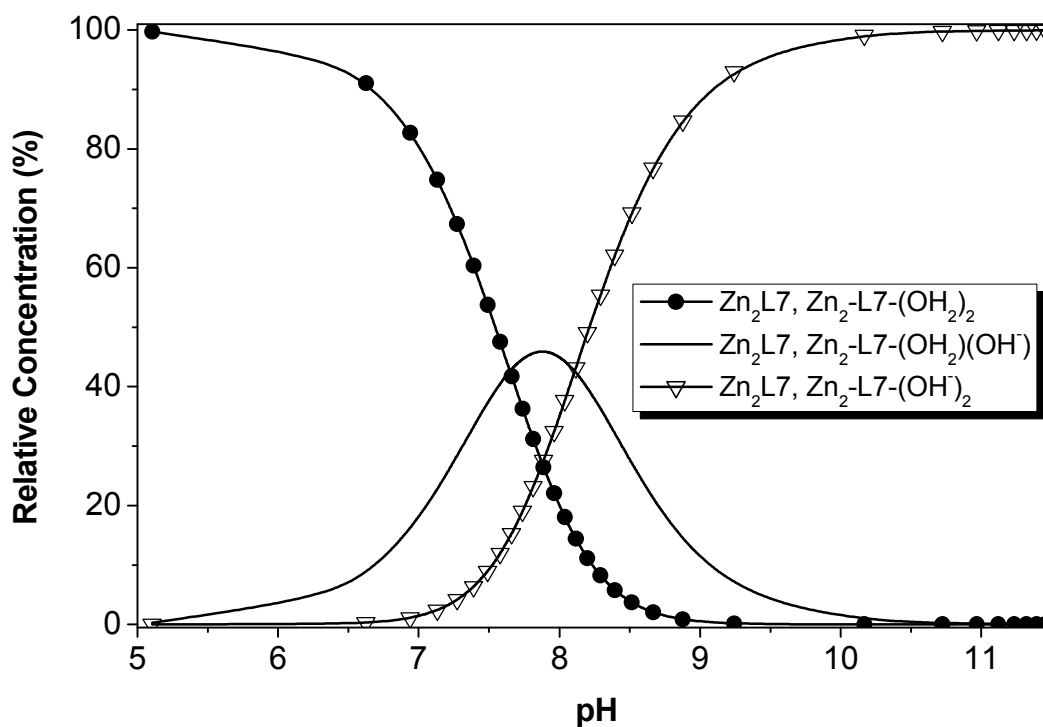


Figure 18. Species distribution diagram for $[\text{Zn}_2\text{L7}](\text{ClO}_4)_4 \cdot \text{CH}_3\text{CN}$ in aqueous solution.

1.4.9 Plots of k_{obs} vs Zn(II) complex concentration

A. Mononuclear Zn(II) complexes (example)

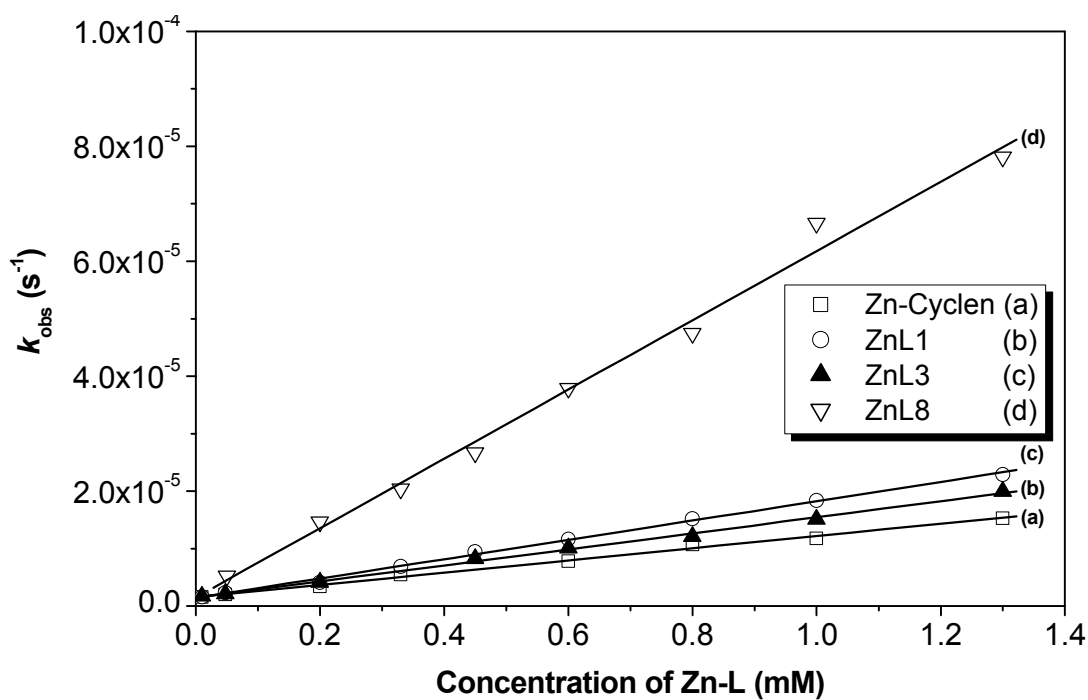
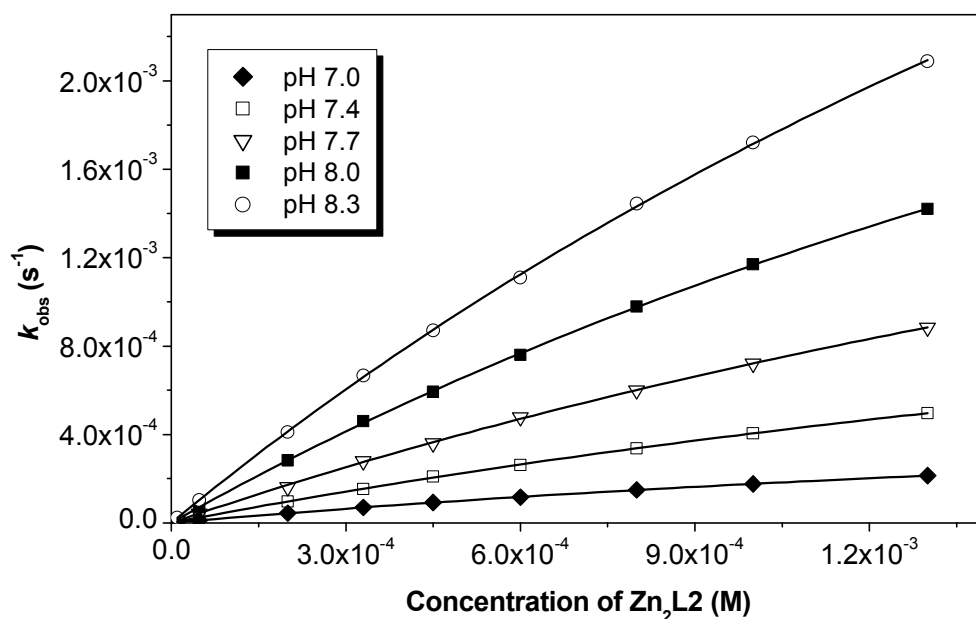


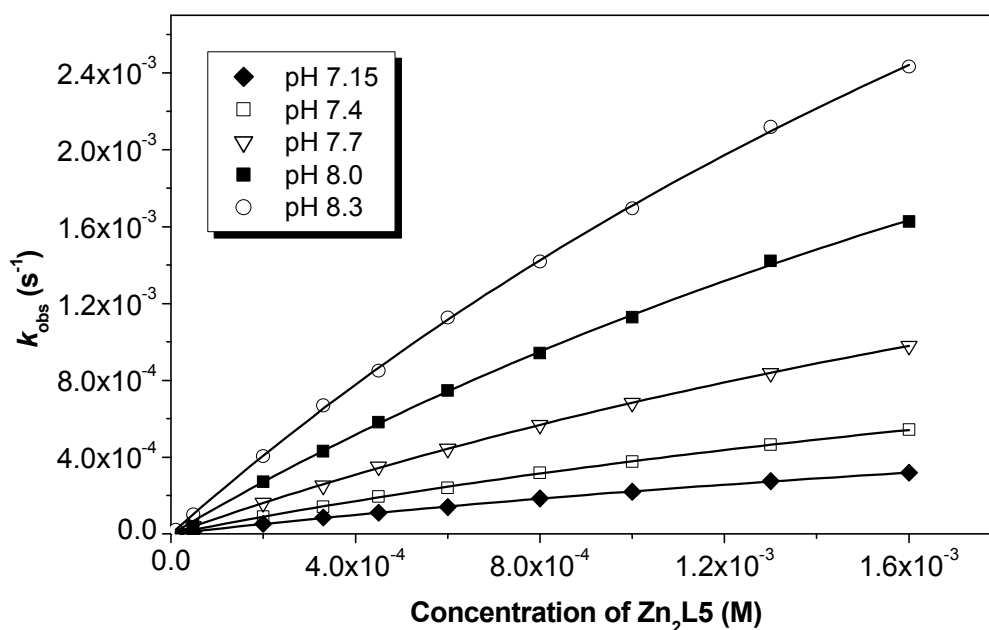
Figure 19: Calculation of the k_{cat} values for the mononuclear complexes at pH 7.

B. Dinuclear Zn(II) complexes



^a 50 mM TRIS/HCl buffer, 10% CH₃CN, *I* = 0.1 M (NaCl), 25 °C, [NA] = 1.0 - 4.0 · 10⁻⁵ mol/L, Δ pH = ± 0.01, Δ *k*_{obs} ± 0.4 - 2.7 %

Figure 20: Saturation kinetics for **Zn₂L2**^a



^a 50 mM TRIS/HCl buffer, 10% CH₃CN, *I* = 0.1 M (NaCl), 25 °C, [NA] = 1.0 - 4.0 · 10⁻⁵ mol/L, Δ pH = ± 0.01, Δ *k*_{obs} ± 0.3 - 3.1 %

Figure 21: Saturation kinetics for **Zn₂L5**^a

The saturation kinetics for these complexes is less obvious due to their lower solubility in aqueous solutions.

1.4.10 Graphical representation of the relationship between measured $k_{\text{cat } 1,2}$, the species-distribution diagram and the calculated $k_{\text{cat } 1}$ and $k_{\text{cat } 2}$ for $\text{Zn}_2\text{L7}$ and $\text{Zn}_2\text{L6}$.

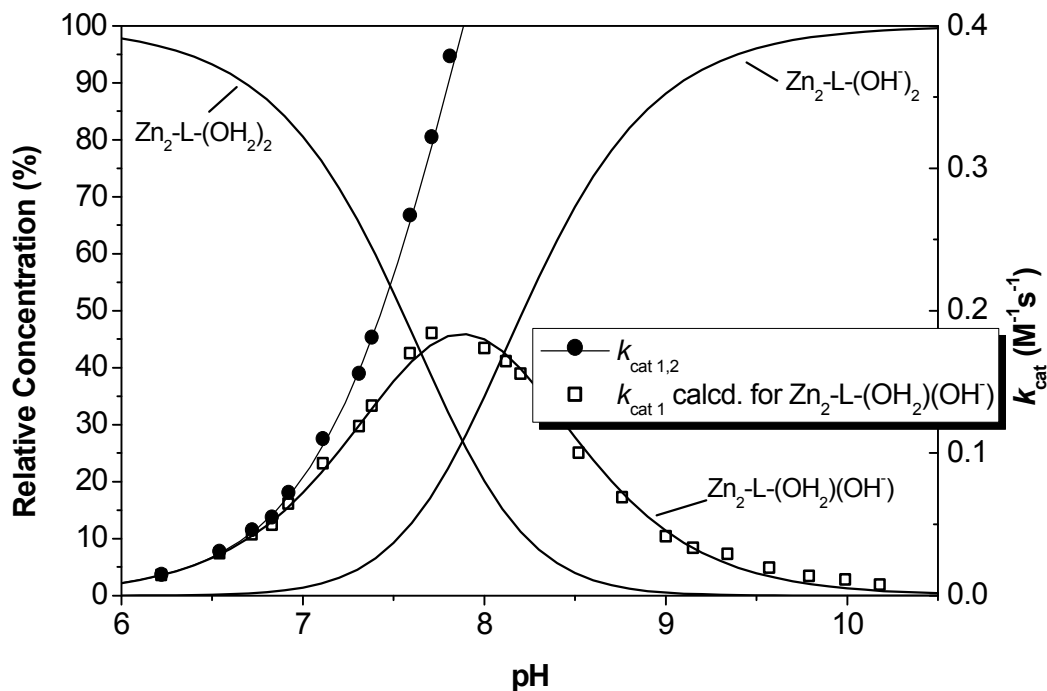


Figure 22: Species-distribution diagram of $\text{Zn}_2\text{L7}$ with measured $k_{\text{cat } 1,2}$ values and calculated $k_{\text{cat } 1}$ values.

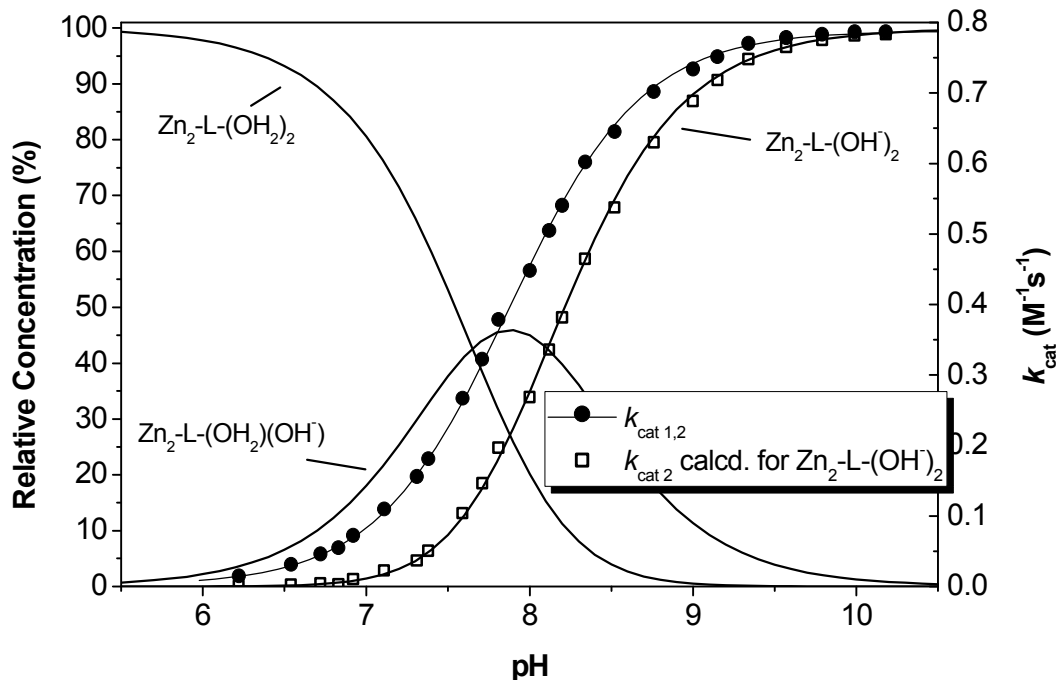


Figure 23: Species-distribution diagram of $\text{Zn}_2\text{L7}$ with measured $k_{\text{cat } 1,2}$ values and calculated $k_{\text{cat } 2}$ values.

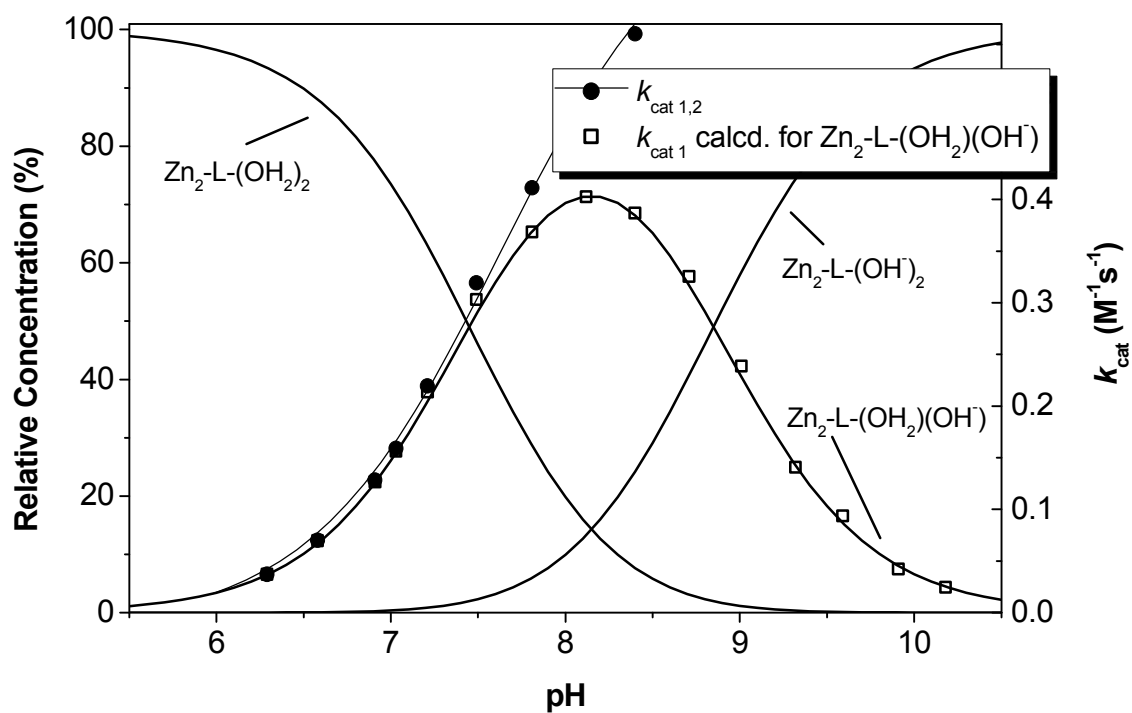


Figure 24: Species-distribution diagram of **Zn₂L6** with measured $k_{\text{cat } 1,2}$ values and calculated $k_{\text{cat } 1}$ values.

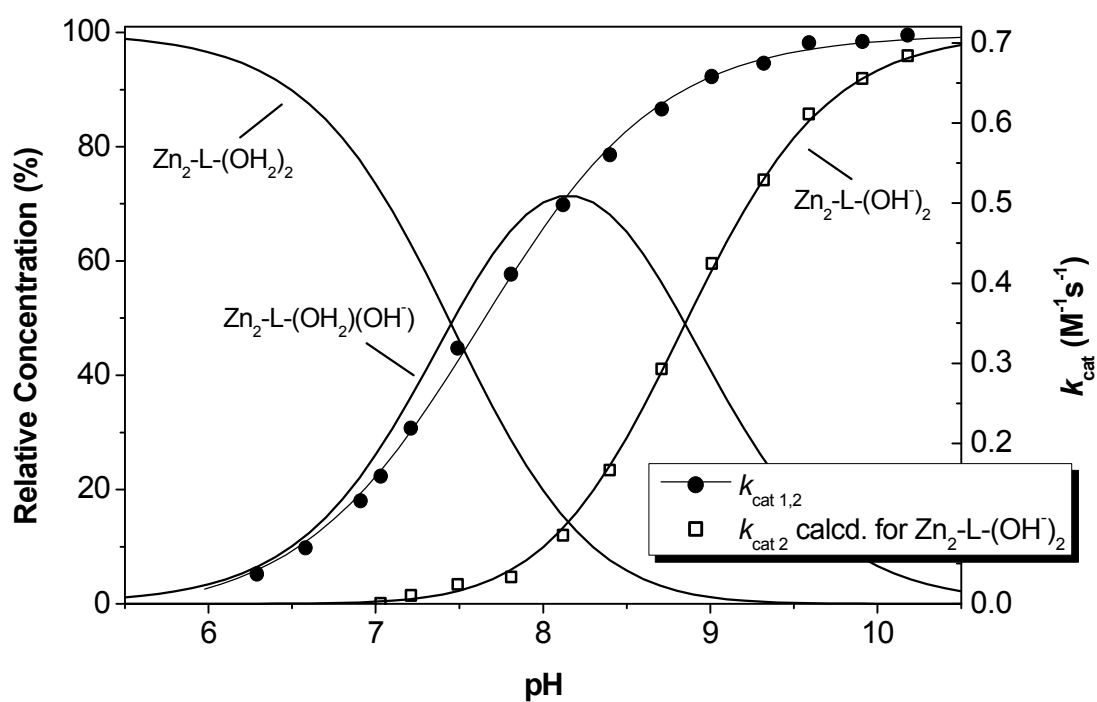


Figure 25: Species-distribution diagram of **Zn₂L6** with measured $k_{\text{cat } 1,2}$ values and calculated $k_{\text{cat } 2}$ values.

1.5 References

-
- ¹ a) Neuberger, A.; Brocklehurst, K. *Hydrolytic Enzymes*, Elsevier Science, Amsterdam, **1987**;
b) Bertini, I.; Luchinat, C.; Maret, W.; Zeppesauer, M. *Zinc Enzymes*, Birkhäuser Ed., Boston, **1986**.
- ² For reviews on metallohydrolases, see: (a) Wilcox, D. E. *Chem. Rev.* **1996**, *96*, 2435. (b) Sträter, N.; Lipscomb, W. N.; Klabunde, T.; Krebs, B. *Angew. Chem. Int. Ed. Engl.* **1996**, *35*, 2024. (c) Lipscomb, W.N.; Sträter, N. *Chem. Rev.* **1996**, *96*, 2375-2433.
- ³ For reviews, see: (a) Chin, J. *Acc. Chem. Res.* **1991**, *24*, 145; (b) Liu, C.; Wang, M.; Zhang, T.; Sun, H. *Coord. Chem. Rev.* **2004**, *248*, 147.
- ⁴ Review on thermodynamic and kinetic data for macrocycle interaction with cations, anions and neutral molecules: Izatt, R. M.; Pawlak, K.; Bradshaw, J. S.; Bruening, R. L. *Chem. Rev.* **1995**, *95*, 2529-2586.
- ⁵ a) Koike, T.; Kajitani, S.; Nakamura, I.; Kimura, E.; Shiro, M. *J. Am. Chem. Soc.* **1995**, *117*, 1210-1219; b) Kimura, E.; Kodama, Y.; Koike, T.; Shiro, M. *J. Am. Chem. Soc.* **1995**, *117*, 8304-8311.
- ⁶ Zhang, Z.; van Eldic, R.; Koike, T.; Kimura, E. *Inorg. Chem.* **1993**, *32*, 5749-5755.
- ⁷ Kim, D.H.; Lee, S.S. *Bioorg & Med. Chem.* **2000**, *8*, 647-652.
- ⁸ Kimura, E.; Shionoya, M.; Hoshino, A.; Ikeda, T.; Yamada, Y. *J. Am. Chem. Soc.* **1992**, *114*, 10134-10137.
- ⁹ Koike, T.; Masahiro, M.; Kimura, E. *J. Am. Chem. Soc.* **1994**, *116*, 8443-8449.
- ¹⁰ a) Belousoff, M. J.; Duriska, M. B.; Graham, B.; Batten, S. R.; Moubaraki, B.; Murray, K. S.; Spiccia, L. *Inorg. Chem.* **2006**, *45*, 3746-3755; b) Burstyn, J. N.; Deal, K. A. *Inorg. Chem.* **1993**, *32*, 3585-3586; c) Deal, K. A.; Burstyn, J. N. *Inorg. Chem.* **1996**, *35*, 2792-2798;
- ¹¹ a) McCue, K. P.; Voss, D. A. Jr.; Marks, C.; Morrow, J. R. *J. Chem. Soc. Dalton Trans.* **1998**, 2961-2963; b) Hegg, E. L.; Deal, K.; Kiessling, L.; Burstyn, J. N. *Inorg. Chem.* **1997**, *36*, 1715-1718;
- ¹² Hegg, E. L.; Burstyn, J. N. *J. Am. Chem. Soc.* **1995**, *117*, 7015-7016;
- ¹³ Kimura, E.; Hashimoto, H.; Koike, T. *J. Am. Chem. Soc.* **1996**, *118*, 10963-10970.
- ¹⁴ a) Hegg, E. L.; Burstyn, J. N. *Coord. Chem. Rev.* **1998**, *173*, 133-165; b) Suh, J. *Acc. Chem. Res.* **1992**, *25*, 273-279.
- ¹⁵ Göbel, M. W. *Angew. Chem. Int. Ed. Engl.* **1994**, *33*, 1141-1143.
- ¹⁶ a) Kovbasyuk, L.; Krämer, R. *Chem. Rev.* **2004**, *104*, 3161-3187; b) Feng, G.; Mareque-Rivas, J. C.; de Rosales, R. T. M.; Williams, N. H. *J. Am. Chem. Soc.* **2005**, *127*, 13470-13471; c) O'Donoghue, A. M.; Pyun, S. Y.; Yang, M.-Y.; Morrow, J. R.; Richard, J. P. *J. Am. Chem. Soc.* **2006**, *128*, 1615-1621.

- ¹⁷ a) Breslow, R.; Berger, D.; Huang, D.-L. *J. Am. Chem. Soc.* **1990**, *112*, 3686-3687; b) Morrow, J. R.; Aures, H.; Epstein, D. *J. Chem. Soc., Chem. Commun.* **1995**, 2431-2432; c) Young, M. J.; Wahnou, D.; Hynes, R. C.; Chin, J. *J. Am. Chem. Soc.*, **1995**, *117*, 9441-9447; d) Chu, F.; Smith, J.; Lynch, V. M.; Anslyn, E. V. *Inorg. Chem.* **1995**, *34*, 5689-5690 (the authors propose that in a Zn complex either imidazole or imidazolium might act as an auxiliary group, providing an 1.5-fold increase in RNA cleavage rate). See, also: e) Hsu, C.-M.; Cooperman, B. S. *J. Am. Chem. Soc.* **1976**, *98*, 5657-5663; f) Koike, T.; Inoue, M.; Kimura, E.; Shiro, M. *J. Am. Chem. Soc.* **1996**, *118*, 3091-3099.
- ¹⁸ Kövari, E.; Krämer, R. *J. Am. Chem. Soc.* **1996**, *118*, 12704-12709.
- ¹⁹ a) Raidt, M.; Neuburger, M.; Kaden, T. A. *Dalton Trans.* **2003**, 1292-1298; b) Kaden, T. A. *Coord. Chem. Rev.* **1999**, *190-192*, 371-389;
- ²⁰ a) Vichard, C.; Kaden, T. A. *Inorg. Chim. Acta* **2002**, *337*, 173-180; b) Vichard, C.; Kaden, T. A. *Inorg. Chim. Acta* **2004**, *357*, 2285-2293.
- ²¹ a) Arca, M.; Bencini, A.; Berni, E.; Caltagirone, C.; Devillanova, F. A. ; Isaia, F. ; Garau, A. ; Giorgi, C. ; Lippolis, V. ; Pera, A. ; Tei, L. ; Valtancoli, B. *Inorg. Chem.* **2003**, *42*, 6929-6939; b) Iranzo, O.; Elmer, T.; Richard, J. P.; Morrow, J. R. *Inorg. Chem.* **2003**, *42*, 7737-7746.
- ²² a) Styka, M. C.; Smierciak, R. C.; Blinn, E. L.; DeSimone, R. E.; Passariello, J. V. *Inorg. Chem.* **1978**, *17*, 82-86; b) Thöm, V. J.; Hosken, G. D.; Hancock, R. D. *Inorg. Chem.* **1985**, *24*, 3378-3381.
- ²³ a) Fabrizzi, L.; Micheloni, M.; Paoletti, P. *Inorg. Chem.* **1980**, *19*, 535-538 ; b) Fabrizzi, L. *Inorg. Chem.* **1977**, *16*, 2667-2668; c) Bencini, A.; Bianchi, A.; Garcia-Espana, E.; Jeannin, Y.; Julve, M.; Marcelino, V.; Philoche-Levisalles, M. *Inorg. Chem.* **1990**, *29*, 963-970.
- ²⁴ a) Fujioka, H.; Koike, T.; Yamada, N.; Kimura, E. *Heterocycles*, **1996**, *42*, 775-787; b) Koike, T.; Takashige, M.; Kimura, E.; Fujioka, H.; Shiro, M. *Chem. Eur. J.* **1996**, *2*, 617-623; c) Kimura, E.; Aoki, S.; Koike, T.; Shiro, M. *J. Am. Chem. Soc.* **1997**, *119*, 3068-3076; d) Aoki, S.; Kimura, E. *J. Am. Chem. Soc.* **2000**, *122*, 4542-4548.
- ²⁵ a) Yashiro, M.; Kaneiwa, H.; Onaka, K.; Komiyama, M. *J. Chem. Soc. Dalton Trans.* **2004**, 605-610; b) Kinoshita, E.; Takahashi, M.; Takeda, H.; Shiro, M.; Koike, T. *J. Chem. Soc. Dalton Trans.* **2004**, 1189-1193.
- ²⁶ a) Yoo, C. E.; Chae, P. S.; Kim, J. E.; Jeong, E. J.; Suh, J. *J. Am. Chem. Soc.* **2003**, *125*, 14580-14589; b) Aoki, S.; Kimura, E. *Rev. Mol. Biotech.* **2002**, *90*, 129-155 and ref. therein.
- ²⁷ Belousoff, M. J.; Duriska, M. B.; Graham, B.; Batten, S. R.; Moubaraki, B.; Murray, K. S.; Spiccia, L. *Inorg. Chem.* **2006**, *45*, 3746-3755.
- ²⁸ El Ghachtouli, S.E.; Cadiou, C.; Deschamps-Olivier, I.; Chuburu, F. ; Aplincourt, M.; Turcry, V. ; Le Baccon, M.; Handel, H. *Eur. J. Inorg. Chem.* **2005**, 2658-2668.
- ²⁹ McCue, K.P.; Morrow, J. *Inorg. Chem.* **1999**, *38*, 6136-6142.
- ³⁰ The experimental conditions (room temperature) cause higher vibrations of the atoms.

- 31 Shionoya, M. ; Kimura, E.; Shiro, M. *J. Am. Chem. Soc.* **1993**, *115*, 6730-6737.
- 32 Koike, T.; Gotoh, T.; Aoki, S.; Kimura, E.; Shiro, M. *Inorg. Chim. Acta* **1998**, *270*, 424-432.
- 33 Aoki, S. ; Kagata, D.; Shiro, M.; Takeda, K.; Kimura, E. *J. Am. Chem. Soc.* **2004**, *126*, 13377-13390.
- 34 Iranzo, O.; Kovalevsky, A.Y.; Morrow, J. R.; Richard, J. P. *J. Am. Chem. Soc.* **2003**, *125*, 1988-1993.
- 35 Bazzicalupi, C.; Bencini, A.; Berni, E.; Bianchi, A.; Fedi, V.; Fusi, V.; Giorgi, C. ; Paoletti, P.; Valtancoli, B. *Inorg. Chem.* **1999**, *38*, 4115-4122.
- 36 a) Koike, T.; Kimura, E.; Nakamura, I.; Hashimoto, Y.; Shiro, M. *J. Am. Chem. Soc.* **1992**, *114*, 7338-7345; b) Koike, T.; Kimura, E. *J. Am. Chem. Soc.* **1991**, *113*, 8935-8941; c) Kimura, E.; Shiota, T.; Koike, T.; Shiro, M.; Kodama Shiro M. *J. Am. Chem. Soc.* **1990**, *112*, 5805-5811; d) Kimura, E.; Nakamura, I.; Koike, T.; Shionoya, M.; Kodama, Y.; Ikeda, T.; Shiro, M. *J. Am. Chem. Soc.* **1994**, *116*, 4764-4771.
- 37 Bazzicalupi, C.; Bencini, A.; Bianchi, A.; Fusi, V.; Giorgi, C. ; Paoletti, P. ; Valtancoli, B.; Zanchi, D. *Inorg. Chem.* **1997**, *36*, 2784-2790.
- 38 Xia, J.; Xu, Y.; Li, S.-A.; Sun, W.-Y.; Yu, K.-B.; Tang, W.-X. *Inorg. Chem.* **2001**, *40*, 2394-2401.
- 39 diTargiani, R. C.; Chang, S.; Salter, M. H.; Hancock, R. D.; Goldberg, D. P. *Inorg. Chem.* **2003**, *42*, 5825-5836.
- 40 Kiefer, L. L.; Fierke, C. A. *Biochemistry* **1994**, *33*, 15233-15240.
- 41 Li, S.-A.; Xia, J.; Yang, D.-X. ; Xu, Y. ; Li, D.-F. ; Wu, M.-F.; Tang, W.-X. *Inorg. Chem.* **2002**, *41*, 1807-1815.
- 42 Voet, D.; Voet, J.G. *Biochemistry*, 2nd edition, Wiley, New York, **1995**, Page 351.
- 43 a) Gomez-Tagle, P.; Yatsimirsky, A.K. *Inorg. Chem.* **2001**, *40*, 3786-3796; b) Roigk, A.; Hettich, R.; Schneider, H.-J. *Inorg. Chem.* **1998**, *37*, 751-756; c) Hettich, R.; Schneider, H.-J. *J. Am. Chem. Soc.* **1997**, *119*, 5638-5647; d) Tecilla, P.; Tonellato, U.; Veronese, A. *J. Org. Chem.* **1997**, *62*, 7621-7628.
- 44 Kim, D. H.; Lee, S. S. *Bioorg. Med. Chem.* **2000**, *8*, 647-652.
- 45 $k_{\text{spontaneous}}$ (s^{-1}) is different for every pH value and does not correspond to the k_{OH} value ($\text{M}^{-1}\text{s}^{-1}$). See also eq. 7 from the supplementary information.
- 46 For the calculation of the pK_a values the highest error for k_{cat} is $\Delta k_{\text{cat}} \pm 8.5 \%$.
- 47 a) Breslow, R.; Singh, S. *Bioorg. Chem.* **1988**, *16*, 408-417; b) Breslow, R.; Nesnas, N. *Tetrahedron Lett.* **1999**, *40*, 3335-3338; c) Akkaya, E. U. ; Czarnik, A. W. *J. Am. Chem. Soc.* **1988**, *110*, 8553-8554.
- 48 Fry, F. H.; Fischmann, A. J.; Belousoff, M. J.; Spiccia, L.; Brügger, J. *Inorg. Chem.* **2005**, *44*, 941-950 and references therein.
- 49 Iranzo, O.; Richard, J. P.; Morrow, J. P. *Inorg. Chem.* **2004**, *43*, 1743-1750.

-
- 50 Xia, J.; Li, S.-A.; Shi, Y.-B. ; Yu, K.-B. ; Tang, W.-X. *J. Chem. Soc., Dalton Trans.* **2001**,
2109-2115.
- 51 Bazzicalupi, C.; Bencini, A.; Berni, E.; Giorgi, C. ; Maoggi, S.; Valtancoli, B. *J. Chem. Soc.,
Dalton Trans.* **2003**, 3574-3580.
- 52 Interpretation of the experimental data at pH 7 using eq. (6): $k'_{\text{cat}} = 2.14 \cdot 10^{-3} \pm 8.0 \cdot 10^{-5} \text{ s}^{-1}$; $K_{\text{M}} = 1.36 \cdot 10^{-2} \pm 5.3 \cdot 10^{-4} \text{ M}$; $k_{\text{cat}} = k'_{\text{cat}}/K_{\text{M}} = 0.157 \text{ M}^{-1}\text{s}^{-1}$; $K_{\text{A}} = 74 \text{ M}^{-1}$ ($R^2 = 0.9998$).
- 53 Bencini, A.; Berni, E.; Bianchi, A.; Fedi, V. ; Giorgi, C. ; Paoletti, P.; Valtancoli, B. *Inorg. Chem.* **1999**, 38, 6323-6325.
- 54 The hydrolysis rate was not measured by a „log-plot” method. The measured absorption is corrected with the molar extinction coefficient ϵ_{NP} using eq. (4) from the supplementary information and then compared to the complex concentration. Correction for the spontaneous hydrolysis of the substrate by the solvent was accomplished by directly measuring a difference between the production of 4-nitrophenolate in the reaction cell and a reference cell containing the same concentration of carboxyester as in the reaction cell in absence of metal complex.
- 55 Subat, M.; Borowik, A. S.; König, B. *J. Am. Chem. Soc.* **2004**, 126, 3185-3190.
- 56 Turygin, D. S.; Subat, M.; Raitman, O. A.; Arslanov, V. V.; König, B.; Kalinina, M. A. *Angew. Chem.* **2006**, 118, 5466-5470.
- 57 Subat, M.; König, B. *Synthesis* **2001**, 12, 1818-1825.

2. 1,4,7,10 – Tetraazacyclododecane Metal Complexes as Potent Promoters of Phosphodiester Hydrolysis under Physiological Conditions

Abstract

Previously reported mono- and dinuclear Zn(II), Cu(II) and Ni(II) complexes of 1,4,7,10-tetraazacyclododecane ([12]aneN₄ or cyclen) with different heterocyclic spacers (triazine, pyridine) of various lengths (bi- and tripyridine) or an azacrown-pendant have been tested for the hydrolysis of bis(4-nitrophenyl)phosphate (BNPP) under physiological conditions (pH 7 - 9, 25 °C). All Zn(II) complexes promote the hydrolysis of BNPP under physiological conditions, while those of Cu(II) and Ni(II) do not have a significant effect on the hydrolysis reaction. The hydrolysis kinetics in buffered solutions (0.05 M Bis/Tris, TRIS, HEPES or CHES, *I* = 0.1 M, NaCl) at 25 °C were determined by the initial slope method (product conversion <5%). Comparison of the second-order pH-independent rate constants (k_{BNPP} , M⁻¹s⁻¹) for the mononuclear complexes **ZnL1**, **ZnL3** and **ZnL6**, which are $6.1 \cdot 10^{-5}$, $5.1 \cdot 10^{-5}$ and $5.7 \cdot 10^{-5}$, respectively, indicate that the heterocyclic moiety improves the rate of hydrolysis up to six times over the parent Zn([12]aneN₄) complex ($k_{\text{BNPP}} = 1.1 \cdot 10^{-5}$ M⁻¹s⁻¹). The reactive species is the Zn(II)-OH⁻ complex, in which the Zn(II)-bound OH⁻ acts as a nucleophile. For dinuclear complexes **Zn₂L2**, **Zn₂L4** and **Zn₂L5** the rate of reaction is defined by the degree of cooperation between the metal centers, which is determined by the spacer length. **Zn₂L2** and **Zn₂L4** possessing shorter spacers are able to hydrolyze BNPP 1 to 2 orders of magnitudes faster than **Zn₂L5**. The second-order rate constants $k_{\text{cat}1,2}$ of **Zn₂L4** and **Zn₂L2** at pH 7, 8 and 9 are significantly higher than those of previously reported related complexes. The high BNPP hydrolytic activity may be related to p-stacking and hydrophobic interactions between the aromatic spacer moieties and the substrate. Complexes **Zn₂L4** and **Zn₂L2** show hydrolytic activity at pH 7 and 8, which allows for the hydrolysis of activated phosphate esters under physiological conditions.

2.1. Introduction

Phosphate esters exist ubiquitously in nature.¹ They are found in nucleoside phosphates (nucleotides) as components of RNA and DNA, in sugar nucleotides for the glycosylation of oligosaccharides and in proteins involved in intracellular signaling and regulation.² Phosphodiester linkages of DNA are very stable to hydrolysis, with a half-life for spontaneous

hydrolysis estimated to be 10^{11} years at pH 7 at 25 °C.³ In nature, many enzymes that catalyze phosphate ester hydrolysis are activated by two or more metal ions.⁴ These include phosphate monoesterases, diesterases and triesterases. Enzymes that catalyze the replication of DNA and RNA and ribozymes that catalyze the intermolecular transesterification of RNA are also activated by more than one metal ion.

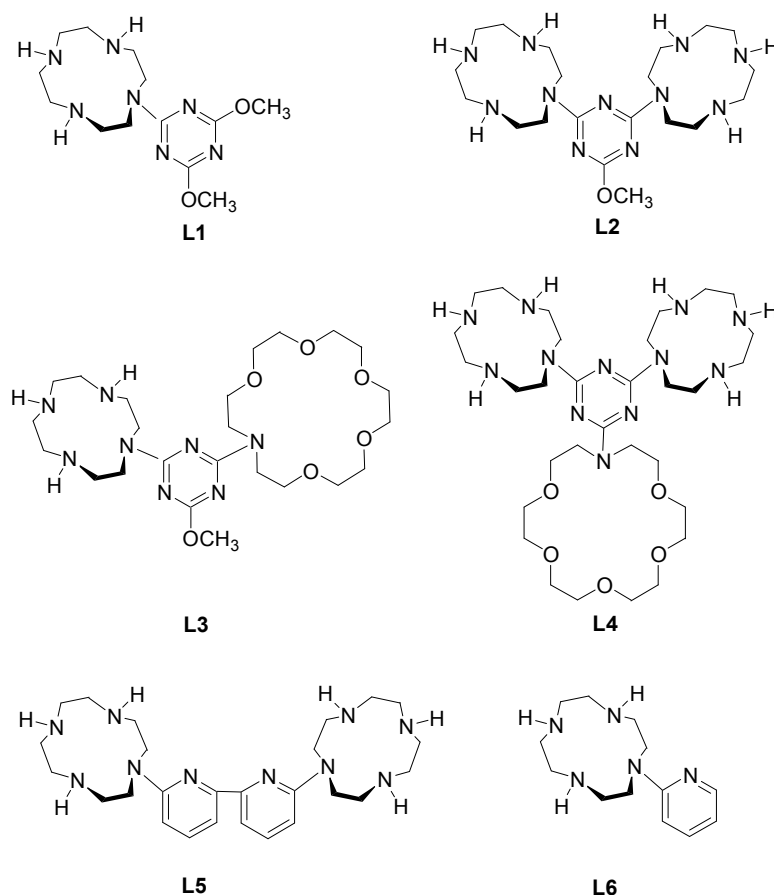
Currently there is considerable interest in understanding the reaction mechanism of such enzymes, especially the role of the metal ions. One goal is developing more reactive chemical systems that efficiently hydrolyze phosphate diester bonds under physiological conditions. Many metal ion based model systems have been reported, generally featuring tridentate or tetradentate ligands with free coordination sites of the metal cation.⁵ However, with only a few exceptions these systems are active either at high pH values (pH =9), elevated temperatures (T =35°C) or show a low solubility in aqueous solutions. For the development of synthetic hydrolases with applications in biotechnology, medicine or environmental sciences, e.g. the detoxification of pesticides like parathion, malathion and other organophosphorus compounds, artificial systems with activity under physiological conditions are required.

The proposed general mechanism of the hydrolysis reaction promoted by these complexes is based on the Lewis acid character of the metal ion reducing the pK_a of the coordinated water. This provides a metal-bound hydroxide nucleophile at neutral pH and at the same time activates a coordinated substrate towards nucleophilic attack by charge neutralization.^{5a,6} For dinuclear species, the two metal ions may act cooperatively in the catalytic process, either one metal ion provides the nucleophile and the other one coordinates the substrate or both metal ions participate in substrate binding, activation and cleavage.⁷ This cooperative action renders dinuclear complexes far more reactive than their mononuclear analogues.

It has been demonstrated that additional substrate interactions next to the metal ion center influence the properties of the metal complexes and that the hydrolytic activity may increase by the attachment of functional groups to a chelate ligand,⁸ such as a basic or nucleophilic auxiliary group⁹ or an NH-acidic group.¹⁰ With the aim to develop more efficient metal complexes possessing hydrolytic activity under physiological conditions, we have previously reported the synthesis of the macrocyclic ligands **L1-L6** (Scheme 1) with different heterocyclic spacers of various lengths and determined the hydrolytic properties of their Zn(II), Cu(II) and Ni(II) complexes in aqueous solution with 4-nitrophenyl acetate (NA).¹¹ We showed that the Zn(II) complexes have a high hydrolytic activity towards NA under physiological conditions compared to other similar macrocyclic compounds. The monohydroxy species $[Zn_2-L-OH_2-OH^-]$ was the active form. The mechanism of reaction,

either following *Michaelis-Menten* type or bimolecular kinetics, depended on the spacer length.

This paper presents kinetic studies of the hydrolysis of bis(4-nitrophenyl)phosphate (BNPP) in aqueous solution at 25 °C in the pH range 7 to 9. The influence of type and length of the spacer bridging the two metal complexes, the metal ions Cu(II), Ni(II) or Zn(II), and of mono- and dinuclear complexes on the hydrolytic efficiency were investigated.



Scheme 1. Structure of the [12]aneN₄ ligands **L1-L6**

2.2. Experimental Section

General information. UV/VIS spectra were recorded on a Varian Cary BIO 50 UV/VIS/NIR spectrophotometer equipped with a jacketed cell holder using 1-cm cuvettes (quartz or glass) from Hellma and on a Zeiss SPECORD M500 equipped with 6 cuvette holders using disposable acrylic (PMMA) 1-cm cuvettes from Sarstedt. For all UV/VIS measurements the temperature was kept constant at 25 °C (± 0.1 °C). EPR spectra in the X-band (9.459 GHz) were recorded with a Bruker System EMX in frozen acetonitrile/butyronitrile (4:1) solution at 110K.

Materials and Reagents. All reagents and solvents used for the synthesis of the metal complexes were of analytical grade. Bis(4-nitrophenyl)phosphate (BNPP) (Fluka) was transformed into the disodium salt form by titration with a 2M NaOH solution. 4-Nitrophenol (4-NP) (Riedel-de Haën), Bis/Tris (bis[2-hydroxyethyl]-imino-tris-[hydroxymethyl]-methane) (Sigma), TRIS (2-amino-2-hydroxymethyl-propane-1,3-diol) (Usb), HEPES (*N*-[2-hydroxyethyl]-piperazine-*N'*-[2-ethanesulfonic acid) (Sigma), CHES (N-cyclohexyl-2-

aminoethanesulfonic acid) (Sigma), were purchased from commercial sources and used without any further purification. The ligands **L1-L6** and their metal complexes were synthesized according to the published procedure.¹¹

Kinetic Measurements. The hydrolysis rate of bis(4-nitrophenyl)phosphate (BNPP) promoted by the ML-OH⁻ species was measured in the pH range 7 to 9 by an initial slope method following the increase in 408 nm-absorption of 4-nitrophenolate in aqueous solution for the Zn(II) complexes and the increase in 400 nm-absorption in aqueous solution for the Cu(II) and Ni(II) complexes (50 mM Bis/Tris, HEPES, TRIS or CHES buffer, $I = 0.1$ M, NaCl) at 25°C. The reactions were corrected for the degree of ionization of the 4-nitrophenol at the respective pH and temperature using the molar extinction coefficients for *para*-nitrophenolate at 400 nm¹¹ and 408 nm¹² previously determined. The kinetic data were collected using the initial slope method (product conversion <5%).¹³ The concentration of the reaction product 4-nitrophenyl phosphate is therefore too low to cause any inhibition of the metal complex. All measurements were performed in triplicate. From the slope [produced 4-nitrophenolate]/time and the concentration of BNPP, the pseudo-first-order rate constant $k_{obs}(\text{BNPP})$ (s⁻¹) was determined. A plot of these k_{obs} values vs metal complex concentrations at a given pH gave a straight line, its slope representing the second-order rate constant $k_{cat}(\text{BNPP})$ (M⁻¹s⁻¹). All correlation coefficients are =0.9992. Correction for the spontaneous hydrolysis of the substrate by the solvent was accomplished either by directly measuring the difference between the production of 4-nitrophenolate in the reaction cell and a reference cell containing the same concentration of phosphate diester as in the reaction cell in absence of metal complex, or by separate measurement of the spontaneous hydrolysis for BNPP under the given experimental conditions and manual subtraction of the measured absorption from the absorption curve of the catalyzed reaction. In comparison with 4-nitrophenyl acetate (NA), the spontaneous hydrolysis of BNPP has a much lower reaction rate when compared to the metal catalyzed reaction, and for pH values <7 the rate of spontaneous hydrolysis of BNPP is too low to be taken into account in the kinetic measurements. Therefore the general rate of spontaneous hydrolysis was not separately determined as previously in the case of NA.¹¹ The reaction solutions contained 0.04-0.5 mM Cu(II)-, 0.16-0.3 mM Ni(II)-, 0.08-18 mM Zn(II)-complex, 0.002-10.0 mM BNPP and 50 mM buffer.

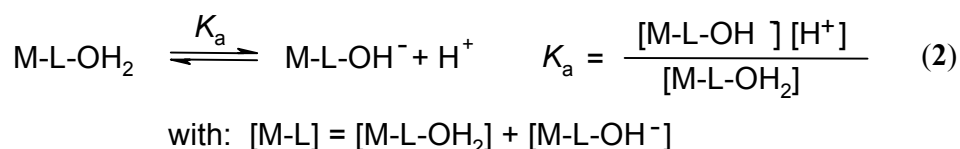
2.3. Results and Discussion

Hydrolysis of bis(4-nitrophenyl)phosphate (BNPP) promoted by the mononuclear metal complexes ZnL1, CuL1, NiL1, ZnL3 and ZnL6.

The reaction rates of ester bond cleavage of BNPP (0.002-10 mM) in aqueous solutions in the pH range 7 - 9 (50 mM HEPES or TRIS buffer, $I = 0.1$ M, NaCl) at 25 °C were measured by an initial slope method following the increase in 408 nm-absorption of 4-nitrophenolate for the Zn(II) complexes and the increase in 400 nm-absorption of 4-nitrophenolate for the Cu(II) and Ni(II) complexes. The reactions were corrected for the degree of ionization of the 4-nitrophenol at the respective pH and temperature. The absorption increase was recorded immediately after mixing and then monitored until 5% reaction conversion. The second-order dependence of the rate constant k_{cat} on the concentration of BNPP and metal complex is described by kinetic equation (1).

$$v_{cat} = \frac{d(Abs)}{d(t) \epsilon_{obs}} = k_{obs} [BNPP] = k_{cat} [M-L] [BNPP] \quad (1)$$

In equation (1) k_{cat} is the observed BNPP hydrolysis rate caused by the metal complex. The term $[M-L]$ describes the total concentration of metal complex and is composed of the concentration of the metal-hydroxy species $[M-L-OH^-]$ and the concentration of the water coordinated complex $[M-L-H_2O]$, depending on the corresponding pK_a of the metal complex. Equation (2) describes this equilibrium:



The corresponding pK_a values of the mononuclear complexes are given in Table 1.

Metal complex	pK_a^a
ZnL1	8.35 ± 0.03
NiL1	11.13 ± 0.02
CuL1 ^b	-
ZnL3	8.28 ± 0.05
ZnL6	7.89 ± 0.05
Zn-[12]aneN ₄	8.06 ± 0.01

^a From ref. 11. ^b Titration was not possible due to insufficient solubility.

Table 1. Deprotonation constants (pK_a) of metal-bound H₂O at 25 °C and $I = 0.10$ (TEAP).

Complex **CuL1** is not sufficiently soluble under the given experimental conditions to allow a potentiometric pH titration. However, its UV and IR spectra indicate a square pyramidal complex with one molecule of water the fifth ligand, as reported in literature.¹⁴ The coordination geometry of the Cu(II) ion is also supported by the electron spin resonance (ESR) spectra of **CuL1** (vide infra). The UV and IR spectra of **NiL1** coincide with the described structure of Ni[12]aneN₄.¹⁵ Among the mononuclear Zn complexes **ZnL6** forms more of the catalytically active species at lower pH values due to its smaller pK_a value. The Lewis acid character of Zn(II) and Ni(II) are reflected in the pK_a values of their cyclen complexes.

Kimura and Norman have shown for the hydrolysis of BNPP and other activated phosphoester derivatives with various Zn[12]aneN₃ and Zn[12]aneN₄ complexes that the active nucleophilic species attacking the phosphate ester is in fact the Zn-L-OH⁻ species.^{16,17,18} The same has been shown for Cu[9]aneN₃ complexes by Burstyn and Spiccia.^{19,20} To our knowledge there are no reported mononuclear macrocyclic Ni(II) complexes which promote the hydrolysis of phosphoesters. However, the reactive species of the dinuclear complex of Ni[9]aneN₃, developed by Kaden *et al.*, is the monohydroxy compound.²¹ Thus equation (1) can be written as follows:

$$v_{\text{cat}} = k_{\text{BNPP}} [\text{M-L-OH}][\text{BNPP}] \quad \text{with} \quad k_{\text{BNPP}} = \frac{[\text{M-L}] k_{\text{cat}}}{[\text{M-L-OH}]} \quad (3)$$

Equations (2) and (3) give equation (4) which describes the relationship between the rate constant k_{cat} , the pH independent reaction rate constant k_{BNPP} and the pH value.

$$k_{\text{cat}} = \frac{k_{\text{BNPP}} K_{\text{a}}}{K_{\text{a}} + [\text{H}^+]} \quad (4)$$

The value of the second-order rate constant k_{cat} (M⁻¹s⁻¹) is equal to the slope of the line obtained in the plot of k_{obs} versus the metal complex concentration at a given pH. The rate constants k_{obs} (s⁻¹) are determined by an initial slope method ([produced 4-nitrophenolate]/time) using the log e values determined previously.^{11,12} All correlation coefficients are = 0.9992. The use of the pH independent second-order reaction rate constant k_{BNPP} (M⁻¹s⁻¹) enables a comparison with previous reports from the literature.

Complex **CuL1** showed poor solubility under the given experimental conditions and could not be used for the hydrolysis experiments. **NiL1** did not show a significant effect on the hydrolysis, with pH dependent k_{obs} values in the range of 10⁻⁸ to 10⁻⁷ s⁻¹. The reactivity increases from pH 7 to pH 9 due to increasing amounts of the active species in solution (0.007% at pH 7, 0.07% at pH 8 and 0.7% at pH 9). Previously reported azamacrocyclic Ni(II) complexes were also active only at pH > 9.²¹

A typical plot of k_{obs} vs Zn(II) complex concentration for the mononuclear Zn(II) complexes is presented in the supporting information. The obtained second-order rate constants k_{cat} (M⁻¹s⁻¹) and the pH-independent hydrolysis rate constants k_{BNPP} (M⁻¹s⁻¹) for the mononuclear Zn(II) complexes are presented in Table 2.

Zn(II)-Cyclen ($pK_a = 7.9$)		ZnL1 ($pK_a = 8.35$)	
pH	$10^6 k_{\text{cat}} (\text{M}^{-1}\text{s}^{-1})$	pH	$10^6 k_{\text{cat}} (\text{M}^{-1}\text{s}^{-1})$
7.51 ^a	3.1	7.12 ^a	3.1
8.00 ^a	6.3	7.53 ^a	7.2
8.52 ^a	8.7	8.00 ^a	18.4
9.00 ^a	9.9	8.49 ^a	32.3
		9.00 ^a	48.4
$10^5 k_{\text{BNPP}} (\text{M}^{-1} \text{s}^{-1})^a = 1.1 \pm 0.3$		$10^5 k_{\text{BNPP}} (\text{M}^{-1} \text{s}^{-1})^a = 6.1 \pm 0.2$	

ZnL3 ($pK_a = 8.28$)					
pH	$10^6 k_{\text{cat}} (\text{M}^{-1}\text{s}^{-1})$	pH	$10^5 k_{\text{cat}} (\text{M}^{-1}\text{s}^{-1})$	pH	$10^5 k_{\text{cat}} (\text{M}^{-1}\text{s}^{-1})$
6.83 ^b	1.7	8.00 ^a	1.70	9.24 ^d	4.60
7.02 ^b	2.3	8.26 ^a	2.31	9.58 ^d	4.89
7.26 ^{a, b, e}	4.2	8.50 ^a	3.13	9.91 ^d	4.99
7.52 ^a	7.7	8.69 ^a	3.66	10.22 ^d	5.05
7.73 ^a	10.3	9.00 ^{a, d, e}	4.38		
$10^5 k_{\text{BNPP}} (\text{M}^{-1} \text{s}^{-1})^{a,b,d} = 5.1 \pm 0.1$					

ZnL6 ($pK_a = 7.89$)					
pH	$10^6 k_{\text{cat}} (\text{M}^{-1}\text{s}^{-1})$	pH	$10^5 k_{\text{cat}} (\text{M}^{-1}\text{s}^{-1})$	pH	$10^5 k_{\text{cat}} (\text{M}^{-1}\text{s}^{-1})$
6.49 ^c	2.1	7.83 ^a	2.42	9.24 ^d	5.35
6.83 ^{b, c, e}	4.2	8.09 ^a	3.42	9.58 ^d	5.60
7.15 ^b	8.2	8.31 ^a	3.93	9.91 ^d	5.58
7.36 ^{a, b, e}	11.4	8.55 ^a	4.61	10.22 ^d	5.65
7.59 ^a	18.7	8.87 ^{a, d, e}	4.98		
$10^5 k_{\text{BNPP}} (\text{M}^{-1} \text{s}^{-1})^{a,b,c,d} = 5.7 \pm 0.1$					

[BNPP] = 0.5 - 10 mM, $\Delta \text{pH} = \pm 0.005$, $\Delta k_{\text{obs}} = 0.3 - 6.8 \%$, $\Delta k_{\text{cat}} = 1.1 - 4.1 \%$, $\Delta T = \pm 0.1 \text{ } ^\circ\text{C}$.

[Zn(II)-Cyclen] = 0.8 - 14 mM, [ZnL1] = 0.5 - 6 mM, [ZnL3] = 0.5 - 15 mM, [ZnL6] = 0.5 - 8 mM.

^a Tris/HCl [50 mM], $I = 0.1 \text{ M}$ (NaCl), $T = 25 \text{ } ^\circ\text{C}$; ^b HEPES [50 mM], $I = 0.1 \text{ M}$ (NaCl), $T = 25 \text{ } ^\circ\text{C}$; ^c Bis/Tris [50 mM], $I = 0.1 \text{ M}$ (NaCl), $T = 25 \text{ } ^\circ\text{C}$; ^d CHES [50 mM], $I = 0.1 \text{ M}$ (NaCl), $T = 25 \text{ } ^\circ\text{C}$; ^e k_{cat} and k_{obs} measured at the same pH value in different buffers are in the given error margins and are listed as average values.

Table 2. Hydrolysis rate constants $k_{\text{cat}} (\text{M}^{-1}\text{s}^{-1})$ and pH-independent hydrolysis rate constants $k_{\text{BNPP}} (\text{M}^{-1}\text{s}^{-1})$ for the mononuclear Zn(II) complexes at 25 $^\circ\text{C}$ in aqueous solution.

Kimura *et al.* have described the hydrolysis of BNPP promoted by the Zn(II)-cyclen complex, but using different reaction conditions ($T = 35\text{ }^{\circ}\text{C}$, $\text{pH} = 9.2$).¹⁶ Kinetic measurements with this complex under our reaction conditions were performed for comparison. The kinetic measurements with **Zn(II)-cyclen** and **ZnL1** were performed in the pH range 7 - 9 in TRIS buffer, while the hydrolysis of BNPP promoted by **ZnL3** and **ZnL6** was measured in the extended pH range 6.5 - 10.3 (50 mM Bis/Tris, HEPES, TRIS or CHES buffer, $I = 0.1\text{ M}$, NaCl). The derived sigmoidal pH-rate profiles (Figure 1) are characteristic of a kinetic process controlled by an acid-base equilibrium and exhibit inflection points corresponding to the pK_a values of the coordinated water molecules of **ZnL3** ($\text{pK}_a = 8.28$) and **ZnL6** ($\text{pK}_a = 7.89$). This indicates that the Zn(II)-OH⁻ complex is the reactive species. The Zn(II)-bound OH⁻ acts as a nucleophile to attack the phosphate atom of the phosphodiester hydrolyzing the bis(4-nitrophenyl)phosphate to 4-nitrophenolate and 4-nitrophenyl phosphate. This mechanism of BNPP hydrolysis has been reported for other Zn(II) cyclen complexes, too.^{16,17,18,22,23} A subsequent hydrolysis of the phosphate monoester to inorganic phosphate was not detected.

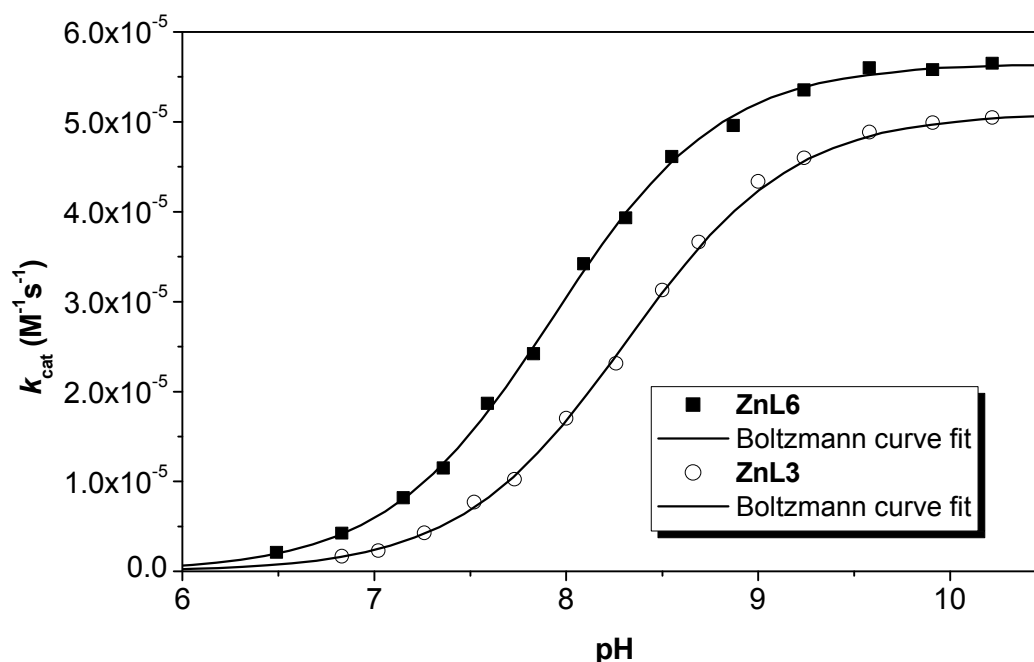
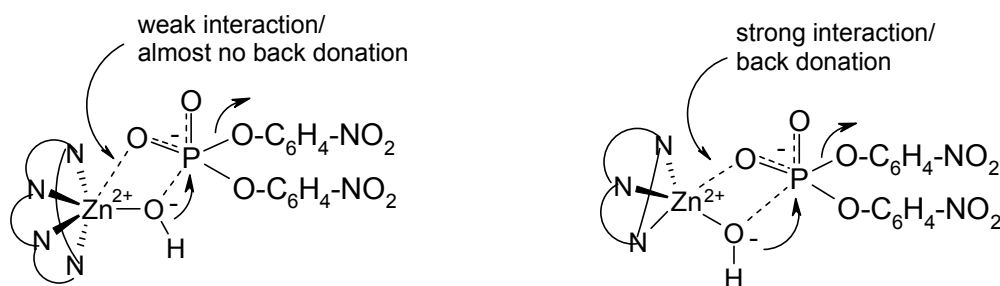


Figure 1. pH-Rate profile for the second-order rate constants of BNPP hydrolysis of **ZnL3** and **ZnL6** at 25 °C and $I = 0.1$ (NaCl) in aqueous solution.

The k_{BNPP} values of our Zn(II) cyclen complexes show a 5 to 6-fold higher hydrolysis rate than the simple Zn[12]aneN₄ system due to the aromatic substituent. π - π interactions of the

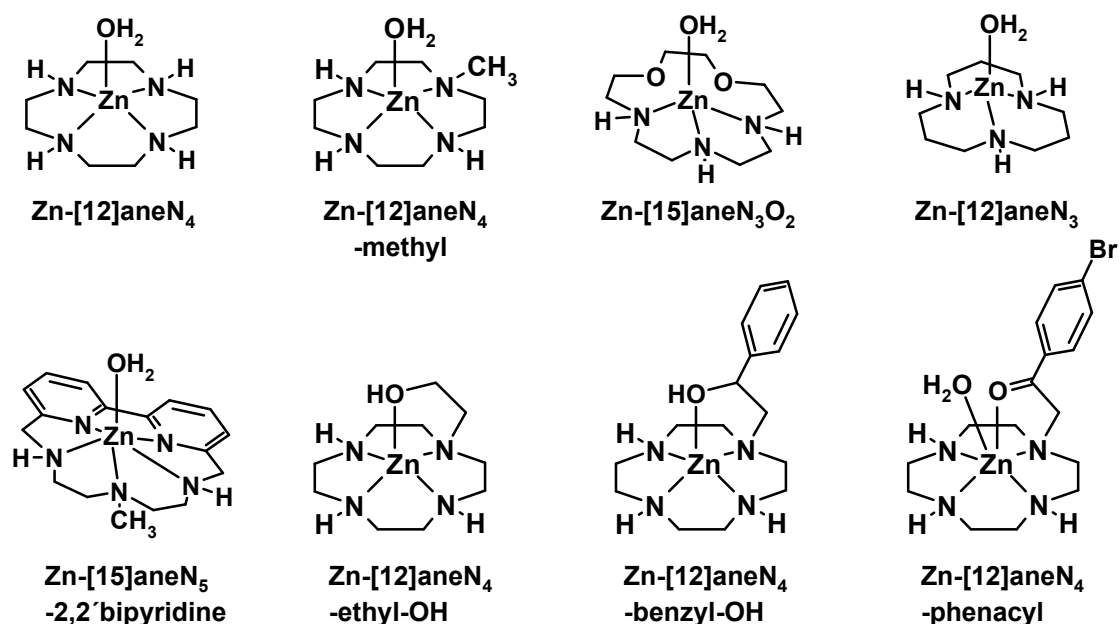
heterocycle with the aromatic ring of the bis(4-nitrophenyl)phosphate leads to a tighter substrate binding. The more hydrophobic environment may result in a higher reactivity of the hydroxy species and a better substrate preorganisation for hydrolysis.²⁴ Tang *et al.* previously reported on the influence of an aromatic substituent, emphasizing on its positive influence on the substrate orientation and stabilisation of the leaving group in the transition state.²⁵

We have previously reported the X-ray structure of **Zn₂L2** showing that the zinc ion is coordinated by only 3 out of four N-atoms of cyclen. The bond to the fourth N-atom is significant longer (2.6 Å).¹¹ Kimura describes the same effect for other Zn cyclen derivatives with electron-poor aromatic substituents.²⁶ The structure of the Zn(II) complexes here reported is in between that of [12]aneN₄²⁷ and of [12]aneN₃, which explains the enhanced hydrolysis rates for BNPP. Complexes of the [12]aneN₃ type promote phosphate diester hydrolysis by coordination of the phosphoester to the metal ion (Scheme 2).



Scheme 2. Proposed transition states of phosphate diesters hydrolysis by azamacrocyclic Zn(II) complexes with tetraza- (left) and triaza-ligands.¹⁶

The structures of previously studied mononuclear azamacrocyclic Zn(II) complexes are depicted in Scheme 3 and their reported second-order reaction rates k_{BNPP} and $\text{p}K_{\text{a}}$ values are summarized in Table 3. Due to the high number of publications in the field of metalloenzyme-promoted phosphate ester hydrolysis, only mononuclear azamacrocyclic Zn(II) complexes promoting the hydrolysis of BNPP have been selected.



Scheme 3. Structures of previously studied mononuclear azamacrocyclic Zn(II) complexes^a

Complex	$10^5 k_{\text{BNPP}} (\text{M}^{-1}\text{s}^{-1})$	Reaction conditions ^a	pK_a^b	Lit.
Zn-[12]aneN₄	2.1 ± 0.2	$I = 0.2$ (NaClO ₄), pH-stat method	7.9	16
Zn-[12]aneN₄-methyl	0.52 ± 0.2	$I = 0.1$ (NaNO ₃), buffer (20 mM) ^c	7.68	9g
Zn-[15]aneN₃O₂	1.37^d	$I = 0.15$ (NaCl), buffer (50 mM) ^e	8.8	28
Zn-[12]aneN₃	8.5 ± 0.2	$I = 0.2$ (NaClO ₄), pH-stat method	7.2	16
Zn-[15]aneN₅-2,2'-bipyridine	11 ± 0.1	$I = 0.1$ (NMe ₄ NO ₃), buffer (50 mM) ^e	10.73	29
Zn-[12]aneN₄-ethyl-OH	50 ± 0.1	$I = 0.1$ (NaNO ₃), buffer (20 mM) ^c	7.6	9g
Zn-[12]aneN₄-benzyl-OH	65 ± 0.1	$I = 0.1$ (NaNO ₃), buffer (20 mM) ^c	7.5	9g
Zn-[12]aneN₄-phenacyl	4.3 ± 0.2	$I = 0.1$ (NaClO ₄), buffer (20 mM) ^c	8.4	30

^a All values were determined in aqueous solutions at 35 °C. ^b pK_a value determined at 25 °C. ^c Goods buffer. ^d k_{BNPP} was calculated from the value of k_{cat} up to pH 10 ($1.3 \pm 0.1 \cdot 10^{-5} \text{ M}^{-1}\text{s}^{-1}$) ^e MOPS, TAPS, CHES, CAPS buffer, depending on the pH range.

Table 3. A comparison of hydrolysis rate constants $k_{\text{BNPP}} (\text{M}^{-1}\text{s}^{-1})$ and pK_a values for previously reported mononuclear Zn(II) complexes.

Zn[12]aneN₃ complexes show higher reaction rates of BNPP hydrolysis than Zn[12]aneN₄ derivatives.³¹ The complexes with an ethyl- and benzylhydroxyl pendant arm show significantly higher hydrolytic activity, due to a different reaction mechanism with the alcoholate as the reactive species: The first reaction step is a transphosphorylation followed by intramolecular

nucleophilic attack of the Zn(II) bound hydroxide ion.^{9,30} Zn-[15]aneN₅-2,2'-bipyridine has the highest reaction rate hydrolyzing BNPP ($1.1 \cdot 10^{-4} \text{ M}^{-1}\text{s}^{-1}$), which is 5-fold higher than the simple Zn[12]aneN₄ system. Complexes **ZnL1**, **ZnL3** and **ZnL6** show k_{BNPP} values in the same range as Zn[12]aneN₃. Due to their lower pK_a values their activity under physiological conditions is high, whereas Zn-[15]aneN₅-2,2'-bipyridine is active only at $\text{pH} > 9$.

Hydrolysis of bis(4-nitrophenyl)phosphate (BNPP) promoted by the dinuclear metal complexes **Zn₂L2**, **Cu₂L2**, **Ni₂L2**, **Zn₂L4** and **Zn₂L5**

The reaction rates of ester bond cleavage of BNPP (0.002-10 mM) in aqueous solutions in the pH range 7 - 9 (50 mM HEPES or TRIS buffer, $I = 0.1 \text{ M}$, NaCl) at 25 °C were measured by an initial slope method. The reaction parameters and method of evaluation of data are identical to those described for the mononuclear complexes.

The reaction rate is proportional to the concentrations of the metal complex and the substrate, such that equation (5) can be postulated, from which equation (6) is then derived.

$$v_{\text{cat}} = k_{\text{cat}} [\text{M-L}]^{\text{Total}} [\text{BNPP}] \quad (5)$$

$$v_{\text{cat}} = \frac{d(\text{Abs})}{d(t) \epsilon_{\text{obs}}} = k_{\text{obs } 1, 2} [\text{BNPP}] = k_{\text{cat } 1, 2} [\text{M-L}]^{\text{Total}} [\text{BNPP}] \quad (6)$$

The reaction rate v_{cat} reflects in this case the contribution of two reactive species, the monohydroxy and the dihydroxy species. Therefore equation (7) can be derived from equation (6).

$$k_{\text{cat } 1, 2} [\text{M-L}]^{\text{Total}} = k_{\text{cat } 1} [\text{M}_2\text{-L-(OH}_2\text{)(OH}^-)] + k_{\text{cat } 2} [\text{M}_2\text{-L-(OH}^-)_2] \quad (7)$$

The contribution of the two reactive species, the monohydroxy and the dihydroxy species depends on the corresponding pK_a of the metal complex.

We have previously shown that for the dinuclear complexes **Zn₂L4** (in aqueous solution) and **Zn₂L2** (in aqueous solution and in MeOH/H₂O 9:1 solution) two distinct buffer regions were determined, one around pH 6, and the other in the pH range 8 - 10, corresponding to three distinct pK_a values¹¹. The proposed chemical model is based on an equilibrium in solution between the μ -hydroxo-bridged species $\text{Zn}_2\text{-L-(}\mu\text{OH}_2\text{)(OH}_2\text{)}$, analogous to the obtained crystal structure of **Zn₂L2**,¹¹ and an open form corresponding to the species where each Zn(II) ion is coordinating a water molecule, $\text{Zn}_2\text{-L-(OH}_2\text{)}_2$. This model is supported by a good match with the calculated and the measured pH profiles, and reports from literature where a similar

equilibrium between open and closed species was postulated.³² The proton independent equilibrium K_{D1} can be determined indirectly. The pK_a values of **Zn₂L2** and **Zn₂L4** are summarized in Table 4.

Metal complex	pK_a^a			$\log K_{D1}$
	pK_{a1}	pK_{a2}	pK_{a3}	
Zn ₂ L2	-	9.72 ± 0.03^b	-	-
Zn ₂ L4	8.27 ± 0.02	9.42 ± 0.06	5.96 ± 0.02	0.47 ± 0.04

^a From ref. 11. ^b The titration curve does not permit a determination of pK_{a1} and pK_{a3} values due to the insufficient solubility of the complex in water and/or MeOH/water 9:1.

Table 4. Deprotonation constants (pK_a) of metal-bound H₂O at 25 °C and $I = 0.10$ (TEAP).

The pK_a value of the μ -hydroxo-coordinated water molecule, pK_{a3} , is smaller than those reported for similar compounds,^{32c} indicating enhanced acidity and stability of the μ -hydroxo-bridge due to the close proximity of the two Zn(II) cyclen moieties. For the dinuclear complexes, **Cu₂L2**, **Ni₂L2** and **Zn₂L5**, the previously described pH profiles¹¹ correspond to the general model³³ with each metal ion coordinating a water molecule and two successive deprotonation steps leading to the species $M_2-L-(OH)_2$.

The pK_a values of these complexes are summarized in **Table 5**.

Metal complex	pK_{a1}	pK_{a2}
Ni ₂ L2	9.75 ± 0.02	10.10 ± 0.02
Cu ₂ L2	8.34 ± 0.03	8.68 ± 0.03
Zn ₂ L5	7.45 ± 0.03	8.85 ± 0.03

Table 5. Deprotonation constants (pK_a) of metal-bound H₂O at 25 °C and $I = 0.10$ (TEAP).¹¹

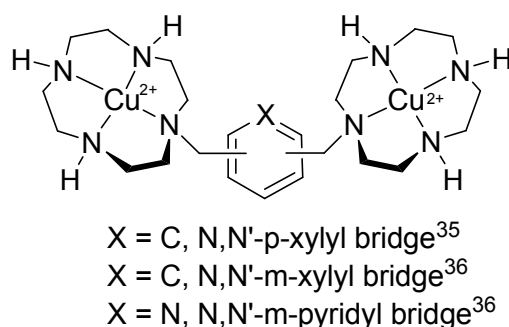
The pH profile, UV and IR spectra of **Cu₂L2** indicate a structure with each Cu(II) ion in square pyramidal geometry,¹⁴ coordinating to the 4 N-atoms of the macrocycle and 1 water molecule. This structure was supported by electron spin resonance (ESR) studies. ESR spectra of acetonitrile/butyronitrile (4:1) solutions of **CuL1** and **Cu₂L2** at 110 K showed characteristic lines for the formation of the mononuclear, respectively dinuclear species, with spectroscopic parameters g_{\parallel} , g_{\perp} and A_{\parallel} similar to those reported for the simple Cu[12]aneN₄

complex³⁴ and the dinuclear Cu[12]aneN₄ complexes bridged by *para*-xylylen,³⁵ *meta*-xylylen or a pyridyl spacer³⁶ (Table 6). The structures of the latter complexes are given in Scheme 6.

Metal complex	g_{\parallel}	g_{\perp}	A_{\parallel} [10^{-4} cm ⁻¹] ^a	D [10^{-4} cm ⁻¹] ^a
CuL1	2.236	2.092	170	
Cu[12]aneN ₄ ^b	2.198	2.057	184	
Cu ₂ L2	2.202	2.052	80	
<i>N,N'</i> - <i>p</i> -xylylenebis(Cu[12]aneN ₄) ^c	2.19	2.06	92	
<i>N,N'</i> - <i>m</i> -xylylenebis(Cu[12]aneN ₄) ^d	2.207	2.065	81	8
<i>N,N'</i> - <i>m</i> -pyridylbis(Cu[12]aneN ₄) ^d	2.193	2.03	90	90

^a Values obtained by simulation. ^b From ref. 33. ^c From ref. 34. ^d From ref. 35.

Table 6. EPR parameters of **CuL1** and **Cu₂L2** in acetonitrile/butyronitrile at 110 K and comparison with previously reported Cu[12]aneN₄ complexes.



Scheme 6. Structures of the dinuclear Cu[12]aneN₄ complexes previously studied by ESR techniques.

The frozen solution ESR spectrum (110 K) of **CuL1** shows a hyperfine splitting (Figure 2), which unfortunately cannot be refined because of the large intrinsic line-width of the signal. A four-line pattern is expected for mononuclear copper(II) complexes due to the coupling of the electron to the 3/2 spin of the copper(II) nucleus.³⁵ The hyperfine coupling constant and g values are close to those found for copper cyclen complexes. The X-band EPR spectrum of **Cu₂L2** exhibits a septuplet around 3000 G (Figure 2) corresponding to the two allowed transitions ($M_S = 1$) in agreement with previous works.^{35,36,37} A half field signal assigned to a forbidden transition ($M_S = 2$) is not observed due to the very low intensity. The observed spectrum shows the characteristic pattern of a dicopper compound with weak intramolecular

exchange between the two copper ions ($I_{\text{Cu}} = 3/2$). The g values are similar for all complexes, indicating the square-pyramidal geometry, while the A_{\parallel} values of **Cu₂L2** are approximately half of those of **CuL1**, which is to be expected for a copper dimer showing magnetic exchange. Unfortunately, the forbidden transition is poorly defined and it is not possible to estimate the Cu-Cu distance from the ratio of the intensity of the forbidden transition to the intensity of the allowed transition.³⁸ Another method for calculation of the distance between the two paramagnetic cations is from the zero-field splitting parameter D ,³⁷ which in our case could not be determined accurately from the simulations.

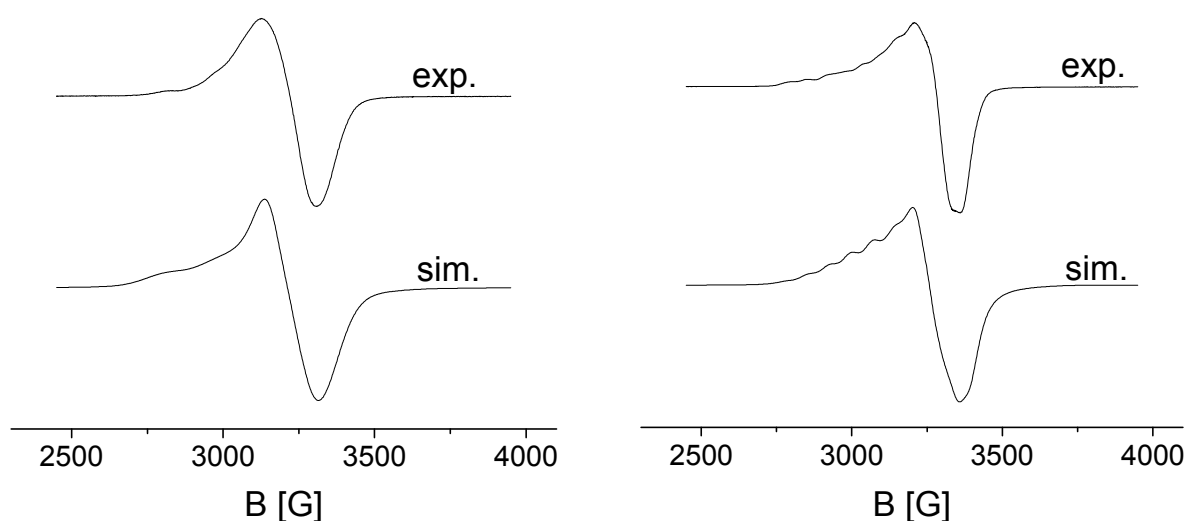


Figure 2. Experimental and simulated EPR spectra of the mononuclear **CuL1** (left) and **Cu₂L2** (right) complexes in acetonitrile/butyronitrile solution at 110 K.

From the data we conclude that **CuL1** and **Cu₂L2** have a typical square-pyramidal geometry, with the Cu(II) ion coordinating to 4 N-atoms of the macrocycle and 1 H₂O molecule. A weak interaction between the two metal centers is shown by the ESR spectra and the small difference between the two pK_a values. A μ -hydroxo bridge between the two metal centers, as in the case of **Zn₂L2** and Cu[9]aneN₃ complexes,^{19,39} can be excluded. In the addition, the coordination of the Cu(II) ions to the N-atom of the bridging hetarene, as seen in a pyridyl-bridged Cu(II) bis(cyclen) complex,³⁶ is not observed. ESR spectra of the Ni(II) complexes gave no signals, even at 4 K. High-field measurement conditions are required, as usual for systems with $S = 1$, to obtain proper spectra.

Complex **Ni₂L2** did not show a significant effect on the hydrolysis (k_{obs} is in the range of 10^{-8} to 10^{-7} s^{-1} , depending on the pH value of the solution) due to the weak Lewis acid character of the metal ion. At physiological pH no active species is present in solution.^{21,40}

For **Cu₂L2**, the k_{obs} values were in the range of 10^{-5} s^{-1} . To the best of our knowledge no discrete Cu(II) or Ni(II) [12]aneN₄ complexes promoting the hydrolysis of a phosphodiester have been reported. Cu[9]aneN₃ complexes^{19,20} and the dinuclear Ni[9]aneN₃ complex, developed by Kaden,²¹ show hydrolytic activity. Suh *et al.* have built artificial enzymes by attaching Cu[12]aneN₄ moieties to cross-linked polystyrene supports, which were capable of cleaving various protein substrates (α -globulin, myoglobin, albumin).⁴¹ The hydrolytic efficiency is ascribed to the high number of Cu[12]aneN₄ moieties, some binding the substrate and some hydrolyzing it, and the reaction medium created by the polymer support. Morrow⁴² and Bursty^{6a,19} have demonstrated that artificial metallohydrolases, mono- as well as dinuclear metal complexes, must possess two *cis*-oriented labile coordination sites in order to simultaneously bind the substrate and the nucleophile. The two metal centers of the **Cu₂L2** complex have only one coordination site available each and do not act cooperatively.

For the dinuclear Zn(II) complexes **Zn₂L2**, **Zn₂L4** and **Zn₂L5** the reaction rates $k_{\text{cat}1,2}$ (from equation (8)) of ester bond cleavage of BNPP (0.01 - 8 mM) were measured in aqueous solutions in the pH range 7 - 9 (50 mM TRIS buffer, $I = 0.1 \text{ M}$, NaCl) at 25 °C following the increase in 408 nm absorption of 4-nitrophenolate. The reaction parameters and method of data evaluation are identical to those described for the mononuclear complexes.²³ The plots of k_{obs} vs Zn(II) complex concentration for the dinuclear Zn(II) complexes are presented in the supporting information. All complexes show second-order kinetics.⁴³ The obtained second-order rate constants $k_{\text{cat}1,2} (\text{M}^{-1} \text{ s}^{-1})$ for **Zn₂L2**, **Zn₂L4** and **Zn₂L5** are summarized in Table 7.

Metal complex	$10^3 k_{\text{cat}1,2} (\text{M}^{-1} \text{ s}^{-1})$ at pH 7 ^a	$10^3 k_{\text{cat}1,2} (\text{M}^{-1} \text{ s}^{-1})$ at pH 8 ^a	$10^3 k_{\text{cat}1,2} (\text{M}^{-1} \text{ s}^{-1})$ at pH 9 ^a
Zn₂L2 ^b	-	1.28	1.35
Zn₂L4	1.03	2.45	2.63
Zn₂L5	0.049	0.244	0.406

[BNPP] = 0.01 - 8 mM, $\Delta \text{pH} = \pm 0.005$, $\Delta k_{\text{obs}} = 2.2 - 9.3 \%$, $\Delta k_{\text{cat}1,2} = 0.8 - 4 \%$, $\Delta T = \pm 0.1 \text{ } ^\circ\text{C}$.

[**Zn₂L2**] = 0.3 - 8 mM, [**Zn₂L4**] = 0.4 - 10 mM, [**Zn₂L5**] = 0.6 - 8 mM.

^a Tris/HCl [50 mM], $I = 0.1 \text{ M}$ (NaCl), $T = 25 \text{ } ^\circ\text{C}$. ^b The measurements with **Zn₂L2** at pH 7 entered the error margin of the apparatus despite numerous attempts, thus making the evaluation of the kinetic measurements inaccurate.

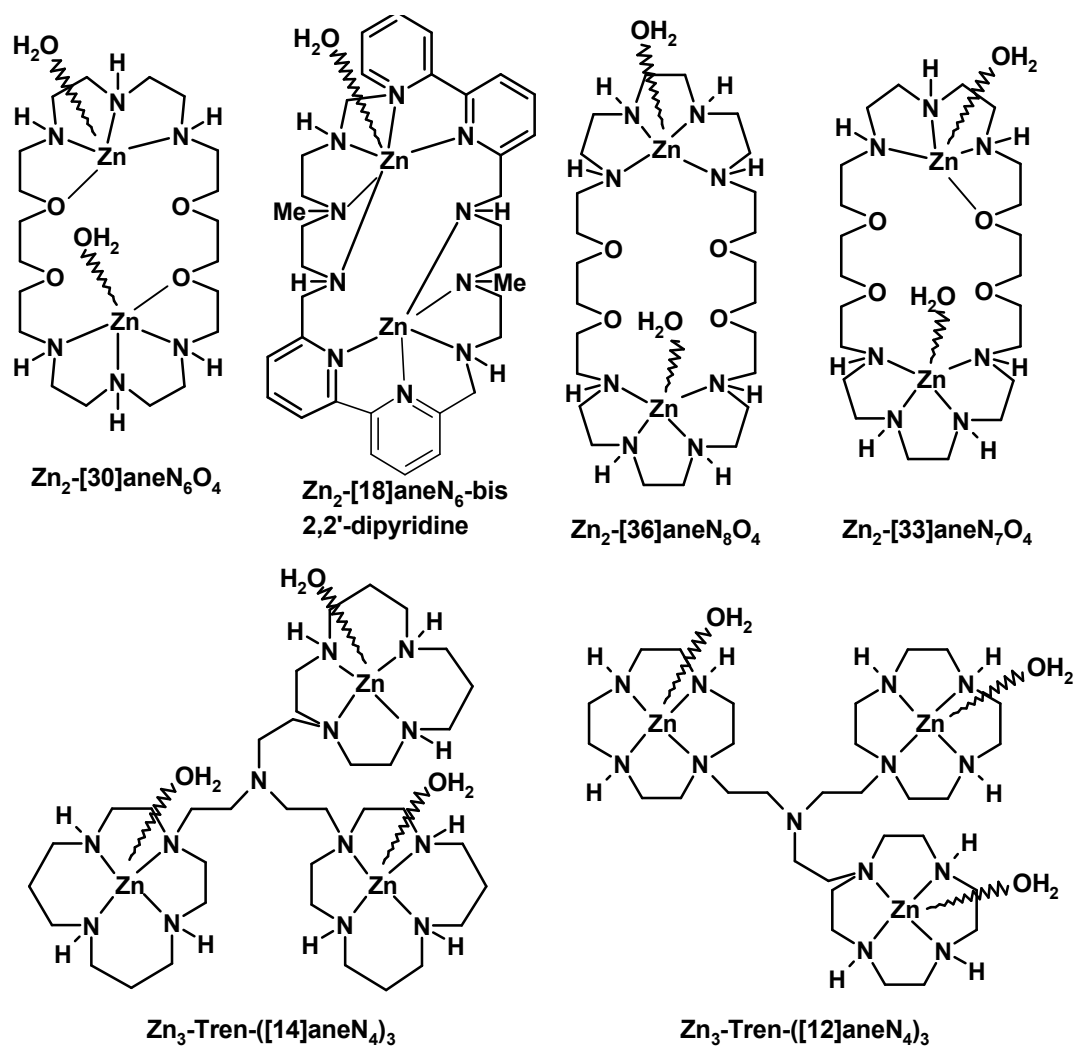
Table 7. Second-order rate constants $k_{\text{cat}1,2} (\text{M}^{-1} \text{ s}^{-1})$ at pH 7, 8 and 9 for the dinuclear Zn(II) complexes at 25 °C in aqueous solution.

From the obtained $k_{\text{cat}1,2}$ values it is obvious that **Zn₂L2** and **Zn₂L4** possessing a shorter spacer are able to hydrolyze BNPP 1 to 2 orders of magnitudes faster than **Zn₂L5**. It has been previously shown that dinuclear Zn(II) complexes with short spacers are able to coordinate the phosphate diester bidentate, thus increasing the activation of the substrate and bringing it closer to the attacking nucleophile.⁴² A short spacer leads to a higher degree of cooperation between the metal centers for the hydrolysis of BNPP. The second-order rate constants increase with pH as expected. For **Zn₂L2** and **Zn₂L4** the increase from pH 8 to pH 9 is very small compared to **Zn₂L5** where the value of $k_{\text{cat}1,2}$ at pH 9 is almost double the value of $k_{\text{cat}1,2}$ at pH 8. The high cooperativity of the two metal centers in **Zn₂L4** leads to faster BNPP hydrolysis, although it is the weaker Lewis acid if compared to **Zn₂L5**.

The hydrolytic activity of the dinuclear Zn(II) complexes is 2 to 3 orders of magnitude higher than that of the corresponding monomers **ZnL1** and **ZnL3**. A direct comparison between **Zn₂L5** and **ZnL6** is not possible due to the different spacer length. The increased rates indicate the importance of cooperativity of the two metal centers for hydrolysis activity.^{6,7,28,29,44}

From the pK_a values and species distribution diagram of **Zn₂L4** (see supporting information) we can assert the monohydroxy species $\text{Zn}_2\text{-L-(OH)}_2(\text{OH}^-)$ in its opened form is the catalytically active species at pH 7 and 8. The bishydroxy form $\text{Zn}_2\text{-L-(OH)}_2$ is present in very low concentration at this pH (less than 3% at pH 8). Even for pH 9 the concentration of the dihydroxy species is only around 25%. Complex **Zn₂L2** behaves similar. For **Zn₂L5** with pK_{a1} and pK_{a2} values of 7.45 and 8.85, the mono- and dihydroxy species are both present pH 7 to 9 and contribute to the BNPP hydrolysis (species distribution diagram, see supporting information).

Scheme 7 gives the structures of previously reported di- and trinuclear metal complexes for BNPP hydrolysis, which showed good activity. The second-order rate constants $k_{\text{cat}1,2}$ ($\text{M}^{-1}\text{s}^{-1}$) at pH 7, 8 and 9 and pK_a values are summarized in Table 8.



^a Charges and counter-ions are omitted for clarity reasons.

Scheme 7. Structures of previously studied di- and trinuclear Zn(II) complexes for the hydrolysis of BNPP.^a

Complex / Nucleophile	$10^5 k_{\text{cat}1,2} (\text{M}^{-1} \text{s}^{-1})^a$			$\text{p}K_a^b$	Lit.
	pH 7	pH 8	pH 9		
$\text{Zn}_2\text{-[30]aneN}_6\text{O}_4 / \text{Zn}_2\text{-(OH)}_2^c$	^{-d}	1.1 ^e	5.11 ^f	9.2	28
$\text{Zn}_2\text{-[18]aneN}_6\text{-bis(2,2'-dipyridine)} / \text{Zn}_2\text{-(OH)}^g$	^{-d}	53	137	8.88	29
$\text{Zn}_2\text{-[36]aneN}_8\text{O}_4 / \text{Zn}_2\text{-(OH)}_2^c$	^{-d}	^{-d}	1.6	9.88	42
$\text{Zn}_2\text{-[33]aneN}_7\text{O}_4 / \text{Zn}_2\text{-(OH)}_2^c$	^{-d}	1.6 ^e	6.4 ^h	9.38	42
$\text{Zn}_3\text{-Tren-([14]aneN}_4\text{)}_3 / \text{Zn}_3\text{-(OH)}_2$ $/\text{Zn}_3\text{-(OH)}_3^{c,i}$	3.8	19.8	30	7.90/8.83 ⁱ	41b
$\text{Zn}_3\text{-Tren-([12]aneN}_4\text{)}_3 / \text{Zn}_3\text{-(OH)}_2$ $/\text{Zn}_3\text{-(OH)}_3^{c,i}$	1.02	3.9	9.4	8.21/9.6 ⁱ	41b

^a Various buffer systems [50 mM], $I = 0.1 - 0.15$ M (NaCl or NMe₄NO₃), 35.1 °C. The values of $k_{\text{cat}1,2}$ were either taken directly from the literature (if reported) or derived from the reported k_{BNPP} (M⁻¹ s⁻¹) values and concentrations. The errors are <5%. ^b 35.1 °C, water. ^c k_{BNPP} values of the monohydroxy species were not determined due to their negligible effect on the hydrolysis. ^d No active species present in solution at the respective pH. ^e pH = 8.1. ^f pH = 9.1. ^g k_{BNPP} values of the dihydroxy species were not determined due to their negligible effect on the hydrolysis. ^h pH = 8.9. ⁱ For these trinuclear complexes it has been shown that the di- and trihydroxy species are the kinetically active species and the $\text{p}K_{\text{a}}$ s of the species are given accordingly.

Table 8: A comparison of second-order rate constants $k_{\text{cat}1,2}$ (M⁻¹s⁻¹) at pH 7, 8 and 9 and $\text{p}K_{\text{a}}$ values for previously reported di- and trinuclear Zn(II) metal complexes.

For all the reported complexes an “associative” mechanism is postulated, in which the substrate approaches the Zn(II) complex and the oxygens of BNPP coordinate to the two electrophilic Zn(II) cations forming a bidentate complex. A zinc-bound hydroxide nucleophile attacks the phosphorous atom. Strong interaction of the BNPP ester with the electrophilic metal centers and a highly nucleophilic character of the Zn-OH, enhances the hydrolytic activity of a complex. The lack of hydrolytic activity of the monohydroxy species of the complexes in Table 8 is attributed to a bridged coordination of the hydroxide anion to two metal centers which reduces the nucleophilicity of the generated hydroxide. This applies similarly to **Zn₂L2** and **Zn₂L4**: the open form monohydroxy species Zn₂-L-(OH₂)(OH⁻) is the catalytically active form and not the closed form with the μ -hydroxo bridge. The high activity of the Zn₂-(OH)₂ complexes in Table 8 is explained by a cooperative role of the two metal ions in the hydrolytic process.

For Zn₂-[18]aneN₆-bis(2,2'-dipyridine)²⁹ the inverse behavior is observed (the monohydroxy species is the active form, while the dihydroxy species is inactive) because each metal ion is coordinated to five N-atoms of the macrocycle, leaving only one coordination site available on each metal ion. In the monohydroxy complex, one Zn(II) ion coordinates to the OH⁻ anion and the second metal center to the substrate BNPP, whereas in the dihydroxy complex, both Zn(II) complexes are occupied by hydroxide anions leaving no binding site available for substrate interaction. The high hydrolytic activity of the monohydroxy complex is attributed to π -stacking and hydrophobic interactions between the nitrophenyl groups and the dipyridine moieties which strengthen the association in the transient state of the hydrolysis.²⁹

The monohydroxy species of **Zn₂L4** and **Zn₂L2** hydrolyze BNPP at pH 7, 8 and 9 with rates that are 1 to 2 orders of magnitude higher than the once previously reported for complexes given in Table 8. Zn₂-[18]aneN₆-bis(2,2'-dipyridine) reaches the same range, but only at higher pH values (pH 9). Furthermore, most of the complexes reported in Table 8 do not

possess hydrolytically active species at $\text{pH} < 9$ and show no hydrolytic activity at physiological pH. **Zn₂L5** has comparable hydrolytic activity to Zn₃-Tren-([14]aneN₄)₃.⁴⁵

2.4. Conclusion

The k_{BNPP} values of mononuclear Zn(II) cyclen complexes reported in this paper show a 5 to 6-fold higher hydrolysis rate than the parent Zn[12]aneN₄ complex, most likely due to the aromatic substituent, which provides a more hydrophobic environment.^{25,27} The reactive species is the Zn(II)-OH⁻ complex, in which the Zn(II)-bound OH⁻ acts as nucleophile to attack the coordinated phosphate diester. The k_{BNPP} values are in the same range as previously reported mononuclear complexes, but have the advantage of activity under physiological conditions.

For dinuclear complexes the rate of reaction is defined by the degree of cooperation between the metal centers, which is influenced by the spacer length. For all the reported dinuclear complexes an “associative” mechanism is postulated, in which the substrate is coordinated to the Zn(II) complex. The phosphor atom of the diester is intramolecularly attacked by the zinc-bound hydroxide nucleophile. Second-order rate constants $k_{\text{cat},2}$ of **Zn₂L4** and **Zn₂L2** at pH 7, 8 and 9 are 1 to 2 orders of magnitude higher than those of previously reported complexes. In contrast to most previously reported compounds of this type, our complexes possess catalytically active species at $\text{pH} < 9$. Their high activity is explained by a cooperative role of the two metals in the hydrolytic process. The analogous Cu(II) and Ni(II) complexes show no significant hydrolytic activity.

In conclusion, complexes **Zn₂L4** and **Zn₂L2** exceed the BNPP hydrolytic activity of previously reported compounds at pH 7 - 9 and 25 °C and are better suited for the hydrolysis of phosphate esters under physiological conditions.

Acknowledgement. K.W. thanks the Deutsche Bundesstiftung Umwelt (DBU) for a graduate scholarship. We would like to thank Prof. Dr. R. Winter from the Institute of Inorganic Chemistry at the University of Regensburg and Dr. Biprajit Sarkar from the University of Stuttgart for the ESR spectra of the Cu(II) complexes and the helpful discussions; and Ms. P. Pellet for help preparing the manuscript. We thank the University of Regensburg and the Fond der Chemischen Industry for financial support.

2.5. Supporting Information

Plots of k_{obs} vs Zn(II) complex concentration

Mononuclear Zn(II) complexes (ZnL1)

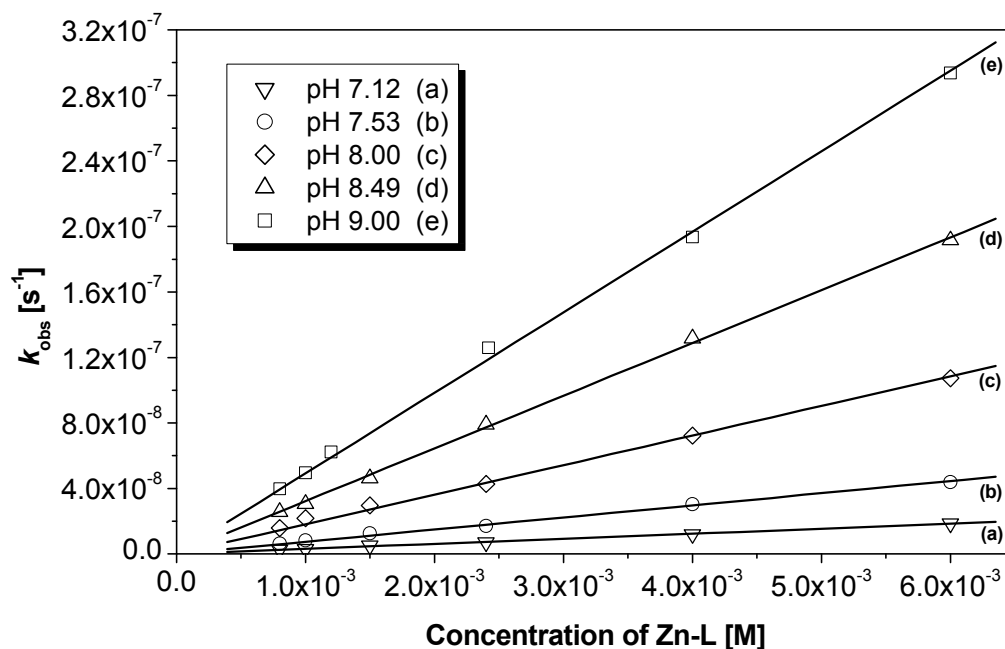


Figure S-1: Calculation of the k_{cat} values for **ZnL1** at various pH values.

Dinuclear Zn(II) complexes

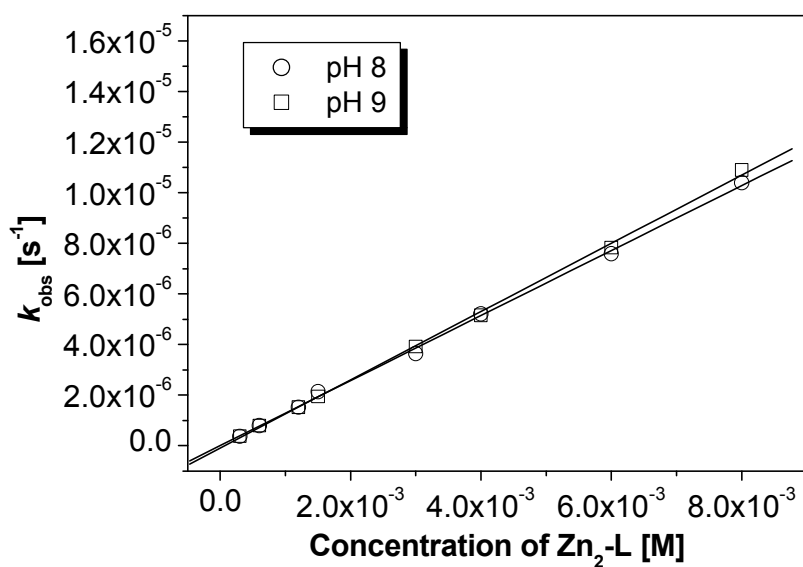


Figure S-2: Calculation of the $k_{\text{cat1,2}}$ values for **Zn₂L2** at various pH values.

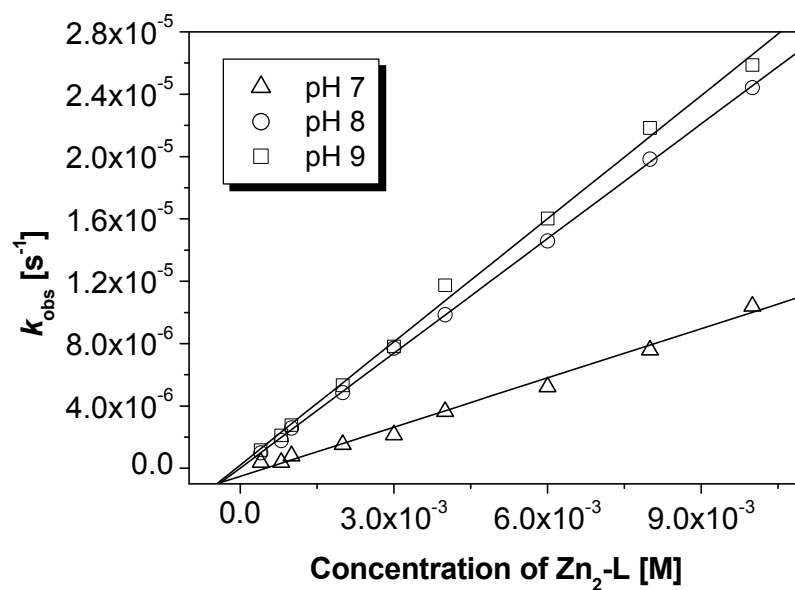


Figure S-3: Calculation of the $k_{\text{cat}1,2}$ values for $\text{Zn}_2\text{L4}$ at various pH values.

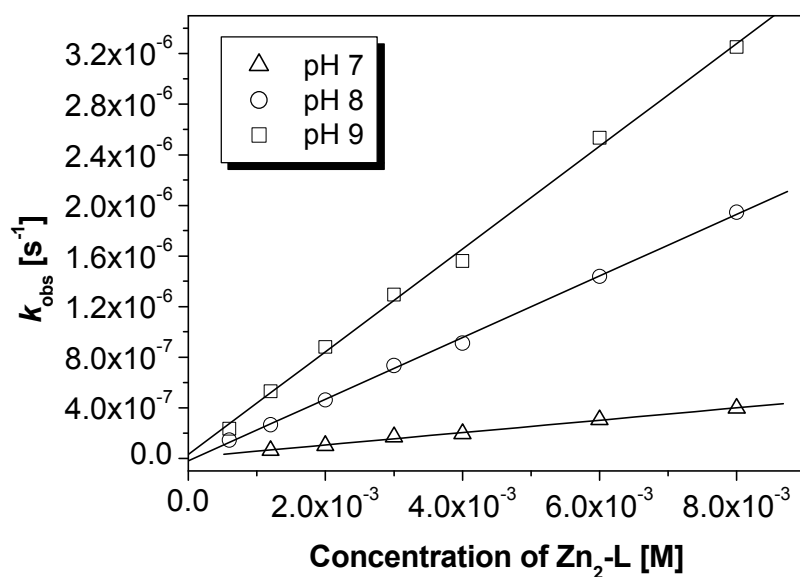


Figure S-4: Calculation of the $k_{\text{cat}1,2}$ values for $\text{Zn}_2\text{L5}$ at various pH values.

2.6. References and Notes

- ¹ Da Silva, J. J. R. Fraústo; Williams, R. J. P. *The biological chemistry of elements*, Clarendon Press, Oxford, **1991**, Chapter 11.
- ² Aoki, S.; Kimura, E. *Rev. Mol. Biol.* **2002**, *90*, 129-155.
- ³ Williams, N. H.; Takasaki, B.; Wall, M.; Chin, J. *Acc. Chem. Res.* **1999**, *32*, 485-493.
- ⁴ For some reviews, see: (a) Wilcox, D. E. *Chem. Rev.* **1996**, *96*, 2435-2458. (b) Sträter, N.; Lipscomb, W. N.; Klabunde, T.; Krebs, B. *Angew. Chem. Int. Ed. Engl.* **1996**, *35*, 2024-2055. (c) Lipscomb, W.N.; Sträter, N. *Chem. Rev.* **1996**, *96*, 2375-2433. (d) Cowan, J. A. *Chem. Rev.* **1998**, *98*, 1067-1087. (e) Jedrzejewski, M. J.; Setlow, P. *Chem. Rev.* **2001**, *101*, 607-618.
- ⁵ For reviews, see: (a) Chin, J. *Acc. Chem. Res.* **1991**, *24*, 145; (b) Liu, C.; Wang, M.; Zhang, T.; Sun, H. *Coord. Chem. Rev.* **2004**, *248*, 147.
- ⁶ a) Hegg, E. L.; Burstyn, J. N. *Coord. Chem. Rev.* **1998**, *173*, 133-165; b) Suh, J. *Acc. Chem. Res.* **1992**, *25*, 273-279.
- ⁷ Göbel, M. W. *Angew. Chem. Int. Ed. Engl.* **1994**, *33*, 1141-1143.
- ⁸ a) Kovbasyuk, L.; Krämer, R. *Chem. Rev.* **2004**, *104*, 3161-3187; b) Feng, G.; Mareque-Rivas, J. C.; de Rosales, R. T. M.; Williams, N. H. *J. Am. Chem. Soc.* **2005**, *127*, 13470-13471; c) O'Donoghue, A. M.; Pyun, S. Y.; Yang, M.-Y.; Morrow, J. R.; Richard, J. P. *J. Am. Chem. Soc.* **2006**, *128*, 1615-1621.
- ⁹ a) Breslow, R.; Berger, D.; Huang, D.-L. *J. Am. Chem. Soc.* **1990**, *112*, 3686-3687; b) Morrow, J. R.; Aures, H.; Epstein, D. *J. Chem. Soc., Chem. Commun.* **1995**, 2431-2432; c) Young, M. J.; Wahnou, D.; Hynes, R. C.; Chin, J. *J. Am. Chem. Soc.*, **1995**, *117*, 9441-9447; d) Chu, F.; Smith, J.; Lynch, V. M.; Anslyn, E. V. *Inorg. Chem.* **1995**, *34*, 5689-5690 (the authors propose that in a Zn complex either imidazole or imidazolium might act as an auxiliary group, providing an 1.5-fold increase in RNA cleavage rate). See, also: e) Hsu, C.-M.; Cooperman, B. S. *J. Am. Chem. Soc.* **1976**, *98*, 5657-5663; f) Koike, T.; Inoue, M.; Kimura, E.; Shiro, M. *J. Am. Chem. Soc.* **1996**, *118*, 3091-3099; g) Kimura, E.; Kodama, Y.; Koike, T.; Shiro, M. *J. Am. Chem. Soc.* **1995**, *117*, 8304-8311.
- ¹⁰ Kövari, E.; Krämer, R. *J. Am. Chem. Soc.* **1996**, *118*, 12704-12709.
- ¹¹ Subat, M.; Woinaroschy, K.; Anthofer, S.; Malterer, B.; Koenig, B. *Inorg. Chem.* **2007**, *46*, 4336-4356.
- ¹² Walenzyk, T.; Koenig, B. *Inorg. Chim. Acta* **2005**, *358*, 2269-2274.
- ¹³ a) Logan, S. R. *Grundlagen der Chemischen Kinetik*, Wiley-VCH, Weinheim, **1997**, Chapter 1-3; b) Perkampus, H.-H.; Kaufmann, R. *Kinetische Analyse mit Hilfe der UV/VIS-Spektrometrie*, Wiley-VCH, Weinheim, **1991**.
- ¹⁴ a) Styka, M. C.; Smierciak, R. C.; Blinn, E. L.; DeSimone, R. E.; Passariello, J. V. *Inorg. Chem.* **1978**, *17*, 82-86; b) Thöm, V. J.; Hosken, G. D.; Hancock, R. D. *Inorg. Chem.* **1985**,

- 24, 3378-3381; c) Thöm, V. J.; Fox, C. C.; Boeyens, J. C. A.; Hancock, R. D. *J. Am. Chem. Soc.* **1984**, *106*, 5947-5955.
- 15 a) Fabrizzi, L.; Micheloni, M.; Paoletti, P. *Inorg. Chem.* **1980**, *19*, 535-538 ; b) Fabrizzi, L. *Inorg. Chem.* **1977**, *16*, 2667-2668; c) Bencini, A.; Bianchi, A.; Garcia-Espana, E.; Jeannin, Y.; Julve, M.; Marcelino, V.; Philoche-Levisalles, M. *Inorg. Chem.* **1990**, *29*, 963-970.
- 16 Koike, T.; Kimura, E. *J. Am. Chem. Soc.* **1991**, *113*, 8935-8941.
- 17 Norman, P. R. *Inorg. Chim. Acta* **1987**, *130*, 1-4.
- 18 Norman, P. R.; Tate, A.; Rich, P. *Inorg Chim. Acta* **1988**, *145*, 211-217.
- 19 a) Deal, K. A. ; Burstyn, J. N. *Inorg. Chem.* **1996**, *35*, 2792-2798; b) Hegg, E. L.; Mortimore, S. H.; Cheung, C. L.; Huyett, J. E.; Powell, D. R. ; Burstyn, J. N. *Inorg. Chem.* **1999**, *38*, 2961-2968.
- 20 a) Fry, F. H. ; Fischmann, A. J.; Belousoff, M. J.; Spiccia, L.; Brügger, J. *Inorg. Chem.* **2005**, *44*, 941-950 and ref. therein. b) Belousoff, M. J.; Duriska, M. B.; Graham, B.; Batten, S. R.; Moubaraki, B.; Murray, K. S.; Spiccia, L. *Inorg. Chem.* **2006**, *45*, 3746-3755. c) Bonora, G. M.; Drioli, S.; Felluga, F.; Mancin, F.; Rossi, P.; Scrimin, P.; Tecilla, P. *Tetrahedron Lett.* **2003**, *44*, 535-538.
- 21 a) Vichard, C.; Kaden, T. A. *Inorg. Chim. Acta* **2002**, *337*, 173-180; b) Vichard, C.; Kaden, T. A.. *Inorg. Chim. Acta* **2004**, *357*, 2285-2293.
- 22 a) Gellman, S. H.; Petter, R.; Breslow, R. *J. Am. Chem. Soc.* **1986**, *108*, 2388-2394. b) Bonfa, L.; Gatos, M.; Mancin, F.; Tecilla, P.; Tonellato, U. *Inorg. Chem.* **2003**, *42*, 3943-3949.
- 23 As shown by previous reports, the mechanism of BNPP hydrolysis by macrocyclic metal complexes implies the following steps: deprotonation of a metal bound water molecule (Ka), binding of the substrate to the metal complex (K), intracomplex nucleophilic attack of the hydroxide (k') with simultaneous departure of the leaving group and, eventually, deprotonation and decomplexation of the substrate to restore the catalyst. The reaction rate is pH dependent and saturation behaviour by formation of the substrate-catalyst complex is expected. However, the affinities of phosphate diesters to Zn(II) complexes are very low and the curvature of the plot is not detectable in the exploitable concentration range. This is common to all reports on metal complexes hydrolysing phosphate diesters. Inhibition of the catalyst by 4-nitrophenyl phosphate is not observed in our reaction conditions (initial slope method, product conversion < 5%).
- 24 a) Costas, M.; Anda, C.; Llobet, A.; Parella, T.; Evans, H. S.; Pinilla, E. *Eur. J. Inorg. Chem.* **2004**, 857-865; b) Gross, F.; Vahrenkamp, H. *Inorg. Chem.* **2005**, *44*, 3321-3329.
- 25 a) Li, S.-A.; Xia, J.; Yang, D.-X. ; Xu, Y. ; Li, D.-F. ; Wu, M.-F.; Tang, W.-X. *Inorg. Chem.* **2002**, *41*, 1807-1815; b) Xia, J.; Li, S.-A.; Shi, Y.-B. ; Yu, K.-B. ; Tang, W.-X. *J. Chem. Soc., Dalton Trans.* **2001**, 2109-2115; c) Li, S.-A.; Li, D.-F.; Yang, D. X.; Huang, J.; Xu, Y.; Tang, W.-X. *Inorg. Chem. Commun.* **2003**, *6*, 221-224.

- 26 a) Koike, T.; Gotoh, T.; Aoki, S.; Kimura, E.; Shiro, M. *Inorg. Chim. Acta* **1998**, 270, 424-432;
b) Aoki, S.; Kagata, D.; Shiro, M.; Takeda, K.; Kimura, E. *J. Am. Chem. Soc.* **2004**, 126,
13377-13390.
- 27 Shionoya, M.; Kimura, E.; Shiro, M. *J. Am. Chem. Soc.* **1993**, 115, 6730-6737.
- 28 Bazzicalupi, C.; Bencini, A.; Bianchi, A.; Fusi, V.; Giorgi, C.; Paoletti, P.; Valtancoli, B.;
Zanchi, D. *Inorg. Chem.* **1997**, 36, 2784-2790.
- 29 Bazzicalupi, C.; Bencini, A.; Berni, E.; Bianchi, A.; Fornasari, P.; Giorgi, C.; Valtancoli, B.
Inorg. Chem. **2004**, 43, 6255-6265.
- 30 Kimura, E.; Gotoh, T.; Koike, T.; Shiro, M. *J. Am. Chem. Soc.* **1999**, 121, 1267-1274.
- 31 The higher Lewis acidic character of the metal ion in Zn[12]aneN3 complexes leads to a
stronger interaction between the metal complex and the phosphodiester, as proposed by
Kimura. In the carboxylic ester hydrolysis promoted by mononuclear complexes, the simple
nucleophilic mechanism is predominant and the Zn(II)-bound hydroxides act as nucleophile to
the carbonyl group. Therefore the Zn[12]aneN3 complexes with higher Lewis acidic character
of the metal ion, but also lower nucleophilic character of the Zn-L-OH- species, have lower
reaction rates in the hydrolysis of carboxyesters than the Zn[12]aneN4 system.
- 32 a) Fujioka, H.; Koike, T.; Yamada, N.; Kimura, E. *Heterocycles*, **1996**, 42, 775-787; b) Koike,
T.; Takashige, M.; Kimura, E.; Fujioka, H.; Shiro, M. *Chem. Eur. J.* **1996**, 2, 617-623; c)
Kimura, E.; Aoki, S.; Koike, T.; Shiro, M. *J. Am. Chem. Soc.* **1997**, 119, 3068-3076; d) Aoki,
S.; Kimura, E. *J. Am. Chem. Soc.* **2000**, 122, 4542-4548.
- 33 a) Yoo, C. E.; Chae, P. S.; Kim, J. E.; Jeong, E. J.; Suh, J. *J. Am. Chem. Soc.* **2003**, 125,
14580-14589; b) Aoki, S.; Kimura, E. *Rev. Mol. Biotech.* **2002**, 90, 129-155 and ref. therein.
- 34 Miyoshi, K.; Tanaka, H.; Tsuboyama, S.; Murata, S.; Shimizu, H.; Ishizu, K. *Inorg. Chim.*
Acta **1983**, 78, 23-30.
- 35 Soibinet, M.; Dechamps-Olivier, I.; Guillon E.; Barbier, J.-P.; Aplincourt, M.; Chuburu, F.;
Le Baccon, M.; Handel, H. *Eur. J. Inorg. Chem.* **2003**, 1984-1994.
- 36 El Ghachtouli, S.; Cadiou, C.; Dechamps-Olivier, I.; Chuburu, F.; Aplincourt, M.; Turcry, V.;
Le Baccon, M.; Handel, H. *Eur. J. Inorg. Chem.* **2005**, 2658-2668.
- 37 Brandes, S.; Gros, C.; Denat, F.; Pullumbi, P.; Guillard, R. *Bull. Soc. Chim. Fr.* **1996**, 133, 65-
73.
- 38 a) Eaton, S. S.; More, K. M.; Sawant, B. M.; Eaton, G. R. *J. Am. Chem. Soc.* **1983**, 105, 6560-
6567. b) Eaton, S. S. *J. Am. Chem. Soc.* **1982**, 104, 5002-5003.
- 39 Belousoff, M. J.; Duriska, M. B.; Graham, B.; Batten, S. R.; Moubaraki, B.; Murray, K. S.;
Spiccia, L. *Inorg. Chem.* **2006**, 45, 3746-3755.
- 40 The k_{obs} values of **Ni₂L2** are about twice the ones of **NiL1**. This may indicate similar
mechanisms of hydrolysis of BNPP by the monohydroxy complex **Ni₂-L-(OH₂)(OH)**, as
previously reported for other dinuclear Ni(II) complexes. However, we refrain from any

mechanistic interpretation for the hydrolysis mediated by **Ni₂L2** or **Cu₂L2**. Their low activity and the concentrations of metal complex and substrate required to reach acceptable experimental errors lead to kinetic data that do not allow a more extended analysis.

⁴¹ a) Jang, B.-B.; Lee, K.-P.; Min, D.-H.; Suh, J. *J. Am. Chem. Soc.* **1998**, *120*, 12008-12016. b) Yoo, C. E.; Chae, P. S.; Kim, J. E.; Jeong, E. J.; Suh, J. *J. Am. Chem. Soc.* **2003**, *125*, 14580-14589. c) Yoo, S. H.; Lee, B. J.; Kim, H.; Suh, J. *J. Am. Chem. Soc.* **2005**, *127*, 9593-9602.

⁴² a) Iranzo, O.; Richard, J. P.; Morrow, J. P. *Inorg. Chem.* **2004**, *43*, 1743-1750; b) Iranzo, O.; Elmer, T.; Richard, J. P.; Morrow, J. P. *Inorg. Chem.* **2003**, *42*, 7737-7746.

⁴³ For previous reports of BNPP hydrolysis by di- or trinuclear Zn(II) macrocyclic complexes, see: a) Arca, M.; Bencini, A.; Berni, E.; Caltagirone, C.; Devillanova, F. A.; Isaia, F.; Garau, A.; Giorgi, C.; Lippolis, V.; Perra, A.; Tei, L.; Valtancoli, B. *Inorg. Chem.* **2003**, *42*, 6929-6939; b) Bazzicalupi, C.; Bencini, A.; Berni, E.; Giorgi, C.; Maoggi, S.; Valtancoli, B. *J. Chem. Soc., Dalton Trans.* **2003**, 3574-3580; c) Bauer-Siebenlist, B.; Meyer, F.; Farkas, E.; Vidovic, D.; Cuesta-Seijo, J. A.; Herbst-Irmer, R.; Pritzkow, H. *Inorg. Chem.* **2004**, *43*, 4189-4202.

⁴⁴ Bazzicalupi, C.; Bencini, A.; Berni, E.; Bianchi, A.; Giorgi, G.; Paoletti, P.; Valtancoli, B. *Inorg. Chem.* **1999**, *38*, 6323-6325.

⁴⁵ The hydrolytic activity of the complexes given in Table 8 were determined at 35.1 °C, whereas the hydrolytic activity of the dinuclear complexes reported in this paper was determined at 25 °C.

3. Study of the Affinity for Phosphate Anions of two Dinuclear Zn(II)(1,4,7,10 – Tetraazacyclododecane) Complexes and Development of a Quantitative Assay for Pyrophosphate under Physiological Conditions

Abstract

Selective recognition of phosphate anions, pyrophosphate PP_i and nucleotides in aqueous solutions under physiological conditions is of current interest for chemists and biologists, due to the biological importance of such ions. We report here the use of two dinuclear zinc(II)-1,4,7,10-tetraazacyclododecane [zinc(II)-cyclen] complexes, **Zn₂L1** and **Zn₂L3**, as binding sites for phosphate anions in aqueous solution at physiological conditions (Hepes or Tris buffer, 10-56 mM, pH 7 or 7.4, 25 °C). Phosphate ion binding was monitored by an indicator displacement assays (IDA) with coumarin methyl sulfonate (**CMS**) as fluorescent indicator or pyrocatechol violet (**PV**) as a colorimetric indicator. The binding of the different phosphate anions is observable with the naked eye. The affinity of both dinuclear zinc(II) metal complexes for phosphate anions increases with the number of negative charges of the anion: ATP, GTP and PP_i show the highest association constants and cAMP binding is the weakest. Binding affinity constants from optical spectroscopy were confirmed by ^{31}P NMR titrations and isothermal titration calorimetry (ITC). The fluorescent complex **Zn₂L3**, containing a dansylamide moiety, does not change its photophysical properties upon phosphate binding, presumably due to the long distance between the dansyl signalling unit and the metal complex binding site.

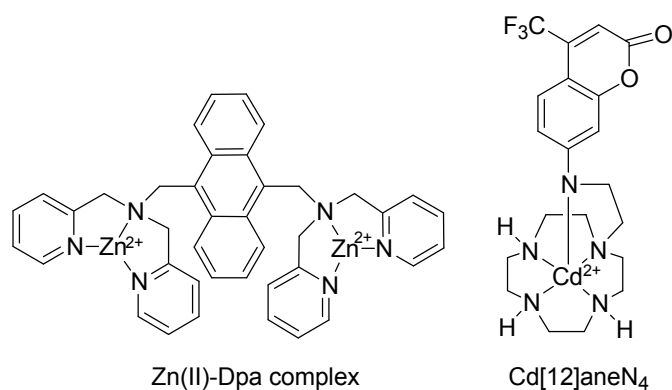
Complex **Zn₂L1** forms a stable 1:1 aggregate with pyrophosphate, showing a slow exchange between free and bound anion once the receptor-substrate complex is formed. This affinity of the dinuclear zinc(cyclen) complex has been used to develop a quantitative assay for micromolar concentrations of PP_i in aqueous solution under physiological conditions.

3.1. Introduction

Phosphate esters exist ubiquitously in nature¹ in form of nucleotides as components of RNA and DNA, as sugar nucleotides in glycosylation of oligosaccharides or in phosphorylated proteins playing a central role in cell regulation.^{2,3} Inorganic phosphate is involved in many metabolic processes, heightened phosphate levels leading to renal failure, while phosphate deficiency to rickets and hyperthyroidism.⁴ The nucleotide adenosine triphosphate (ATP) is the molecular currency for intracellular energy transfer,⁵ and pyrophosphate ($\text{P}_2\text{O}_7^{4-}$, PP_i), the product of ATP hydrolysis, plays an important role in intracellular signalling.⁶ Phospholipids

are key cell membrane components and the study of apoptotic mechanisms focus on the phospholipid bilayer deterioration.⁷ Organophosphorus pesticides and nerve agents as highly toxic substances present a considerable environmental danger.⁸ Therefore development of artificial phosphate anion receptors in aqueous solutions under physiological conditions remains a challenging task. Such sensors could be useful tools for the detection, transport and separation of biologically important phosphates,⁹ with applications in various fields, most importantly in medicinal chemistry, molecular biology and environmental sciences.

Previous reports on phosphate receptors in aqueous solution show that there are generally two different approaches for designing such a sensor. The first approach is the design of a chemosensor, by attaching the phosphate binding unit to a fluorescent molecule which acts as the signalling group reporting the binding by an increase, decrease or shift of its fluorescence emission. Czarnik *et al.* was the first to report such a chemosensor for pyrophosphate in aqueous solution, based on a polyammonium complex with an anthracene spacer as signalling unit.¹⁰ However, this sensor cannot be used in biological experiments, because the polyamine ligand chelates also metal ions. Recent reports reveal that transition metal complexes with vacant coordination sites are well suited to serve as phosphate ion binding sites. The most used binding unit in chemosensors for phosphates nowadays is the zinc(II)-dipicolylamine (Dpa) complex developed by Hamachi *et al.* (**Scheme 1**).¹¹ Hamachi *et al.* used this Zn(II) complex in combination with anthracene as a chemosensor for phosphorylated peptides¹¹, ATP¹² and UDP (in a glycosyltransferase assay)¹³, in combination with xanthone for the detection of nucleoside pyrophosphates¹⁴ and in combination with stilbazole bound to a natural phosphoprotein binding domain for the recognition of phosphopeptides.¹⁵ Several other groups have used the Zn(II)-Dpa binding motif: Hong *et al.* reported fluorescent pyrophosphate ($P_2O_7^{4-}$, PP_i) sensors based on a *p*-nitrophenylazo-¹⁶ or a naphthalene-Dpa system,¹⁷ Smith *et al.* a chemosensor for phosphatidylserine-containing membranes¹⁸ and membranes of bacterial cells¹⁹ and recently, Das *et al.* a dimethylamino-phenylazo-Dpa system for the selective naked-eye detection of ATP.²⁰ Another useful phosphate binding unit besides Dpa is a macrocyclic polyamine-transitional metal complex, such as the Cd(II)-cyclen (1,4,7,10-tetraazacyclododecane, [12]aneN₄) complex reported by Kikuchi *et al.*²¹ with a pendant amino-coumarin as a fluorescent reporter and switch (**Scheme 1**). Kimura reported also a luminescent supramolecular sensor for inositol-1,4,5-triphosphate (IP_3) based on a Zn(II)-cyclen complex.²²

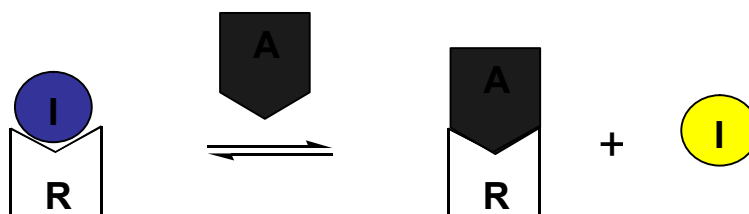


^a counteranions are omitted for clarity reasons.

Scheme 1^a

The obvious drawbacks of designing a chemosensor are its often difficult synthesis and the uncertainty whether the sensor will then really detect the binding or show selectivity among the various phosphates. Indeed many of the aforementioned chemosensors show also a lower affinity for other phosphate anions present in solution, the selectivity being generally attributed to the difference in the number of the anionic charges of the phosphate species.

Thus, a second approach for designing a sensor for phosphate anions in aqueous solution is the use of an indicator-displacement assay (IDA), a simple and increasing popular strategy, similar to the antibody-based biosensors in competitive immunoassays. In an indicator displacement assay, a receptor with an affinity for a given analyte forms a reversible non-covalent complex with an indicator, usually a fluorescent or UV/Vis dye. Upon complexation with the receptor, the spectral properties of the indicator undergo some change (shift, enhancement or quenching of signal). Treatment of the receptor-indicator complex with the analyte displaces the indicator from the receptor, thereby restoring the indicator's original spectral properties and providing a means of assessing analyte presence and quantifying its concentration spectroscopically (**Scheme 2**).²³



^a Emission or absorption intensity of the indicator may be also enhanced or reduced upon complexation with receptor.

Scheme 2. Principle of the indicator displacement assay (IDA); I = Indicator, R = Receptor, A = Analyte^a

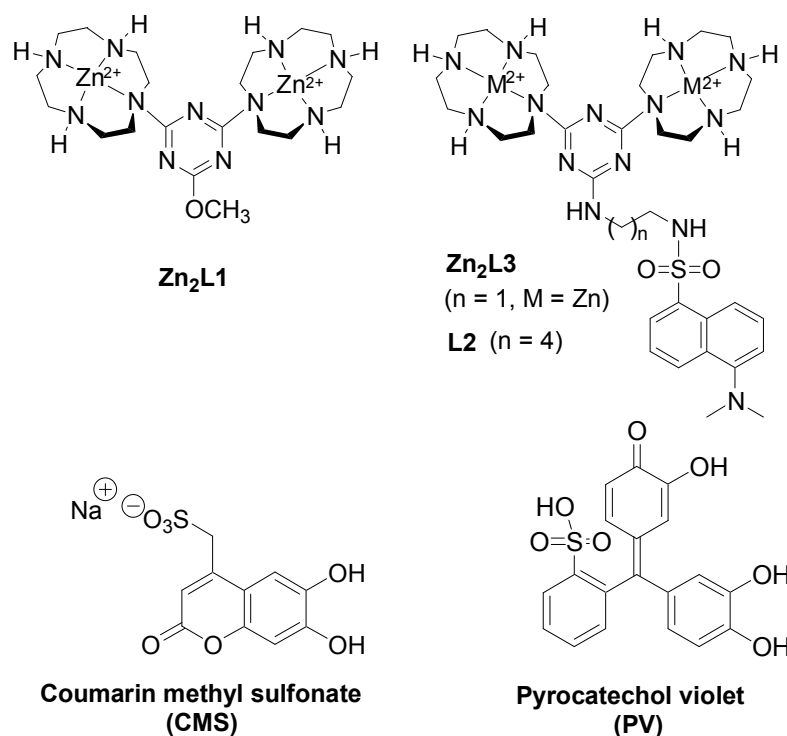
Anslyn introduced first this type of assay and used it for detection of the polyanionic second messenger inositol-1,4,5-triphosphate (IP₃) with a macrocyclic guanidinium cleft and 5-carboxyfluorescein as indicator²⁴, as well as for the detection of inorganic phosphate in saliva using a Cu(II) trispyridyl complex.²⁵ Fabrizzi *et al.* reported also a dicopper(II) macrocyclic complex able to quench the fluorescence of the coordinated indicator, which is then restored upon receptor binding selectively pyrophosphate.²⁶ Kim *et al.* used the simple phosphate binding unit we described before for chemosensors, Zn(II)-Dpa (two such units were linked by a 4-methyl-phenol spacer to yield a ditopic receptor) with pyrocatechol violet as non-covalently bound indicator, to detect phosphate anions (RPO₄²⁻)²⁷ and monitored with this ensemble cyclic nucleotide phosphodiesterase activity.²⁸ Using a similar approach Smith *et al.* reported an indicator displacement system for fluorescent detection of phosphate oxyanions²⁹ and bilayer membranes enriched in phosphatidylserine³⁰ under physiological conditions. Recently, Joliffe *et al.* reported also a ditopic Zn(II)-Dpa receptor with a cyclic peptide spacer for pyrophosphate detection using the IDA approach.³¹

The IDA approach offers several advantages: (i) the receptor is not covalently attached to the indicator, therefore no extra synthetic steps are necessary, allowing one to focus on the synthesis of the host and simply choose the appropriate indicator; (ii) the assay works well both in aqueous solution and organic solvents; (iii) the indicator can be changed at will. The last property offers to this approach a secondary tuning of sensitivity and selectivity due to the participation of the indicator to the sensing process. Indeed, by finding an indicator I with lower affinity for receptor than the analyte A, but higher affinity for the receptor than another competing analyte A', that is $K_{A'} < K_I < K_A$, the selectivity can be tuned for each single receptor, as demonstrated in a recent study by Smith *et al.*³² and previously shown by Anslyn³³ and Fabrizzi.²⁶

Kimura *et al.* have shown that azamacrocyclic zinc complexes such as Zn[12]aneN₄ and Zn[12]aneN₃ are good models for zinc enzymes³⁴ and thus, based on the fact that phosphates act as substrates or inhibitors of these enzymes, the Zn(II) complexes have been found to be a novel family of selective sensors of phosphates.^{22,35}

Based on the previous reports of Kimura and our group^{36,37}, we report here the synthesis of the new bis(1,4,7,10-tetrazacyclododecane) ligands **L2** and **L3** and of the dinuclear Zn(II) complex **Zn₂L3** (Scheme 3). As part of an ongoing effort to develop sensors of phosphate anions in aqueous solutions, we studied the binding affinity of the new complex **Zn₂L3** and of the previously reported dinuclear zinc(II) complex **Zn₂L1**³⁶ for phosphate anions in aqueous solution at physiological conditions (Hepes or Tris, 10-56 mM, pH 7 or 7.4, 25 °C) by means

of the indicator displacement assays with coumarin methyl sulfonate (**CMS**) as fluorescent indicator or pyrocatechol violet (**PV**) as a colorimetric indicator.

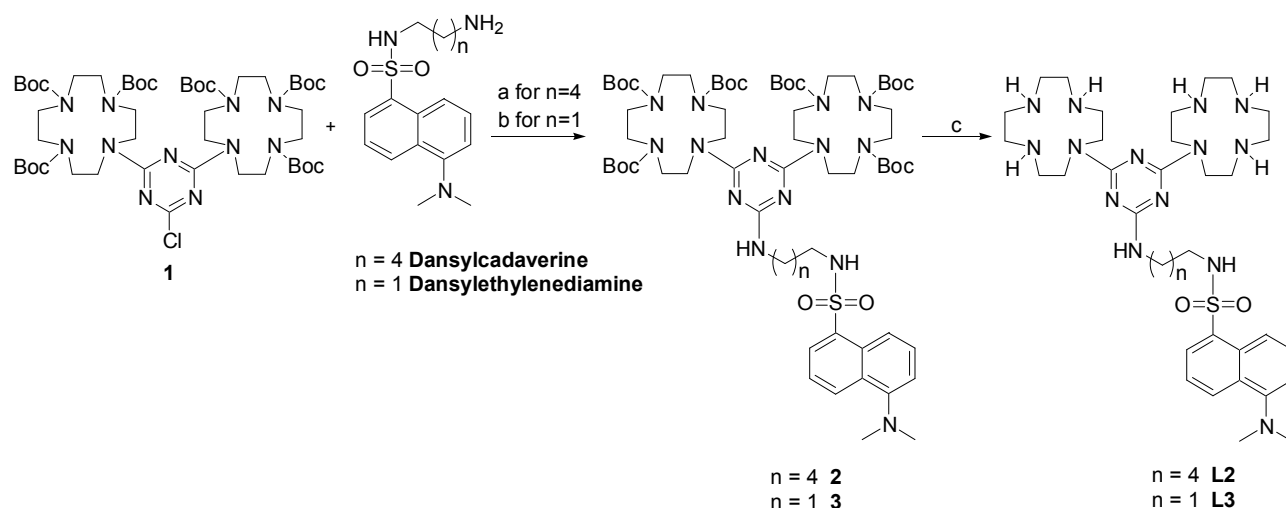


Scheme 3. Studied [12]aneN₄ metal complexes **Zn₂L1**, **Zn₂L3**, ligand **L2** and the indicators used for indicator displacement assay.

3.2. Results and Discussion

Syntheses of the macrocyclic ligands L2 and L3 and their Zn(II) complexes. The syntheses of ligands **L2** and **L3**, containing a dansylamide moiety follows a previous reported procedure.³⁶ The ligands are obtained from the previously reported compound **1**³⁷ by nucleophilic substitution with the respective amine in dioxane at reflux, deprotection of the Boc-groups with TFA and elution from basic ion-exchange resin (**Scheme 4**). Dansylethylenediamine was obtained according to a published procedure.³⁸

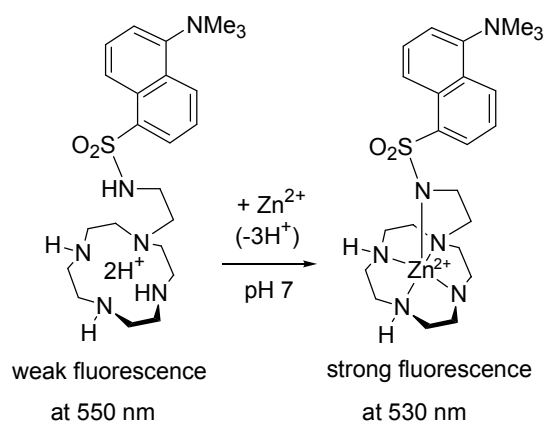
The synthesis of **3** requires higher temperatures and longer times of reaction due to the lower reactivity of the dansyl-(2-amino-ethyl)-amide. The lower yield in the deprotection of **3** is explained by the high acidity of the sulphonamide, due to which quantitative product isolation from the basic ion-exchange resin is not possible. However, this drawback is compensated by the fact that the starting materials are easily prepared in high amounts.



a: Dansylcadaverine (1 eq.), K_2CO_3 (2.5 eq.), dioxane, reflux at 120 °C, 12h, 75%; **b:** Dansylethylenediamine (2.5 eq), K_2CO_3 (5 eq.), dioxane, reflux at 140 °C, 72h, 75%; **c:** TFA (80 eq.), DCM, RT, 12h (for **2**) and 24h (for **3**), then column with basic ion-exchange resin, quantitative yield (**L2**), 62% (**L3**).

Scheme 4. Synthesis of **L2** and **L3**.

By attachment of the fluorescent dansyl moiety to the dinuclear metal binding unit we envisaged the design of a chemosensor, with the pendant dansyl unit as a fluorescent reporter and switch similar to the compound reported by Kikuchi et al.²¹ (see **Scheme 1**). The choice of the dansyl group was inspired by previous reports by Kimura,³⁹ in which the interaction between a zinc(II)cyclen complex and the dansyl sulphonamide led to an enhanced fluorescence (**Scheme 5**).

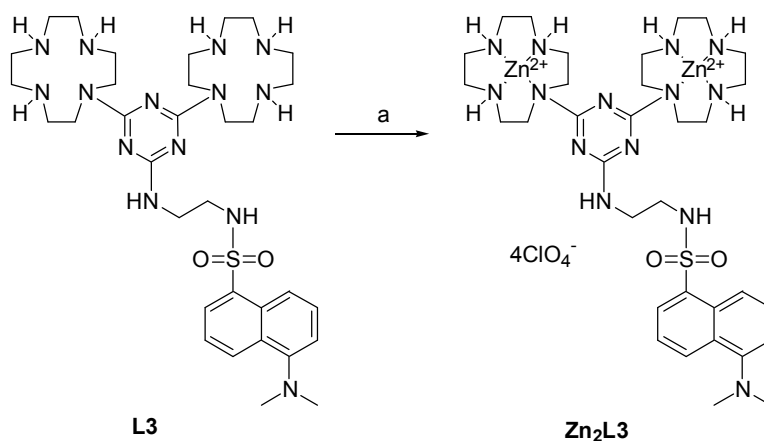


Scheme 5. Kimura's zinc(II)cyclen complex with a dansyl sulphonamide pendant.³⁹

The complexation step with $\text{Zn}(\text{ClO}_4)_2 \cdot 6\text{H}_2\text{O}$ proved difficult for **L2**, leading to mixtures of mono- and dinuclear metal complexes indifferent of the reaction conditions and purification methods used. Purification by HPLC is not possible due to the high polarity of the molecules.

In addition, the dinuclear Zn(II) complex of **L2** (90% purity from ESI spectrum) has not a good solubility in water, acetonitrile, methanol or ethanol, due to the longer alkyl chain. The addition of DMSO to increase the solubility was unsatisfactory and is not recommended due to reports of DMSO as fluorescence quencher.⁴⁰ Therefore **Zn₂L2** does not fulfil the conditions to work as a phosphate anion sensor in aqueous solutions and was not studied further.

The dinuclear Zn(II) complex **Zn₂L3** was isolated in analytical purity with very good yield (91%) from the reaction of the ligand with zinc perchlorate salt in aqueous solution and recrystallization from EtOH and was characterized by different methods (¹H NMR, ¹³C NMR, UV/Vis, IR, ESI, elemental analysis) to show a stoichiometry of 2:1 metal cation/ligand (**Scheme 6**).



a: Zn(ClO₄)₂·6H₂O (2.1 eq.), H₂O, aq. LiOH until pH = 8-9, reflux, 4h, recrystallization from EtOH, 91%.

Scheme 6. Synthesis of **Zn₂L3**.

Binding ability of Zn₂L1 towards pyrophosphate anions in aqueous solution. The binding affinity and stoichiometry of **Zn₂L1** to pyrophosphate tetrasodium salt (PP_i⁴⁻) in buffered solutions (Tris 56 mM, pH 7, 300 K, 10% D₂O) was investigated by ³¹P NMR titrations. A first titration experiment of PP_i (56 mM) with increasing amounts of **Zn₂L1** (**Figure 1**) shows the formation of the receptor-substrate complex, reflected in the appearance of a new downfield peak at -4.05 ppm. With increasing amounts of metal complex, the resonance signal of free PP_i broadens and decreases in intensity, whereas the new peak increases in intensity, until for the ratio 1:1 **Zn₂L1** to PP_i the resonance signal of free pyrophosphate has completely disappeared. No further change in chemical shift at higher concentrations of **Zn₂L1** (see supporting information for further titration experiments) strongly suggests 1:1 complexation. The samples were measured every six hours for 24h and some of them also after five days to exclude changes in time due to slow kinetics of reactions and indicated the

formation of a stable 1:1 complex. The titrations are typical of a slow-exchange between free and bound PP_i with an exchange rate constant k of 80 Hz.

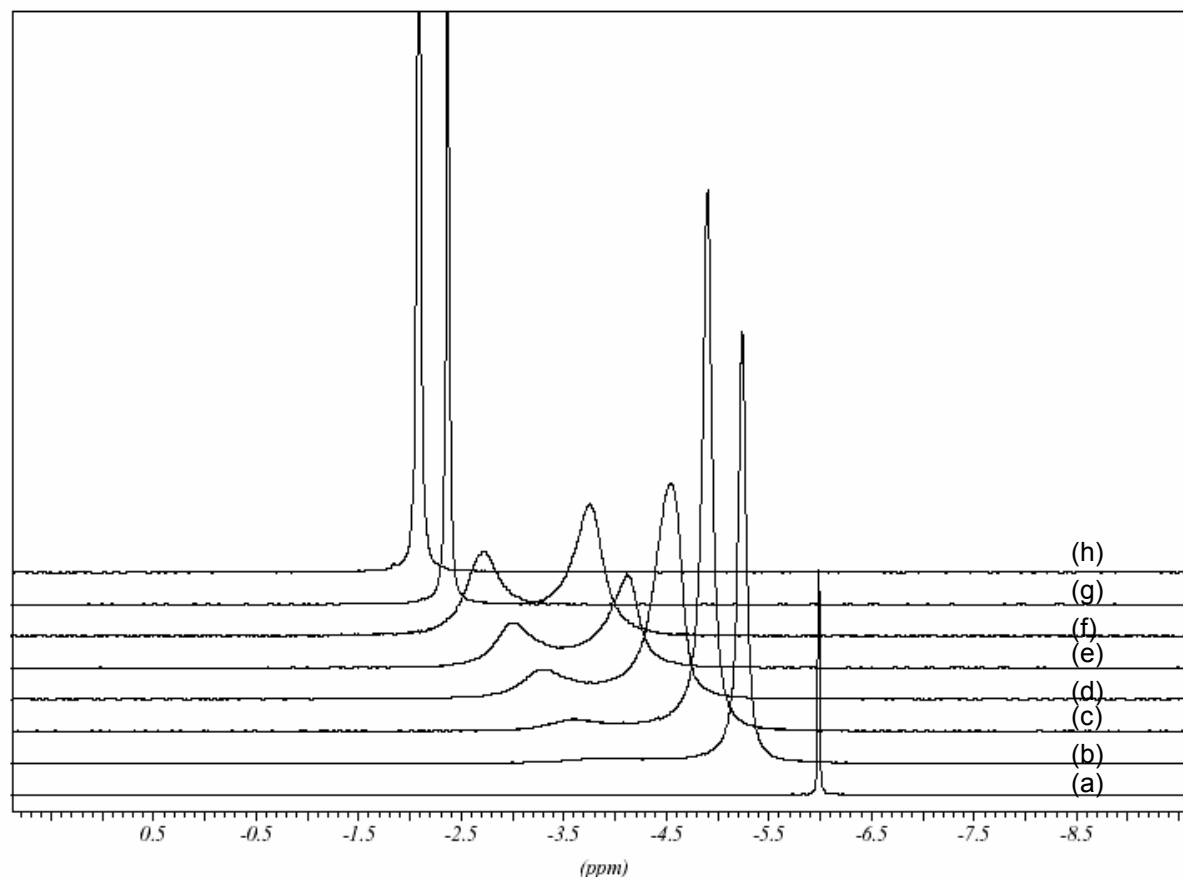


Figure 1. Partial ^{31}P NMR spectra of the titration of **Zn₂L1** to a 56 mM solution of PP_i (0.7 mL Tris buffer 56 mM, pH 7, 10% D₂O, 300 K). X -increment=-0.28 ppm. Total amount of equivalents of **Zn₂L1** present in solution: (a) 0 eq. (free pyrophosphate); (b) 0.1 eq.; (c) 0.15 eq.; (d) 0.2 eq.; (e) 0.33 eq.; (f) 0.5 eq.; (g) 1 eq.; (h) 1.1 eq.

Our observations fit to previous reports of downfield shifts of the phosphate resonance signal upon binding,^{12,20,31,35,41} due to the shielding effect of the coordinated Zn(II) ions. Di- and triphosphates have been shown to bind to ditopic Zn(II) complexes in a bridging fashion with two oxygens on each P atom coordinating one zinc ion.^{13,26,31,41} Based on these results, we propose the same binding motif for **Zn₂L1** and performed a low temperature measurement of a sample with the ratio 1:1.5 **Zn₂L1** to PP_i (see supporting information). No split of the resonance signal at -4.05 ppm was observed, but as the solvent was water, the temperature could be lowered only to a minimum of 278 K. A change in solvent would permit lower temperatures, but would not reflect the situation in aqueous solution. The experiment emphasized the high stability of the formed complex.

Isothermal calorimetric titration (ITC)⁴² of PP_i to **Zn₂L1** (presented in the supporting information) under the same experimental conditions (Tris buffer 56 mM, pH 7, 298 K) confirmed the formation of a stable 1:1 complex. The values for the binding stoichiometry (*n*) and the thermodynamic parameters of interaction (enthalpy of binding ΔH , binding constant *K*, entropy change ΔS and, consequently, free energy change ΔG) are summarized in **Table 1**.

	stoichiometry	Binding	Binding	Entropy	Free energy
	<i>n</i>	constant <i>K</i>	enthalpy ΔH	change ΔS	change ΔG
		[10 ⁻⁶ M ⁻¹]	[cal mol ⁻¹]	[cal mol ⁻¹ K ⁻¹]	[cal mol ⁻¹]
Zn₂L1	0.9 ± 0.1	1.7 ± 0.3	-6209 ± 91	7.66	-8490

Table 1. Thermodynamic parameters and association constant (*K*) for the binding of PP_i to **Zn₂L1** in aqueous solution (Tris 56 mM, pH 7) at 25 °C.

The binding process is predominantly enthalpically driven, which suggests strong coordinative interactions, while the positive value of ΔS is a strong indication that water molecules have been expelled from the complex interface.⁴² The calorimetric curve indicated a second exothermic non-binding process taking place after the formation of the receptor-substrate complex, a process which was not visible in NMR. This process could not be determined more accurately, and we can only assume it to be a change in the complex geometry to give maximum binding interaction, as is the case with enzymes.⁴³

Indicator displacement assay (IDA) of Zn₂L1 with pyrocatechol violet (PV). Pyrocatechol violet (**PV**) is a catechol-type pH-sensitive dye, which upon coordination to zinc ions is reported to change its colour from yellow ($\lambda_{\text{max}} = 443$ nm) to blue ($\lambda_{\text{max}} = 636$ nm).^{27,28,32,44} Therefore, the displacement of the receptor-bound pyrocatechol violet by a phosphate anion would be communicated visually as well spectrophotometrically. A preliminary “naked-eye test” of **Zn₂L1** with **PV** in buffered solutions (Hepes 10 mM, pH 7.4) confirmed the previous reported affinity and selectivity of Zn(II)-cyclen compounds for phosphate anions.^{22,35} The indicator is released only in the presence of phosphates, and the degree of its release is clearly influenced by the number of negative charges on the phosphate, (**Figure 2**). The UV/Vis absorption spectra of these titrations are presented in the supporting information.

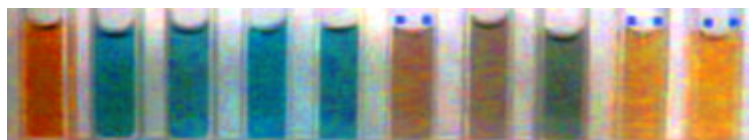


Figure 2. Colour of a solution of **PV** (50 μM) and **Zn₂L1** (50 μM) in the presence and absence of phosphate anions (250 μM). From left to right: **PV** alone, 1:1 mixture of **PV** to **Zn₂L1**, NO_3^- , CO_3^{2-} , CH_3CO_2^- , H_2PO_4^- , HPO_4^{2-} , PhPO_4^{2-} , PP_i and ATP. Titrations were performed at 25 $^\circ\text{C}$ in 10 mM Hepes buffer, pH 7.4.

The typical UV/Vis titration spectra of **PV** with **Zn₂L1** (**Figure 3** top) showed an isosbestic point, indicating a defined receptor-indicator complex stoichiometry, similar to previous reports.^{27,28,44} With increasing amounts of metal complex, the absorption of the free yellow indicator at $\lambda_{\text{max}} = 443 \text{ nm}$ decreased and shifted to $\lambda_{\text{max}} = 636 \text{ nm}$, giving a blue coloured solution. The 1:1 stoichiometry between **Zn₂L1** and indicator was supported by the Job plot (inset in **Figure 3** bottom) and by the linear increase in absorption at 636 nm up to 1 equivalent of added receptor. The structure of the formed receptor-indicator complex was reported by Kim et al.^{27, 28}

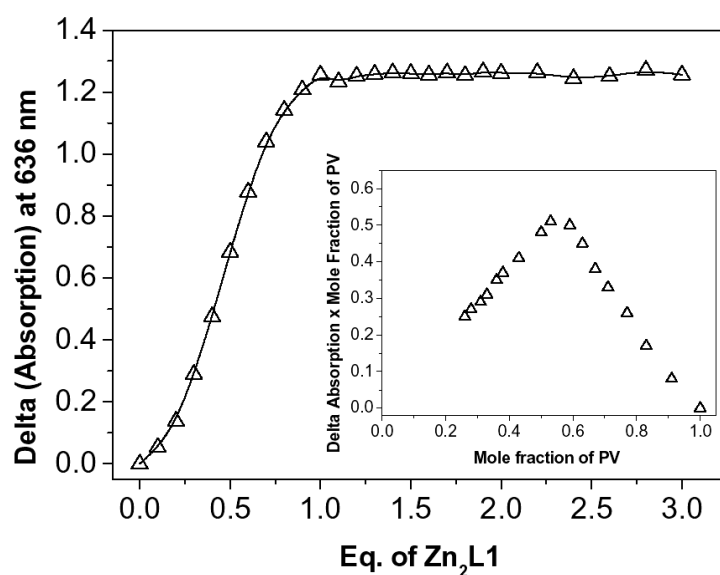
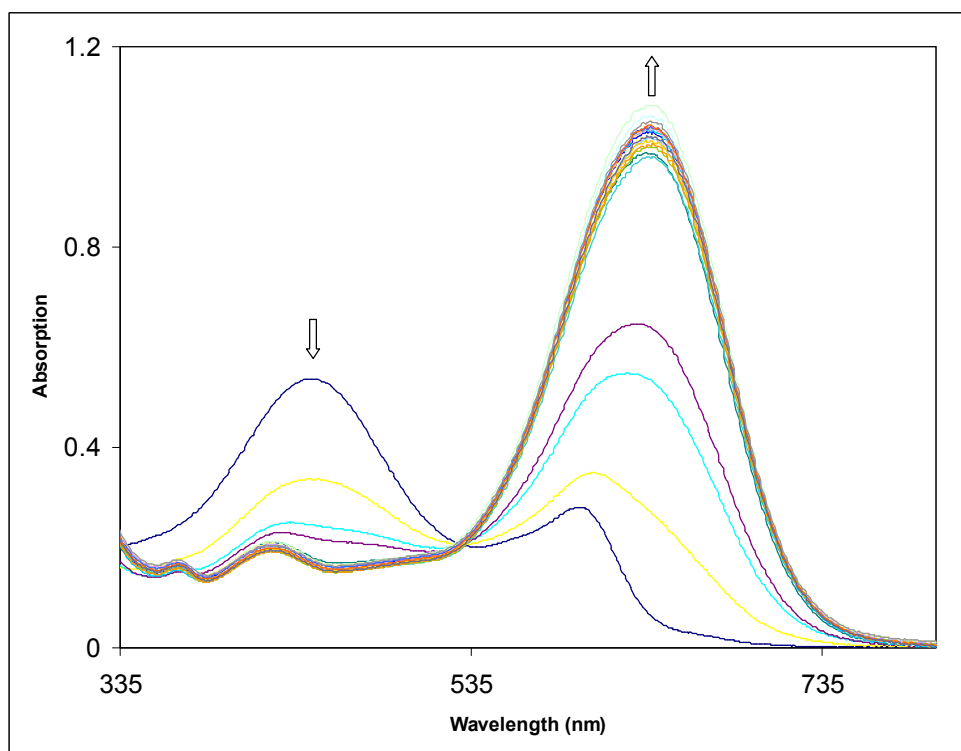


Figure 3. Top: UV/Vis absorption spectra of **PV** (constant concentration 35 μM) upon addition of **Zn₂L1** (0-105 μM). Bottom: Plot of the change in absorption at 636 nm, corresponding to the receptor-indicator complex, vs. the number of equivalents of **Zn₂L1** present in solution. **Zn₂L1** (0-105 μM) was added to a constant concentration of **PV** (35 μM). Inset: Jobs plot indicating a 1:1 stoichiometry. Titrations were performed at 25 $^{\circ}\text{C}$ in 10 mM Hepes buffer, pH 7.4.

ITC data could be described by a ‘one-site binding’ model with stoichiometry n equal to 1 and an association constant K of **Zn₂L1** for **PV** of $(4.23 \pm 0.21) \times 10^5 \text{ M}^{-1}$. The thermodynamic parameters of interaction (enthalpy of binding ΔH , binding constant K , entropy change ΔS and, consequently, free energy change ΔG) are summarized in **Table 2**.

	n	10⁻⁵ K [M ⁻¹]	ΔH [cal mol ⁻¹]	ΔS [cal mol ⁻¹ K ⁻¹]	ΔG [cal mol ⁻¹]
Zn₂L1	1.12 ± 0.01	4.23 ± 0.21	-8828 ± 121	-3.865	-7676.23

Table 2. Binding stoichiometry n , thermodynamic parameters and association constant (K) for the interaction of **PV** with **Zn₂L1** in aqueous solution (Hepes 10 mM, pH 7.4) at 25 °C.

The obtained thermodynamic data fit with previous reports of **PV** interaction with Zn(II) complexes²⁷: the process is enthalpically driven, while the unfavorable entropic contribution to the binding of the indicator ($\Delta S = -3.865 \text{ cal mol}^{-1} \text{ K}^{-1}$) compared to that of the pyrophosphate anion ($\Delta S = 7.66 \text{ cal mol}^{-1} \text{ K}^{-1}$) was suggested to be due to ordering of water molecules at the complex interface in the binding process. The binding constant K_{PV} of **Zn₂L1** is one order of magnitude higher than the one reported by Kim et al. for a dinuclear Zn(II)-Dpa complex,²⁷ therefore our IDA assembly will be more sensitive, as lower concentrations of anionic substrates will be needed for displacement of the indicator. The calorimetric titration curve is presented in the supporting information.

Addition of aliquots of aqueous solutions (Hepes buffer 10 mM, pH 7.4) of the sodium and/or potassium salts of ATP, ADP, cAMP, GTP, PP_i, hydrogen phosphate and phenyl phosphate to a 1:1 mixture of **Zn₂L1** and **PV** (35 μM) were able to displace the indicator with various degrees. The UV/Vis titration spectra (see supporting information) did not present an isosbestic point, although we demonstrated previously the 1:1 binding motif for pyrophosphate. Spectrophotometrical methods are very sensitive to any secondary interactions taking place in solution (aggregations etc.) and it is possible that the aforementioned second exothermic non-binding process observed in the ITC experiment with PP_i is the cause of the absence of a clean isosbestic point.

The association constants K for the various phosphates were derived from the concentrations of **PV** and respective phosphate at 50% release of indicator and are presented in **Table 3**.

Phosphate	Binding Const $K (\times 10^5 \text{ M}^{-1})^a$
ATP	7.0 ± 0.15
ADP	4.70 ± 0.35
cAMP	0.06 ± 0.007^b
GTP	6.68 ± 0.31
PP _i	8.4 ± 0.15
Na ₂ HPO ₄	0.77 ± 0.045
Na ₂ H ₂ PO ₄	0.11 ± 0.065^b

^a All titrations were performed at 25 °C in aqueous solutions buffered at pH 7.4 with 10 mM HEPES. Each value represents the average of three separate experiments. ^b The value of K is approximated (after 6 eq. of phosphate added there was only 15-20% release of **PV**).

Table 3. Binding constants K of **Zn₂L1** with various phosphate anions determined by the IDA technique with **PV**.

As observed in the “naked-eye test”, the binding affinity is clearly influenced by the number of negative charges on the phosphate, as was previously reported for other phosphate anion receptors.^{20,21,25b,28,29,45} ATP, GTP and PP_i have the highest negative charge and thus show the highest binding constants, whereas for cAMP with one negative charge partial displacement of the indicator was observed only upon addition of more than 6 equivalents of analyte. The binding constant obtained for PP_i ($K_{\text{PP}_i} = 8.4 \pm 0.15 \times 10^5 \text{ M}^{-1}$) matches the value obtained by ITC measurements ($K_{\text{PP}_i} = 1.67 \pm 0.3 \times 10^6 \text{ M}^{-1}$), the slight difference being perhaps due to the difference in pH and buffer (for ITC measurement Tris buffer 56 mM with pH 7 was used).

Interaction of Zn₂L3 with phosphate anions. We envisaged the complex **Zn₂L3** with the dansyl unit coordinating to one of the Zn(II) centres, as reported previously by Kimura *et al.*³⁹ (the alkyl chain would allow a certain flexibility to the dansyl moiety, needed for coordination; this would be more difficult if the fluorescent pendant molecule were attached directly to the triazine), resulting in an enhanced emission of the complex, and the displacement of the pendant ligand by phosphate anions would trigger an optical response. The emission response of compound **Zn₂L3** was tested by fluorescence titrations with various phosphates and nucleotides (5 equivalents of PP_i, ATP, GTP, ADP, Na₂HPO₄, GDP and other nucleotides) to show however no notable change or shift in intensity (**Figure 4**).

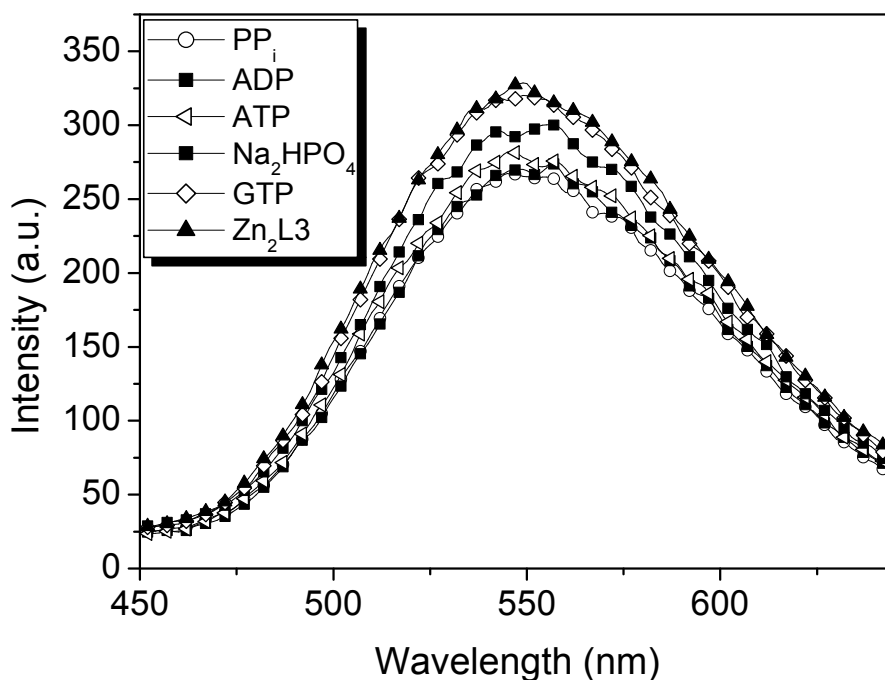


Figure 4. Excitation spectra of **Zn₂L3** (80 μ M) upon addition of various nucleotides and phosphates (400 μ M). Titrations were performed at 25 $^{\circ}$ C in 10 mM Hepes buffer, pH 7.4 ($\lambda_{\text{exc}} = 330$ nm). The same curve shapes were obtained with GDP and CTP and are not represented for clarity reasons.

Therefore the planned interaction between binding and signalling unit was not present. Indeed, the characteristic blue shift or increase in fluorescence intensity reported by Kimura³⁹ and Kikuchi²¹ upon pendant coordination is not visible in our case, similar emission and excitation spectra of ligand **L3** (80 μ M), the dinuclear metal complex **Zn₂L3** (80 μ M) and dansylamide, both at pH 7.4 (Hepes, 10 mM) and pH 13.5 (aq. NaOH solution 1M) indicating no coordination of the dansylamide to zinc complexes (see supporting information). The deprotonation and reversible coordination of the dansyl sulphonamide, which is the origin of changes in emission properties in the presence of an analyte competing for binding to the metal complex, is missing in compound **Zn₂L3**.

Hence, the phosphate binding affinity of **Zn₂L3** was studied by the IDA approach. The use of pyrocatechol violet (**PV**) as indicator, like in the case of **Zn₂L1**, had a major drawback in that an overlap between the absorption band at 331 nm of **Zn₂L3** and that of **PV** at 443 nm could lead to errors of measurement. This fact, paired with the different properties of the receptor and indicator (one is fluorescent, the other a colorimetric indicator) and the fact that fluorescence measurements need lower concentrations of analytes and are more sensitive than

UV/Vis titrations, led us to make use of one of the major advantages offered by the IDA technique, the free choice of the indicator, and chose the fluorescent indicator coumarin methyl sulfonate (**CMS**) for the IDA approach with **Zn₂L3**. For good comparison of data, we studied also the binding affinity of **CMS** to **Zn₂L1**.

Indicator displacement assay of Zn₂L1 and Zn₂L3 with coumarin-methylsulfonate (CMS). Coumarin methyl sulfonate has been used as an indicator in measurements with dinuclear Zn(II)-dipicolylamine complexes to detect low concentration of pyrophosphate under physiological conditions^{29,31} and phosphatidylserine in bilayer membrane surfaces.³⁰ It is a highly water soluble pale yellow solid, exhibits very stable fluorescence emission at 480 nm and was easily prepared following the reported procedure²⁹ in 47% yield by treatment of 6,7-dihydroxy-4-chloromethyl coumarin with sodium sulfite.

Zn₂L1 was capable of quenching the fluorescence emission of **CMS** in a concentration dependent fashion at 25 °C in aqueous solution (pH 7.4, Hepes 10 mM) (**Figure 5**).

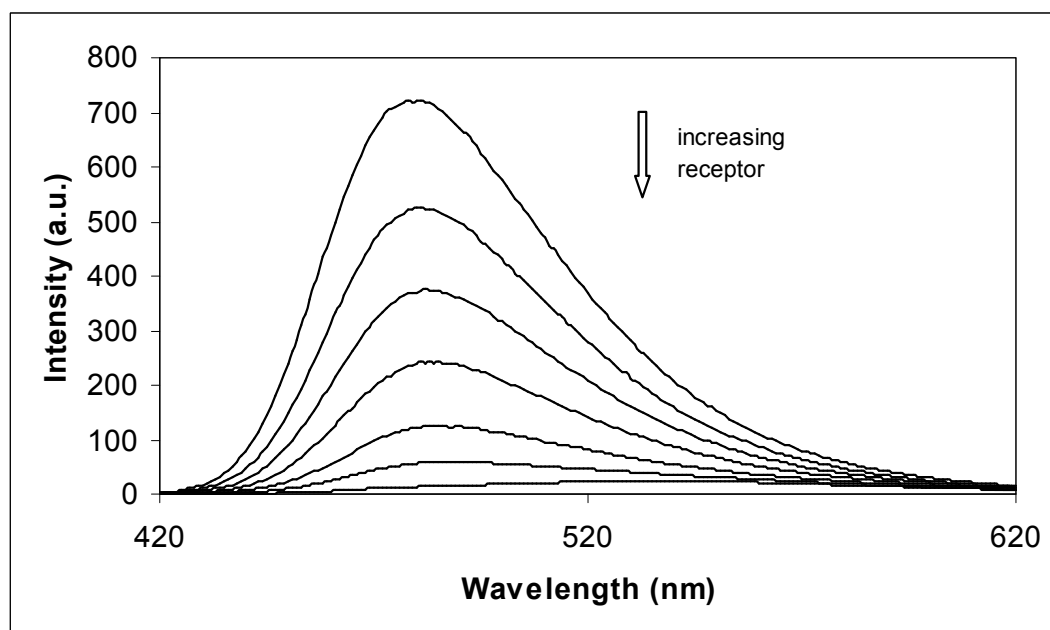


Figure 5. Fluorescence emission spectra of **CMS** (80 μ M) following the addition of increasing amounts of **Zn₂L1** (0-192 μ M). Titrations were performed at 25 °C in 10 mM Hepes buffer, pH 7.4 (λ_{exc} = 396 nm, λ_{em} = 480 nm, 550V).

In contrast to the previous reports, the Job plot indicated 1:2 receptor-indicator binding stoichiometry, supported also by the titration curve (**Figure 6**). All titrations were corrected for the dilution due to the addition of aliquots of **Zn₂L1**.

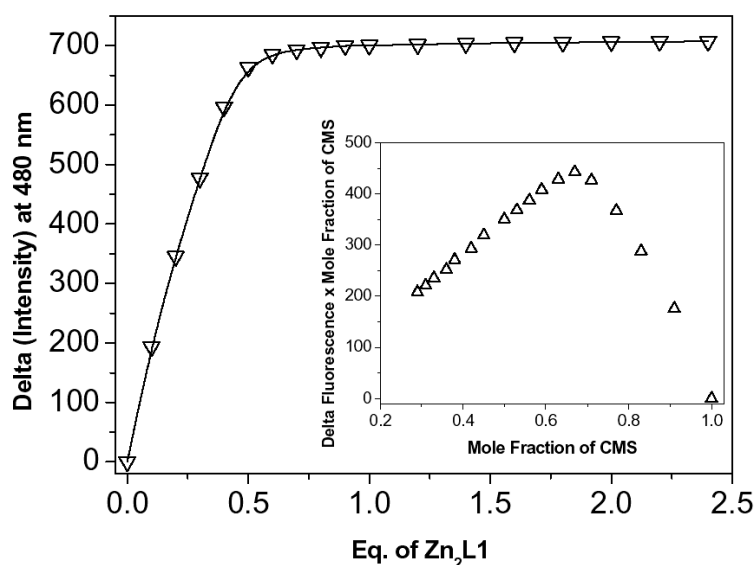


Figure 6. Fluorescence intensity of **CMS** (80 μM) at 480 nm upon addition of **Zn₂L1** (0-192 μM). Inset: Jobs plot for the receptor-indicator binding of **CMS** and **Zn₂L1** indicating a 1:2 stoichiometry. Titrations were performed at 25 $^{\circ}\text{C}$ in 10 mM Hepes buffer, pH 7.4 and the titrations were corrected for dilution.

ITC measurements performed under the same reaction conditions fitted the “one-binding site” model with a stoichiometry of 1:2. The value of the determined association constant K was of $2.5 \pm 0.1 \times 10^5 \text{ M}^{-1}$. The ITC titration curve is presented in the supporting information together with the thermodynamic parameters of interaction.

Preliminary excitation and emission titration experiments of **CMS** and **Zn₂L3** (presented in the supporting information) provided the excitation wavelength of 396 nm as ideal for the IDA approach, with only the indicator **CMS** emitting at this wavelength without interference from the dansyl moiety of the dinuclear metal complex. This excitation wavelength was also used in the previous measurements with **Zn₂L1** for a good comparison of data. The fluorescence emission intensities at 480 nm obtained upon addition of aliquots of **Zn₂L3** to an aqueous solution (10 mM Hepes buffer, pH 7.4) of **CMS** gave distinct 1:1 binding curves, with complete quenching of the indicator emission after addition of 1 equivalent of metal complex (inset in **Figure 7**). Non-linear least square fitting of the titration curves to a standard 1:1 binding model^{46,47} (**Figure 7**) yielded the value of the association constant $K = (4.64 \pm 0.06) \times 10^4 \text{ M}^{-1}$.

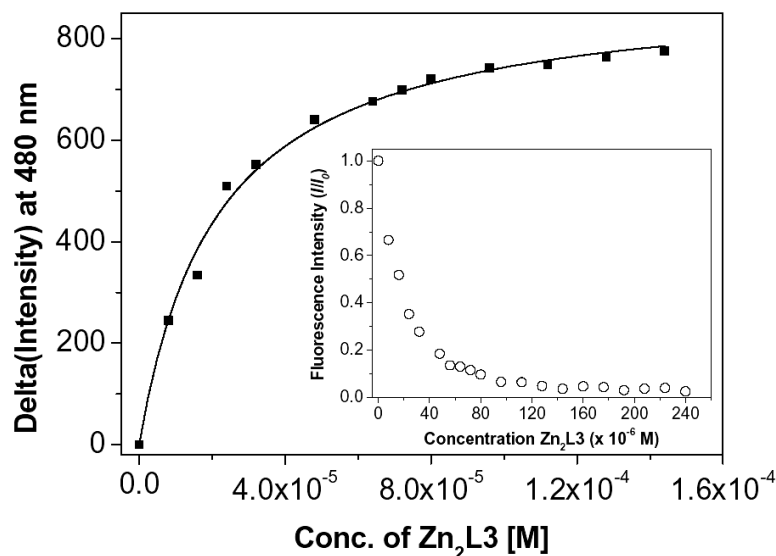


Figure 7. Fluorescence titration curve and calculated non-linear fit for the addition of aliquots of **Zn₂L3** to **CMS** (80 μ M). Inset: plot of the fluorescence intensity (I/I_0) at 480 nm of **CMS** (80 μ M) vs. total concentration of **Zn₂L3** present in solution at 25 $^{\circ}$ C in 10 mM Hepes buffer, pH 7.4. All titrations were corrected for dilution.

The different binding stoichiometry of **Zn₂L1** and **Zn₂L3** to **CMS** is not yet fully understood. At present, there is no crystallographic report or any other study of the complex formed between **CMS** and Zn(II) receptor molecules, and we can only suppose that the long and bulky spacers of the dinuclear metal complexes (for **Zn₂L3** the triazine-dansyl moiety, Smith had *m*- and *p*-xylene spacers,²⁹ and Joliffe reported a bulky cyclic peptide spacer³¹) could induce steric and electronic effects upon binding **CMS**. The association constants K_{CMS} of **Zn₂L1** and **Zn₂L3** are in the range reported for other Zn(II) complexes,^{29,31} with **Zn₂L1** binding the indicator 5 times more tightly than **Zn₂L3**.

The previously described procedure for the IDA measurement of **Zn₂L1** with **PV** was also used in the case of **Zn₂L3** and **CMS** and the same substrates were tested for binding affinity. The association constants K for the various phosphates were derived from the concentrations of **CMS** and respective phosphate at 50% release of indicator and presented in **Table 4**.

Phosphate	Binding Const $K (\times 10^4 \text{ M}^{-1})^a$
ATP	3.44 ± 0.13
ADP	2.94 ± 0.27
cAMP	0.13 ± 0.1^b
GTP	3.86 ± 0.3
PP _i	5.02 ± 0.13
Na ₂ HPO ₄	1.05 ± 0.24
Na ₂ PhPO ₄	0.464 ± 0.02

^a All titrations were performed at 25 °C in aqueous buffer solutions (HEPES 10mM, pH 7.4). Each value represents the average of at least three separate experiments. ^b The value of K is approximated (after 10 eq. cAMP added there was only 13% release of indicator for cAMP).

Table 4. Binding constants K of **Zn₂L3** for various phosphate anions determined by the IDA technique with **CMS**.

Similar to **Zn₂L1**, the binding affinity of **Zn₂L3** increases with the number of negative charges on the phosphate and a “naked-eye test” was developed through irradiation of the samples with a fluorescent lamp, as shown in **Figure 8**.

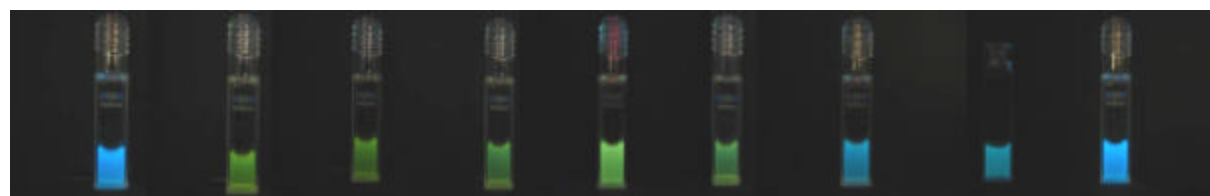


Figure 8. Colour of solutions of **CMS** (80 μM) and **Zn₂L3** (80 μM) upon irradiation in the presence and absence of phosphate anions (80 μM). From left to right: **CMS** alone, 1:1 mixture of **CMS** to **Zn₂L3**, cAMP, HPO₄²⁻, PhPO₄²⁻, ADP, GTP, ATP and PP_i. Titrations were performed at 25 °C in 10 mM Hepes buffer, pH 7.4.

Quantitative assay for phosphate anions in aqueous solution under physiological conditions. The properties of **CMS** and the availability of **Zn₂L1**³⁶ led us to develop an analytical assay for the detection of phosphate anions in aqueous solution, shown in **Figure 9**. The present ensemble shows under a fluorescent lamp release of **CMS** only with addition of phosphate anions, the degree of the release being proportional to the number of negative charges of the phosphate. Thus, almost no release was observed in the presence of an equivalent of inorganic phosphate, phenylphosphate and cAMP, while a return to the initial emission wavelength and intensity of **CMS** is visible with the nucleotides ATP, ADP, GTP

and GDP and the pyrophosphate. No release was observed by addition of 10 eq. of other anions.

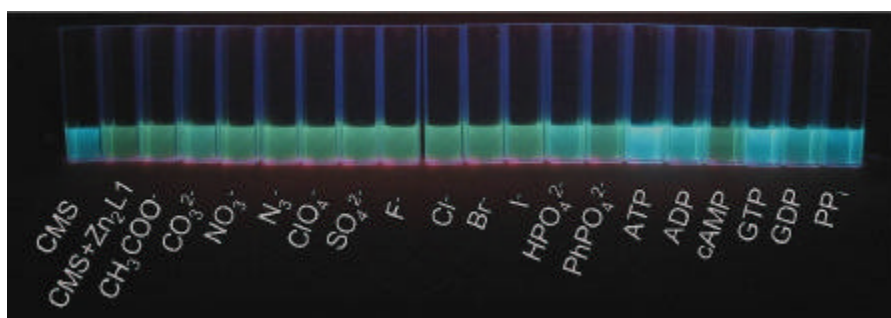
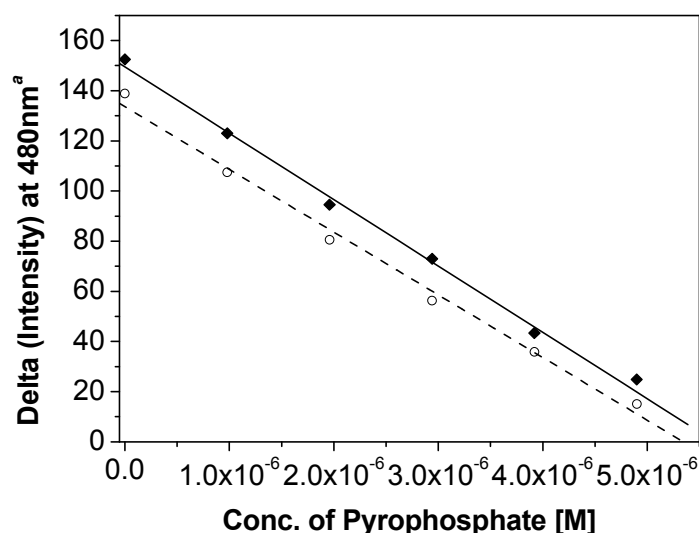


Figure 9. Colour of the mixture (80 μM **CMS**, 40 μM **Zn₂L1**) upon irradiation in the presence and absence of various anions (800 μM) and phosphate anions (80 μM). Titrations were performed at 25 $^{\circ}\text{C}$ in 10 mM Hepes buffer, pH 7.4.

Based on the properties of this assembly we developed a quantitative assay for μM concentrations of PP_i in aqueous solution under physiological conditions in the presence of other anions (**Figure 10**), offering a new application of transitional metal complexes of azamacrocycles. Only three other reports of such an assay for PP_i are found in literature, using either the Zn(II)-Dpa unit^{16,17,31} or a dicopper(II) macrocyclic complex.²⁶



^a Delta (Intensity) = Intensity of free indicator CMS (10 μM) – Measured Intensity.

Figure 10. Plot of the difference in intensity at 480 nm^a against concentration of PP_i in HEPES solution (pH 7.4, 10 mM) in the absence (●, —) and presence (○, ---) of other ions (50 μM of NaCl, 50 μM NaOAc, 50 μM Na_2CO_3 and 50 μM Na_2SO_4). The concentration of the indicator **CMS** was kept constant at 10 μM and that of **Zn₂L1** at 5 μM .

3.3. Conclusion

The previous reported complex **Zn₂L1**³⁶ showed from ³¹P NMR and ITC titrations in aqueous solution under physiological conditions (Tris 56 mM, pH 7, 25 °C) the formation of a very stable 1:1 complex with pyrophosphate, with a slow exchange taking place between free and bound anion. Displacement measurements with **PV** in buffered solutions (Hepes 10 mM, pH 7.4, 25 °C) indicated that the receptor can distinguish phosphate anion derivatives from other anionic species, with binding affinities proportional to the number of negative charges on the anion.

We have reported the synthesis of a new dinuclear Zn(II) (cyclen) complex, **Zn₂L3**, containing the dansylamide moiety bound to the triazine spacer. **Zn₂L3** does not behave as a chemosensor upon binding of phosphate esters, because the deprotonation and reversible coordination of the dansyl sulphonamide to one of the metal centres, which is the origin of changes in emission properties in the presence of an analyte competing for binding to the metal complex, is missing, probably due to the long distance between the dansyl signalling unit and the binding site. Indicator displacement assay with **CMS** as florescent indicator led to similar results as for **Zn₂L1**, with ATP, GTP and PP_i possessing the highest association constants and cAMP the lowest.

The affinity of **Zn₂L3** for the various phosphates can be directly detected with the naked eye through irradiation of the samples with a fluorescent lamp.

The association constants for **Zn₂L1** are around one order of magnitude higher than those of **Zn₂L3** due to electronic and steric influences of the bulky spacer. The binding constant of **Zn₂L1** for PP_i ($K_{PP_i} = 8.4 \pm 0.15 \times 10^5 \text{ M}^{-1}$) obtained from the IDA approach matches the value obtained by ITC measurements ($K_{PP_i} = 1.67 \pm 0.3 \times 10^6 \text{ M}^{-1}$), the slight difference being caused by the difference in pH and buffer for the two measuring techniques. As an application, we developed a quantitative assay for PP_i in aqueous solution under physiological conditions down to the concentration range of 1 μM in the presence of other anions (excluding other phosphate anions), offering a new application of transitional metal complexes of azamacrocycles.

The binding properties and affinities of **Zn₂L1** and **Zn₂L3** towards phosphate anions could be further tuned for selective recognition of a specific phosphate by the choice of the indicator, as demonstrated in a recent study by Smith *et al.*³² and previously shown by Anslyn³³ and Fabrizzi.²⁶ Such assemblies, where a single receptor could be used with a range of indicators to give different selectivities may find applications in biological and biochemical assays.

3.4. Experimental Section

General information. UV/VIS spectra were recorded on a Varian Cary BIO 50 UV/VIS/NIR spectrophotometer equipped with a jacketed cell holder using 1-cm cuvettes (quartz or glass) from Hellma. Fluorescence measurements were performed in 1 cm quartz cuvettes (Hellma) and recorded on a Varian 'Cary Eclipse' fluorescence spectrophotometer. For all UV/Vis and fluorescence measurements the temperature was kept constant at 25 °C (± 0.1 °C). IR spectra were recorded on a Bio-Rad FT-IR FTS 155 spectrometer and a Bruker Tensor 27 spectrometer with an ATR unit. Elemental analysis was performed on a Vario EL III. Mass spectra were performed on a ThermoQuest Finnigan TSQ 7000 (ESI) and Finnigan MAT 95 (HRMS). ^1H , and ^{13}C NMR spectra were obtained on the following machines: Bruker AC-250 (^1H : 250.1 MHz, ^{13}C : 62.9 MHz, 24 °C), Bruker Avance 300 (^1H : 300.1 MHz, ^{13}C : 75.5 MHz, 27 °C), Bruker Avance 400 (^1H : 400.1 MHz, ^{13}C : 100.6 MHz, 27 °C), Bruker Avance 600 (^1H : 600.1 MHz, ^{13}C : 150.1 MHz, 27 °C). Melting points were determined with a Büchi SMP 20 and are uncorrected. ^{31}P NMR spectra were recorded on a Bruker Avance 400 at 300 K with phosphoric acid as external reference.

Materials and Reagents. All reagents and solvents used for the synthesis of the metal complexes were of analytical grade. Dansylcadaverine (Fluka), pyrophosphate tetrasodium salt (Acros) and the other reagents were purchased from commercial sources and used without any further purification.

Caution: Although no problems were encountered in this work, metal perchlorate complexes are potentially explosive. They should be handled with care and the complexes should be prepared in small quantities.

4,6-Bis-(1,4,7,10-tetraaza-cyclododecane-1,4,7-tricarboxylic acid tri-*tert*-butyl ester)-2-dansylcadaverine-[1,3,5]-triazin (2)

Dansylcadaverine (0.047 g, 0.142 mmol) and 1^{37} (0.150 g, 0.142 mmol) were dissolved in 10 mL dioxane and stirred for 5 minutes under inert atmosphere. Then K_2CO_3 (0.05 g, 0.355 mmol, 2.5 eq.) was added. The mixture was refluxed for 24h at 110 °C under inert atmosphere. After completion, the reaction mixture was filtered in order to remove all inorganic salts and the solvent was removed under reduced pressure. The raw product (0.196 g, 0.144 mmol) was purified by column chromatography on neutral alumina (EE/PE 60:40, then 100:0, then DCM). The product was obtained as a slightly turquoise solid (0.145 g, 0.107 mmol, 75 %).

Melting point 104°C; ^1H NMR (300 MHz, CDCl_3 , 25°C, TMS): δ =1.23 (m, 2H, CH_2); 1.41 (m, 58 H, CH_3 -Boc and CH_2); 2.86 (m, 8H, CH_3N and $\text{CH}_2\text{NH}\text{SO}_2$); 3.18-3.68 (m, 34H, CH_2

Cyclen and CH_2NH -triazine); 4.67 (bs, 1H, NHSO_2); 7.16 (d, 1H, $^2J=7.59$ Hz, CH 6); 7.49 (dd, 1H, $^2J=7.29$, 8.52 Hz, CH 3); 7.53 (dd, 1H, $^2J=7.59$, 8.60 Hz, CH 7); 8.21 (dd, 1H, $^2J=7.29$, 1.28 Hz, CH 2); 8.31 (d, 1H, $^2J=8.60$ Hz, CH 8); 8.51 (dd, 1H, $^2J=8.52$, 1.28 Hz, CH 4); ^{13}C NMR (300 MHz, CDCl_3 , 25°C, TMS): δ =23.59 (CH_2); 28.44, 28.47 (CH_3 -Boc); 29.30, 29.40 (CH_2); 39.98 (CH_2NH -Triazine); 43.03 ($\text{CH}_2\text{NH}\text{SO}_2$); 45.35 (CH_3N); 50.22 (CH_2 Cyclen); 79.71 (C_{quat} -Boc); 115.08 (CH_{arom} 6), 118.93 (CH_{arom} 8), 123.13 (CH_{arom} 3), 128.19 (CH_{arom} 7), 129.40 (CH_{arom} 2), 129.66 (CH_{arom} 4), 129.87, 130.15 (CH_{arom}); 135.07 (C_{quat} - SO_2); 151.90 (C_{quat} -N-(CH_3)₂); 156.29 (COO -Boc); 165.76 (C_{quat} triazine); IR (KBr): $\tilde{\nu}$ =3385, 3270, 2974, 2933, 2868, 2789, 2361, 1695, 1542, 1474, 1411, 1366, 1250, 1164, 1105, 972, 946, 860, 777 cm^{-1} ; UV/Vis (MeOH): λ_{max} (lg ϵ)=335 (3.668); MS (ESI, DCM/MeOH + 10 mmol/l NH_4Ac): m/z (%): 678.6 (65) [$(\text{M}+2\text{H}^+)^{2+}$]; 1356.1 (100) [MH^+]; elemental analysis calcd (%) for $\text{C}_{66}\text{H}_{110}\text{N}_{14}\text{O}_{14}\text{S} \cdot \text{CH}_2\text{Cl}_2$: C 55.86, H 7.84, N 13.61; found: C 56.12, H 8.23, N 13.42.

4,6-Bis-(1,4,7,10-tetraaza-cyclododecane-1,4,7-tricarboxylic acid tri-*tert*-butyl ester)-2-(dansyl-(2-amino-ethyl)-amide)-[1,3,5]-triazin (3)

A solution of **1**³⁷ (0.886 g, 0.838 mmol) in 25 mL dioxane p.a. was stirred under nitrogen for 5 minutes, then a solution of Dansyl-(2-amino-ethyl)-amide (0.615 g, 2.096 mmol, 2.5 eq.) in 75 mL dioxane p.a. was added dropwise. Then K_2CO_3 (0.580 g, 4.19 mmol, 5 eq.) was added. The mixture was refluxed for 72h at 140 °C under inert atmosphere. After completion, the reaction mixture was filtered in order to remove all inorganic salts and the solvent was removed under reduced pressure. The raw product (1.434 g) was purified by column chromatography on neutral alumina (EE/PE 30:70 to 40:60). The product was obtained as a yellow solid (0.820 g, 0.624 mmol, 75%).

Melting point 113 °C (sublimation); ^1H NMR (400 MHz, CDCl_3 , 25°C, TMS): δ =1.41 (bs, 54H, CH_3 -Boc); 2.86 (s, 6H, CH_3N); 3.10-3.68 (m, 36H, CH_2 chain and CH_2 Cyclen); 4.77 (bs, 1H, NHSO_2); 6.95 (bs, 1H, NH -triazin); 7.13 (d, 1H, $^3J=7.58$ Hz, CH 6); 7.47 (dd, 1H, $^3J=7.58$, 8.65 Hz, CH 7); 7.48 (dd, 1H, $^3J=7.34$, 8.54 Hz, CH 3); 8.21 (d, 1H, $^3J=7.34$ Hz, CH 2); 8.36 (d, 1H, $^2J=8.65$ Hz, CH 8); 8.48 (d, 1H, $^2J=8.54$ Hz, CH 4); ^{13}C NMR (400 MHz, CDCl_3 , 25°C, TMS): δ =28.53 (CH_3 -Boc); 41.79 ($\text{CH}_2\text{NH}\text{SO}_2$); 43.57 (CH_2NH -Triazine); 45.42 (CH_3N); 50.09, 50.16, 50.25, 50.29 (CH_2 Cyclen); 79.78, 80.09, 80.3 (C_{quat} -Boc); 115.02, 123.14, 127.78, 127.82, 129.79, 129.84, 129.87, 129.92 (CH_{arom}); 135.08 (C_{quat} - SO_2); 151.73 (C_{quat} -N-(CH_3)₂); 156.24 (C_{quat} , C=O Boc); 165.76 (C_{quat} triazine); IR (KBr): $\tilde{\nu}$ =3414, 3267, 2975, 2933, 2361, 2200, 1686, 1541, 1499, 1474, 1410, 1366, 1321, 1249, 1163, 1106, 1050, 970, 946, 858, 777; UV/Vis (CH_2Cl_2): λ_{max} (lg ϵ)=340 (3.655); MS (ESI, DCM/MeOH

+ 10 mmol/l NH₄Ac): *m/z* (%):1313.9 (100) [MH⁺]; elemental analysis calcd (%) for C₆₃H₁₀₄N₁₄O₁₄S: C 57.59, H 7.98, N 14.93; found: C 57.22, H 8.11, N 14.66.

4,6-Bis-(1,4,7,10-tetraaza-cyclododecane)-2-dansylcadaverine-[1,3,5]-triazin (L2)

A solution of **2** (0.073 g, 0.05 mmol) in CH₂Cl₂ was treated with TFA (0.45 g, 0.3 ml, 4 mmol, 80 eq.) and the reaction mixture was stirred overnight. After completion of reaction the solvent was removed under reduced pressure. The obtained pale yellow solid (quantitative yield) was solved in water and passed through a column of pre-swelled (pH = 7) basic ion-exchange resin. The fractions having a basic pH were collected and the resulting aqueous solution was frozen in liquid nitrogen and lyophilised. The ligand **L2** was obtained as a colourless solid in quantitative yield (40 mg, 0.05 mmol).

Melting point 102 °C (sublimation); ¹H NMR (400 MHz, MeOD, 25°C, TMS): *δ*=1.17-1.27 (m, 2H, CH₂); 1.30-1.41 (m, 4H, CH₂); 2.64-2.70 (m, 8H, CH₂ Cyclen); 2.71-2.77 (m, 8H, CH₂ Cyclen); 2.83 (t, 2H, ³*J* = 6.96 Hz, CH₂NHSO₂); 2.87 (s, 6H, CH₃N); 2.95 (bs, 8H, CH₂ Cyclen); 3.08 (bs, 1H, NHSO₂); 3.16 (t, 2H, ³*J*=6.89 Hz, CH₂NH-Triazine); 3.38 (bs, 1H, NH-triazine); 3.73 (m, 8H, CH₂ Cyclen); 7.26 (d, 1H, ³*J*=7.57 Hz, CH 6); 7.56 (dd, 1H, ³*J*=7.30, 8.54 Hz, CH 3); 7.57 (dd, 1H, ³*J*=7.57, 8.69 Hz, CH 7); 8.17 (d, 1H, ³*J*=7.30 Hz, CH 2); 8.35 (d, 1H, ³*J*=8.69 Hz, CH 8); 8.55 (d, 1H, ³*J*=8.54 Hz, CH 4); ¹³C NMR (400 MHz, MeOD, 25°C, TMS): *δ*=24.94 (CH₂); 30.50, 30.52 (CH₂); 41.23 (CH₂NH-Triazine); 43.88 (CH₂NHSO₂); 45.87 (CH₃N); 46.42, 46.81, 49.54, 49.69, 49.75 (CH₂ Cyclen); 116.46 (CH_{arom} 6); 120.68 (CH_{arom} 8); 124.34 (CH_{arom} 3); 129.09 (CH_{arom} 7); 130.11 (CH_{arom} 2); 131.07 (CH_{arom} 4); 131.11, 131.29 (CH_{arom} quat.); 137.33 (C_{quat}-SO₂); 153.26 (C_{quat}-N-(CH₃)₂); 167.15, 168.025 (C_{quat} triazine); IR (KBr): $\tilde{\nu}$ =3427, 2927, 2852, 2361, 1542, 1489, 1418, 1362, 1299, 1142, 833, 797, 720; UV/Vis (MeOH): λ_{max} (lg *e*)=336 (3.552); Fluorescence (MeOH): λ_{exc} =336 nm, λ_{em} =518 nm, Intensity=226.611 (c=1.25e-05 M); MS (ESI, AcN/TFA): *m/z* (%): 252.5 (30) [(M+3H⁺)³⁺]; 266.1 (100) [(M+3H⁺+CH₃CN)³⁺]; 378.3 (75) [(M+2H⁺)²⁺]; HRMS (PI-EIMS, 70 eV): calcd. for C₃₆H₆₁N₁₄O₂S [(M-H)⁺] 753.4823, found 753.4827 (0.57 ppm).

4,6-Bis-(1,4,7,10-tetraaza-cyclododecane)-2-(dansyl-(2-amino-ethyl)-amide)-[1,3,5]-triazin (L3)

A solution of **3** (0.770 g, 0.586 mmol) in CH₂Cl₂ was treated with TFA (5.36 g, 3.6 mL, 47 mmol, 80 eq.) and the reaction mixture was stirred for 24h. After completion of reaction the solvent was removed under reduced pressure. The obtained pale yellow solid (quantitative yield) was solved in water and passed through a column of pre-swelled (pH = 7) basic ion-exchange resin. The fractions having a basic pH were collected and the resulting aqueous

solution was frozen in liquid nitrogen and lyophilised. The product was obtained as a colourless solid (0.258 g, 0.362 mmol, 62%).

Melting point 92 °C; ^1H NMR (300 MHz, MeOD, 25°C, TMS): δ =2.62 (bs, 8H, CH_2 Cyclen); 2.70 (bs, 8H, CH_2 Cyclen); 2.87 (s, 14H, CH_3N and CH_2 Cyclen); 3.00 (t, 2H, 3J =6.03 Hz, $\text{CH}_2\text{NH-Triazine}$); 3.32 (t, 2H, 3J =6.03 Hz, CH_2NHSO_2); 3.7 (bs, 8H, CH_2 Cyclen); 7.23 (d, 1H, 3J =7.59 Hz, CH 6); 7.50 (dd, 1H, 3J =7.59, 8.58 Hz, CH 7); 7.55 (dd, 1H, 3J =7.32, 8.47 Hz, CH 3); 8.17 (d, 1H, 3J =7.32 Hz, CH_2 2); 8.26 (d, 1H, 3J =8.58 Hz, CH 8); 8.53 (d, 1H, 3J =8.47 Hz, CH 4); ^{13}C NMR (300 MHz, MeOD, 25°C, TMS): δ =41.19 (CH_2NHSO_2); 44.54 ($\text{CH}_2\text{NH-Triazine}$); 45.84 (CH_3N); 46.94, 48.59, 48.73, 48.87 (CH_2 Cyclen); 116.28 (CH 6), 120.36 (CH 8), 124.24 (CH 3), 128.99 (CH 7), 130.09 (CH 2), 130.99 (CH_{quat} arom.), 131.11 (CH 4), 131.22 (CH_{quat} arom.); 136.92 ($\text{C}_{\text{quat-SO}_2}$); 153.20 ($\text{C}_{\text{quat-N-(CH}_3)_2}$); 167.16 (C_{quat} triazine, C-Cyclen), 168.01 (C_{quat} triazine, C-NH); IR (KBr): ν =3397, 2938, 2840, 2361, 2200, 1542, 1497, 1416, 1362, 1294, 1142, 1063, 940, 792, 625, 572; UV/Vis (MeOH): λ_{max} (lg ϵ)= 336 (3.766); Fluorescence (MeOH): λ_{exc} =336 nm, λ_{em} =522 nm, Intensity=700.936 ($c=2.5\text{e-}05$ M); MS (ESI, TFA/AcN/ H_2O): m/z (%): 357.4 (100) [$(\text{M}+2\text{H}^+)^{2+}$]; 713.6 (20) [MH^+]; HRMS (PI-EIMS, 70 eV): calcd. for $\text{C}_{33}\text{H}_{56}\text{N}_{14}\text{O}_2\text{S}$ [$(\text{M-H})^+$] 712.4331, found 712.4421 (1.46 ppm).

[Zn₂L3](ClO₄)₄ · CH₃CH₂OH

The aqueous solutions of ligand (0.080 g, 0.112 mmol) and $\text{Zn}(\text{ClO}_4)_2 \cdot 6\text{H}_2\text{O}$ (0.088 g, 0.235 mmol, 2.1 eq.) were added drop wise in the same time in a warm aqueous solution (5 mL). An aqueous LiOH solution was added until pH = 8-9. The reaction mixture was refluxed for 4h. The product was recrystallized from EtOH (2mL) as a pale yellow solid (127 mg, 0.1 mmol, 91%).

Melting point 180-182°C (sublimation); ^1H NMR (300 MHz, $\text{CH}_3\text{CN-}d_3$, 25°C, TMS): δ =2.65-2.9 (m, 18H, 12H CH_2 Cyclen and 6H CH_3N); 2.94-3.15 (m, 14H, 12H CH_2 Cyclen and CH_2NHSO_2); 3.23-3.46 (m, 6H, CH_2 Cyclen and $\text{CH}_2\text{NH-triazine}$); 4.24-4.44 (m, 4H, CH_2 Cyclen); 6.11 (m, 1H, NH-triazine); 7.23 (d, 1H, 3J =7.43 Hz, CH 6); 7.53 (dd, 1H, 3J =7.43, 8.78 Hz, CH 7); 7.57 (dd, 1H, 3J =7.41, 8.23 Hz, CH 3); 8.15 (d, 1H, 3J =7.41 Hz, CH 2); 8.18 (d, 1H, 3J =8.78 Hz, CH 8); 8.51 (d, 1H, 3J =8.23 Hz, CH 4); ^{13}C NMR (300 MHz, $\text{CH}_3\text{CN-}d_3$, 25°C, TMS): δ = 41.89 ($\text{CH}_2\text{NH-triazine}$); 43.04 (CH_2NHSO_2); 44.39 (CH_3N); 45.33, 45.80, 46.05, 46.43 (CH_2 Cyclen); 114.85, 118.34, 123.08, 127.93, 128.61, 128.92, 129.25, 129.91 (CH arom); 134.98 ($\text{C}_{\text{quat-SO}_2}$); 151.71 ($\text{C}_{\text{quat-N-(CH}_3)_2}$); 165.48 (C_{quat} triazine); IR (KBr): ν =3427, 3283, 2931, 2361, 2200, 1636, 1560, 1419, 1346, 1312, 1143, 1110, 1090, 979, 795, 627, 575 cm^{-1} ; UV/Vis (Tris 10 mM pH 7.4): λ_{max} (lg ϵ)=331 (3.587);

Fluorescence (Tris 10 mM pH 7.4, 650V): $\lambda_{\text{exc}}=330$ nm, $\lambda_{\text{em}}=551$ nm, Intensity=367.584 (c=6.25E-05 M); MS (ESI, H₂O/AcN): m/z (%): 450.3 (100) [(M⁴⁺+ 2CO₃²⁻)²⁺]; elemental analysis calcd (%) for C₃₃H₅₆N₁₄O₁₈SCl₄Zn₂ · EtOH: C 32.65, H 4.85, N 15.23; found: C 32.52, H 4.87, N 15.04.

Binding Studies by Isothermal Titration Calorimetry (ITC). All ITC experiments were performed in buffered aqueous solution (Tris 56 mM, pH 7 or HEPES, 10 mM, pH 7.4) at 25 °C using an ultrasensitive VP-ITC calorimeter from MicroCal (Northampton, MA, U.S.A.). The titrant and sample solutions were prepared from the same stock buffer solution, and both solutions were thoroughly degassed under vigorous stirring before each titration. The reference cell contained Millipore water. During the ITC experiment the cell solution was stirred at 430 rpm by syringe to ensure rapid mixing and 60 x 5 μ L of titrant were injected over 10 s with a spacing time between each injection of two minutes in order to allow complete equilibration. A background titration, consisting of the identical titrant solution, but only the buffer solution in the sample cell, was subtracted from each experimental titration to account for heat of dilution. Data analysis was performed with the Windows-based Origin software package supplied by MicroCal. The Origin software uses a nonlinear least-squares algorithm (minimization of χ^2) and the concentrations of the titrant and the sample to fit the heat flow per injection to an equilibrium binding equation, providing best fit values of the stoichiometry (n), change in enthalpy (ΔH°), and binding constant (K). Using these values, the entropy change ΔS and, consequently, free energy change ΔG are determined.

3.5. Supporting Information

NMR spectra of Zn₂L3

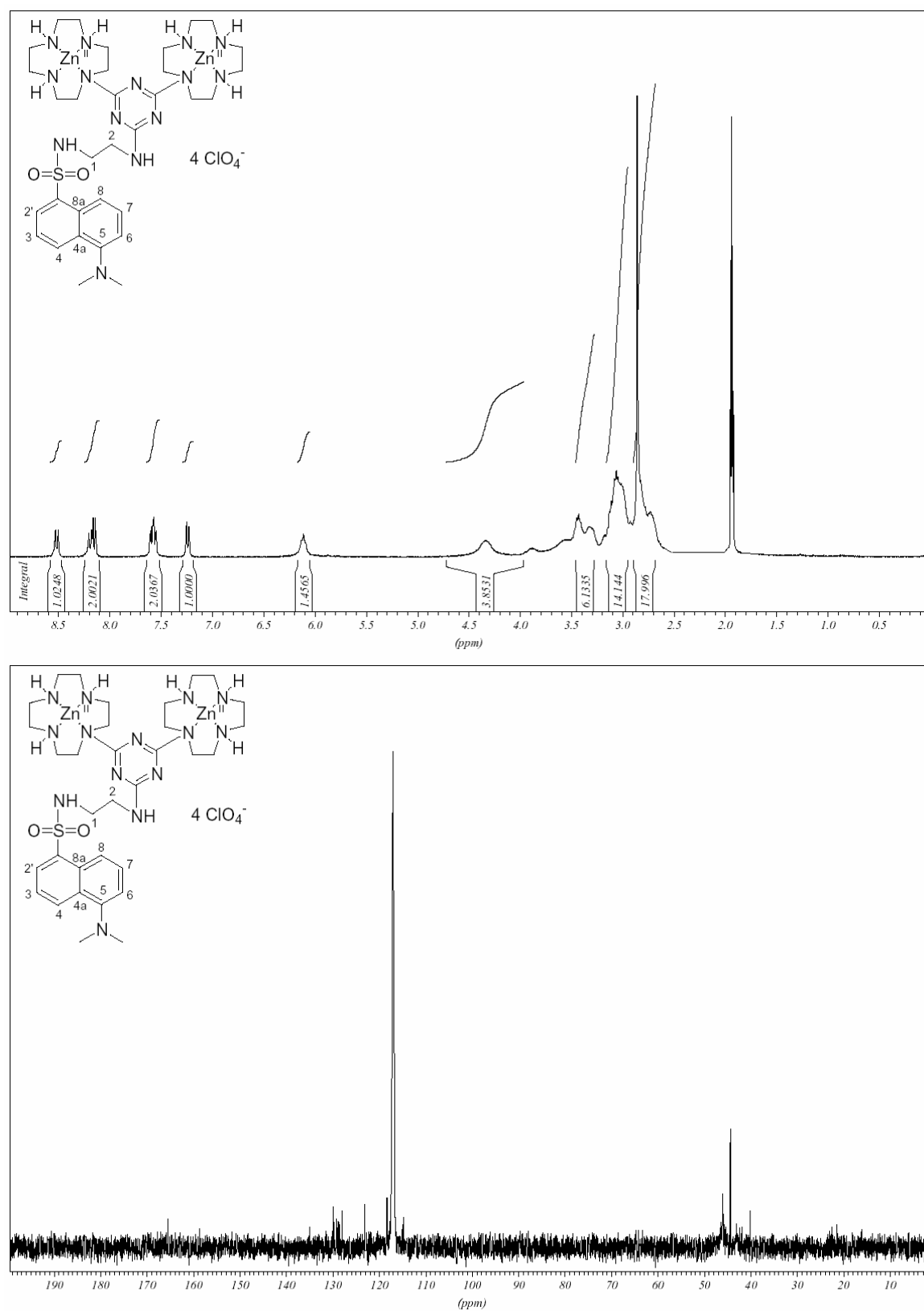


Figure S-1. ¹H-NMR and ¹³C-NMR spectra of Zn₂L3.

^{31}P -NMR spectra of the titrations of $\text{Zn}_2\text{L1}$ to PP_i

^{31}P -NMR spectra of the titration of $\text{Zn}_2\text{L1}$ to PP_i (20 mM).

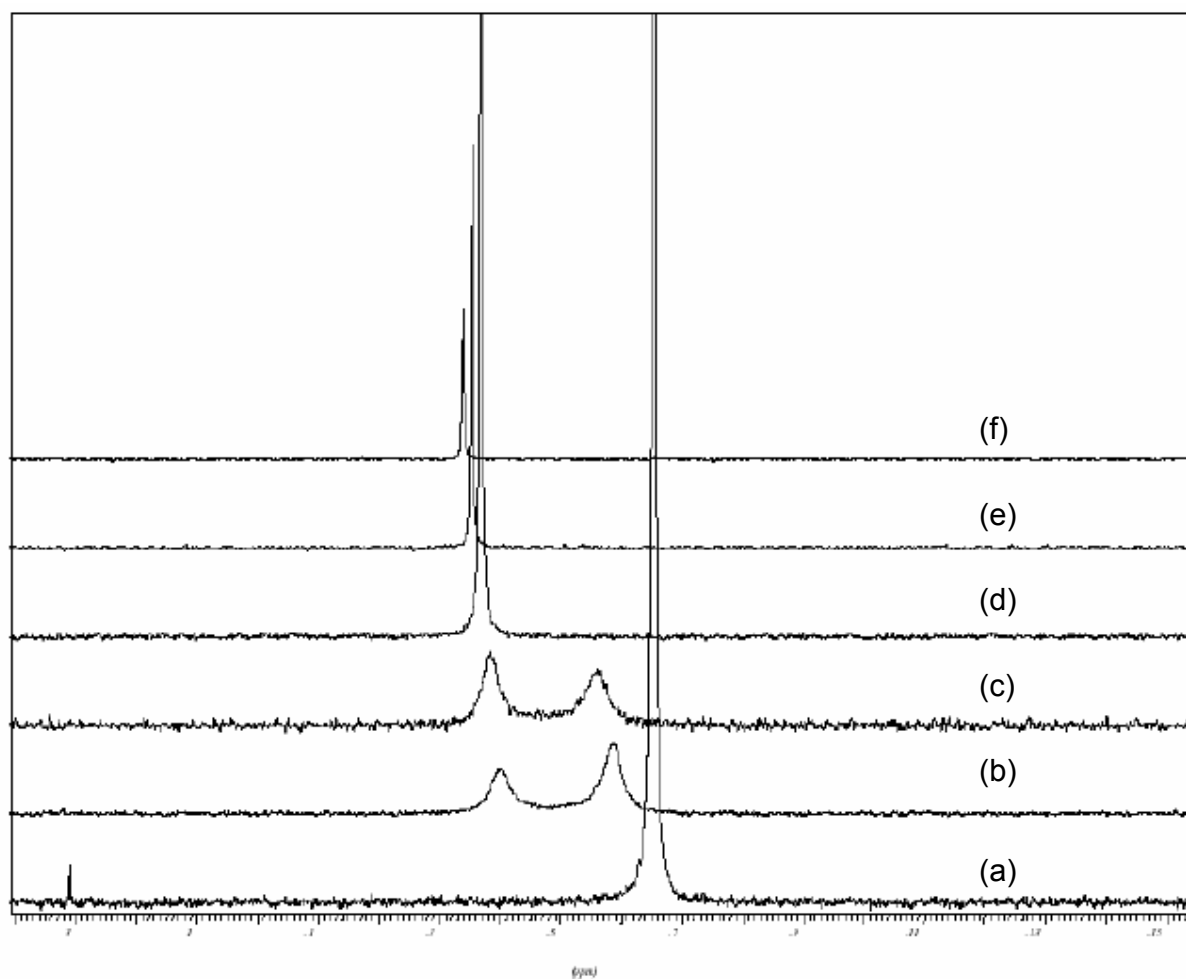


Figure S-2. Partial ^{31}P NMR spectra of the titration of aliquots of **$\text{Zn}_2\text{L1}$** solution (20 mM) to a 20 mM solution of PP_i (total volume 0.6 mL Tris buffer 56 mM, pH 7, 10% D_2O , 300 K). X -increment = -0.14 ppm. Total amount of equivalents of **$\text{Zn}_2\text{L1}$** present in solution: (a) 0 eq. (free pyrophosphate); (b) 0.2 eq.; (c) 0.5 eq.; (d) 1 eq.; (e) 2 eq.; (f) 5 eq.

³¹P-NMR low temperature measurement.

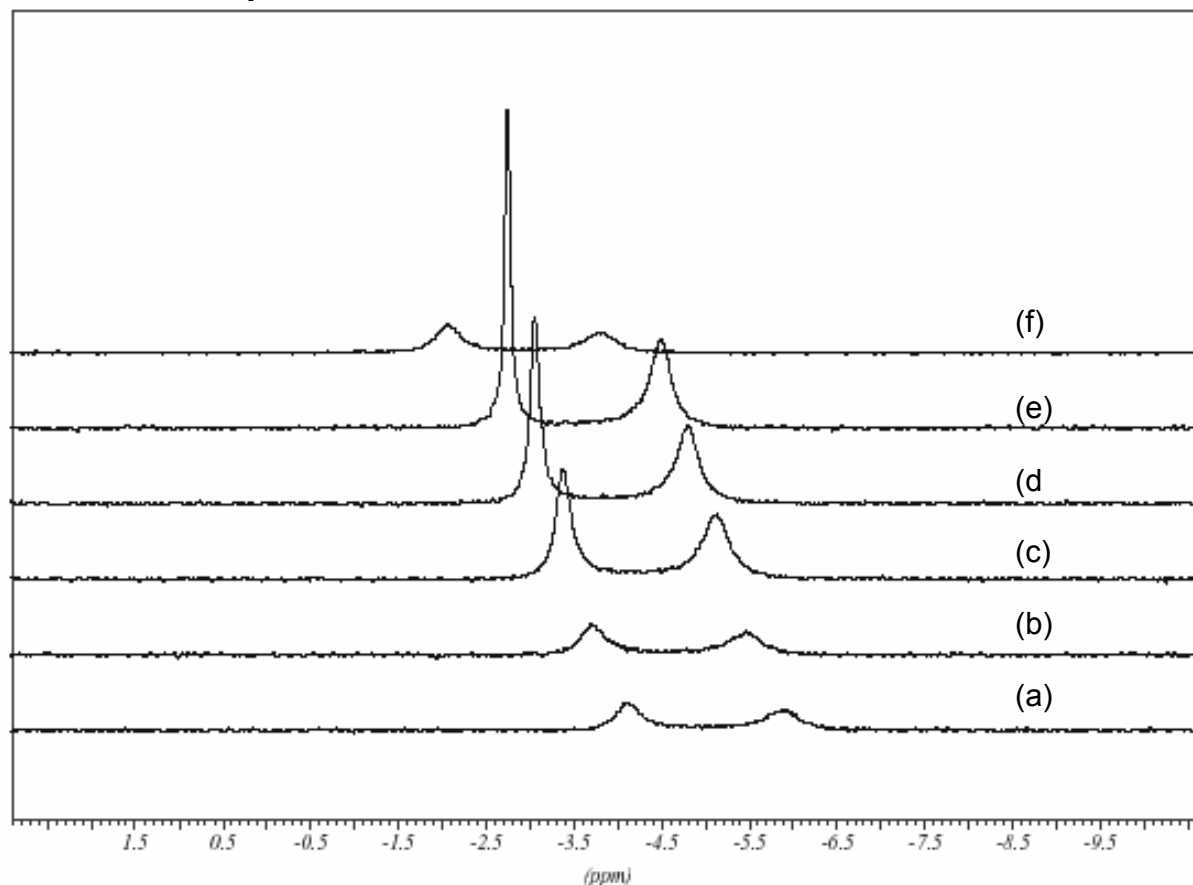


Figure S-3. Partial ³¹P NMR low temperature measurement of a sample with the ratio 1:1.5 **Zn₂L1** to PP_i (0.6 mL Tris buffer 56 mM, pH 7, 10% D₂O). *X*-increment = -0.41 ppm. (a) 300 K, 0h; (b) 300 K, after 24h; (c) 294 K, after 44h; (d) 288 K, after 45h; (e) 282 K, after 46h; (f) 300 K, after 47h.

Binding Studies by Isothermal Titration Calorimetry (ITC).

All ITC experiments were performed in buffered aqueous solution (Tris 56 mM, pH 7 or HEPES, 10 mM, pH 7.4) at 25 °C using an ultrasensitive VP-ITC calorimeter from MicroCal (Northampton, MA, U.S.A.). The titrant and sample solutions were prepared from the same stock buffer solution, and both solutions were thoroughly degassed under vigorous stirring before each titration. The reference cell contained Millipore water. During the ITC experiment the cell solution was stirred at 430 rpm by syringe to ensure rapid mixing and 60 x 5 μL of titrant were injected over 10 s with a spacing time between each injection of two minutes in order to allow complete equilibration. A background titration, consisting of the identical titrant solution, but only the buffer solution in the sample cell, was subtracted from each experimental titration to account for heat of dilution. Data analysis was performed with the Windows-based Origin software package supplied by MicroCal. The Origin software uses

a nonlinear least-squares algorithm (minimization of χ^2) and the concentrations of the titrant and the sample to fit the heat flow per injection to an equilibrium binding equation, providing best fit values of the stoichiometry (n), change in enthalpy (ΔH°), and binding constant (K). Using these values, the entropy change ΔS and, consequently, free energy change ΔG are determined.

ITC experiment of PP_i vs Zn₂L1.

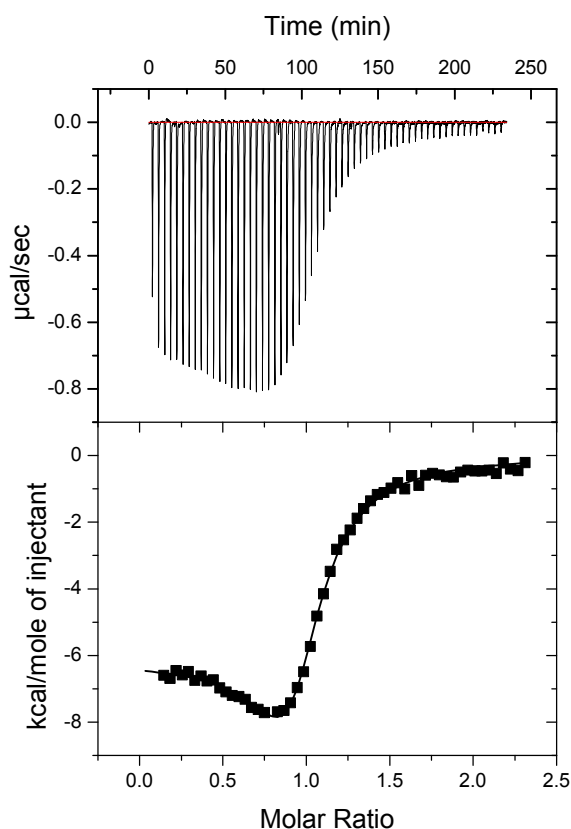


Figure S-4. ITC of Zn₂L1 (0.05 mM) with PP_i (0.52 mM) in buffer solution (Tris 56 mM, pH 7) at 25 °C.

ITC experiment of PV vs $\text{Zn}_2\text{L1}$.

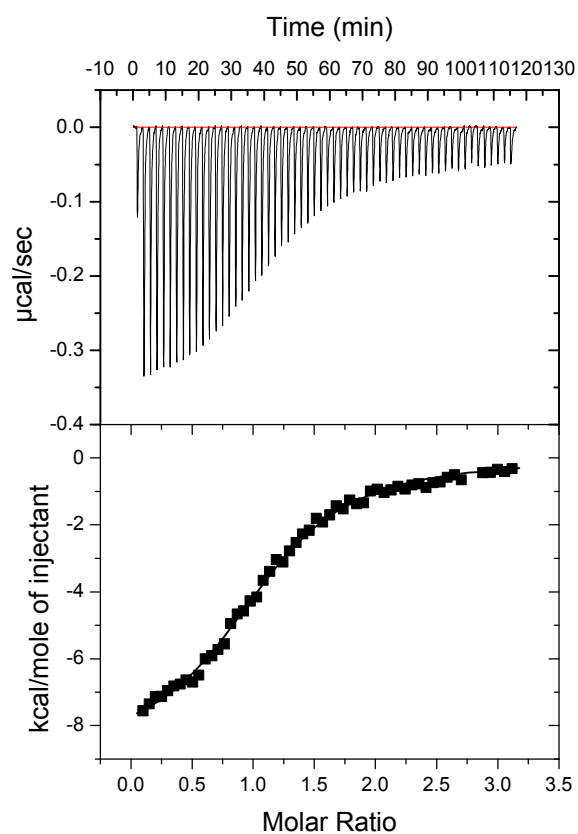


Figure S-5. ITC of $\text{Zn}_2\text{L1}$ (0.014 mM) with PV (0.2 mM) in Hepes (10 mM, pH 7.4) at 25°C.

ITC experiment of CMS vs Zn₂L1.

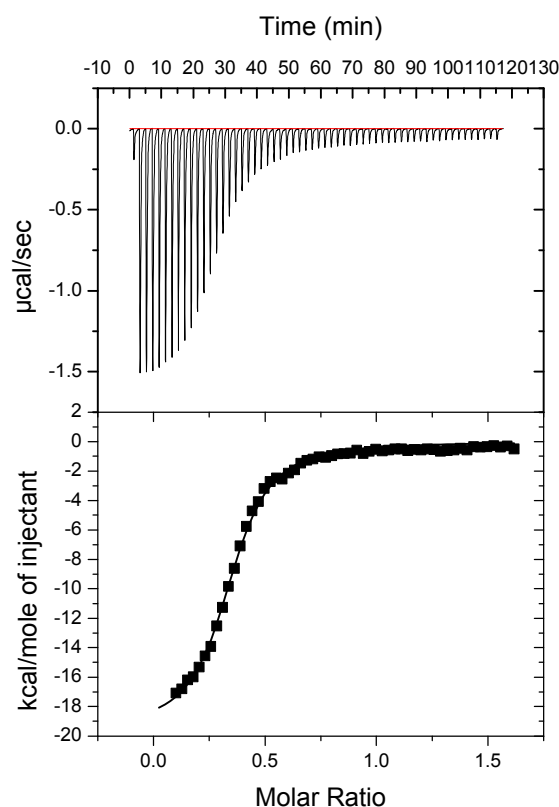


Figure S-6. ITC of **Zn₂L1** (0.4 mM) with **CMS** (0.055 mM) in Hepes (10 mM, pH 7.4) at 25°C.

	n	10⁻⁵ K	ΔH	ΔS	ΔG
		[M ⁻¹]	[cal mol ⁻¹]	[cal mol ⁻¹ K ⁻¹]	[cal mol ⁻¹]
Zn₂L1	2.83 ± 0.02	2.47 ± 0.15	-6901 ± 58.29	1.533	-7357.84

Table S-1. Binding stoichiometry *n*, thermodynamic parameters and association constant (*K*) for the interaction of **CMS** with **Zn₂L1** in aqueous solution (Hepes 10 mM, pH 7.4) at 25 °C.

Fluorescence and UV/Vis-spectra

UV/Vis spectra of a 1:1 mixture of $\text{Zn}_2\text{L1}$ and PV (50 μM) upon addition of various anions.

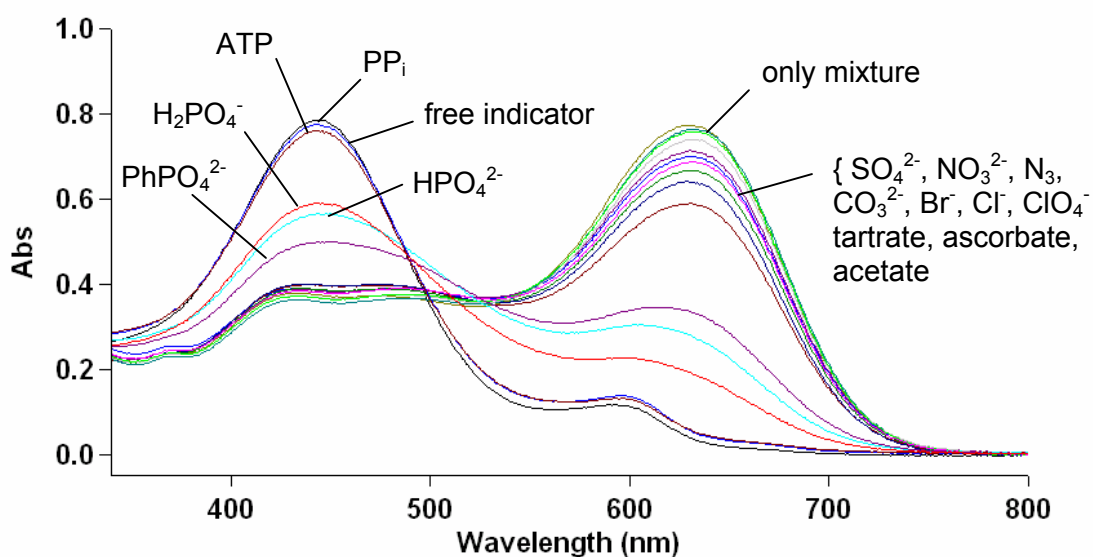


Figure S-7. UV/Vis absorption spectra of a 1:1 mixture $\text{Zn}_2\text{L1}$ and PV (50 μM , $\lambda_{\text{max}} = 636$ nm) in the presence of various anions (250 μM). Only phosphate anions are able to displace the indicator with $\lambda_{\text{max}} = 443$ nm. The displacement, and therefore the binding ability of $\text{Zn}_2\text{L1}$, is proportional to the number of negative charges on the phosphate.

UV/Vis spectra of a 1:1 mixture of $\text{Zn}_2\text{L1}$ and PV (35 μM) upon addition of PP_i .

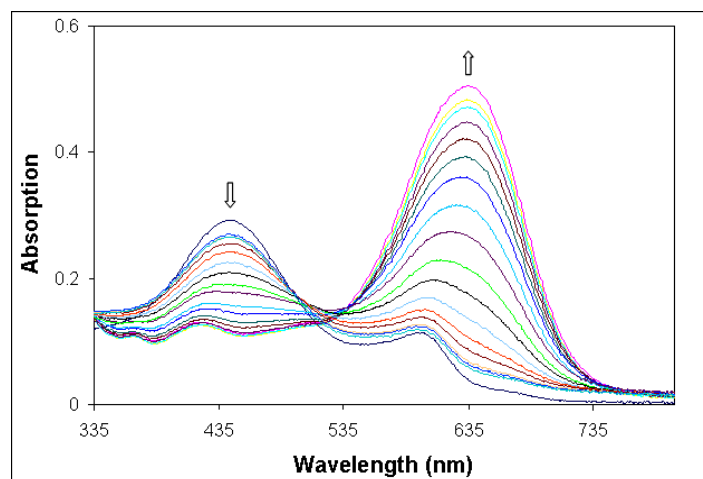


Figure S-8. Addition of PP_i (0-70 μM) to a solution containing both $\text{Zn}_2\text{L1}$ (35 μM) and PV (35 μM). Titrations were performed at 25 $^{\circ}\text{C}$ in 10 mM Hepes buffer, pH 7.4. The spectrum has been corrected for dilution.

Excitation spectra of L3 (80 μ M) and Zn₂L3 (80 μ M) at pH 7.4 and 13.5.

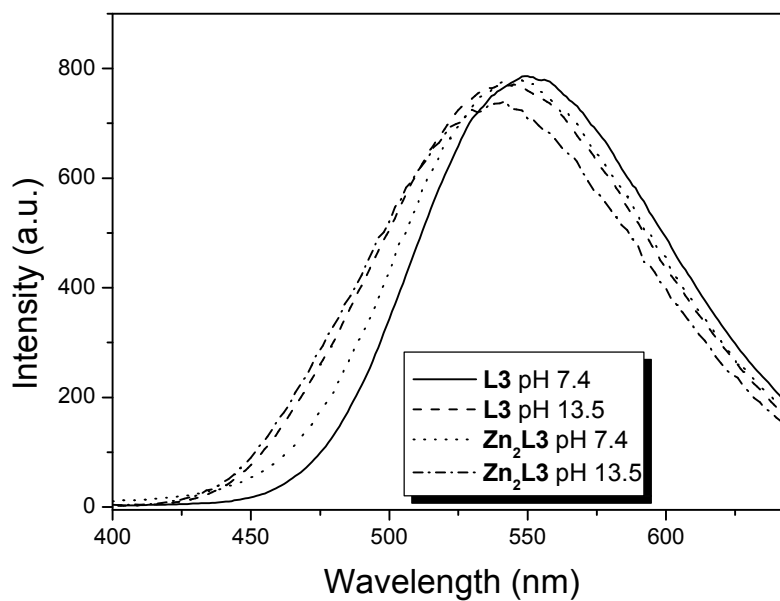


Figure S-9. Excitation spectra of **L3** (80 μ M) and **Zn₂L3** (80 μ M) at pH 7.4 (Hepes 10 mM) and 13.5 (aq. NaOH 1M) at 25 °C ($\lambda_{\text{exc}} = 330$ nm).

The characteristic emission wavelength of the two measured molecules and the intensity of the signal are resumed in **Table S-2**.

Molecule	pH 7.4	pH 13.5
L3	$\lambda_{\text{em}} = 550$ nm (789)	$\lambda_{\text{em}} = 547$ nm (777)
Zn₂L3	$\lambda_{\text{em}} = 548$ nm (779)	$\lambda_{\text{em}} = 542$ nm (740)

Table S-2. Excitation spectra of **L3** and **Zn₂L3** at pH 7.4 and 13.5.

UV/Vis-spectra of $\text{Zn}_2\text{L3}$ (80 μM) at pH 7.4 and 13.5.

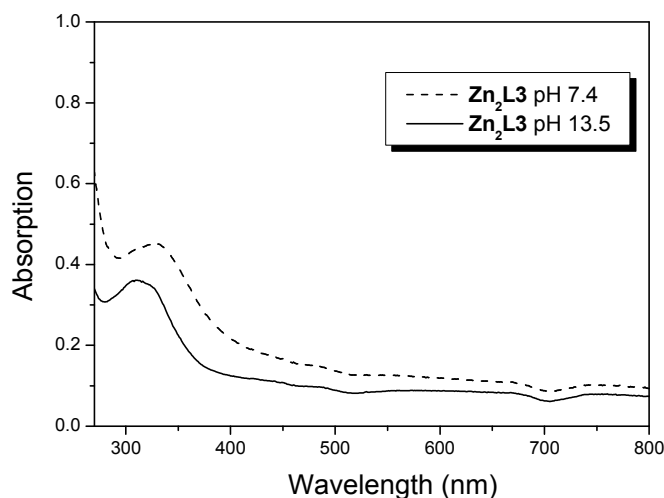


Figure S-10. UV/Vis-spectra of $\text{Zn}_2\text{L3}$ (80 μM) at pH 7.4 (Hepes 10 mM, $\lambda_{\text{max}} = 331$ nm) and pH 13.5 (aq. NaOH 1M, $\lambda_{\text{max}} = 313$ nm) at 25 $^{\circ}\text{C}$. As a comparison dansylamide was reported¹ at pH 7.3 as neutral molecule to show a band at $\lambda_{\text{max}} = 327$ nm and at pH 12.1, where it is present in its monoanionic form, a band at 316 nm.

UV/Vis spectra of $\text{Zn}_2\text{L3}$ and CMS (both 80 μM)

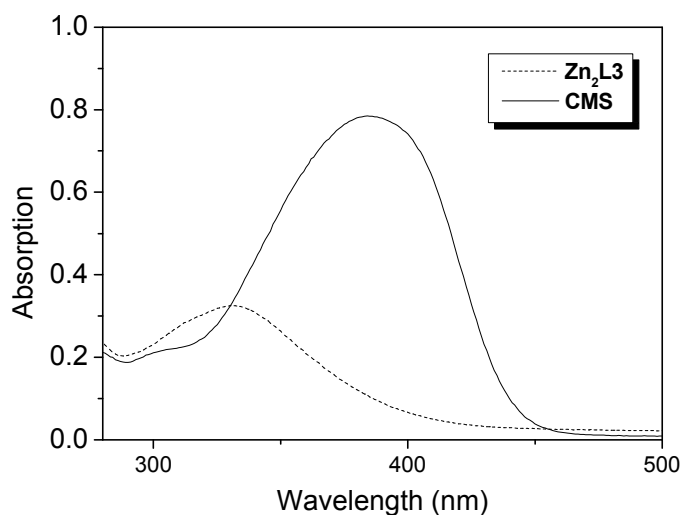


Figure S-11. UV/Vis spectra of $\text{Zn}_2\text{L3}$ (80 μM) with $\lambda_{\text{max}} = 331$ nm and CMS (80 μM) with $\lambda_{\text{max}} = 384$ nm (Hepes 10 mM, pH 7.4, 25 $^{\circ}\text{C}$).

¹ T. Koike, T. Watanabe, S. Aoki, E. Kimura, M. Shiro, *J. Am. Chem. Soc.* **1996**, *118*, 12696-12703.

Excitation spectra of CMS (80 mM) and Zn₂L3 (80 mM) for $\lambda_{\text{exc}} = 396 \text{ nm}$.

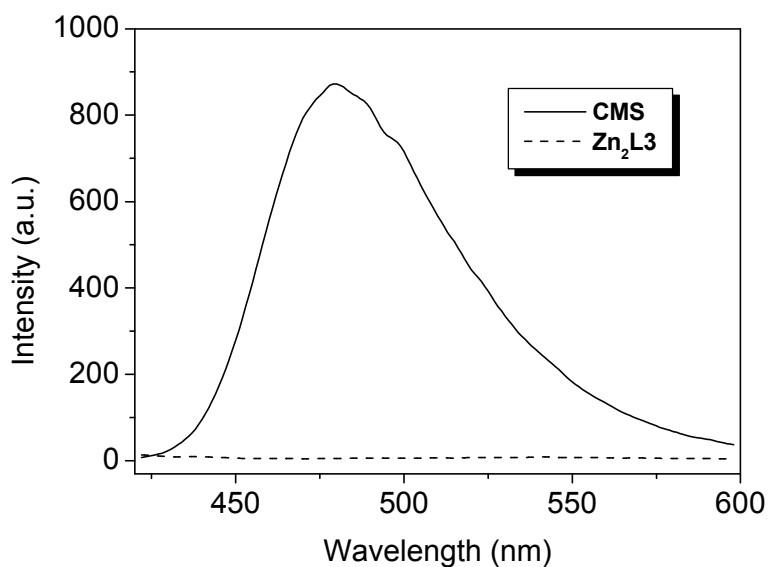


Figure S-12. Fluorescence emission spectra of **CMS** (80 μM , $\lambda_{\text{em}} = 480 \text{ nm}$) and **Zn₂L3** (80 μM) for $\lambda_{\text{exc}} = 396 \text{ nm}$. Titrations were performed in Hepes 10 mM, pH 7.4 at 25 °C.

Excitation spectra of CMS (80 μM) upon addition of Zn₂L3 (0-128 μM).

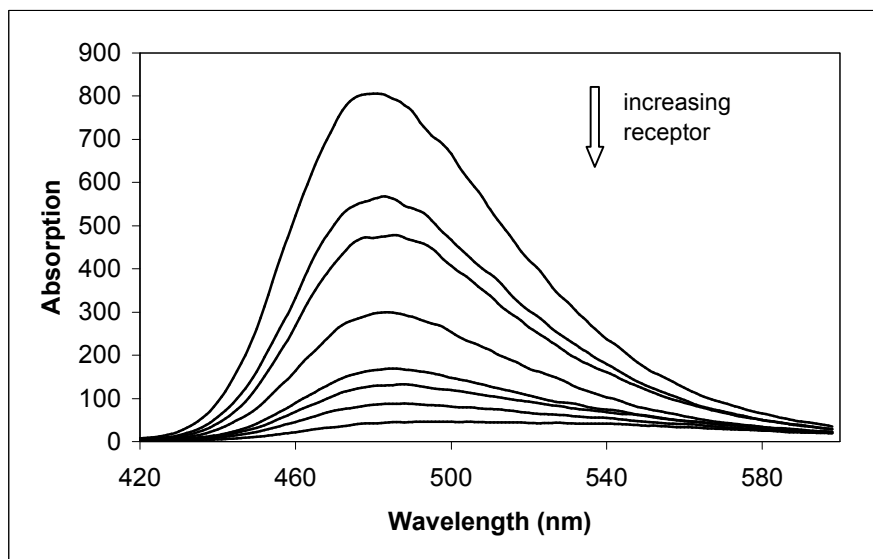


Figure S-13. Fluorescence emission spectra of **CMS** (80 μM) following the addition of increasing amounts of **Zn₂L3** (0-128 μM). Titrations were performed at 25 °C in 10 mM Hepes buffer, pH 7.4 ($\lambda_{\text{exc}} = 396 \text{ nm}$).

3.6. References

- ¹ J. J. R. Fraústo, Da Silva,; R. J. P. Williams, *The biological chemistry of elements*, Clarendon Press, Oxford, **1991**, Chapter 11.
- ² S.Aoki, E. Kimura, *Rev. Mol. Biol.* **2002**, *90*, 129-155 and references therein.
- ³ a) *The Biochemistry of Nucleic Acids*, 10th ed. (Eds.: R.L. P. Adams, J. T. Knower, D. P. Leader), Chapman and Hall, New York, **1986**; b) W. Saenger, *Principles of Nucleic Acid Structure*, Springer, New York, **1998**.
- ⁴ E. Takeda, Y. Taketani, N. Sawada, T. Sato, H. Yamamoto, *BioFactors* **2004**, *21*, 345-355.
- ⁵ W. N. Lipscomb, N. Straeter, *Chem. Rev.* **1996**, *96*, 2375-2433.
- ⁶ H. R. Horton, L. A. Moran, K. G. Scrimgeour, M. D. Perry, J. D. Rawn, *Principles of Biochemistry*, 4th ed., Pearson Prentice Hall, Upper Saddle River, NY, **2006**.
- ⁷ M. Soederberg, C. Edlund, K. Kristensson, G. Dallner, *Lipids* **1991**, *26*, 421-425.
- ⁸ a) Y.-C. Yang, *Acc. Chem. Res.* **1999**, *32*, 109-115; b) Y.-C. Yang, J. A. Baker, J. R. Ward, *Chem. Rev.* **1992**, *92*, 1729-1743.
- ⁹ For recent reports on membrane or solid state phosphate sensor devices. See: a) T. Kidosaki, S. Takase, Y. Shimizu, *Chem. Sens.* **2006**, *22*, 49 – 51; b) S. Suzuki, S. Takase, Y. Shimizu, *Chem. Sens.* **2006**, *22*, 46 – 48; c) X. Lin, X. Wu, Z. Xie, K.-Y. Wong, *Talanta* **2006**, *70*, 32 – 36; d) J. Wang, P. L. Bishop, *Environment. Technol.* **2005**, *26*, 381 – 388; e) review: J. D. R. Thomas, *Pure Appl. Chem.* **2001**, *73*, 31 - 38.
- ¹⁰ A. W. Czarnik, *Acc. Chem. Res.* **1994**, *27*, 302-308 and references therein.
- ¹¹ a) A. Ojida, Y. Mito-oka, M. Inoue, I. Hamachi, *J. Am. Chem. Soc.* **2002**, *124*, 6256-6258. b) The use of Dpa metal complexes for phosphate recognition goes back to the earlier report of Vahrenkamp et al. of the crystal structure of a phosphate - Zn(II)-Dpa complex of the composition [(Dpa-Zn)₃(tolyl-OPO₃)₂]HPO₄: F. Groß, A. Müller-Hartmann, H. Vahrenkamp, *Eur. J. Inorg. Chem.* **2000**, *12*, 2363.
- ¹² A. Ojida, S.-K. Park, Y. Mito-oka, I. Hamachi, *Tetrahedron Lett.* **2002**, *43*, 6193-6195.
- ¹³ J. Wongkongkatap, Y. Miyahara, A. Ojida, I. Hamachi, *Angew. Chem. Int. Ed.* **2006**, *45*, 665-668.
- ¹⁴ A. Ojida, H. Nonaka, Y. Miyahara, S.-I. Tamaru, K. Sada, I. Hamachi, *Angew. Chem. Int. Ed.* **2006**, *45*, 5518 – 5521.
- ¹⁵ T. Anai, E. Nakata, Y. Koshi, A. Ojida, I. Hamachi, *J. Am. Chem. Soc.* **2007**, *129*, 6232-6239.
- ¹⁶ D. H. Lee, J. H. Im, S. U. Son, Y. K. Chung, J. I. Hong, *J. Am. Chem. Soc.* **2003**, *125*, 7752-7753.
- ¹⁷ D. H. Lee, S. Y. Kim, J. I. Hong, *Angew. Chem. Int. Ed.* **2004**, *43*, 4777-4780.
- ¹⁸ C. Lakshmi, R. G. Hanshaw, B. D. Smith, *Tetrahedron*, **2004**, *60*, 11307-11315.

- ¹⁹ a) W. M. Leevy, J. R. Johnson, C. Lakshmi, J. Morris, M. Marquez, B. D. Smith, *Chem. Commun.* **2006**, 1595-1597; b) W. M. Leevy, S. T. Gammon, H. Jiang, J. R. Johnson, D. J. Maxwell, E. N. Jackson, M. Marquez, D. Piwnica-Worms, B. D. Smith, *J. Am. Chem. Soc.* **2006**, *128*, 16476-16477.
- ²⁰ D. A. Jose, S. Mishra, A. Ghosh, A. Shrivastav, S. K. Mishra, A. Das, *Org. Lett.* **2007**, *9*, 1979-1982.
- ²¹ S. Mizukami, T. Nagano, Y. Urano, A. Odani, K. Kikuchi, *J. Am. Chem. Soc.* **2002**, *124*, 3920-3925.
- ²² S. Aoki, M. Zulkefeli, M. Shiro, M. Kohsako, K. Takeda, E. Kimura, *J. Am. Chem. Soc.* **2005**, *127*, 9129-9139.
- ²³ For a recent review on indicator displacement measurements for detection of inorganic anions and various biomolecules, see: S. L. Wiskur, H. Ait-Haddou, J. J. Lavigne, E. V. Anslyn, *Acc. Chem. Res.* **2001**, *34*, 963-972.
- ²⁴ K. Niikura, A. Metzger, E. V. Anslyn, *J. Am. Chem. Soc.* **1998**, *120*, 8533-8534.
- ²⁵ a) S. L. Tobey, E. V. Anslyn, *Org. Lett.* **2003**, *5*, 2029-2031; b) T. Zhang, E. V. Anslyn, *Tetrahedron* **2004**, *60*, 11117-11124.
- ²⁶ L. Fabrizzi, N. Marcotte, F. Stomeo, A. Taglietti, *Angew. Chem. Int. Ed.* **2002**, *41*, 3811-3814.
- ²⁷ M.S. Han, D. H. Kim, *Angew. Chem. Int. Ed.* **2002**, *41*, 3809-3811.
- ²⁸ M.S. Han, D.H. Kim, *Bioorg. Med. Chem. Lett.* **2003**, *13*, 1079-1082.
- ²⁹ R.G. Hanshaw, S.M. Hilkert, H. Jiang, B.D. Smith, *Tetrahedron Lett.* **2004**, *45*, 8721-8724.
- ³⁰ R.G. Hanshaw, E. J. O'Neil, M. Foley, R.T. Carpenter, B. D. Smith, *J. Mater. Chem.* **2005**, *15*, 2707-2713.
- ³¹ M. McDonough, A. Reynolds, W. Y. G. Lee, K. A. Jolliffe, *Chem. Commun.* **2006**, *28*, 2971 - 2973.
- ³² B. P. Morgan, S. He, R. C. Smith, *Inorg. Chem.* **2007**, *46*, 9262-9266.
- ³³ L. Zhu, Z. Zhong, E.V. Anslyn, *J. Am. Chem. Soc.* **2005**, *127*, 4260-4269.
- ³⁴ a) E. Kimura, T. Shiota, T. Koike, M. Shiro, *J. Am. Chem. Soc.* **1990**, *112*, 5805-5811; b) T. Koike, S. Kajitani, I. Nakamura, E. Kimura, M. Shiro, *J. Am. Chem. Soc.* **1995**, *117*, 1210-1219.
- ³⁵ a) E. Kimura, S. Aoki, T. Koike, M. Shiro, *J. Am. Chem. Soc.* **1997**, *119*, 3068-3076. b) S. Aoki, E. Kimura, *Rev. Mol. Biotechnol.* **2002**, *90*, 129-155 and references therein.
- ³⁶ M. Subat, K. Woinaroschy, S. Anthofer, B. Malterer, B. Koenig, *Inorg. Chem.* **2007**, *46*, 4336-4356.
- ³⁷ D. S. Turygin, M. Subat, O. A. Raitman, V. V. Arslanov, B. König, M. A. Kalinina, *Angew. Chem. Int. Ed.* **2006**, *45*, 5340-5344.
- ³⁸ E. L. Doyle, C. A. Hunter, H. C. Phillips, S. J. Webb, N. H. Williams, *J. Am. Chem. Soc.* **2003**, *125*, 4593-4599.

-
- ³⁹ a) T. Koike, T. Watanabe, S. Aoki, E. Kimura, M. Shiro, *J. Am. Chem. Soc.* **1996**, *118*, 12696-12703; b) Kimura, E.; Aoki, S.; Kikuta, E.; Koike, T. *Proc. Nat. Acad. Of Science*, **2003**, *100*, 3731-3736; c) T. Koike, E. Kimura, I. Nakamura, Y. Hashimoto, M. Shiro, *J. Am. Chem. Soc.* **1992**, *114*, 7338-7345.
- ⁴⁰ R. P. Haugland, *Invitrogen Handbook - A guide to fluorescent probes and labelling technologies*, **2005**.
- ⁴¹ C. Bazzicalupi, A. Bencini, A. Bianchi, A. Danesi, C. Giorgi, C. Lodeiro, F. Pina, S. Santarelli, B. Valtancoli, *Chem. Commun.* **2005**, 2630-2632.
- ⁴² I. Jelesarov, H. R. Bosshard, *J. Mol. Recognit.* **1999**, *12*, 3-18.
- ⁴³ A. K. H. Hirsch, F. R. Fischer, F. Diederich, *Angew. Chem. Int. Ed.* **2007**, *46*, 338-352.
- ⁴⁴ H. Ait-Haddou, S. L. Wiskur, V. M. Lynch, E. V. Anslyn, *J. Am. Chem. Soc.* **2001**, *123*, 11296-11297.
- ⁴⁵ C. Li, M. Numata, M. Takeuchi, S. Shinkai, *Angew. Chem. Int. Ed.* **2005**, *44*, 6371-6374.
- ⁴⁶ P. Gans, A. Sabatini, A. Vacca, *Talanta* **1996**, *43*, 1739.
- ⁴⁷ K. A. Connors, *Binding Constants, the Measurement of Molecular Complex Stability*, John Wiley & Sons, New York, **1987**.

4. Synthesis and characterization of 1-(2H-Tetrazol-5-yl)-1,4,7,10-tetraaza-cyclododecane and its Zn(II), Ni(II) and Cu(II) complexes¹

Abstract

As part of an ongoing effort to develop new metal complexes of tetraazamacrocycles with novel properties in coordination or functionalization we report here the synthesis of a new derivative of 1,4,7,10-tetraazacyclododecane (cyclen) with a tetraazole moiety directly bound to the azamacrocycle. The new ligand was obtained by reaction with cyanogen bromide giving the cyanamide, followed by a [2+3] cycloaddition with NaN₃ to yield the tetraazole. The ligand and its Zn(II), Ni(II) and Cu(II) complexes were fully characterised by analytical methods. X-ray structure analysis of the Ni(II) compound shows the formation of a stable dimer by coordination of each of the two tetraazole substituents to the neighboring metal cation. Potentiometric titrations of the metal complexes indicate a possible conversion of the monomer to the dimeric structure in solution and show the pK_a of the NH-atom on the tetraazole substituent to be between 4.03 and 5.3 depending on the metal ion coordinated by cyclen.

4.1 Introduction

Polyamine macrocyclic compounds have attracted great interest in host-guest and supramolecular chemistry due to their intriguing structural and spectroscopic properties.¹ One of their most remarkable properties is their ability to adapt to many metal ion coordination geometries,² offering multiple donor sites and being therefore often used as model systems for metalloenzymes or sensors.³ In addition, tetradentate macrocyclic compounds such as tetraazamacrocycles can be easily functionalized⁴ on their secondary nitrogen atoms yielding novel properties in coordination, electro- or photo chemistry, and catalysis. Tetraazoles, on the other hand are interesting heterocycles⁵ with uses in coordination chemistry as ligands, in medicinal chemistry as metabolically stable surrogates for carboxylic acid groups,⁶ in pharmaceutical sciences as lipophilic spacers and in various material science applications, including explosives. They are also used as precursors to a variety of nitrogen-containing heterocycles.

¹ The results of this chapter are submitted for publication:

Woinaroschy, K.; Ursu, A.; Koenig B. *Heterocycles* **2007**, submitted.

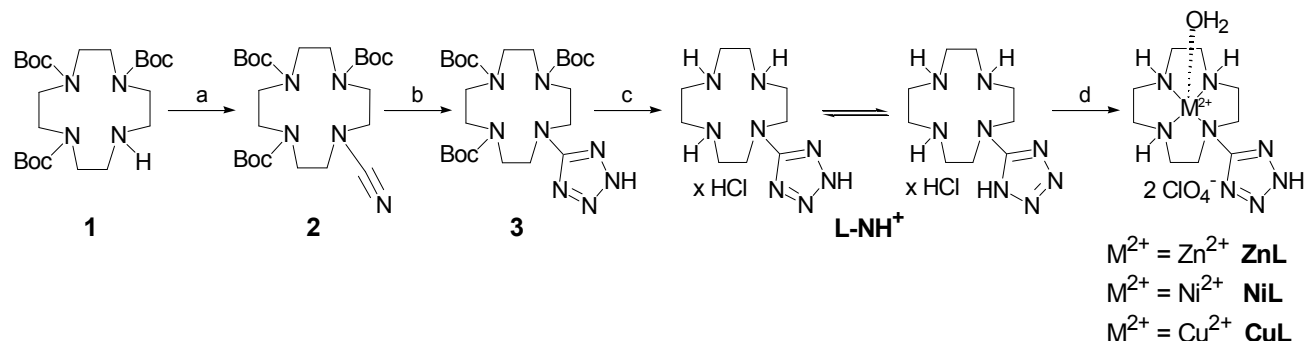
As part of an ongoing effort to develop new metal complexes of tetraazamacrocycles with novel properties in coordination or functionalization we report here the synthesis of a new derivative of 1,4,7,10-tetraazacyclododecane (cyclen) with the tetraazole moiety directly bound to the azamacrocycle. This is, to the best of our knowledge, the first application of the [2+3] cycloaddition procedure reported by Demko and Sharpless⁷ for an azamacrocyclic compound. The ligand and its Zn(II), Ni(II) and Cu(II) complexes were obtained by solution synthesis and not by solvothermal techniques, as frequently reported for tetrazol transition metal complexes, and they were fully analytically characterised. X-ray structure analysis of the Ni(II) compound shows the formation of a stable dimer by coordination of each of the two tetraazole substituents to the neighboring metal cation.

4.2 Results and Discussion

4.2.1 Syntheses of the macrocyclic tetraazole ligand and its metal complexes ZnL, CuL and NiL.

The synthesis of the novel ligand, containing the azamacrocyclic moiety bound to a tetraazole unit, starts from the previously reported compound 1,4,7,10-tetraaza-cyclododecane-1,4,7-tricarboxylic acid tri-tert-butyl ester (shortly 3-Boc-cyclen) **1**⁸, which was reacted in THF at reflux with cyanogen bromide following a modified literature procedure⁹ to yield monosubstitution product **2** (**Scheme 1**). The reaction does not lead to the expected di(3-Boc-cyclen)methanimine, a precursor of polysubstituted guanidine products, as in previous reports.⁹ This could be due to the fact that the electrophilicity of the cyanamide is significantly decreased after reaction with the first cyclen moiety, but also to the lower nucleophilicity of the cyclen. A reaction of **2** with an excess amount of **1** under various reaction conditions did not lead to any new products and showed that **2** is thermally labile as it decomposed completely after 5 hours of reflux. Further addition reactions of *n*-BuNH₂ and Et₂NH to the cyanamide **2** to obtain the guanidinium functionality failed. It has been reported that additions of amines to cyanamides require harsh reaction conditions¹⁰, but even the use of high temperatures (130 °C), higher pressures (sealed tubes) or fluorinated alcohols, such as trifluoroethanol, as solvents (their polarity should facilitate the addition while their lack of nucleophilicity should retard the formation of the *O*-fluoroalkyl isoureas) did not give the desired guanidines. A [2+3] cycloaddition reaction of **2** with NaN₃ following the procedure reported by Demko and Sharpless⁷ yielded **3**. The compound was treated with diethyl ether saturated with HCl to remove all Boc protecting groups to give ligand **L-NH⁺** in form of the ammonium chloride salt (**Scheme 1**). Other deprotecting methods, such as treatment with

TFA, led to a mixture of the desired product with various unidentified decomposition product. The ligand could not be neutralised to the free base form **L-NH** by passing it through a basic ion exchange resin column due to its decomposition on the basic resin and was therefore neutralised *in situ* in the next reaction step.



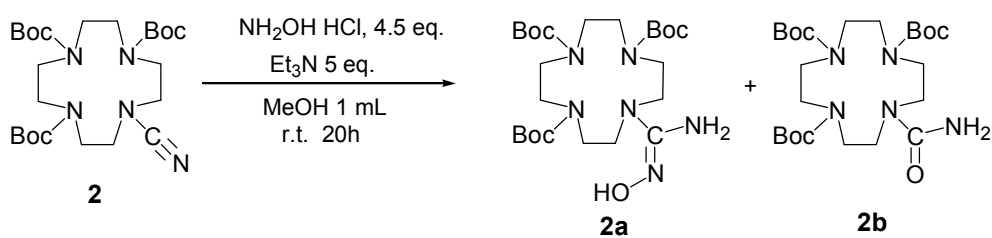
a: BrCN (0.52 eq.), K₂CO₃, THF, reflux 3h, 82% ; **b:** NaN₃ (1.1 eq.), ZnBr₂, H₂O/MeOH 2:1, reflux 20h, 72% ; **c:** Et₂O/HCl, MeOH, RT, 24h, 99% ; **d:** M(ClO₄)₂ · 6H₂O (M = Zn, Ni, Cu) (1.1 eq.), aq. LiOH (pH = 8-9), reflux 4h, quantitative yield.

Scheme 1. Synthesis of **L-NH⁺** and its corresponding metal complexes.

Metal complexes were isolated with good yields from the reaction of the ligand with metal perchlorate salts in aqueous solutions and were characterized by different analytical (¹H NMR and ¹³C NMR for **ZnL**, UV/Vis, IR, ESI, elemental analysis, HRMS) to show a stoichiometry of 1:1 metal cation/ligand.¹¹

We tried to apply the procedure for the [2+3] cycloaddition reaction of **2** to benzylazide (obtained from benzylbromide following the reported procedure),¹² but no conversion was observed. Use of previously reported other reaction conditions¹³ also failed. It has already been shown that nitriles are not sufficient dipolarophiles to react with organic azides in a cycloaddition reaction.¹⁴ At present, only a few highly electron-deficient nitriles are known to undergo this reaction.¹⁵ Shapless *et al.* have reported the [2+3] cycloaddition of aromatic azides to sulfonyl¹⁴ and acyl cyanides.¹⁶ As can be observed from all these reports, the reaction is favoured by strong electron-withdrawing substituents on the nitrile, while in our case the azamacrocyclic substituent acts as an electron donating group. The large substituent may additionally impose steric hindrance on the reaction.

In our attempt to gain new cyclen derivatives by functionalization of **2**, we would also like to report here the synthesis of the hydroxyguanidine **2a** and the thermodynamically more stable compound, the amide **2b**, obtained by following a literature procedure (**Scheme 2**).¹⁷



Scheme 2. Synthesis of the new cyclen derivatives **2a** and **2b**.

4.2.2 X-ray Crystal Structure of the dimer $[\text{Ni}_2(\text{LH}_1)_2(\text{H}_2\text{O})_2](\text{ClO}_4)_2$.

The heteroaromatic spacer is directly connected to the macrocycle, without any pendant arm, leading to a rather rigid structure. The pure **NiL** obtained by recrystallization from EtOH as a pale violet solid was dissolved in a small amount of water and was left at room temperature. After two weeks pale violet crystals were collected. **Figure 1** shows an ORTEP drawing of the complex with 50% probability thermal ellipsoids.

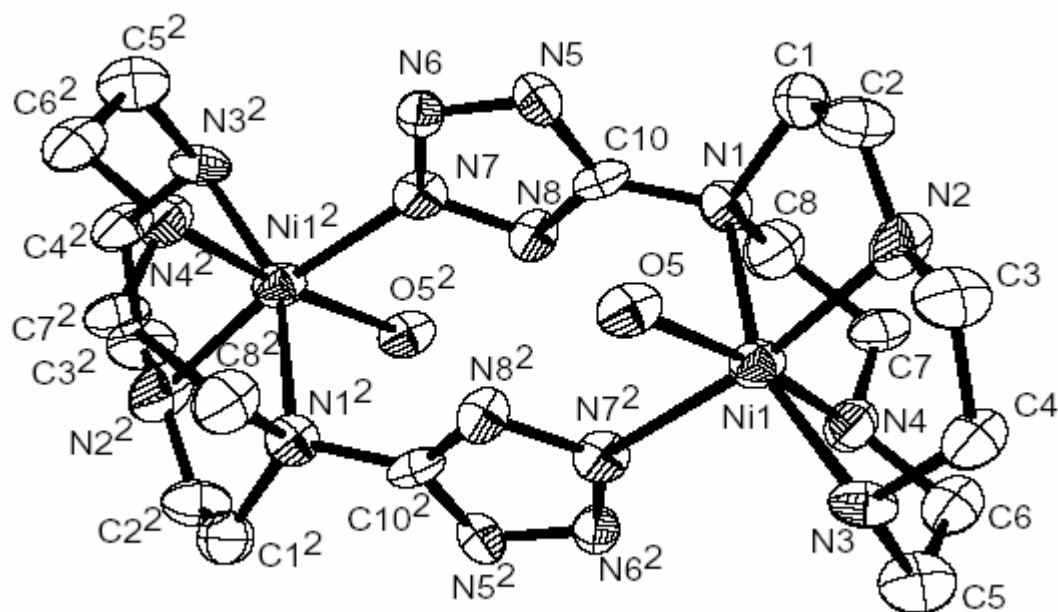


Figure 1. ORTEP drawing (50% probability ellipsoids) of $[\text{Ni}_2(\text{LH}_1)_2(\text{H}_2\text{O})_2](\text{ClO}_4)_2$. All hydrogen atoms and two perchlorate anions are omitted for clarity.

Selected bond lengths and bond angles around the Ni(II) ions are presented in **Table 1**. Crystal data and data collection parameters, atomic positional parameters with standard deviations, bond lengths and bond angles are available upon request.

Bond distances, Å			
Ni(1)-O(5)	2.153	Ni(1)-N(4)	2.050
Ni(1)-N(1)	2.271	Ni(1)-N(7 ²)	2.051
Ni(1)-N(2)	2.060	N(1)-C(10)	1.409
Ni(1)-N(3)	2.100	C(10)-N(5)	1.354
Bond angles, deg			
O(5)-Ni(1)-N(1)	99.18	N(1)-Ni(1)-N(2)	80.24
O(5)-Ni(1)-N(2)	90.57	N(1)-Ni(1)-N(3)	157.55
O(5)-Ni(1)-N(3)	96.66	N(1)-Ni(1)-N(4)	81.91
O(5)-Ni(1)-N(4)	172.74	N(2)-Ni(1)-N(3)	83.81
O(5)-Ni(1)-N(7 ²)	82.63	N(2)-Ni(1)-N(4)	96.69
N(7 ²)-Ni(1)-N(1)	95.18	N(3)-Ni(1)-N(4)	84.38
N(7 ²)-Ni(1)-N(3)	102.57	Ni(1)-N(1)-C(10)	110.98
N(7 ²)-Ni(1)-N(4)	90.13	Ni(1)-N(7 ²)-N(8 ²)	119.96
N(1)-C(10)-N(5)	123.35	N(1)-C(10)-N(8)	122.58
Distances Ni(1)-Ni(1 ²), O(5)-O(5 ²), N(7)-C(10 ²), O(5)-C(10)			
Ni(1)-Ni(1 ²)	6.087	N(7)-C(10 ²)	3.225
O(5)-O(5 ²)	6.525	N(8)-N(8 ²)	2.925
O(5)-C(10)	3.476	N(8)-N(5 ²)	3.552
N(7)-O(5 ²)	2.777	N(8)-O(5 ²)	2.752

Table 1. Bond distances, bond angles and atomic distances for [Ni₂(LH₁)₂(H₂O)₂](ClO₄)₂.

Figure 1 shows the symmetrical structure and geometry of the Ni(II) complex. **NiL** forms a dimer by coordination of the tetraazole substituent to the neighboring metal cation. The coordination takes place through the N2-position on the tetraazole and not N1, minimizing steric constraints.¹⁸

Each Ni(II) ion has a distorted octahedral coordination geometry as previously reported for the Ni([12]aneN₄)²⁺ complex,¹⁹ with the macrocycle coordinated in a folded configuration to four sites around the central nickel atom (one of which is axial), the other two sites being occupied by a water molecule in an axial position and one deprotonated N-atom of the tetraazole.

The distances between the Ni atom and the N atoms of cyclen lie in the range 2.05-2.1 Å, as it is generally reported for Ni-N distances found in octahedral polyamine complexes.^{19,20} The longer distance to N(1) is explained by the influence of the tetraazole, which withdraws as an electron-poor aromatic system electron density of cyclen nitrogen atom thus making the coordination to the metal ion weaker. The tetraazole could also induce a steric constrain as reflected by the short bond length N(1)-C(10). The short distance between the nickel atom and the tetraazole N-atom, comparable to the distance Ni(1)-N(2) and Ni(1)-N(4) indicates a strong interaction and the formation of a stable compound. The two tetraazole bridges are in parallel planes separated by approx. 3 Å, indicating stabilization of the complex by an intramolecular p-p stacking interaction. The tetraazole rings are perfectly planar, with almost equal bond lengths in the range 1.318-1.37 Å. There is practical no difference between the C-N and N-N bond length, which indicates strong p-electron delocalization in the tetraazole ring. The angles between the adjacent atoms in the ring lie in the range 103.18-113.83°, close to that expected for a regular pentagon, 108°. All the data of the tetraazoles coincide to previous reports.²¹ The two metal ions are separated by 6 Å, therefore the electrostatic interaction between them is weak.

4.2.3 Deprotonation Constants (pK_a) of the metal complexes.

The pK_a values of **ZnL**, **NiL** and tetraazole (Fluka, contains ~10 % H₂O) were determined by pH-metric titrations in aqueous solutions under nitrogen at 25 °C and $I = 0.1$ (tetraethylammonium chloride TEACl). Various small amounts of HClO₄ 0.1 M (0.2 - 1.2 mL) were added to the titration solution in order to determine values in the pH range of 3 to 8. No pK_a value could be determined for **CuL** in the pH range 3-11. For each metal complex at least two independent titrations were performed. The pH profiles of **ZnL**, **NiL** and of the simple tetraazole (Fluka, contains ~10 % H₂O) are given in the **Figures 2-4**. The pK_a values are summarized in **Table 2**.

Metal complex	pK_a		
	pK_{a1}	pK_{a2}	pK_{a3}
ZnL	4.54 ± 0.02	5.32 ± 0.02	8.74 ± 0.02
NiL	4.03 ± 0.02	4.9 ± 0.02	-
TA	4.88 ± 0.02	-	-

Table 2. Deprotonation constants (pK_a) of the metal complexes at 25 °C and $I = 0.10$ (TEAP).

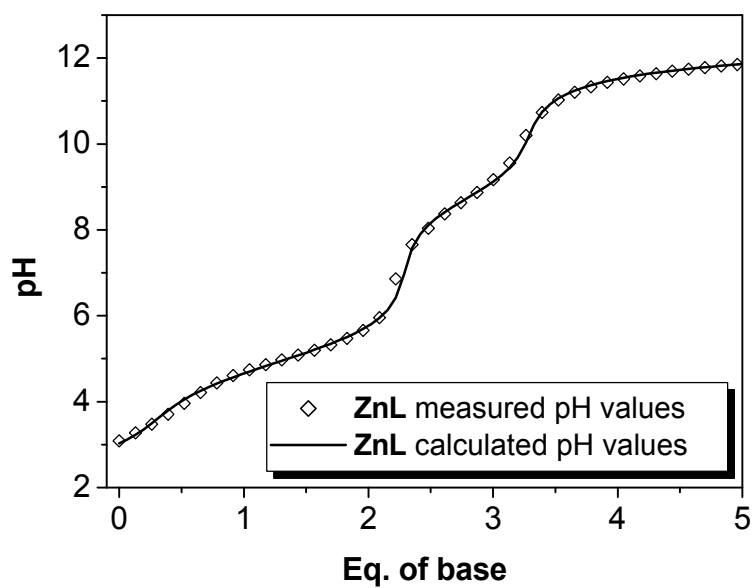


Figure 2. Titration curve for the complex $[\text{ZnL}](\text{ClO}_4)_2$ in aqueous solution (2 eq. HClO_4)

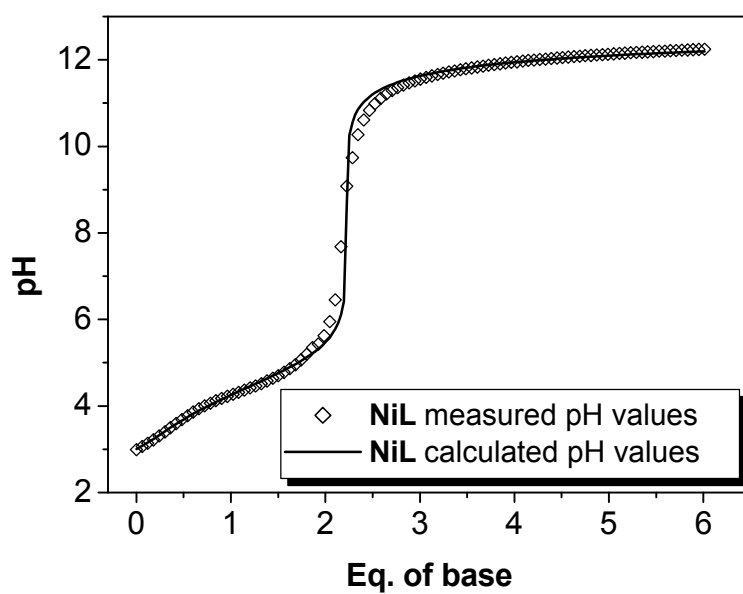


Figure 3. Titration curve for the complex $[\text{NiL}](\text{ClO}_4)_2$ in aqueous solution (2 eq. HClO_4)

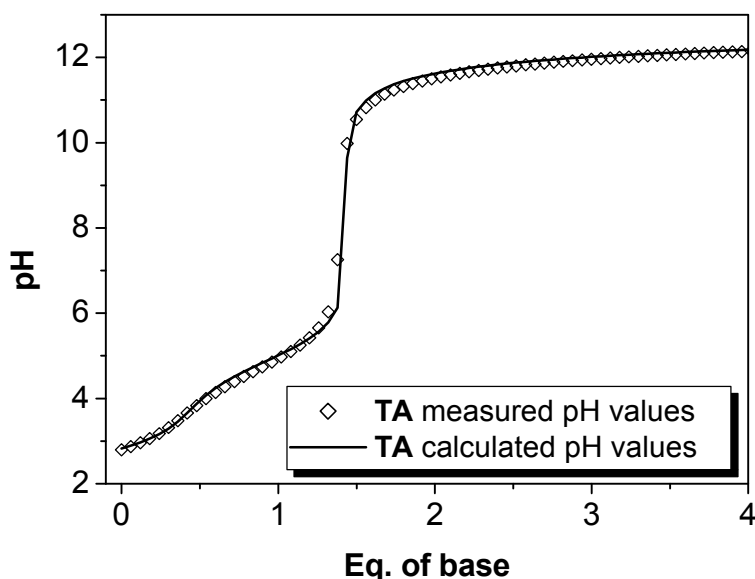
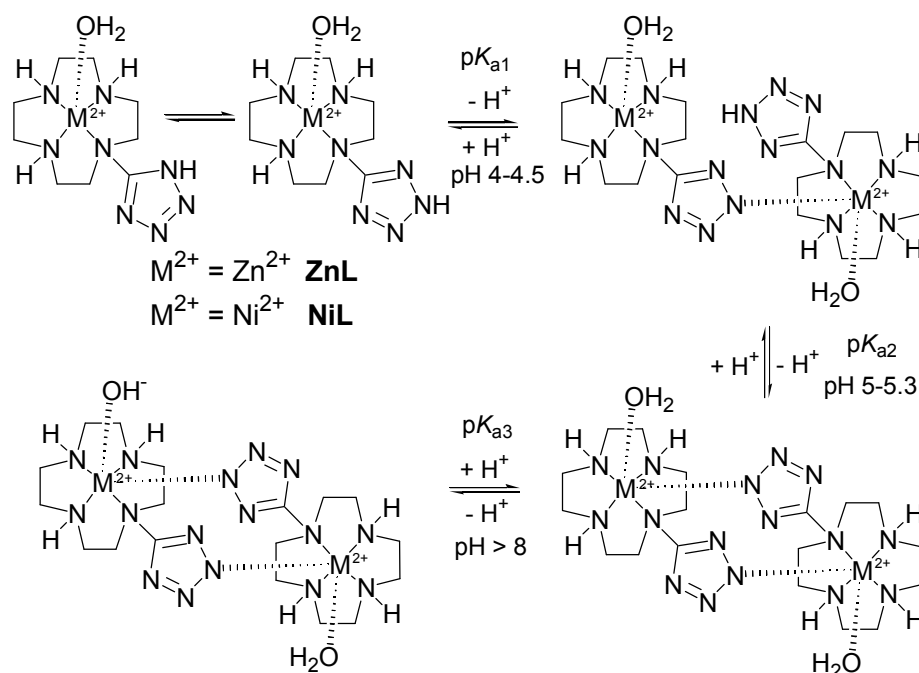


Figure 4. Titration curve of tetraazole (Fluka, 10% H₂O) in aqueous solution (0.2 eq. HClO₄)

The obtained pK_a values indicate a possible conversion in solution from the monomeric to the dimeric structure, as pK_{a1} and pK_{a2} of **ZnL** and **NiL** are as shown in **Table 2** to be in the range of that of the tetraazole. Indeed it is known that tetraazoles have pK_a values in the range of 3 to 5⁷ and as there are no other acidic protons in the molecule (cyclen has pK_a values <2 and >10²² and the water molecules coordinated to the metal centers should have pK_a values around 8 for **ZnL**^{22,23} and >11 for **NiL**²³) we propose the first two deprotonation steps to belong to the two bridging tetraazole units. This would be consistent with the crystallographic structure of **NiL** described earlier. Another support of the idea of formation of a dimer in solution is the value of the third pK_a obtained for **ZnL**, $pK_{a3} = 8.74$, which could be attributed to one of the water molecules coordinated on the Zn(II) ion. Its value is in the range reported for water molecules coordinated to a Zn(cyclen) compound.^{22,23} For **NiL** no third deprotonation is visible, in consistence with the weak Lewis acidic character of nickel leading to coordinated water molecules to be deprotonated at pH values >11.²³

From the data obtained by potentiometric titrations we propose therefore a conversion in solution with increasing pH from the monomeric to the stable dimeric form (**Scheme 3**).



Scheme 3. Proposed model for the deprotonation steps of **ZnL** and **NiL**

From synthesis the metal complexes **ZnL** and **NiL** were obtained in their monomeric form as indicated by the analytical data (elemental analysis of **NiL**, mass spectroscopy of **ZnL** and **NiL**, UV and NMR spectra). The IR spectra show bands around 1400 and 1150 cm^{-1} which are characteristic for the tetraazole moiety,²⁴ and which are not shifted as expected upon coordination to a metal cation.

Most previously reported metal-tetrazole complexes were obtained by solvothermal techniques^{24,25} and analysed by elemental analysis and crystallographic studies only. So we report one of the first examples of tetrazole metal complexes obtained by solution methods and characterised spectroscopically. The described new azamacrocyclic tetrazole complexes may find use in catalysis or as building blocks for self-assembled supramolecular coordination compounds.

4.3 Experimental section

4.3.1 General information.

UV/VIS spectra were recorded on a Varian Cary BIO 50 UV/VIS/NIR spectrophotometer equipped with a jacketed cell holder using 1-cm cuvettes (quartz or glass) from Hellma. For all UV/VIS measurements the temperature was kept constant at 25 °C (± 0.1 °C). IR spectra were recorded on a Bio-Rad FT-IR FTS 155 spectrometer and a Bruker Tensor 27 spectrometer with an ATR unit. Elemental analysis was performed on a Vario EL III. Mass spectra were performed on a ThermoQuest Finnigan TSQ 7000 (ESI) and Finnigan MAT 95

(HRMS). Potentiometric titrations were performed with a Metrohm Dosimat 665. ^1H and ^{13}C NMR spectra were obtained on the following machines: Bruker AC-250 (^1H : 250.1 MHz, ^{13}C : 62.9 MHz, 24 °C), Bruker Avance 300 (^1H : 300.1 MHz, ^{13}C : 75.5 MHz, 27 °C), Bruker Avance 400 (^1H : 400.1 MHz, ^{13}C : 100.6 MHz, 27 °C), Bruker Avance 600 (^1H : 600.1 MHz, ^{13}C : 150.1 MHz, 27 °C). Melting points were determined with a Büchi SMP 20 and are uncorrected.

4.3.2 Materials and Reagents.

All reagents and solvents used for the synthesis of the metal complexes were of analytical grade. Cyanogen bromide (Fluka), sodium azide (Acros), tetraazole (Fluka) and the various metal salts were purchased from commercial sources and used without any further purification. Cyclen was a generous gift from Schering and was used without further purification.

4.3.3 Crystallographic Study.

Translucent light blue triclinic crystals of the dimer $[\text{Ni}_2(\text{LH}_1)_2(\text{H}_2\text{O})_2](\text{ClO}_4)_2$ (0.25 x 0.05 x 0.01 mm) were used for data collection at 123 (\pm 1) K with graphite-monochromated Cu-K α radiation (λ = 1.54184 Å) on a Oxford Diffraction Gemini Ultra diffractometer. The structure of the compound $[\text{Ni}_2(\text{LH}_1)_2(\text{H}_2\text{O})_2](\text{ClO}_4)_2$ was solved by direct methods SIR97 and refined by full-matrix least-squares on F^2 using SHELXL-97. The molecular structure is illustrated in **Figure 1** by ORTEP drawing with 50% probability thermal ellipsoids. Selected interatomic distances and bond angles around the Ni(II) are presented in **Table 1**.

Crystal data for $[\text{Ni}_2(\text{LH}_1)_2(\text{H}_2\text{O})_2](\text{ClO}_4)_2$: $\text{C}_{18}\text{H}_{42}\text{Cl}_2\text{N}_{16}\text{Ni}_2\text{O}_{10}$, M_r = 831, triclinic, space group P -1, a = 7.4827 (8) Å, b = 9.1044 (9) Å, c = 11.1784 (15) Å, α = 91.665 (9)°, β = 96.656 (10)°, γ = 90.375 (8)°, V = 756.04 (15) Å³, Z = 1, D_x = 1.825 Mg/m³, μ = 3.896 mm⁻¹, $F(000)$ = 432, θ -range for data collection from 3.98 to 51.58, index ranges $-7 < h < 7$, $-9 < k < 9$, $-11 < l < 11$, reflection collected = 4551, unique reflections = 1529, R_{int} = 0.0946, data/restraints/parameters 1529/0/217, goodness-of-fit on F^2 is 1.005, final R-index R_1 = 0.1362 (wR_2 = 0.1983), ρ_{min} = -0.480 e Å⁻³, ρ_{max} = 0.708 e Å⁻³.

4.3.4 Potentiometric pH Titrations.

The pH titrations were carried out under N₂ at 25 °C with a computer controlled pH-meter (pH 3000, WTW) and dosimat (Dosimat 665 and 765, Metrohm). Aqueous solutions of the metal complexes (0.05 mM) were titrated with 0.02 M tetraethylammoniumhydroxide

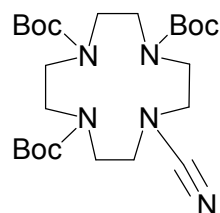
(TEAOH) aqueous solution. The ionic strength was adjusted to $I = 0.1$ with tetraethylammoniumchloride (TEAC). The TEAOH solutions were calibrated with kalium hydrogen phthalate. A titration of 0.1 M perchloric acid with TEAOH solution was used for calibration and to determine $\log K_W$. The Irving-factor (A_I) was determined according to $\text{pH}_{\text{measurement}} = \text{pH}_{\text{real}} + A_I$. Various small amounts of HClO_4 0.1 M (0.2 - 1.2 mL) were added to the titration solution in order to determine values in the pH range of 3 to 8. For each metal complex at least two independent titrations were made. Data analysis was performed with the program Hyperquad2000 (Version 2.1, P. Gans) and Origin 6.0.

Caution: Although no problems were encountered in this work, metal perchlorate complexes as well as tetraazoles are potentially explosive. They should be handled with care, and the complexes should be prepared in small quantities.

4.3.5 Synthesis of the macrocyclic tetraazole ligand and its metal complexes.

The synthetic intermediate 1,4,7,10-tetraaza-cyclododecane-1,4,7-tricarboxylic acid tri-tert-butyl ester **1** was prepared according to the published method.

10-Cyano-1,4,7,10tetraaza-cyclododecane-1,4,7-tricarboxylic acid tri-tert-butyl ester (**2**)

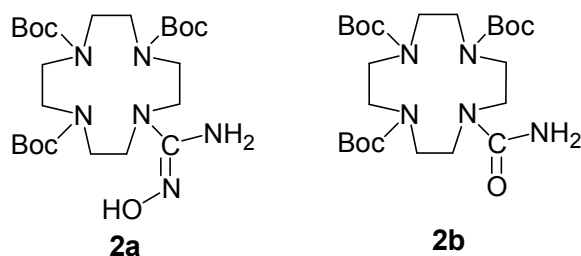


3-Boc-Cyclen (0.4 g, 0.846 mmol) was solved in 10 mL THF and the cyanogen bromide was added (0.047 g, 0.440 mmol, 0.52 eq.) followed by K_2CO_3 (0.117 g, 0.846 mmol). The reaction mixture was refluxed for 3h. At the end of reaction, the excess K_2CO_3 was filtered off, the solvent was removed by reduced pressure and the crude mixture (413 mg) was purified by column chromatography (EE/PE 50:50). The product was obtained as a colourless solid ($R_f = 0.5$, ethyl acetate/petroleum ether, 1:1). Yield: 0.18 g, 0.361 mmol, 82%.

Melting point: 58 - 60 °C; UV/VIS (MeOH) λ_{max} [nm] ($\lg \epsilon$) = 193 (4.524), 203 (3.983), 205 (3.912); IR (KBr): $\tilde{\nu}$ [cm^{-1}] = 2976, 2933, 2361, 2209, 1688, 1463, 1417, 1366, 1249, 1165, 1033, 977, 941, 858, 773; $^1\text{H-NMR}$ (300 MHz, CDCl_3): d = 1.39 (bs, 18H, $\text{COOC}(\text{CH}_3)_3$); 1.40 (bs, 9H, $\text{COOC}(\text{CH}_3)_3$); 3.19 (bs, 4H, CH_2 Cyclen); 3.33 (bs, 4H, CH_2 Cyclen); 3.39-3.44 (m, 8H, CH_2 Cyclen); $^{13}\text{C-NMR}$ (300 MHz, CDCl_3): d = 28.41 ($\text{COOC}(\text{CH}_3)_3$); 28.65 ($\text{COOC}(\text{CH}_3)_3$); 47.92, 49.90, 54.13 (CH_2 Cyclen); 79.69 ($\text{COOC}(\text{CH}_3)_3$); 80.46

(COOC(CH₃)₃); 116.98 (N-CN); 155.21 (COOC(CH₃)₃); MS (ESI, AcN/H₂O/TFA) : *m/z* (%) = 498.3 (100) [MH⁺], 515.3 (80) [(M + NH₄)⁺]. Anal. Calcd for C₂₄H₄₃N₅O₆: C 57.93, H 8.71, N 14.07. Found: C 57.34, H 8.75, N 13.51.

10-(N-Hydroxycarbamimidoyl)-1,4,7,10-tetraaza-cyclododecane-1,4,7-tricarboxylic acid tri-tert-butyl ester (2a) and 10-Carbamoyl-1,4,7,10-tetraaza-cyclododecane-1,4,7-tricarboxylic acid tri-tert-butyl ester (2b)



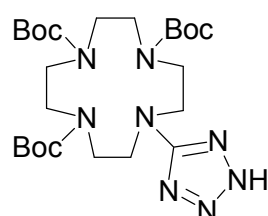
To 3-Boc-Cyclen-cyanamide **2** (0.1 g, 0.2 mmol) was added Et₃N (14 mL, 1 mmol, 5 eq.) then MeOH, followed immediately by NH₂OH HCl (0.064 g, 0.9 mmol, 4.5 eq.). For rinsing some MeOH was used. The reaction was stirred for 20h at r.t. (no more educt is present after this period). Two more polar products appear, the less polar is more concentrated (the amide). The solvent was eliminated under reduced pressure to give 0.23 g raw material. Then it was solved in CHCl₃ and PE was added. The formed precipitate was filtered off (0.065 g), the solvent was eliminated to yield 0.16 g raw material which was purified by column chromatography (5:95 MeOH/EE). The hydroxyguanine **2a** was obtained as minor product as a colourless solid (0.013 g, 0.024 mmol, 12%, *R_f* = 0.3, ethyl acetate/methanol 9:1). The amide **2b** was obtained as major product as a colourless solid (0.029 g, 0.056 mmol, 28%, *R_f* = 0.48, ethyl acetate/methanol 9:1).

2a: Melting point: 92-93 °C; UV/VIS (CHCl₃) λ_{max} [nm] (lg ε) = 330 (2.662); IR (KBr): $\tilde{\nu}$ [cm⁻¹] = 3371, 2977, 2932, 2428, 1690, 1583, 1473, 1413, 1366, 1251, 1167, 1106, 1023, 968, 937, 858, 775; ¹H-NMR (400 MHz, CDCl₃): d = 1.46 (bs, 27H, COOC(CH₃)₃); 3.34-3.51 (m, 18H, CH₂ Cyclen and NH₂); 4.94 (bs, 1H, OH); ¹³C-NMR (400 MHz, CDCl₃): d = 28.46 (COOC(CH₃)₃); 28.58 (COOC(CH₃)₃); 49.32; 50.88; 51.17 (CH₂ Cyclen); 79.82 (COOC(CH₃)₃); 80.32 (COOC(CH₃)₃); 155.75 (COOC(CH₃)₃); 156.58 (COOC(CH₃)₃); 159.89 (C_{quat} hydroxycarbamimidoyl); MS (ESI, DCM/MeOH + 10 mmol/l NH₄Ac) : *m/z* (%) = 531.4 (100) [MH⁺]; HRMS (PI-LSI-MS, MeOH/Glycerin) calculated for (C₂₄H₄₇N₆O₇)⁺ 531.3506 found 531.3492 ± 2.67 ppm.

2b: Melting point: 98 - 99 °C; UV/VIS (CHCl₃) λ_{max} [nm] (lg ε) = 327 (1.808); IR (KBr): $\tilde{\nu}$ [cm⁻¹] = 3453, 3364, 2976, 2932, 2360, 1691, 1602, 1475, 1413, 1366, 1251, 1165, 1105,

1024, 970, 935, 858, 777; $^1\text{H-NMR}$ (400 MHz, CDCl_3): δ = 1.44 (bs, 27H, $\text{COOC}(\text{CH}_3)_3$); 3.39 (bs, 12H, CH_2 Cyclen); 3.46 (bs, 4H, CH_2 Cyclen); 4.68 (bs, 2H, NH_2); $^{13}\text{C-NMR}$ (400 MHz, CDCl_3): δ = 28.40 ($\text{COOC}(\text{CH}_3)_3$); 28.47 ($\text{COOC}(\text{CH}_3)_3$); 50.23; 50.50; 50.62 (CH_2 Cyclen); 80.04 ($\text{COOC}(\text{CH}_3)_3$); 80.33 ($\text{COOC}(\text{CH}_3)_3$); 156.25 ($\text{COOC}(\text{CH}_3)_3$); 156.69 ($\text{COOC}(\text{CH}_3)_3$); 159.63 ($\text{C}_{\text{quat. amide}}$); MS (ESI, DCM/MeOH + 10 mmol/l NH_4Ac) : m/z (%) = 516.2 (100) [MH^+]. Anal. Calcd for $\text{C}_{24}\text{H}_{45}\text{N}_5\text{O}_7 \cdot \text{CH}_3\text{OH}$: C 54.83, H 9.02, N 12.79. Found: C 55.14, H 9.49, N 12.94. HRMS (PI-EI-MS, CH_2Cl_2) calculated for $(\text{C}_{24}\text{H}_{45}\text{N}_5\text{O}_7)^+$ 515.3319 found 515.3310 ± 1.74 ppm.

10-(2H-Tetrazol-5-yl)-1,4,7,10-tetraaza-cyclododecane-1,4,7-tricarboxylic acid tri-tert-butylester (3)

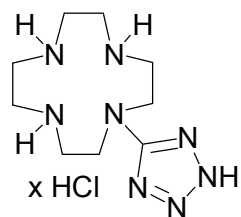


3-Boc-Cyclen-Cyanamide **2** (0.1 g, 0.2 mmol, 1 eq.), NaN_3 (0.014 g, 0.220 mmol, 1.1 eq.) and ZnBr_2 (0.045 g, 0.2 mmol, 1 eq.) were solved in water. If there are clumps of undissolved nitrile, MeOH or iPrOH or glycerol is added (no more than 50% v/v). The reaction mixture was refluxed for 20h under **vigorous stirring**. A more polar product appears. The reaction was stopped and the aqueous phase was extracted 3 times with EE. The combined organic layers were evaporated, 8 mL of a 0.25 N NaOH solution was added and the mixture was stirred for 30 min, until the original precipitate was dissolved and a suspension of zinc hydroxide was formed. The suspension was filtered, the solid washed with 1 mL 1 N NaOH. To the filtrate was added a solution of HCl until pH = 5, with vigorous stirring, causing the tetraazole zwitterion to precipitate. The tetraazole was filtered and dried (if it is a too small amount of pp, solve it in DCM and dry it). If little or no precipitate was formed upon final acidification, the aqueous layer was saturated with NaCl and extracted 3 times with EE, the organic layer is dried over Na_2SO_4 and evaporated to dryness. We obtain 0.078 g (0.144 mmol, 72%) of product as colourless solid (R_f = 0.3, ethyl acetate/methanol, 9:1).

Melting point: 68 - 70 °C; UV/VIS (MeOH) λ_{max} [nm] (lg e) = 200.9 (4.215), 203.9 (4.123); 316 (2.501); IR (KBr): $\tilde{\nu}$ [cm^{-1}] = 3446, 2977, 2933, 2361, 1693, 1467, 1414, 1367, 1250, 1166, 1039, 974, 947, 857, 777; $^1\text{H-NMR}$ (400 MHz, CDCl_3): δ = 1.44 (bs, 27H, $\text{COOC}(\text{CH}_3)_3$); 3.29 (bs, 4H, CH_2 Cyclen); 3.39 (bs, 4H, CH_2 Cyclen); 3.58 (m, 4H, CH_2 Cyclen); 3.61-3.62 (m, 4H, CH_2 Cyclen); 13.5 (very bs, 1H, NH tetraazole); $^{13}\text{C-NMR}$ (400

MHz, CDCl₃): d = 28.41 (COOC(CH₃)₃); 28.56 (COOC(CH₃)₃); 48.39 (CH₂ Cyclen); 49.33 (CH₂ Cyclen); 50.70 (CH₂ Cyclen); 53.93 (CH₂ Cyclen); 79.98 (COOC(CH₃)₃); 80.95 (COOC(CH₃)₃); 155.61 (COOOC(CH₃)₃); 157.01 (COOOC(CH₃)₃); 160.40 (C_{quat}. tetraazole); MS (-p ESI, DCM/MeOH + 10 mmol/l NH₄Ac) : *m/z* (%) = 539.4 (100) [(M-H⁺)⁻]; HRMS (PI-EI-MS, CH₂Cl₂) calculated for (C₂₄H₄₄N₈O₆)⁺ 540.3384 found 540.3376 ± 1.44 ppm.

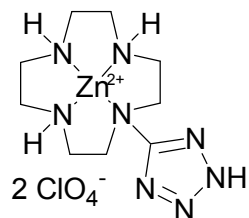
1-(2H-Tetrazol-5-yl)-1,4,7,10-tetraaza-cyclododecane hydrochloric salt (L-NH⁺)



3-Boc-Cyclen-Tetraazole (0.107 g, 0.198 mmol) was solved in MeOH (2 mL) and the solution was cooled in an ice-bath. HCl/Ether (1 mL) was added and the reaction was mixed for 24h. After reaction completion, the solvent was eliminated under reduced pressure to obtain 69 mg (0.197 mmol, 99%) of the HCl salt as colourless solid (*R_f* = 0, dichloromethane/methanol, 9:1).

Melting point: > 180 °C; UV/VIS (Millipore H₂O) λ_{\max} [nm] (lg ϵ) = 220 (3.359); IR (KBr): $\tilde{\nu}$ [cm⁻¹] = 3429, 2985, 2820, 2769, 2664, 2571, 2496, 2393, 1603, 1543, 1443, 1357, 1287, 1251, 1150, 1076, 1005, 957, 760; ¹H-NMR (300 MHz, D₂O): d = 3.09-3.21 (m, 12H, CH₂ Cyclen); 3.62-3.68 (m, 4H, CH₂ Cyclen); ¹³C-NMR (300 MHz, D₂O): d = 43.56, 44.4, 45.03 (CH₂ Cyclen); 49.25 (CH₂ Cyclen); 160.53 (C_{quat}. tetraazole); MS (+p ESI, H₂O/AcN/TFA) : *m/z* (%) = 241.1 (100) [MH⁺]; HRMS (PI-LSI-MS, MeOH/Glycerin) calculated for (C₉H₂₁N₈)⁺ 241.1889 found 241.1888 ± 0.48 ppm.

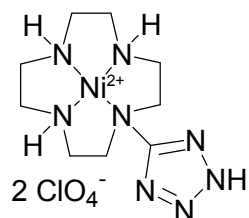
1-(2H-Tetrazol-5-yl)-(Zinc-1,4,7,10-tetraaza-cyclododecane) perchlorate (ZnL)



The aqueous solutions of ligand (0.1 g, 0.286 mmol) and Zn(ClO₄)₂ · 6H₂O (0.117 g, 0.314 mmol, 1.1 eq.) were added drop wise in the same time in a warm aqueous solution (5 mL). An aqueous LiOH solution was added until pH = 8-9. The reaction mixture was refluxed for 4h. The product was obtained quantitatively by lyophilization as hygroscopic colorless solid.

UV/VIS (Millipore H₂O) λ_{\max} [nm] (lg e) = broad band from the lower wavelength region up to 250 nm; IR (KBr): $\tilde{\nu}$ [cm⁻¹] = 3165 (s), 2945, 2820, 2199, 1637, 1492, 1446, 1412, 1357, 1287, 1222, 1141, 1082, 979, 628; ¹H-NMR (400 MHz, D₂O): d = 2.82-3.11 (m, 10H, CH₂ Cyclen); 3.25-3.38 (m, 4H, 2H CH₂ Cyclen and 2H CH₂ Cyclen); 3.51-3.64 (m, 2H, CH₂ Cyclen); ¹³C-NMR (400 MHz, D₂O): d = 43.52, 43.76, 45.03 (CH₂ Cyclen); 51.38 (CH₂ Cyclen); 167.79 (C_{quat.} tetraazole); MS (+p ESI, H₂O/MeOH + 10 mM NH₄Ac) : *m/z* (%) = 339 (100) [M²⁺ + Cl]⁺; 363.1 [M²⁺ + CH₃COO]⁺.

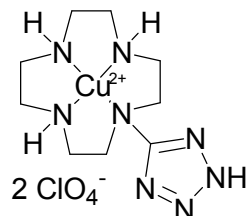
1-(2H-Tetrazol-5-yl)-(Nickel-1,4,7,10-tetraaza-cyclododecane) perchlorate (NiL)



The aqueous solutions of ligand (0.1 g, 0.286 mmol) and Ni(ClO₄)₂ · 6H₂O (0.115 g, 0.314 mmol, 1.1 eq.) were added drop wise in the same time in a warm aqueous solution (5 mL). An aqueous LiOH solution was added until pH = 8-9. The reaction mixture was refluxed for 4h. The product was recrystallized from EtOH as pale violet solid (0.094 g, 0.189 mmol, 66%).

Melting point: > 180 °C; UV/VIS (Millipore H₂O) λ_{\max} [nm] (lg e) = 348 (2.255); 552 (2.024); 964 (2.0); IR (KBr): $\tilde{\nu}$ [cm⁻¹] = 3430, 3324, 3257, 2933, 2364, 2038, 1647, 1491, 1443, 1363, 1103, 1085, 1004, 973, 764; MS (+p ESI, H₂O/MeOH + 10 mM NH₄Ac) : *m/z* (%) = 357.1 (100) [M²⁺ + CH₃COO]⁺; Anal. Calcd for C₉H₂₀N₈O₈Cl₂Ni · H₂O: C 20.95, H 4.30, N 21.72. Found: C 21.14, H 5.07, N 21.76.

1-(2H-Tetrazol-5-yl)-(Copper-1,4,7,10-tetraaza-cyclododecane) perchlorate (CuL)



The aqueous solutions of ligand (0.05 g, 0.143 mmol) and Cu(ClO₄)₂ · 6H₂O (0.058 g, 0.158 mmol, 1.1 eq.) were added drop wise in the same time in a warm aqueous solution (5 mL). An aqueous LiOH solution was added until pH = 8-9. The blue reaction mixture was refluxed for 2h. Then the mixture was left to reach r.t and EtOH was added. The mixture was left in the fridge over-night and the brown residue which appeared was filtered out the next day. The

resulting clear blue solution was lyophilized to give the desired product quantitatively as a dark blue hygroscopic solid.

UV/VIS (Millipore H₂O) λ_{max} [nm] (lg ϵ) = 280 (3.023); 613 (2.022); IR (KBr): $\tilde{\nu}$ [cm⁻¹] = 3600-3200 (br s), 2362, 2199, 1635, 1481, 1442, 1147, 1115, 1085, 985, 626; MS (+pESI, H₂O/AcN/MeOH + 10 mM NH₄Ac) : m/z (%) = 302 (25) [2M²⁺-2H⁻]²⁺; 338 (45) [M²⁺ + Cl]⁺; 362 (100) [M²⁺ + CH₃COO⁻]⁺.

4.4 References

- ¹ P. D. Beer, N. G. Berry, A. R. Cowley, E. J. Hayes, E. C. Oates, and W. W. H. Wong, *Chem. Commun.* 2003, 2408; C. Bucher, R. S. Zimmerman, V. Lynch, and J. L. Sessler, *Chem. Commun.* 2003, 1646; M. Albrecht, S. Schmid, M. de- Groot, P. Weis, and R. Fröhlich, *Chem. Commun.* 2003, 2526; J. Farkas Jr, S. J. Stoudt, E. M. Hanawalt, A. D. Pajerski, and H. G. Richey Jr, *Organometallics* 2004, **23**, 423; J. Nelson, M. Nieuwenhuyzen, I. Pál, and R. M. Town, *Dalton Trans.* 2004, 229; B. Bag, and P. K. Bharadwaj, *Inorg. Chem.* 2004, **43**, 4626; B. Dietrich, P. Viout, J.-M. Lehn, 'Macrocyclic Chemistry: Aspects of Organic and Inorganic Supramolecular Chemistry', VCH, New York, 1993 and references therein; H.-J. Schneider, and A. Yatsimirsky, 'Principles and Methods in Supramolecular Chemistry', John Wiley&Sons, New York, 1999 and references therein.
- ² Review on thermodynamic and kinetic data for macrocycle interaction with cations, anions and neutral molecules: R. M. Izatt, K. Pawlak, J. S. Bradshaw, and R. L. Bruening, *Chem. Rev.* 1995, **95**, 2529-2586.
- ³ For reviews, see: (a) J. Chin, *Acc. Chem. Res.* 1991, **24**, 145; C. Liu, M. Wang, T. Zhang, H. Sun, *Coord. Chem. Rev.* 2004, **248**, 147.
- ⁴ M. V. Baker, D. H. Brown, B. W. Skelton, and A. H. White, *J. Chem. Soc., Dalton Trans.* 2000, 4607; B.-C. Tzeng, W.-C. Lo, C.-M. Che, and S.-M. Peng, *Chem. Commun.* 1996, 181; P. Planinic, D. Matkovic-Calogovic, and H. Meider, *J. Chem. Soc., Dalton Trans.* 1997, 3445 ; L. Burai, É. Tóth, G. Moreau, A. Sour, R. Scopelliti, and A. E. Merbach, *Chem. Eur. J.* 2003, **9**, 1394; M. E. Padilla-Tosta, J. M. Lloris, R. Martonez-Manez, A. Benito, J. Soto, T. Pardo, M. A. Miranda, and M. D. Marcos, *Eur. J. Inorg. Chem.* 2000, 741; N. W. Alcock, K. P. Balakrishnan, P. Moore, *J. Chem. Soc., Dalton Trans.* 1986, 743.
- ⁵ A. R. Katritzky, C. W. Rees, E. F. V. Scriven, and R. N. Butler, 'Comprehensive Heterocyclic Chemistry', Pergamon, Oxford, UK, 1996, Vol. 4.
- ⁶ H. Singh, A. S. Chawla, V. K. Kapoor, D. Paul, and R. K. Malhotra, *Prog. Med. Chem.* 1980, **17**, 151.
- ⁷ P. Demko, and K. B. Sharpless, *J. Org. Chem.*, 2001, **66**, 7945; F. Himo, Z. P. Demko, L. Noodleman, and K. B. Sharpless, *J. Am. Chem. Soc.* 2002, **124**, 12210; F. Himo, Z. P. Demko, L. Noodleman, and K. B. Sharpless, *J. Am. Chem. Soc.* 2003, **125**, 9983.
- ⁸ M. Brandes, C. Gros, F. Denat, and R. Grilaud, *Bull. Chem. Soc. Chim. Fr.*, 1996, **133**, 3068.
- ⁹ S. Thambidurai, K. Jeyasubramanian, and S. K. Ramalingam, *Polyhedron*, 1996, **15**, 4011; J. P. Ferris, C. H. Huang, and W. J. Hagan, *Nucleosides Nucleotides*, 1989, **8**, 407; A. R. Katritzky, B. V. Rogovoy, C. Chassaing, and V. Vvedensky, *J. Org. Chem.* 2000, **65**, 8080; Y.-Q. Wu, S. K. Hamilton, D. E. Wilkinson, and G. S. Hamilton, *J. Org. Chem.* 2002, **67**, 7553.

- ¹⁰ B. B Snider, and S. M. O'Hare, *Tetrahedron Lett.* 2001, **42**, 2455 and references therein; B.B. Snider, Y. Ahn, and S. M. O'Hare, *Org. Lett.* 2001, **3**, 4217; M. Shimizu, A. Oishi, Y. Taguchi, Y. Gama, and I. Shibuya, *Chem. Pharm. Bull.* 2002, **50**, 426.
- ¹¹ ZnL and CuL are very hygroscopic solids, which prohibited obtaining accurate elemental analysis or X-ray structure analyses. The small molecular mass with two positive charges did not allow for HRMS.
- ¹² S. G. Alvarez, and M. T. Alvarez, *Synthesis* 1997, 413.
- ¹³ L. Bosch, and J. Vilarrasa, *Angew. Chem.* 2007, **119**, 4000.
- ¹⁴ Z. P. Demko, and K. B. Sharpless, *Angew. Chem. Int. Ed.* 2002, **41**, 2110.
- ¹⁵ H. Quast, and L. Bieber, *Tetrahedron Lett.* 1976, **18**, 1485; W. R. Carpenter, *J. Org. Chem.* 1962, **27**, 2085; M. M. Krayushin, A.M. Beskopylnyi, S. G. Slotin, O. A. Lukyanov, and V. M. Zhulin, *Izv. Akad. Nauk. SSSR Ser. Khim.* 1980, **11**, 2668.
- ¹⁶ Z.P. Demko, and K.B. Sharpless, *Angew. Chem. Int. Ed.* 2002, **41**, 2113.
- ¹⁷ S.D. Luzzi, and M.A. Marletta, *Bioorg. Med. Chem. Lett.* 2005, **15**, 3934.
- ¹⁸ H. Gallardo, I. M. Begnini, A. Neves, and I. Vencato, *J. Braz. Chem. Soc.* 2000, **11**, 274; H. Gallardo, E. Mayer, A. J. Bertoluzzi, F. Molin, and A. S. Mangrich, *Inorg. Chim. Acta*, 2004, **357**, 505 and references therein; W. R. Ellis Jr., and I. W. Purcell, *Inorg. Chem.* 1982, **21**, 834.
- ¹⁹ M. Ciampolini, M. Micheloni, N. Nardi, P. Paoletti, P. Dapporto, and F. Zanobini, *J. Chem. Soc. Dalton Trans.* 1984, 1357; J. H. Coates, D. A. Hadi, S. F. Lincoln, H. W. Dodgen, and J. P. Hunt, *Inorg. Chem.* 1981, **20**, 707; A. Bencini, A. Bianchi, E. Garcia-Espana, Y. Jeannin, M. Julve, V. Marcelino, and M. Philoche-Levisalles, *Inorg. Chem.* 1990, **29**, 963.
- ²⁰ S. C. Nyburg, and J. S. Wood, *Inorg. Chem.* 1964, **3**, 468.
- ²¹ R. Das, P. Paul, K. Nag, and K. Venkatsubramanian, *Inorg. Chim. Acta*, 1991, **185**, 221; V. P. Sinditskii, M. D. Dutov, A. E. Fogelzang, T. Y. Vernidub, V. I. Sokol, and M. A. Porai-Koshits, *Inorg. Chim. Acta*, 1991, **189**, 259; R. Guillard, N. Jagerovic, A. Tabard, P. Richard, L. Courthaudon, A. Lonati, C. Lecomte, and K. M. Kadish, *Inorg. Chem.* 1991, **30**, 16.
- ²² T. Koike, S. Kajitani, I. Nakamura, E. Kimura, and M. Shiro, *J. Am. Chem. Soc.*, 1995, **117**, 1210.
- ²³ M. Subat, K. Woinaroschy, S. Anthofer, B. Malterer, and B. Koenig, *Inorg. Chem.* 2007, **46**, 4336 and references therein.
- ²⁴ X-S. Wang, Y.-Z. Tang, X.-F. Huang, Z.-R. Qu, C.-M. Che, P. W. H. Chan, and R.-G. Xiong, *Inorg. Chem.* 2005, **44**, 5278; S. Cralkjey, R. H. Findlay, and M. H. Palmer, *Tetrahedron* 1973, **29**, 2173.
- ²⁵ M. A. M. Abu-Youssef, F. A. Mautner, A. A. Massoud, and L. Oehrstroem, *Polyhedron*, 2007, **26**, 1531; X.-M. Zhang, Y.-F. Zhao, H.-S. Wu, S. R. Batten, and S.W. Ng, *Dalton Trans.*

2006, 3170; H. Zhao, Q. Ye, Q. Wu, Y.-M. Song, Y.-J. Liu, and R.-G. Xiong, *Z. Anorg. Allg. Chem.* 2004, **630**, 1367.

C. Summary

This PhD thesis is a study of cyclen transition metal complexes as biomimetic catalysts, phosphate anion sensors and building-blocks in supramolecular assemblies. We have synthesised new Cu(II) and Ni(II) complexes of macrocyclic ligands and compared their hydrolytic properties in aqueous solution towards 4-nitrophenyl acetate and bis(4-nitrophenyl)phosphate with that of identical Zn(II) complexes. Unlike the Zn(II) complexes, the Cu(II) and Ni(II) complexes do not promote the hydrolysis of the substrates, as they do not fulfil one of the two conditions needed for an artificial metallohydrolase: the Cu(II) complexes do not possess two *cis*-oriented coordination sites on the metal ion for binding the substrate and a water molecule, while Ni(II) is not a strong Lewis acid and does not facilitate deprotonation of the coordinated water to generate the hydroxide nucleophile. Two dinuclear Zn(II) complexes showed the formation of a very stable 1:1 complex with pyrophosphate, with a slow exchange taking place between free and bound anion. Indicator displacement measurements with pyrocatechol violet and coumarin methylsulphonate in buffered solutions (pH 7.4, 25 °C) indicated that the receptor can distinguish phosphate anion derivatives from other anionic species, with binding affinities proportional to the number of negative charges on the anion. The binding affinity can be detected with the naked eye. We report here the synthesis of a new derivative of Cyclen with a tetraazole moiety directly bound to the azamacrocycle and its Zn(II), Ni(II) and Cu(II) complexes. X-ray structure analysis of the Ni(II) compound shows the formation of a stable dimer by coordination of each of the two tetraazole substituents to the neighboring metal cation. Potentiometric titrations of the metal complexes indicate a possible conversion of the monomer to the dimeric structure in solution and show the pK_a of the NH-atom on the tetraazole substituent to be between 4.03 and 5.3 depending on the metal ion coordinated by cyclen.

D. Appendix

Publication list

Subat, M.; Woinaroschy, K.; Anthofer, S.; Malterer, B.; Koenig B.

“1,4,7,10-Tetraazacyclododecane metal complexes as potent promoters of carboxyester hydrolysis under physiological conditions” *Inorg. Chem.* **2007**, *46*(10) pp 4336 - 4356.

Woinaroschy, K ; Ursu, A. ; Koenig, B.

“Synthesis and characterization of 1-(2H-Tetrazol-5-yl)-1,4,7,10-tetraaza-cyclododecane and its Zn(II), Ni(II) and Cu(II) complexes”, *Heterocycles*, submitted.

CURRICULUM VITAE

Kristina-Michaela WOINAROSCHY

DATE OF BIRTH: 13. 10. 1979

NATIONALITY: Romanian

Married

EDUCATION

- Oct. 2003 - Sept. 2007 **University of Regensburg, Germany: PhD in Organic Chemistry**
Thesis submitted, defending date : 27th of November 2007
- 2002 - 2003 **Ecole Polytechnique, Paris, France: DEA Multinational de Chimie Moléculaire** (equivalent to a **Master Degree** in Organic Chemistry)
- 2001 - 2002 **École Polytechnique, Paris, France:** Erasmus student
Graduated with "High Honours"
- 1998 - 2003 **"Politehnica" University, Bucharest, Romania: Bachelor of Science**
Department of Engineering Sciences, Chemistry Division, English Stream
Final average: 10 out of 10

WORK AND RESEARCH EXPERIENCE

- July 2005 - Dec. 2006 **Scientific assistant of the biotech company Entelechon GmbH, Regensburg, Germany**
Position: Responsible for the market launch, advertising, marketing, distribution and customer support of the innovative product QconCATs.
- Oct. 2003 - Sept. 2007 **PhD in organic chemistry at the University of Regensburg**
Supervisor, Prof. Dr. B. König
Subject: "Cyclen transition metal complexes as biomimetic catalysts, phosphate anion sensors and building-blocks in supramolecular assemblies"
- Oct. 2003 - July 2004 **Scientific assistant at the University of Regensburg**
- Sept. 2002 - April 2003 **MSc thesis at the Ecole Polytechnique, Paris, France**
Supervisor Dr. Joëlle Prunet
Subject: "Synthesis of a model of the fragment C16-C30 of Dolabelide C"
- April - July 2002 **Scientific research project at the Ecole Polytechnique, Paris, France**
Supervisor: Dr. Joëlle Prunet
Subject: "Diastereoselective synthesis of 1,2,4-triols by intermolecular conjugated addition"
- April - July 2000 **Scientific research project at Manchester Metropolitan University, UK**
Supervisor: Dr. Julia M. Dickinson
Subject: "Hydroxy pyridones as potential sequestering iron chelates"

SCIENTIFIC CONFERENCES AND TRAINING COURSES

2007	Project management course (innovation management, corporate strategy, product management, competitive analysis) organized by the German Chemical Society in order to obtain the title " <u>Certified project manager in chemical economics</u> ".
11 - 14 Sept. 2005	Annual meeting of the German Chemical Society (GdCh), Düsseldorf, Germany " Photooxidation of environmental pollutants using flavin systems " (poster presentation)
17 - 21 July 2005	XXX International Symposium on Macrocyclic Chemistry, Dresden, Germany " New metal cyclen complexes as catalytic reagents for phosphodiester and carboxyester hydrolysis " (poster presentation)
August - Sept. 1999	Product Development summer course organized by BEST (Board of European Students of Technology) at the "Friedrich-Alexander" University in Erlangen and "Technische Universität" in Dresden, Germany.

AWARDS

July 2004 - June 2007	PhD scholarship awarded by the German Environmental Foundation
Sept. 2002 - Aug. 2003	Scholarship granted by EGIDE , France
Oct. 2001 - July 2002	Scholarship granted by the Foundation of the Ecole Polytechnique , Paris, France
April - July 2000	Erasmus/Socrates scholarship

ENGAGEMENT AND HOBBYS

Member of the German Chemical Society (**GdCh**);
Play acting (former member of the student theatre company „**Babylon**“)
Sport (fitness, skiing, skating)